DOCUMENT NO. W-134
DATE 9/6/73 COPY NO. 1

(NASA-CR-135774) APPLICATIONS OF LASER RANGING AND VLBI OBSERVATIONS FOR SELENODETIC CONTROL Interim Report (Ohio State Univ. Research Foundation) 243 p HC $14.25 CSCL 20E G3/16
N73-33404
Unclas 19395

Reports of the Department of Geodetic Science

Report No. 157

# APPLICATIONS OF LASER RANGING AND VLBI OBSERVATIONS FOR SELENODETIC CONTROL

by

Francis A. Fajemirokun

Prepared for

National Aeronautics and Space Administration
Manned Spacecraft Center
Houston, Texas

Contract No. NAS 9-9695
OSURF Project No. 2841
Interim Report No. 6

NOV 1973
RECEIVED
NASA STI FACILITY
INPUT BRANCH

TECHNICAL LIBRARY COPY
NASA - WALLOPS STATION
WALLOPS ISLAND, VA.

SEP 1973
RECEIVED
NASA STI FACILITY
INPUT BRANCH

The Ohio State University
Research Foundation
Columbus, Ohio 43212

November, 1971

9-4-73

Reports of the Department of Geodetic Science

Report No. 157

# APPLICATIONS OF LASER RANGING AND VLBI OBSERVATIONS FOR SELENODETIC CONTROL

by

Francis A. Fajemirokun

Prepared for

National Aeronautics and Space Administration
Manned Spacecraft Center
Houston, Texas

Contract No. NAS 9-9695
OSURF Project No. 2841
Interim Report No. 6

The Ohio State University
Research Foundation
Columbus, Ohio 43212

November, 1971

## PREFACE

This project is under the supervision of Ivan I. Mueller, Professor of the Department of Geodetic Science at The Ohio State University, and it is under the technical direction of Mr. Richard L. Nance, Photogrammetry and Cartography Section, NASA/MSC, Houston, Texas. The contract is administered by the Space Sciences Procurement Branch, NASA/MSC, Houston, Texas.

A revised version of this report has been submitted to the Graduate School of The Ohio State University in partial fulfillment of the requirements for degree Doctor of Philosophy.

## ABSTRACT

This study was undertaken so as to develop the observation equations necessary to utilize lunar laser ranging and Very Long Baseline Interferometry (VLBI) measurements for the establishment of a primary control network on the moon. The network consists of coordinates of moon points in the selenodetic Cartesian coordinate system, which is fixed to the lunar body, oriented along the three principal axes of inertia of the moon, and centered at the lunar center of mass.

The determination of coordinates of points on the moon using earth-based observations requires the knowledge of the following dynamic behavior of the earth and the moon: the orbital motion of the moon about the barycenter, the rotation of the moon on its axis and the motion of the earth about its center of mass. In addition, the knowledge of the geocentric positions of the terrestrial stations is essential.

Since our knowledge of the parameters related to the above phenomena can be improved simultaneously with the determination of coordinates of lunar points, the observation equations derived in this study are based on a general model in which the unknown parameters included the following:

(a) The selenodetic Cartesian coordinates.

(b) The geocentric coordinates of earth stations.

(c) Parameters of the orientation of the selenodetic coordinate system with respect to a fixed celestial system.

(d) The parameters of the orientation of the "average" terrestrial coordinate system with respect to a fixed celestial coordinate system.

(e) The geocentric coordinates of the center of mass of the moon, given by a lunar ephemeris.

The orientation parameters of both the earth-fixed and the moon-fixed coordinate system were represented in this study by three Eulerian angles which, along with their time rates, could be obtained by numerically integrating the differential equations of motion of the respective bodies. This resulted in the reduction of the number of parameters (in the adjustment model), which are related to the orientation of the two bodies. The general adjustment model developed for the analyses of laser and VLBI observations is based on the theory of adjustment computations with matrix algebra.

The numerical tests performed in this study with simulated as well as real data demonstrated that the numerical integration of the earth's orientation angles yields values which are very close to the classically computed angles, and that the initial conditions for the integration are capable of being solved in an adjustment process. Also, the results of the numerical experiments performed with simulated laser data confirmed the feasibility of the method developed in this study.

ACKNOWLEDGEMENTS

The author wishes to express his deep gratitude to the many persons, without whom this work would not have been possible.

First and foremost, the author is grateful to the Department of Geodetic Science and themembers of its staff, for the financial support and academic guidance given to him during his studies here. In particular, the author wishes to thank his adviser Professor Ivan I. Mueller, for his encouragement, patience and guidance through the various stages of this work. Professors Urho A. Uotila, Richard H. Rapp and Gerald H. Newsom served on the author's reading committee, and offered many valuable suggestions to help clarify many points.

The author has also enjoyed working with other graduate students in the department, especially with the group at 231 Lord Hall, where there was always an atmosphere of enthusiastic learning and of true friendship.

The author is grateful to the various scientists outside the department, with whom he had discussions on the subject of this work, especially to the VLBI group at the Smithsonian Astrophysical Observatory in Cambridge, Massachussetts.

A large amount of computer time needed for the study was provided by the Instruction and Research Computer Center (IRCC) of The Ohio State University, and the author was able to make full use of its facilities through the assistance of Mr. John M. Snowden of the IRCC. Partial support for this study was also furnished by the Mapping Sciences Laboratory of the National Aeronautics and Space Administration, Manned Spacecraft Center, Houston, Texas under Contract No. NAS 9-9695.

The author is greatly indebted to his wife, Dorothy, and to his children - Bola and Wale - for their patience, support, encouragement and love which

sustained him during his years of concentrated study here.

Finally, the author wishes to thank Miss Barbara Beer who, with exceptional skill and expertise, typed most of this work. He also wishes to thank Mrs. Evelyn Rist who, outside her regular work, helped in typing parts of this presentation.

TABLE OF CONTENTS


| | Page |
|---|---|
| PREFACE | ii |
| ABSTRACT | iii |
| ACKNOWLEDGEMENT | v |
| LIST OF TABLES | x |
| LIST OF FIGURES | xi |
| 1. INTRODUCTION | 1 |
| 1.1 General Discussion | 1 |
| 1.2 Review of Past Methods | 3 |
| 1.3 Future Observational Systems for Selenodetic Control | 5 |
| 2. APPLICATION OF LASER RANGING TO SELENODETIC CONTROL | 11 |
| 2.1 Historical Background | 11 |
| 2.2 Basic Operating Principles of Laser Ranging Systems | 13 |
| 2.3 Earth-Moon Distance Equations | 15 |
| 2.31 The "Average" Terrestrial Coordinate System | 16 |
| 2.32 The Selenodetic Coordinate System | 17 |
| 2.33 The Geocentric Coordinates of the Selenocenter | 19 |
| 2.34 Parameters of the Orientation of the Moon | 21 |
| 2.35 The Parameters of Earth's Orientation | 24 |
| 2.36 Computation of Distances between Points on the Earth and on the Moon | 26 |

Page

2.4 Formulation of Observation Equations for Earth-Moon Distances . . . . . 35

2.5 Observation Equations when Orientation Angles are Obtained through Numerical Integration Process . . . . . 60

2.6 Summary . . . . . 65

3. APPLICATION OF THE VLBI TO SELENODETIC CONTROL . . . . . 66

3.1 Introduction . . . . . 66

3.2 Basic Operating Principles of the VLBI . . . . . 68

3.3 Equations for VLBI Measured Time Delays . . . . . 76

3.31 Earth-Earth VLBI Equations . . . . . 77

3.32 Moon-Moon VLBI Equations . . . . . 95

3.33 Earth-Moon VLBI Equations . . . . . 109

3.4 Summary . . . . . 122

4. NUMERICAL INTEGRATION OF THE ORIENTATION OF AN EARTH-FIXED COORDINATE SYSTEM WITH RESPECT TO AN INERTIAL SYSTEM . . . . . 123

4.1 Introduction . . . . . 123

4.2 The Equations of Motion of a Rigid Body . . . . . 126

4.3 The Rotation of the Earth About its Center of Mass . . . . . 128

4.31 The Dynamical Equations of Motion . . . . . 128

4.32 Euler's Geometric Equations . . . . . 134

4.33 Differential Equations of Motion of the Earth . . . . . 136

4.4 Numerical Integration of the Earth's Orientation Angles . . . . . 137

4.41 Calculation of Initial Values . . . . . 139

4.42 Parameters of Integration . . . . . 143

Page

4.5 Adjustment of Initial Condition . . . . . 146

4.51 Evaluation of the State Transition and the Parameter Sensitivity Matrices . . . . 149

4.52 Numerical Fit of the Numerically Integrated Angles to the Calculated Angles. . . . . 151

4.6 Numerical Experiments and Results . . . . . 155

4.61 Fitting the Numerically Integrated Eulerian Angles to the Simulated Angles . . . . . 157

4.62 Comparison of Numerically Integrated Eulerian Angles to those Obtained through Classical Method . . . . . 163

5. ADJUSTMENT MODEL FOR LASER AND VLBI OBSERVATIONS . . . . . 172

5.1 Introduction . . . . . 172

5.2 Classification of Parameters in the Solution . . . . . 174

5.3 Generalized Adjustment Model . . . . . 178

5.31 Formation of Normal Equations . . . . . 178

5.32 Solution of Normal Equations . . . . . 181

5.4 Numerical Experiments. . . . . 186

6. SUMMARY AND CONCLUSIONS . . . . . 207

APPENDIX A: Equations for Earth-Based VLBI Observations of an Artificial Source. . . . . 211

APPENDIX B: Systematic Errors Affecting Earth-Based Lunar Observations . . . . . 215

BIBLIOGRAPHY . . . . . 223

LIST OF TABLES

Page

4.1 Gravitational Constants. . . . . 146

4.2 Starting Initial Conditions for Three Test Cases . . . . . 158

4.3 Recovered Initial Conditions for Three Test Cases after Two Iterations . . . . . 159

4.4 Correlation Matrix for Adjusted Initial Values in the Simulated Case . . . . . 162

4.5 Weight Coefficient Matrix for Adjusted Initial Values in the Simulated Case . . . . . 162

4.6 Correlation Matrix for Adjusted Initial Conditions in the Real Case . . . . . 168

4.7 Weight Coefficient Matrix for Adjusted Initial Conditions in the Real Case . . . . . 168

5.1 Types of Observations . . . . . 177

5.2 Types of Parameters (Pseudo Observations) . . . . . 178

5.3 The Geocentric Cartesian Coordinates of Three Laser Stations. . 188

5.4 Selenodetic Cartesian Coordinates of Three Lunar Retroreflectors . . . . . 188

5.5 Variances of Parameters for Case (1), With One Laser Station Observing . . . . . 197

5.6 Variances of Parameters for Case (2), Period of Observation Varied. . . . . 199

5.7 Variances of Parameters for Case (3), With Three Laser Stations Observing . . . . . 200

5.8 Correlation Matrix for Case (3), 200 Observations Over a One Year Period. . . . . 202

5.9 Shifts Introduced to Parameters and Corrections from Solution . . . . . 206

## LIST OF FIGURES


| | | Page |
|---|---|---|
| 2.1 | The Selenodetic Coordinate System | 18 |
| 2.2 | The Moon's Eulerian Angles | 22 |
| 2.3 | The Earth's Orientation Angles | 26 |
| 2.4 | Laser Station (P) and Retroreflector (M) | 27 |
| 2.5 | Topocentric Mean Ecliptic (1950.0) Coordinates of Retroreflector (M) | 31 |
| 3.1 | Equipment for a VLBI Observing System | 69 |
| 3.2 | Clipped Signal in Relation to the Received Signal | 71 |
| 3.3 | Basic Geometrical Relationships in Interferometry | 73 |
| 3.4 | Clipped Signal Received at Two Stations and Time Delay | 73 |
| 3.5 | Fringe Amplitude Plotted Against Time Delays | 75 |
| 3.6 | Earth-Earth VLBI Observations | 77 |
| 3.7 | Moon-Moon VLBI Observations | 95 |
| 3.8 | Earth-Moon VLBI Observations | 110 |
| 4.1 | Rigid Body and a Fixed System | 127 |
| 4.2 | The Fundamental Coordinate Systems and the Eulerian Angles | 129 |
| 4.3 | Calculation of Eulerian Angles and Their Rates | 140 |
| 4.4 | Residuals in $\vartheta$ and $\psi$ Before and After Adjustment (Simulated Case) | 160 |
| 4.5 | Residuals in $\Phi$ Before and After Adjustment (Simulated Case) | 161 |
| 4.6 | Residuals in $\vartheta$ and $\psi$ Over One Year Period | 166 |
| 4.7 | Residuals in $\Phi + \psi$ Over One Year Period | 167 |
| 4.8 | Residuals for $\vartheta$ and $\psi$ Before and After Adjustment (Real Case) | 169 |

Page

4.9 Residuals in $\Phi + \psi$ Before and After Adjustment (Real Case) . . . . . 170

5.1 Location of the Three Lunar Retroreflectors . . . . . 189

A.1 Earth-Based VLBI with Artificial Source . . . . . 312

# 1 INTRODUCTION

## 1.1 General Discussion.

The science of lunar mapping is an old one whose origin can be traced to the beginning of telescopic astronomy, started by Galileo Galilei in the seventeenth century. Since the first lunar map was published by Galilei around 1610, numerous authors have been engaged in mapping the earth's closest celestial object. Traditionally, this field has been part of the domain of astronomers. However, things changed during the advent of the space age, and scientists of differing disciplines became interested in lunar mapping and related subjects. The quality of published maps of the moon improved with time, due to the advancement in both theory and instrumentation. A detailed history of lunar mapping has been published by Kopal in Chapter 15 of his book on the moon [51].

The mapping of an area requires as a first step, the establishment of a consistent network of control points, whose coordinates have been obtained in a unified and well-defined coordinate system. As opposed to the method of establishing geodetic control for earth mapping, past selenodetic controls have been obtained through the use of earth-based observations. Thus, the determination of coordinates of points on the moon through classical methods is rigorously tied to the following extraneous parameters:

(i) the coordinates of the moon's center of mass in a geocentric inertial coordinate system

(ii) the orientation of an earth-fixed coordinate system with respect to an inertial coordinate system

(iii) the orientation of a defined set of moon-fixed coordinate axes with respect to an earth-fixed coordinate system

(iv) the atmospheric refraction model used for reducing the earth-based observations.

Our knowledge of these parameters is constantly improving due to a natural loop of events, in which improvement in the various theories demands better instrumentation and observation reduction procedures, while more accurate observations demand improvements in existing theories.

The classical types of observations used in lunar position determination were the heliometer observations and earth-based lunar photography. In many instances, the same observations (with or without additional observations) were re-evaluated many times as a result of significant improvements in theory. It now appears that further refinements in the reduction methods for the old observations can neither significantly improve positional accuracy of lunar control points, nor contribute to further improvement in theory. Hence, over the past few decades, new forms of observations have been used to provide selenodetic control, and the application of new instrumentation for selenodetic control has been suggested. The main objective of this study is to investigate how two of the new observational systems can be applied for establishing a primary network of lunar control.

In the section that follows, a brief review of past methods of determining coordinates of lunar features will be presented. The last section of this introductory chapter lists the new observational systems suggested, the problem areas to be investigated and the approach used in this study.

## 1.2 Review of Past Methods.

The classical method of determining the moon's rotational constants (I - the mean inclination of the moon's equator with respect to the mean ecliptic and f - the moon's so-called mechanical flattening), its geometrical figure and the physical libration uses the reduction of heliometer observations. The heliometer is a refracting telescope of small aperture which measures angular distances between a "first fundamental" point on the moon and other lunar features and the moon's limb. The "first fundamental" point is Mösting A, a medium-sized crater situated close to the center of the moon's disc. The basic observation technique designed by Bessel in 1839 has been used with certain modifications to obtain the numerous heliometer observations available today [39].

Those heliometer observations involving the moon's apparent limb and Mösting A have been used by many famous astronomers to simultaneously solve for the lunar physical librations and the coordinates of Mösting A. The adjustment procedure involves the fit of a best fitting sphere to the observed moon's limb, and the coordinates of Mösting A obtained in this manner are referenced to the center of figure.

The determination of coordinates of other fundamental control points on the moon utilizes the heliometer observations made between lunar features and Mösting A. Using the available physical libration parameters, these positions are determined relative to the "first fundamental" point. In 1899, Franz, a German astronomer determined the coordinates of eight fundamental control points on the moon [27]. Later, coordinates of four addi-

tional craters were obtained by Hayn. Most of the existing coordinates of lunar features today are based on the coordinates of these fundamental control points.

The extension of lunar control was achieved through the use of earth-based photography. In general there are two types of lunar photography, namely phase and full-moon photography, each possessing its own advantages and disadvantages. Furthermore, moon photography is either with or without star background. The star background provides the orientation of the camera system as well as the focal length of the telescope. On the other hand, photographs without star background rely on the fundamental points for scale and orientation.

With the use of full-moon photographs taken at Lick Observatory at different librations, Franz extended the original eight points of Franz into a system of 150 points [28]. For the first half of this century this set of points was used as the primary control network on the moon. Later, in 1956-58, an Austrian astronomer Schrutka-Rechtenstamm undertook an extensive review of the moon libration theory, and then recomputed Franz's 150 points [89]. Thus, the Schrutka-Rechtenstamm system was established, and has since been used for further control densification.

In the late 1950's and early 1960's, there was a great need for more accurate control extensions on the moon so as to provide a basis for lunar cartography and to meet the needs of the manned lunar explorations. Several individuals and agencies became involved in the lunar control and lunar mapping work, among whom were two U.S. agencies - the Aeronautical Chart and Information Center (ACIC) and the Army Map Service (AMS, now TOPOCOM). Using different types of moon photography as well as reduction

procedures, each agency obtained a set of coordinates for lunar features. In spite of large differences between the two systems, a combined solution was performed by the Army Map Service in which both the ACIC data and the AMS data were used to obtain selenodetic coordinates of 734 craters. This solution is now referred to as the Department of Defense (DOD) Selenodetic Control System 1966 [ 7 ].

Another direct result of man's lunar exploration over the past few decades is the addition of satellite-borne methods of determining coordinates of features on the moon to the classical methods mentioned above. These methods include photography of the moon by lunar satellites and direct angular observations of features of the moon by astronauts in a manned spacecraft. These and other methods are discussed in [ 78].

The main features of the classical methods of obtaining selenodetic features as reviewed above are that they are based on earth-based photographs and on a fundamental control network established through heliometer measurements. The earth-based photographs suffer from scale and resolution limitations, and the heliometer is a short-focal length telescope with limited resolution. Coordinates of points on the moon tied to fundamental control points are affected by the center of figure - center of mass bias. Relative accuracies of positions of lunar features from earth-based photography are approximately 1 and 1.5 km near the origin, in the horizontal and vertical components respectively, and degenerate rapidly towards the lunar limb [75].

### 1.3 Future Observational Systems for Selenodetic Control.

In the summer of 1965, the National Aeronautics and Space Administration (NASA) sponsored a Lunar Exploration and Science Conference in Falmouth, Massachusetts [74]. Two years later, a follow-up conference was held at Santa Cruz, California [75]. Among the groups participating in each of these lunar conferences was a Geodesy and Cartography working

group. This group, after clarifying its scientific objectives, went on to suggest ways of achieving these goals. The scientific objectives agreed upon at the meetings included the following:

(a) more accurate determination of the position and orientation of the moon (and their variations with time) with respect to the earth

(b) determination of the mass and gravitational field of the moon

(c) determination of the physical size and shape of the moon, measurements of topographic variations and development of a lunar geodetic network over the entire lunar surface.

In order to achieve these goals, the group suggested the use of observational systems (some new and others old) such as

(i) laser ranging (to the moon and lunar satellites)

(ii) earth-based radio tracking of the moon and lunar satellites (with Doppler and ranging transponders on the moon and on the lunar satellites)

(iii) orbiting camera systems

(iv) independent-clock radio interferometry (VLBI)

(v) surface gravimetry, and gradiometer measurements taken from lunar satellites.

To this list was later added satellite altimetry, satellite-to-satellite tracking and earth-moon, moon-moon Very Long Baseline Interferometry (VLBI) [18].

Since these new observational systems were proposed, few papers have been presented at different scientific meetings on what some of the above instrumentation (notably the laser and VLBI) could achieve in the field of selenodesy. However, these papers are usually of a general nature, without specific and detailed mathematical development of how these instru-

ments can be used to improve selenodetic control and related parameters.

The primary aim of this study is to develop observation equations which could be used with new observations to achieve some of the goals listed above. In doing this, only the lunar laser ranging and the VLBI have been considered. These observational systems offer a means by which a new primary lunar control network can be established, while at the same time the position and orientation parameters of the moon can be improved. Such a primary control network established through the instrumentation considered in this work can be extended through other modern methods (see [78]) together with lunar surface measurements. The current status of the position and orientation parameters of the moon will be discussed briefly below.

Lunar Position.

The problem of finding the position of the center of mass of the moon in a geocentric inertial coordinate system has attracted the attention of numerous scientists since the time of Newton. This has resulted in a few lunar theories, each one being an attempt to analytically solve the differential equations of motion of a perturbed two-body system. A general account of the different methods used in obtaining the moon's motion in space is contained in a book by Brown [11].

The result of any lunar theory is the lunar ephemeris which contains the positions of the moon in tabulated form. The ephemeris in general use today is based on the Hill-Brown theory, with corrections by Eckert [20]. Over the past few years, the Jet Propulsion Laboratory (JPL) has introduced another method of obtaining lunar position. This involves the numerical integration of the equations of motion using digital computers. The

last of the series of numerical lunar ephemeris published by JPL and available on magnetic tape (DE-69), is the LE-16 [77] which is believed to be gravitationally consistent and the most accurate ephemeris available today. Nevertheless the estimated uncertainty in the ephemeris is about 50 meters in range and 100-150 meters in position. The expected precision of laser and VLBI measurements is much higher than that of any lunar ephemeris available, and thus the expectation that the new observations can be used to improve the current status of the lunar theory.

Moon's Orientation.

Traditionally, the orientation of the moon in space is defined by three Eulerian angles between a moon-fixed set of axes and the mean ecliptic coordinate system. The orientation angles are obtained through the solution of the moon's rotational equations of motion. The rotation of the moon follows approximately the empirical Cassini laws, and the deviations of the true motion from that defined by the Cassini laws are the physical librations of the moon.

The physical libration of the moon is traditionally solved by applying heliometer observations to the linearized forms of the equations of motion. Hence the accuracy of these angles depends on the accuracy of the heliometer observations as well as the errors introduced in the process of obtaining the linearized form of the equations of motion. Currently, lunar orientation (i.e. physical libration) is estimated to be accurate to about 20" of arc (about 200-m on lunar surface) [75].

It has been recently proposed that the lunar orientation angles be obtained by direct integration of the original equations of motion [78]. The resulting angles and their rates will depend only on the six initial conditions and the

moon's physical parameters (for example the principal moments of inertia). These parameters can then be corrected in an adjustment using the new types of observations.

Earth's Orientation.

Since the laser and the earth-moon VLBI are observations involving earth stations, the orientation of the earth in space must also be known. The earth's orientation in the past has been calculated through precession, nutation, and polar motion and its accuracy is considered to be within that demanded by current types of astronomical observations.

The use of modern instrumentation of higher accuracy such as the VLBI and laser introduces the possibility of updating our present knowledge about precession nutation and polar motion. In order to do this without having to adjust all the numerous coefficients of the series expressions for nutation and precession, it has been proposed in this work that the orientation of the earth with respect to an inertial system be defined by three Eulerian angles. These angles and their time rates can be obtained by direct numerical integration of earth's equations of motion in its original form. The advantage of this method is that the earth's orientation parameters are reduced to the six initial conditions only.

In this study, both the earth and the moon have been assumed to be rigid bodies, and the equations developed are valid for a rigid earth and moon. The effects of non-rigidity of both celestial bodies on the equations derived are two-fold. Firstly, there is the direct effect of earth tides and lunar tides on the geocentric and selenodetic coordinates of earth and moon stations respectively. Some discussion on this effect has been included in Appendix B. The non-rigidity of the earth and the moon also affects the rotational equations of motion of the two celestial bodies in a rather complicated manner. Investigations on these two effects are continuing.

The presentation of this work is organized as follows: The next chapter presents the equations related to laser measured distances. Partial derivatives necessary for the evaluation of observation equations are fully derived. Most of the equations in this work are expressed in compact forms using either vector or matrix notations. In Chapter 3, equations for the VLBI measurements are derived for three cases (earth-moon baseline, moon-moon baseline, earth-earth baseline). The numerical integration method of calculating the earth's orientation angles is presented in Chapter 4. The equations of motion are derived for the case of a rigid earth without any other assumptions, and preliminary computational results are included.

In the fifth chapter, equations for a least-squares adjustment procedure for the laser and VLBI observations are given, and preliminary computational results using simulated laser observations are presented. The last chapter contains the summary of the work done on this study and the conclusions reached.

## 2. APPLICATION OF LASER RANGING TO SELENODETIC CONTROL

### 2.1 Historical Background

Laser, an acronym for light amplification by stimulated emission of radiation, is the result of an extension of the principles of microwave amplifiers (MASERS) to amplification and generation of electromagnetic radiation in or near the optical region. With the laser, it became possible to generate and control coherent light through the use of electronic transitions in atoms.

The first successful construction of light amplifier (laser) was made by Maiman in 1960 [56]. Since then, numerous modifications and improvements have been made to the laser, and at present, laser has become one of the most important sources or generators of radiation.

The main properties of the laser are directionality, high intensity, coherency, and narrow frequency width (monochromaticity). Radiation generated by laser can either be pulsed or continuous. Because of its properties, the laser has many applications in numerous scientific fields such as in distance measurements, communication, medical and biological research, and in the general sciences [60].

In geodetic science, the laser has been used for the construction of precise electromagnetic distance measuring equipment. Also, laser ranging systems have been built, for the purpose of satellite tracking and obtaining accurate ranges to the moon. Today, a few satellite tracking stations have been equipped with lasers, and there is a lunar laser ranging station in the United States, actively engaged in ranging to the corner reflectors on the moon.

In 1965, Alley at al. [ 1 ] proposed the use of a Q-switched ruby laser in conjunction with a corner reflector located on the moon for making accurate range measurements between the earth and the moon. This proposal was independently advocated by a group of Russian scientists in the same year [48]. A group of

scientists and engineers was subsequently formed with the purpose of investigating and planning the lunar laser ranging experiment (LURE). In 1967, the National Aeronautics and Space Administration officially endorsed the emplacement of a retroreflector on the moon as part of the surface experiments to be performed on some of the Apollo lunar landing missions. The first retroreflector was placed on the moon two years later by the crew of the first landing mission, and the second retroreflector was deposited on the moon by the crew of the Apollo 14 mission. A third retroreflector is expected to be placed on the moon by the Apollo 15 astronauts.

Shortly after the first laser ranging retroreflector (LRRR) was placed on the moon, reflected laser pulses from the LRRR were acquired with the 120-inch telescope at Lick Observatory of the University of California, located at Mt. Hamilton, California [26]. Subsequently, successful acquisition of reflected laser signals were also reported by two other observatories. These are the Lunar Laser Observatory of the Air Force Cambridge Research Laboratories (AFCRL), located in the Catalina Mountains near Tucson, Arizona, and the McDonald Observatory of the University of Texas at Fort Davis, Texas. After the initial signal acquisition phase, only the 107-inch telescope of the McDonald Observatory is now being used for continuing measurements to both retroreflectors on the moon. So far, a range precision of ±0.3m has been achieved [4], and improvement to ±0.15m or better is expected shortly.

The life expectancy of the retroreflector is in excess of ten years [26]. Long-term precise range measurements to retroreflectors on the moon could not only be used to establish a primary control network on the moon, but could also be used for improving our present knowledge of astronomical, geophysical and lunar parameters. In [43], Kaula summarized the various geophysical problems to whose solution lunar laser ranging might contribute. These problems include short- and long-term wobble (of the earth's pole) and variations in the earth's rotation, earth tides, tidal dissipation and plate tectonics. However, for the successful application of laser ranging to these and other problems, stations actively engaged in making continuing measurements to retroreflectors

on the moon need to be established, while more retroreflectors should be placed on the moon.

## 2.2 Basic Operating Principles of Laser Ranging Systems.

The general theory of the generation and amplification of light by stimulated emission is a subject that is well treated in books on lasers and in modern physics textbooks. It is not intended here to give a detailed description of the laser theory , nor a complete technical description of laser ranging systems. Rather, in this section, the basic characteristics of any laser ranging system will be treated briefly for completeness, and in order to make the equations developed in the rest of this chapter clearer.

The main components of a laser ranging system consists of the laser, transmitting and receiving telescopes and a correlator.

The laser component serves as a light source, and generates a laser beam which may be either continuous or pulsed. The pulsed beam is used in the laser ranging systems. Also, all present lunar ranging stations are equipped with Q-switched ruby lasers consisting of an oscillator and three amplifiers.

The laser pulses are transmitted through a telescope which tracks the corner reflector on the moon's surface. A small part of the reflected light is collected by the same telescope (or another telescope serving as a receiving telescope). The same telescope can be used as a transmitter and a receiver partly because the light travel time of about 2.5 seconds between transmitting and receiving allows the mechanical insertion of a mirror which directs the returning photons collected by the telescope into a photomultiplier detector.

The correlator of the ranging system measures the light travel time to the reflector and back. As the laser pulse is fired, a start signal is generated to start the travel time counter, and detection of the return beam generates a stop signal to stop the travel time counter. With current

laser and timing techniques, an uncertainty of ±1 nsec in the absolute measurements of the round trip travel time is possible. This is equivalent to ±15cm in the one way distance.

Other minor features in some of the laser ranging systems include an optical offset guider. This feature is used for pointing to the retroreflector when the retroreflector is on the dark portion of the moon, by optically offsetting the main telescope from a given identifiable lunar feature. When the corner reflector is on the illuminated portion of the moon, the signal-to-noise ratio of the return laser pulse is considerably lower for smaller telescopes due to the background light gathered from the surface of the moon.

The laser ranging retroreflectors were designed to serve as reference points on the lunar surface to be used for point-to-point distance measurements. The two retroreflectors already deposited on the moon by U.S. astronauts are each 46cm-square arrays, consisting of 100 fused silica corner reflectors (3.8cm in diameter), each recessed by 1.9cm in an aluminium panel. The corner reflectors are uncoated and use total internal reflection. Each corner reflector has the unique property that light shining into the corner reflector will be sequentially reflected from its three faces and will come out in a path parallel to the incident light. The third retroreflector array which will be placed on the moon by the crew of the Apollo 15 mission is similar to the previous two arrays, but consists of three times as many corner reflectors.

The design of the LRRR is such that the reflectors will perform under essentially isothermal conditions throughout lunar nights and most of lunar days, thereby ensuring adequate return of signals at all times. The array also allows for the velocity-aberration displacement of up to 1.6km without any significant loss of signal. The most important function of the array, however, is that it eliminates the stretching in time of the return signal which would otherwise be produced by the curvature and irregularity of the moon's surface.

## 2.3 Earth-Moon Distance Equations.

The primary purpose of this chapter is to investigate how lunar laser ranges can be used to establish a selenodetic control network on the moon. The retroreflectors would serve as the "benchmarks", whose coordinates could be determined using the lunar ranges from laser stations on the earth. However, the relative position of a lunar point such as the retroreflector with respect to an earth station depends on a number of physical and geometric parameters of the earth, moon and the earth-moon dynamic system. It is therefore logical to expect a refinement of these parameters in any adjustment of lunar laser distances for the purpose of establishing a selenodetic control system.

Before one can use lunar laser distances for the purpose mentioned above, the mathematical relationship between the measured distances and the following list of parameters have to be established:

(a) The selenodetic coordinates of the lunar retroreflector (M)

(b) The geocentric coordinates of the selenocenter (C)

(c) The geodetic coordinates of the laser station (P)

(d) Parameters of the orientation of a moon-fixed coordinate system with respect to an inertial coordinate system. These are given by the physical libration angles $\sigma$, $\rho$, $\tau$ and the mean orientation angles as defined by the Cassini laws

(e) Parameters defining the orientation of the "average" terrestrial coordinate system with respect to an inertial system. In Classical Astronomy, these parameters are usually given by the precessional elements ($\xi_0$, $\theta_1$, $z$), the nutational parameters ($\Delta\epsilon$, $\Delta\psi$), time (represented by Greenwich Apparent Sidereal Time (GAST)), and the position of the instantaneous true pole with respect to the Conventional Internation Origin (CIO pole), given by $x_p$ and $y_p$ [69].

From the review of existing literature on this subject, one could find that a few mathematical formulas have been derived, which express the earth-moon distance as a function of some of the parameters listed above. For example, Alley and Bender treated the problem of using laser distances to improve our knowledge of geocentric longitude in [2], while Alley et al. offered a simplified model for estimating the expected accuracies with which some geophysical and lunar parameters can be determined in [3]. A relatively more detailed mathematical model was developed by Kokurin et al. for improving certain astronomical parameters in [48] and [49]. Their approach was based on geometric consideration of the earth's and lunar positions at the epoch of observation. In this section, a different approach will be used, based on the consideration of the various coordinate systems involved, which can be transformed to a uniform coordinate system through the use of rotation matrices (composed of functions of the orientation parameters) and translations. The main goal will be to express the coordinates of the lunar point at the observation epoch, in a coordinate system topocentered at the observing station. The earth-moon distance can then be deduced as a function of these topocentric coordinates.

Before going into the development of the laser equations, the various coordinate systems involved and the parameters connected with them will be given brief treatments.

### 2.31 The "Average" Terrestrial Coordinate System.

The average terrestrial coordinate system is defined by the average terrestrial pole of 1900-05 (designated as the Conventional International Origin (CIO)), and an average terrestrial equator [69]. It is the system to which absolute geodetic and reduced astronomic coordinates of any physical point on the earth are referred.

The average terrestrial Cartesian coordinate system (U, V, W) has its origin at the center of mass of the earth, and its axes are fixed with respect to the earth's body. The positive W axis is directed toward the CIO pole, the positive U axis is directed towards the Greenwich Mean Astronomic meridian as defined by the Bureau International de l'Heure (BIH), and the V axis completes a right-handed rectangular system.

In computing geodetic coordinates of points on the earth's surface, a reference figure (the reference ellipsoid) is usually introduced. An absolute geodetic coordinate system can be defined, which is geocentered and has its axes coincident with the U, V, W axes defined above. If the absolute geodetic coordinates of an earth station is given as ($\varphi$, $\lambda$, h), then the Cartesian coordinates can be computed from:

$$\begin{bmatrix} U \\ V \\ W \end{bmatrix} = \begin{bmatrix} (N+h)\cos\varphi\cos\lambda \\ (N+h)\cos\varphi\sin\lambda \\ (N(1-e^2)+h)\sin\varphi \end{bmatrix}$$

where

$N = \dfrac{a}{(1-e^2\sin^2\varphi)^{\frac{1}{2}}}$, the transverse radius of curvature,

$e^2 = 2f - f^2$, the first eccentricity,

and

a, f are parameters of the earth-ellipsoid, denoting the semi-major axis and flattening of the ellipsoid respectively.

2.32 <u>The Selenodetic Coordinate System.</u>

On the moon, we use spherical coordinates - longitude $\ell$, latitude b and radius r - to define the location of a point on the lunar surface. Similar to the geodetic coordinate system, the selenodetic coordinate system is fixed

with respect to the lunar body.

The selenodetic latitude is measured from the lunar equator, defined as the plane passing through the center of mass, perpendicular to the axis of rotation. Latitude is measured in degrees positive toward the north lunar pole and negative toward the south pole.

The prime meridian, $\ell = 0$ is a plane which contains the axis of rotation and the Earth-Moon line when the node and the perigee coincide (i.e. at zero geometric libration). The longitude is measured in degrees, positive in the direction of rotation (eastwards) from 0° to 180° and westwards from 0° to -180°.

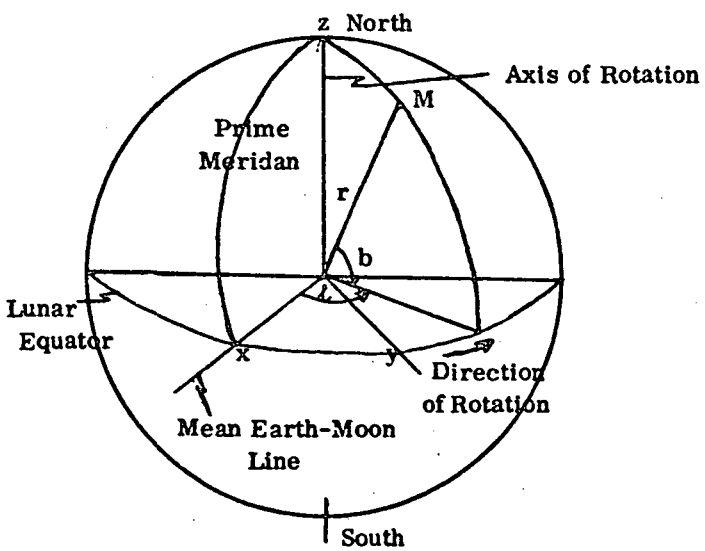


Figure 2.1 The Selenodetic Coordinate System.

The Cartesian selenodetic coordinates of any lunar point (denoted by x, y, z) is related to the spherical coordinates of that point by the equation:

$$\begin{bmatrix} x \\ y \\ z \end{bmatrix} = \begin{bmatrix} r & \cos b & \cos \ell \\ r & \cos b & \sin \ell \\ r & \sin b & \end{bmatrix}.$$

The xyz system is centered at the moon's center of mass. The z axis is coincident with the moon's axis of rotation. the x axis coincides with the mean Earth-Moon line (sometimes referred to as "first radius") and the y axis is perpendicular to both x and z axes and completes a right-handed rectangular system.

The selenodetic coordinate system is related to the ecliptic system by the three Eulerian angles, which will be treated in more detail in section 2.34.

2.33 <u>The Geocentric Coordinates of the Selenocenter.</u>

In developing the equations for measured lunar laser distances, the coordinates of the lunar center of mass with respect to the geocenter are needed. These coordinates are obtainable from any lunar ephemeris which gives the coordinates of the moon, relative to the earth, as a function of time. All ephemerides in present use are the result of a particular lunar theory which attempts to apply the law of gravity to the motion of the moon.

The lunar theory is a subject that has been discussed and treated by various scientists from the time of Newton to the present day. Although different authors employ different methods in arriving at their lunar theory, they all start from the differential equations of a perturbed two-body system. The main problem is to integrate the equations of motion of a perturbed two-body system given by

$$\ddot{\vec{r}} + G(M_D + M_L)\frac{\vec{r}}{r^3} = \frac{\partial R}{\partial r}$$

where:

$\vec{r}$ is the earth-moon vector

G is the gravitational constant

$M_{\oplus}$, $M_{☽}$ are the earth's and moon's mass respectively

and

R is the "disturbing function". If there were no perturbing bodies, R would be zero and the resulting motion would be elliptic. If the sun acts as the only perturbing body, then R is given by

$$R = GM_{\odot} \left( \frac{1}{\rho} - \frac{\vec{r} \cdot \vec{r}'}{r'^3} \right)$$

where

$\rho$ is the moon-sun distance

$r'$ is the earth-sun distance

$M_{\odot}$ is the mass of the sun.

The disturbing function generally used in any of the lunar theories is modified to account for the presence of other perturbing bodies, i.e., the planets.

The analytical integration of the equations of motion for three or more bodies in a closed form is not generally obtainable. Consequently, there are two basic ways in which the lunar ephemeris is obtained:

In the first method, the elements of the equations of motion are expanded as Fourier series, yielding a sequence of terms that are analytically integrated, and resulting in lengthy analytical expressions for the lunar ephemeris. In the alternate method the original unexpanded equations of motion are numerically integrated. The analytical method has been used by classical lunar theorists and its main disadvantage is that the expression for the lunar ephemeris is truncated. The number of terms in the final expression depends on the number

of bodies and types of perturbations treated as well as on the accuracy of the high-order terms required. The present most widely used lunar ephemeris - which is the result of the Hill-Brown theory [12] with modifications by Eckert [20] - uses the Fourier series development method.

The numerically integrated lunar ephemeris, which was initiated by the Jet Propulsion Laboratory (JPL), is made possible by the advent of digital computers and is noted for its gravitational consistency. All the planetary effects are well taken care of and any differences between the ephemeris and the true coordinates of the moon are a direct result of inadequacies in the theory itself. The numerical ephemeris is also clearly superior to the analytically obtained ephemeris in terms of accuracy as demonstrated by the JPL [72]. Consequently, the position of the center of the moon, to which corrections are to be computed and which should be used in the prediction equations for laser distances, should be that from the latest of the numerical lunar ephemeris - LE16 which is contained in the JPL Development Ephemeris Tape 69 (DE-69) [77].

2.34 Parameters of the Orientation of the Moon.

The laser distances, like any other earth-moon observation, is a function of the parameters that define the orientation of the moon. The orientation of the moon is related to the moon's rotation on its axis in the same way as the lunar ephemeris is related to the orbital motion.

The moon's rotation follows, to a high degree of approximation, the empirical Cassini laws. The physical deviation of the moon's motion from the described by the Cassini laws is known as the physical libration of the moon.

The moon's orientation in space is defined by the three Eulerian angles, which define the orientation of a moon-fixed coordinate system with respect

to an inertial system. Traditionally, the inertial system chosen is the mean ecliptic coordinate system of date which is not truly inertial, but has secular changes due to planetary precession.

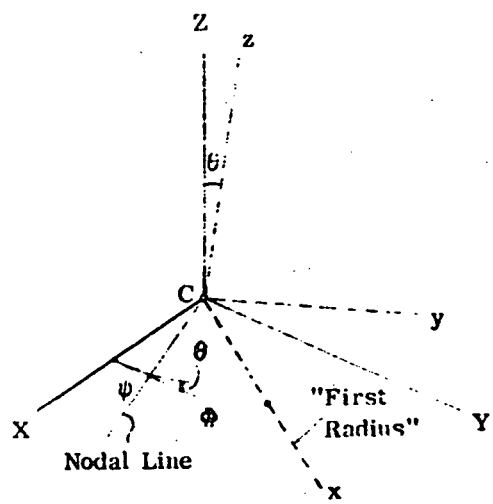


Figure 2.2. The Moon's Eulerian Angles.

Figure 2.2 shows the xyz coordinate system which is fixed to the body of the moon, and the XYZ system representing the mean ecliptic system of date. The Eulerian angles are denoted by $\theta$, $\psi$ and $\Phi$.

The Eulerian angles are composed of two parts, namely the mean angles (which are the mathematical expressions of the Cassini laws) and the perturbations (given by the physical libration angles). The angles are given by the following expressions:

$$\Phi = L + \pi - \Omega + \tau - \sigma$$

$$\psi = \Omega + \sigma$$

$$\theta = I + \rho$$

where

$L$ is the mean longitude of the moon in its orbit

$\Omega$ is the longitude of the mean ascending node of the moon's orbit

$I$ is the mean inclination of the lunar equator to the ecliptic

$\tau$ is the physical libration in longitude

$\sigma$ is the physical libration in node

and

$\rho$ is the physical libration in inclination.

The mean angles L and $\Omega$ are obtainable as explicit functions of time from the following expressions taken from [65].

$$L = 270^\circ.4341639 + 481{,}267^\circ.8831117\,T - 0^\circ.1133333 \times 10^{-2}\,T^2 + 0^\circ.1888889 \times 10^{-5}\,T^3$$

$$\Omega = 259^\circ.1832750 - 1{,}934^\circ.1420083\,T + 0^\circ.2077778 \times 10^{-2}\,T^2 + 0^\circ.2222222 \times 10^{-5}\,T^3$$

where T is the time in Julian centuries of 36525.0 ephemeris days from January 0.5 1900 (J.D. = 2415020.0). The mean inclination I is given by:

$$I = 5521''.5.$$

The physical libration angles are expressed as harmonic series having fixed coefficients and arguments which are expressed as functions of time:

$$\tau = \sum_i A_i \cos(a_i t + b_i)$$

with similar expressions for $\sigma$ and $\rho$.

The Eulerian angles which define the orientation of a set of moon-fixed axes with respect to an inertial system are obtained through the solution of the equations of motion for the rotation of the moon. Classically, the differential equations (represented by the Euler's dynamical equations) are

analytically solved by series expansion, and actual observations (usually heliometric observations) are used to solve for the coefficients of the harmonic expressions. Recently, the numerical integration of the differential equations of motion in their original form has been proposed, [78]. By using this method, the Eulerian angles would be obtained directly by integration without splitting the angles into two parts - the mean angles and the physical libration angles. Inaccuracies in the orientation angles obtained by numerical integration can only result from inadequacies in the lunar rotational theory, and not in the type of linearization and approximations that are essential for solving analytically the differential equations of motion.

2.35 The Parameters of Earth's Orientation.

In observations made from an earth point to a moon point, the relative orientation of an earth-fixed coordinate system with respect to a moon-fixed coordinate system is needed. The coordinates of the earth station are expressed in an earth-fixed system while the moon station coordinates are in a moon-fixed system. In practice, the problem of determining the relative orientation of the moon with respect to the earth at any epoch is solved by finding the orientations of the earth and the moon with respect to an inertial system.

The orientation of the earth in an inertial coordinate system is also needed in geodetic astronomy, where observations are made to celestial objects, whose positions are given in a celestial coordinate system of a standard epoch. The precessional elements ($\zeta_0$ $\vartheta_1$ and $z_1$) define the orientation of the mean celestial equator and equinox of date with respect to the mean equator and equinox of an initial epoch. The orientation of the true equatorial coordinate system to the mean equatorial system is also defined by the nutation in longitude and obliquity ($\Delta\psi$, $\Delta\epsilon$).

Lastly, the orientation of the average terrestrial coordinate system with respect to the true celestial equatorial system is given by the two coordinates of the true pole from the average (CIO) pole, together with the Greenwich hour angle of the true vernal equinox (Greenwich Apparent Sidereal Time).

The expressions for precession and nutation elements are obtained from the analytical solution of the differential equations of motion representing the rotation of the earth on its axis. The nutation series that are currently in use in astronomical work are those obtained by Woolard [94]. The accuracy of the precessional and nutational elements obtained through the use of current expressions are consistent with the accuracies of present day observational systems. However, in using observations made by future systems which are expected to be more accurate, there is a possibility of improving the accuracies of the elements of precession and nutation. The constants for the expressions that give $\zeta_0$, $\theta_1$ and $z_1$ as well as those for the nutation series can be regarded as parameters to be adjusted in addition to other parameters of interest.

Another way in which the orientation of an earth-fixed coordinate system can be obtained from the earth's rotational theory is proposed in this work. Essentially, this method considers the orientation of the terrestrial coordinate system with respect to a fixed mean ecliptic system as made up of three Eulerian angles. The three angles and their time derivatives can be obtained from the three second order differential equations of motion for the rotation of the earth in its complete form by numerical integration process. This topic is being given a complete treatment in Chapter 4.

Figure 2.3 shows the relationship between the average terrestrial coordinate system (UVW) and a mean ecliptic coordinate system (XYZ) of a standard epoch. The earth's Eulerian angles are denoted by $\theta_\varepsilon$, $\psi_\varepsilon$, and $\Phi_\varepsilon$.

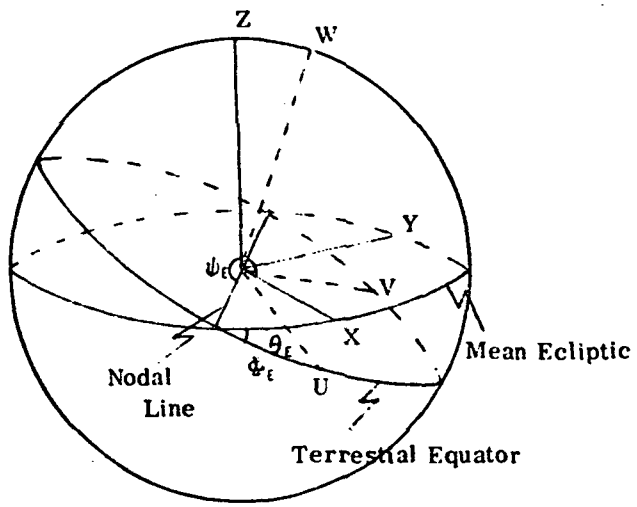


Figure 2.3 The Earth's Orientation Angles.

The advantage of the numerical integration method of obtaining the orientation of the earth over the classical analytic method is the fact that the angles obtained depend only on the initial conditions represented by six constants. Consequently, only six parameters need be added to the parameters list if the values of precession and nutation elements obtained from existing expressions are to be taken as variable quantities.

2.36 Computation of Distances between Points on the Earth and on the Moon.

In Figure 2.4, P is a station on the earth making distance measurements to a moon point M. The geodetic coordinates of P are given by $\varphi$, $\lambda$ and h. The Cartesian coordinates of P in the UVW system are given by

$$\begin{bmatrix} U \\ V \\ W \end{bmatrix} = \begin{bmatrix} (N + h) \cos\varphi \cos\lambda \\ (N + h) \cos\varphi \sin\lambda \\ (N(1 - e^2) + h) \sin\varphi \end{bmatrix} . \tag{2.1}$$

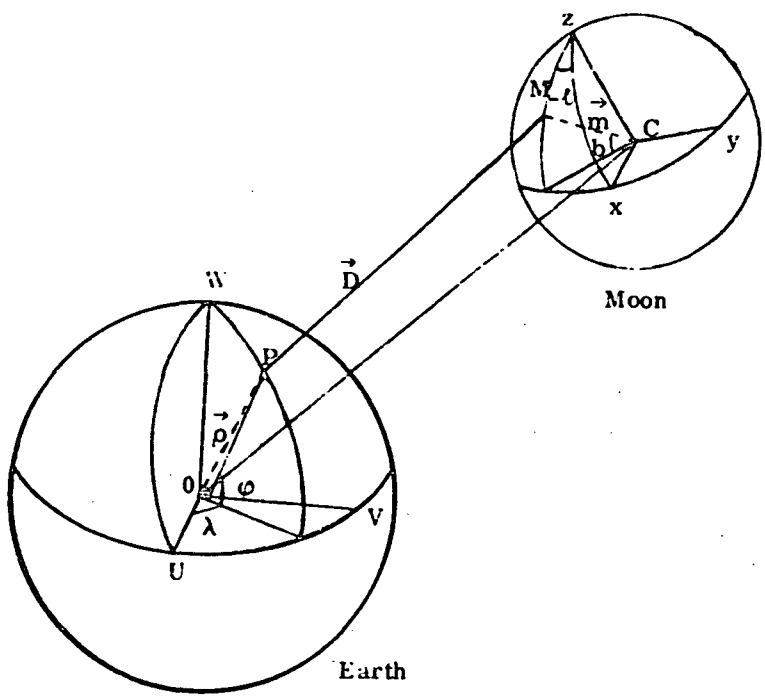


Figure 2.4. Laser Station (P) and Retroreflector (M)

Similarly, we let $\ell$, b, r be the selenodetic coordinates of point M. Then the Cartesian coordinates of M in the xyz system are given by

$$\begin{bmatrix} x_M \\ y_M \\ z_M \end{bmatrix} = \begin{bmatrix} r \cos b \cos \ell \\ r \cos b \sin \ell \\ r \sin b \end{bmatrix} . \tag{2.2}$$

The geocentric Cartesian coordinates of the lunar center $X_c$, $Y_c$, and $Z_c$ at the epoch of observation is taken from any lunar ephemeris. In the derivations to be made here, it will be assumed that the $X_{cQ}$, $Y_{cQ}$, $Z_{cQ}$ coordinates of the selenocenter is obtained from the latest numerically integrated lunar ephemeris - the LE16. In this ephemeris, the coordinates are expressed in the 1950.0 mean equatorial system.

The coordinates of the laser station P can be expressed in the 1950.0 mean ecliptic coordinate system by applying a series of orthogonal transformations [69]:

$$\begin{bmatrix} X_P \\ Y_P \\ Z_P \end{bmatrix}_{ecl.\ 1950.0} = R_1(\epsilon_0)\, P^T N^T S^T \begin{bmatrix} U \\ V \\ W \end{bmatrix} \tag{2.3}$$

where P, N, S are 3 x 3 orthogonal transformation matrices as follows

$$\begin{aligned} P &= R_3(-z_1)\, R_2(\theta_1)\, R_3(-\zeta_0) \\ N &= R_1(-\epsilon - \Delta\epsilon)\, R_3(-\Delta\psi)\, R_1(\epsilon) \\ S &= R_2(-x_P)\, R_1(-y_P)\, R_3(\mathrm{GAST}). \end{aligned} \tag{2.4}$$

The conventional orthogonal rotation matrices $R_1(\alpha)$, $R_2(\alpha)$ and $R_3(\alpha)$ are often used (as in this case) to rotate a general system by angle $\alpha$ about the axes X, Y, Z respectively. These matrices, consistent with a right handed coordinate system are given by:

$$R_1(\alpha) = \begin{bmatrix} 1 & 0 & 0 \\ 0 & \cos\alpha & \sin\alpha \\ 0 & -\sin\alpha & \cos\alpha \end{bmatrix}$$

$$R_2(\alpha) = \begin{bmatrix} \cos\alpha & 0 & -\sin\alpha \\ 0 & 1 & 0 \\ \sin\alpha & 0 & \cos\alpha \end{bmatrix}$$

$$R_3(\alpha) = \begin{bmatrix} \cos\alpha & \sin\alpha & 0 \\ -\sin\alpha & \cos\alpha & 0 \\ 0 & 0 & 1 \end{bmatrix}.$$

The parameters $z_1$, $\theta_1$ and $\zeta_0$ are the precession elements for the period between 1950.0 and the epoch of observation; $\Delta\epsilon$ and $\Delta\psi$ are nutation in obliquity and longitude respectively at the epoch of observation; $\epsilon$ is the mean obliquity of the equator of date; GAST represents the Greenwich Apparent Sidereal Time and $x_p$, $y_p$ are the polar motion parameters. $\epsilon_0$ is the mean obliquity of the equator at the epoch 1950.0. Equation 2.3 could be equivalently written as

$$\begin{bmatrix} X_p \\ Y_p \\ Z_p \end{bmatrix}_{ecl.1950.0} = R_1(\epsilon_0)R_3(\zeta_0)R_2(-\theta_1)R_3(z)R_1(-\epsilon)R_3(\Delta\psi)R_1(\epsilon+\Delta\epsilon)R_3(-GAST)R_1(y_p)R_2(x_p)\begin{bmatrix} U \\ V \\ W \end{bmatrix}. \tag{2.5}$$

In a similar manner, the coordinates of lunar retroreflector (M) can be expressed in the 1950.0 mean ecliptic system as follows:

$$\begin{bmatrix} X_M \\ Y_M \\ Z_M \end{bmatrix}_{ecl.1950.0} = R_1(\epsilon_0)P^T R_1(-\epsilon)R_3(-\psi)R_1(\theta)R_3(-\Phi)\begin{bmatrix} x_M \\ y_M \\ z_M \end{bmatrix}. \tag{2.6}$$

In equation (2.6), $\psi$, $\theta$ and $\Phi$ are the Eulerian angles which define the orientation of the selenodetic (x, y, z) coordinate system with respect to the mean ecliptic system of date. The three angles have been treated in Section 2.34.

If

$$T_1 = R_3(\Phi)\, R_1(-\theta)\, R_3(\psi)$$

then equation (2.6) becomes

$$\begin{bmatrix} X_M \\ Y_M \\ Z_M \end{bmatrix}_{Ec1.1950.0} = R_1(\epsilon_0) P^T R_1(-\epsilon) T_1^T \begin{bmatrix} x_M \\ y_M \\ z_M \end{bmatrix} . \qquad (2.7)$$

Since the geocentric mean equatorial (of 1950.0) coordinates of the lunar center as obtained from the LE-16 or any other lunar ephemeris are given by

$$\begin{bmatrix} X_{CQ} \\ Y_{CQ} \\ Z_{CQ} \end{bmatrix},$$

the geocentric coordinates of the selenocenter, expressed in the mean ecliptic 1950.0 system are given by

$$\begin{bmatrix} X_C \\ Y_C \\ Z_C \end{bmatrix}_{Ec1.1950.0} = R_1(\epsilon_0) \begin{bmatrix} X_{CQ} \\ Y_{CQ} \\ Z_{CQ} \end{bmatrix} \qquad (2.8)$$

where $\epsilon_0$ as defined earlier, is the mean obliquity of the equator at 1950.0.

Thus, the topocentric coordinates of the lunar reflector (M), with the laser station (P) at center are obtained, by considering Figure 2.5, as

$$\begin{bmatrix} X_M \\ Y_M \\ Z_M \end{bmatrix}_{topoc.} = \begin{bmatrix} X_C \\ Y_C \\ Z_C \end{bmatrix}_{Ecl.1950.0} + \begin{bmatrix} X_M \\ Y_M \\ Z_M \end{bmatrix}_{Ecl.1950.0} - \begin{bmatrix} X_P \\ Y_P \\ Z_P \end{bmatrix}_{Ecl.1950.0} . \qquad (2.9)$$

The topocentric coordinates of the moon point obtained by equation (2.9) are expressed in the mean ecliptic coordinate system of 1950.0. It should be noted, however, that since distances between two points are independent of the coordinate system, the topocentric coordinates could have been expressed in any coordinate system. The 1950.0 mean ecliptic coordinate system has been chosen because it is a near-inertial coordinate system which will also be used in the case of VLBI observations involving directions.

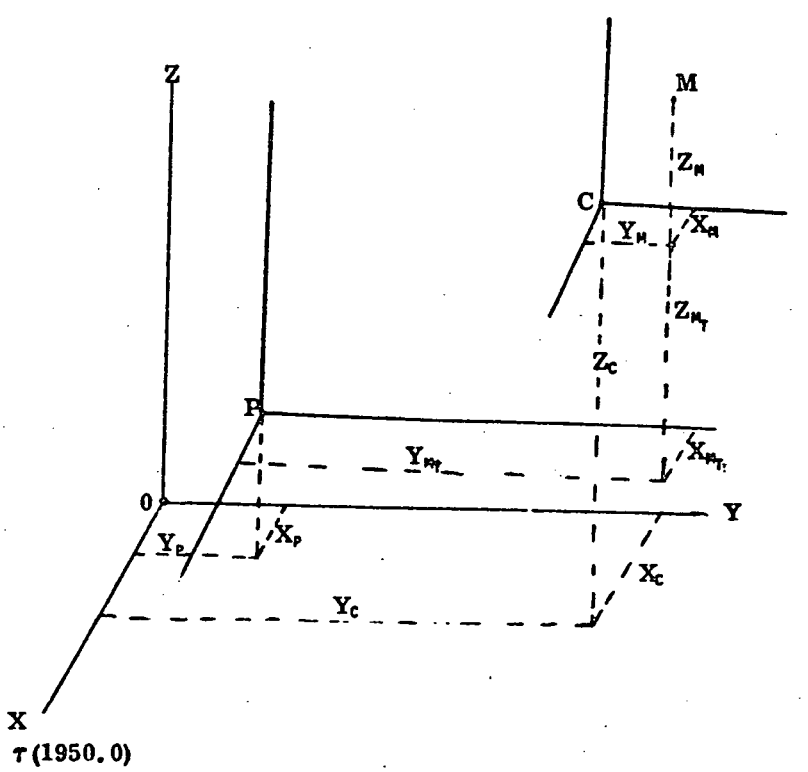


Figure 2.5. Topocentric Mean Ecliptic (1950.0) Coordinates of Retroreflector (M).

Into equation (2.9), we substitute expressions for

$$\begin{bmatrix} X_c \\ Y_c \\ Z_c \end{bmatrix}, \quad \begin{bmatrix} X_M \\ Y_M \\ Z_M \end{bmatrix} \quad \text{and} \quad \begin{bmatrix} X_p \\ Y_p \\ Z_p \end{bmatrix}$$

to obtain

$$\begin{bmatrix} X_M \\ Y_M \\ Z_M \end{bmatrix}_{topoc.} = R_1(\epsilon_0) \begin{bmatrix} X_{CQ} \\ Y_{CQ} \\ Z_{CQ} \end{bmatrix} + R_1(\epsilon_0) P^T R_1(-\epsilon) T_1^T \begin{bmatrix} x_M \\ y_M \\ z_M \end{bmatrix} - R_1(\epsilon_0) P^T N^T S^T \begin{bmatrix} U \\ V \\ W \end{bmatrix} \tag{2.10a}$$

which is fully expressed as

$$\begin{bmatrix} X_M \\ Y_M \\ Z_M \end{bmatrix}_{topoc} + R_1(\epsilon_0) \begin{bmatrix} X_{CQ} \\ Y_{CQ} \\ Z_{CQ} \end{bmatrix} + R_1(\epsilon_0) R_3(\zeta_0) R_2(-\theta_1) R_3(z_1) R_1(-\epsilon) R_3(-\psi) R_1(\theta) R_3(-\Phi) \begin{bmatrix} x_M \\ y_M \\ z_M \end{bmatrix}$$

$$- R_1(\epsilon_0) R_3(\zeta_0) R_2(-\theta_1) R_3(z_1) R_1(-\epsilon) R_3(\Delta\psi) R_1(\epsilon + \Delta\epsilon) R_3(-GAST) R_1(y_p) R_2(x_p) \begin{bmatrix} U \\ V \\ W \end{bmatrix} \tag{2.10b}$$

or,

$$\begin{bmatrix} X_M \\ Y_M \\ Z_M \end{bmatrix}_{topoc.} = R_1(\epsilon_0)\left\{\begin{bmatrix} X_{CQ} \\ Y_{CQ} \\ Z_{CQ} \end{bmatrix} + R_3(\zeta_0)R_3(-\theta_1)R_3(z_1)R_1(-\epsilon)\left(R_3(-\psi)R_1(\theta)R_3(-\varphi)\begin{bmatrix} x_M \\ y_M \\ z_M \end{bmatrix}\right.\right.$$

$$\left.\left. - R_3(\Delta\psi)R_1(\epsilon+\Delta\epsilon)R_3(-GAST)R_1(x_p)R_2(y_p)\begin{bmatrix} U \\ V \\ W \end{bmatrix}\right)\right\}. \qquad (2.10c)$$

In vector form, equation (2.10) can be expressed as

$$\vec{X}_T = M_1\vec{X}_{CQ} + M_2\vec{X}_M - M_3\vec{X}_P \qquad (2.11)$$

where

$\vec{X}$ - is position vector, the subscripts indicating

T - moon point in a topocentric coordinate system

CQ - geocentric equatorial coordinates of moon's center of mass

M - moon point in selenodetic coordinate system

P - earth observing station in average terrestrial coordinate system

$M_1$, $M_2$, $M_3$ are orthogonal transformation matrices for expressing each position vector in a coordinate system parallel to that of the 1950.0 mean ecliptic system.

The rotation matrices in equation (2.5) were used in order to transform from the average terrestrial system to the mean ecliptic system. It has been explained in Section 2.35 that the orientation of the average terrestrial system to the 1950.0 mean ecliptic system could be defined by a set of three Eulerian angles - $\theta_E$, $\psi_E$, and $\varphi_E$. If the three orientation angles are available, then equation (2.5) can be written as

$$\begin{bmatrix} X_P \\ Y_P \\ Z_P \end{bmatrix}_{\text{ecl. 1950.0}} = T_a^T \begin{bmatrix} U \\ V \\ W \end{bmatrix} = R_3(-\psi_\varepsilon)\, R_1(\theta_\varepsilon)\, R_3(-\Phi_\varepsilon) \begin{bmatrix} U \\ V \\ W \end{bmatrix} \tag{2.12}$$

if

$$T_a = R_3(\Phi_\varepsilon)\, R_1(-\theta_\varepsilon)\, R_3(\psi_\varepsilon) \tag{2.13}$$

In a similar manner, the numerically obtained Eulerian angles for the moon's orientation (see Section 2.34) could define the orientation of the selenodetic coordinate system to an inertial system such as the mean ecliptic system of 1950.0. Therefore equation (2.7) could also be written as

$$\begin{bmatrix} X_M \\ Y_M \\ Z_M \end{bmatrix}_{\text{ecl. 1950.0}} = T_1^T \begin{bmatrix} x_M \\ y_M \\ z_M \end{bmatrix} = R_3(-\psi_M)\, R_1(\theta_M)\, R_3(-\Phi_M) \begin{bmatrix} x_M \\ y_M \\ z_M \end{bmatrix} \tag{2.14}$$

where $\psi_M$, $\theta_M$, $\Phi_M$ are the numerically integrated moon's Eulerian angles defining the orientation of the selenodetic system with respect to an inertial system (in this case, the 1950.0 mean ecliptic system).

As an alternate expression to equations (2.10), equation (2.9) could be expressed as follows:

$$\begin{bmatrix} X_M \\ Y_M \\ Z_M \end{bmatrix}_{\text{topoc.}} = R_1(\epsilon_0) \begin{bmatrix} X_{CQ} \\ Y_{CQ} \\ Z_{CQ} \end{bmatrix} + R_3(-\psi_M)\, R_1(\theta_M)\, R_3(-\Phi_M) \begin{bmatrix} x_M \\ y_M \\ z_M \end{bmatrix}$$

$$- R_3(-\psi_\varepsilon)\, R_1(\theta_\varepsilon)\, R_3(-\Phi_\varepsilon) \begin{bmatrix} U \\ V \\ W \end{bmatrix}. \tag{2.15}$$

Equations (2.10) express the topocentric coordinates of a moon point at any epoch in terms of astronomical parameters in current usage in most astronomical work. On the other hand, equation (2.15) gives the same topocentric coordinates of the moon, but expressed in terms of Eulerian angles defining the orientation of the earth-fixed and the moon-fixed coordinate systems with respect to the 1950.0 mean ecliptic coordinate system.

The distance from the earth point to the moon point is a function of the topocentric coordinates of the moon point as follows:

$$D = (X_{MT}^2 + Y_{MT}^2 + Z_{MT}^2)^{\frac{1}{2}} \qquad (2.16)$$

where D is the distance and the $X_{MT}$, $Y_{MT}$, $Z_{MT}$ are topocentric coordinates of the lunar point at the epoch of observation given by any of equations (2.10) or equivalently, equation (2.15).

## 2.4 Formulation of Observation Equations for Earth-Moon Distances

In Section (2.36) a set of equations have been derived, by which the distance between any point on the earth and another point on the moon can be predicted for any epoch of observation. In general, the predicted and the observed values of the distance will not be identical due to many factors. These include the fact that some or all of the parameters used in predicting the distance may be inaccurately known, and the fact that the observed distances themselves may suffer from systematic errors, in addition to the common accidental observational errors.

In this section, the effect of small variations in the parameters on the calculated distance will be derived, which together with the differences in observed and calculated values, could be used to correct initial values of the parameters. It is assumed here that the measured distances have been

corrected for all instrumental and other systematic errors (such as atmospheric refraction). Consequently, no systematic error models are introduced into the observation equations. Rather, the equations can serve as a general model which can be used to adjust any type of distance observations from an earth point to a moon point if such observed ranges are freed from systematic errors.

From equation (2.16), the distance equation can be written as

$$D = f_1([X_T]) \tag{2.17}$$

where D is distance and $[X_T]$ is column vector of topocentric coordinates of the lunar point.

Also, from equation (2.10), if GAST = $\Theta$

$$[X_T] = f_2(\epsilon_0, \epsilon, \zeta_0, \theta_1, z_1, \Delta\psi, \Delta\epsilon, \Theta, x_p, y_p, \psi, \vartheta, \Phi, U, V, W, x_M, y_M, z_M, X_{CQ}, Y_{CQ}, Z_{CQ}) \tag{2.18}$$

and if the parameters listed in equation (2.18) are represented by a column vector $[x]$, then

$$[X_T] = f_2[x]. \tag{2.19}$$

The mathematical structure represented by equation (2.17) with equation (2.19) is of the type

$$L_a = F(X_a) \tag{2.20}$$

where $L_a$ is a vector of the adjusted values of observed quantities, and $X_a$ is the vector of adjusted values of parameters. The Taylor series linearization of (2.20) leads to the observation equations [94]

$$V = AX + L \tag{2.21}$$

where

$$A = \frac{\partial L_a}{\partial X_a}$$

$$X = X_a - X_0 \qquad (2.22)$$

$$L = L_0 - L_b$$

$$L_0 = F(X_0)$$

and

$X_0$ is the vector of initial values of parameters

$L_b$ is the vector of observed values

$V$ is the vector of residuals.

In this case, the design matrix [A] is given by:

$$A = \frac{\partial D}{\partial x} = \frac{\partial D}{\partial X_T}\frac{\partial X_T}{\partial x} \qquad (2.23)$$

where D, $x$, $X_T$ are all column vectors. For each measured distance $d_i$, the ith row of matrix A is given by

$$\frac{\partial d_i}{\partial x} = \frac{\partial d_i}{\partial X_T}\frac{\partial X_T}{\partial x}. \qquad (2.24)$$

From equations (2.16) and (2.17),

$$f_i(X_T) = (X_{M_T}^2 + Y_{M_T}^2 + Z_{M_T}^2)^{\frac{1}{2}} = D.$$

Therefore

$$\frac{\partial d_i}{\partial X_T^i} = \frac{1}{d_i}\left[X_{M_T}^i \;\vdots\; Y_{M_T}^i \;\vdots\; Z_{M_T}^i\right] \qquad (2.25)$$

and

$$\frac{\partial D}{\partial X_T} = \begin{bmatrix} \frac{1}{d_1}\left[X_{M_T}^1 \quad Y_{M_T}^1 \quad Z_{M_T}^1\right] \\ \vdots \\ \frac{1}{d_n}\left[X_{M_T}^n \quad Y_{M_T}^n \quad Z_{M_T}^n\right] \end{bmatrix} \qquad (2.26)$$

where n is the number of observations.

In order to find $\frac{\partial X_T}{\partial \chi}$, it can be seen that the function $f_2$ in equation (2.18) includes rotation matrices, which also have to be differentiated. Differentials of rotation matrices are easily obtained through the use of special skew matrices (hereafter referred to as Lucas matrices), whose properties are such that when the skew matrix is either pre-multiplied or post-multiplied by a rotation matrix, the resulting matrix is the partial derivative of the original rotation matrix [58].

Define:

$$L_1 = \begin{bmatrix} 0 & 0 & 0 \\ 0 & 0 & 1 \\ 0 & -1 & 0 \end{bmatrix},$$

$$L_2 = \begin{bmatrix} 0 & 0 & -1 \\ 0 & 0 & 0 \\ 1 & 0 & 0 \end{bmatrix},$$

$$L_3 = \begin{bmatrix} 0 & 1 & 0 \\ -1 & 0 & 0 \\ 0 & 0 & 0 \end{bmatrix}.$$

Then as an example, if $R_n(\alpha)$ represents a $3 \times 3$ rotation matrix, $(n = 1, 2, 3)$,

$$\frac{\partial R_n(\alpha)}{\partial \alpha} = L_n \cdot R_n(\alpha) = R_n(\alpha) \cdot L_n$$

$$\frac{\partial R_n(-\alpha)}{\partial \alpha} = -L_n \cdot R(\alpha) \tag{2.27}$$

Also, if

$$M = R_n(\alpha)\, R_m(\beta)\, R_j(\gamma),$$

then

$$\frac{\partial M}{\partial \alpha} = L_n R_n(\alpha) R_m(\beta) R_j(\gamma) = L_n M$$

$$\frac{\partial M}{\partial \beta} = R_n(\alpha) L_m R_m(\beta) R_j(\gamma)$$

and

$$\frac{\partial M}{\partial \gamma} = R_n(\alpha) R_m(\beta) R_j(\gamma) L_j = M L_j. \qquad (2.28)$$

The partials $\frac{\partial X_T}{\partial \varkappa}$ will now be derived from equation (2.10), for each element of the $\varkappa$ vector individually:

(1) For the mean obliquity of the equator at the epoch 1950.0, ($\epsilon_0$):

$$\frac{\partial X_T}{\partial \epsilon_0} = \frac{\partial \begin{bmatrix} X_M \\ Y_M \\ Z_M \end{bmatrix}_{\text{epoc.}}}{\partial \epsilon_0} = L_1 R_1(\epsilon_0) \left( \begin{bmatrix} X_{CQ} \\ Y_{CQ} \\ Z_{CQ} \end{bmatrix} + P^T T_1^T \begin{bmatrix} x_M \\ y_M \\ z_M \end{bmatrix} - P^T N^T S^T \begin{bmatrix} U \\ V \\ W \end{bmatrix} \right)$$

or

$$\frac{\partial X_T}{\partial \epsilon_0} = L_1 X_T = L_1 \begin{bmatrix} X_M \\ Y_M \\ Z_M \end{bmatrix}_{\text{epoc.}} = \begin{bmatrix} 0 \\ Z_M \\ -Y_M \end{bmatrix}. \qquad (2.29)$$

(2) For the mean obliquity of the equator of date ($\epsilon$):

$$\frac{\partial X_T}{\partial \epsilon} = R_1(\epsilon_0)\left(-P^T L_1 \left\{ R_1(-\epsilon) T_1^T \begin{bmatrix} x_M \\ y_M \\ z_M \end{bmatrix} - N^T S^T \begin{bmatrix} U \\ V \\ W \end{bmatrix} \right\} - P^T N^T L_1 S^T \begin{bmatrix} U \\ V \\ W \end{bmatrix}\right) \quad (2.30)$$

(3) For the precessional elements $\zeta_0$, $\theta_1$, and $z_1$:

$$\frac{\partial X_T}{\partial \zeta_0} = R_1(\epsilon_0) L_3 P^T \left( R_1(-\epsilon) T_1^T \begin{bmatrix} x_M \\ y_M \\ z_M \end{bmatrix} - N^T S^T \begin{bmatrix} U \\ V \\ W \end{bmatrix} \right) \quad (2.31)$$

$$\frac{\partial X_T}{\partial \theta_1} = -R_1(\epsilon_0) R_3(\zeta_0) L_2 R_2(-\theta_1) R_3(z_1) \left( R_1(-\epsilon) T_1^T \begin{bmatrix} x_M \\ y_M \\ z_M \end{bmatrix} - N^T S^T \begin{bmatrix} U \\ V \\ W \end{bmatrix} \right) \quad (2.32)$$

$$\frac{\partial X_T}{\partial z_1} = R_1(\epsilon_0) P^T L_3 \left( R_1(-\epsilon) T_1^T \begin{bmatrix} x_M \\ y_M \\ z_M \end{bmatrix} - N^T S^T \begin{bmatrix} U \\ V \\ W \end{bmatrix} \right). \quad (2.33)$$

(4) For the nutation in obliquity and longitude, $\Delta\epsilon$ and $\Delta\psi$:

$$\frac{\partial X_T}{\partial \Delta\epsilon} = -R_1(\epsilon_0) P^T N^T L_1 S^T \begin{bmatrix} U \\ V \\ W \end{bmatrix} \quad (2.34)$$

and

$$\frac{\partial X_T}{\partial \Delta\psi} = -R_1(\epsilon_0) P^T R_1(-\epsilon) L_3 R_3(\Delta\psi) R_1(\epsilon + \Delta\epsilon) S^T \begin{bmatrix} U \\ V \\ W \end{bmatrix}. \quad (2.35)$$

(5) For the moon's Eulerian angles, $\theta$, $\psi$, and $\Phi$:

$$\frac{\partial X_T}{\partial \theta} = R_1(\epsilon_0)\, P^T R_1(-\epsilon) R_3(-\psi) L_1 R_1(\theta) R_3(-\Phi) \begin{bmatrix} x_M \\ y_M \\ z_M \end{bmatrix} \tag{2.36}$$

$$\frac{\partial X_T}{\partial \psi} = -R_1(\epsilon_0) P^T R_1(-\epsilon)\; L_3\; T_1^T \begin{bmatrix} x_M \\ y_M \\ z_M \end{bmatrix} \tag{2.37}$$

and

$$\frac{\partial X_T}{\partial \Phi} = -R_1(\epsilon_0) P^T R_1(-\epsilon)\, T_1^T\, L_3 \begin{bmatrix} x_M \\ y_M \\ z_M \end{bmatrix}. \tag{2.38}$$

(6) For the coordinates of the true pole $x_p$, $y_p$ and the Greenwich Apparent Sidereal Time $\Theta$:

$$\frac{\partial X_T}{\partial x_p} = -R_1(\epsilon_0) P^T N^T S^T L_2 \begin{bmatrix} U \\ V \\ W \end{bmatrix} \tag{2.39}$$

$$\frac{\partial X_T}{\partial y_p} = -R_1(\epsilon_0) P^T N^T R_3(-\Theta) L_1 R_1(y_p) R_2(x_p) \begin{bmatrix} U \\ V \\ W \end{bmatrix} \tag{2.40}$$

$$\frac{\partial X_T}{\partial \Theta} = R_1(\epsilon_0) P^T N^T L_3 S^T \begin{bmatrix} U \\ V \\ W \end{bmatrix}. \tag{2.41}$$

(7) In order to find the partials with respect to the coordinates (of earth point, moon point and moon's center), let the column vectors $X_{CQ}$, $X_M$ and $X_P$ be given as (see equation (2.10)):

$$X_{CQ} = \begin{bmatrix} X_{CQ} \\ Y_{CQ} \\ Z_{CQ} \end{bmatrix}, \quad X_M = \begin{bmatrix} x_M \\ y_M \\ z_M \end{bmatrix}, \quad X_P = \begin{bmatrix} U \\ V \\ W \end{bmatrix}.$$

If

$$I = \text{identity matrix} = \begin{bmatrix} 1 & 0 & 0 \\ 0 & 1 & 0 \\ 0 & 0 & 1 \end{bmatrix}$$

then

$$\frac{\partial X_T}{\partial X_{CQ}} = R_1(\epsilon_0) \cdot I = R_1(\epsilon_0). \tag{2.42}$$

Similarly,

$$\frac{\partial X_T}{\partial X_M} = R_1(\epsilon_0) P^T R_1(-\epsilon) T_1^T \tag{2.43}$$

and

$$\frac{\partial X_T}{\partial X_P} = -R_1(\epsilon_0) P^T N^T S^T. \tag{2.44}$$

Each of equations (2.42) to (2.44) is a 3 x 3 matrix, with the three columns representing the three coordinates (of selenocenter, lunar point and earth station), while the rows represent the three topocentric coordinates of the lunar point.

In using measured laser distances as observed quantities it will be impracticable to use some of the parameters that have so far been used in finding the partials represented by equations (2.29) to (2.44) due to one main reason. Some parameters, in their present form, change from epoch to epoch and the total number of parameters to be solved for will always be larger than the number of observations. Such parameters that vary with time include the precessional elements, the mean obliquity of the equator of date, nutation in obliquity and longitude, the Greenwich Apparent Sidereal Time, the Eulerian angles of the moon and the geocentric coordinates of the selenocenter. It is therefore necessary to express these variable parameters as functions of time or like arguments, and to regard the coefficients of these arguments as the parameters.

Suppose a variable parameter, q can be expressed as a function of time:

$$q = g_0 + g_1 t + g_2 t^2 + \cdots + g_n t^n$$

i.e.

$$q = f(G, t)$$

where

G is a column vector of coefficients $g_0, g_1 \cdots$

and t is some time unit, or similar argument.

Then

$$\frac{\partial X_T}{\partial G} = \frac{\partial X_T}{\partial q} \cdot \frac{\partial q}{\partial G} .$$

Each variable parameter will now be considered.

The Mean Obliquity of the Equator of Date.

An expression for the mean obliquity of the equator of date ($\epsilon$) is given by [65]:

$$\epsilon = 23\overset{\circ}{.}4522944 - 0\overset{\circ}{.}01301250t - 0\overset{\circ}{.}1638889 \times 10^{-5}t^2 + 0\overset{\circ}{.}5027778 \times 10^{-6}t^3$$

or

$$\epsilon = a_0 + a_1 t + a_2 t^2 + a_3 t^2$$

where t is in tropical centuries from 1900.0

$$\therefore \quad \frac{\partial X_T}{\partial [a_0, \cdots a_3]^T} = \frac{\partial X_T}{\partial \epsilon} \cdot \frac{\partial \epsilon}{\partial [a_0, \cdots a_3]^T}$$

and

$$\frac{\partial \epsilon}{\partial [a_0, \cdots a_3]^T} = [1 \;\vdots\; t \;\vdots\; t^2 \;\vdots\; t^3].$$

If the variable parameter $\epsilon$ is then replaced by the coefficients $a_0$, $a_1$, $a_2$, $a_3$, then equation (2.30) is replaced by

$$\frac{\partial X_T}{\partial [a_0, \cdots a_3]^T} = \frac{\partial X_T}{\partial \epsilon} \cdot [1 \quad t \quad t^2 \quad t^3] \qquad (2.45)$$

where $\frac{\partial X_T}{\partial \epsilon}$ is a column vector given by equation (2.30). The right hand side of equation (2.45) is a 3 x 3 matrix which will have to be pre-multiplied by equation (2.25) so as to obtain a row vector that represents the partials of the lunar distance with respect to the coefficient $a_0, \cdots a_3$, i.e.,

$$\frac{\partial d_l}{\partial [a_0, \cdots a_3]^T} = \frac{\partial d_l}{\partial X_T^l} \cdot \frac{\partial X_T}{\partial \epsilon} \cdot \frac{\partial \epsilon}{\partial [a_0, \cdots a_3]^T}. \qquad (2.46)$$

The Precessional Elements.

The expressions for the precessional elements are given as [65]:

$$\zeta_o = 2304''.951665\,t + 0''.302165\,t^2 + 0''.018\,t^3$$

$$\theta_1 = 2004''.258257\,t - 0''.426885\,t^2 - 0''.0418\,t^3$$

$$z_1 = 2304''.951615\,t + 1''.095195\,t^2 + 0''.01832\,t^3$$

where $t$ represents the elapsed time since the reference epoch of 1950.0, in tropical centuries. The above equations can be written, in matrix form as

$$\zeta_o = B_1^T T^*$$

$$\theta_1 = B_2^T T^*$$

$$z_1 = B_3^T T^*$$

where $B_1$, $B_2$, $B_3$ are column vectors of coefficients and

$$T^* = \begin{bmatrix} t \\ t^2 \\ t^3 \end{bmatrix}.$$

Thus,

$$\frac{\partial \zeta_o}{\partial B_1} = [t \;\vdots\; t^2 \;\vdots\; t^3] = T^{*T} \quad \text{(i.e. } T^* \text{ transposed)}$$

and

$$\frac{\partial X_J}{\partial B_1} = \frac{\partial X_J}{\partial \zeta_o} \cdot T^{*T}. \tag{2.47}$$

Similarly,

$$\frac{\partial X_J}{\partial B_2} = \frac{\partial X_J}{\partial \theta_1} \cdot T^{*T} \tag{2.48}$$

$$\frac{\partial X_J}{\partial B_3} = \frac{\partial X_J}{\partial z_1} \cdot T^{*T}. \tag{2.49}$$

From equations (2.47), (2.48), (2.49) and (2.25) the partials of the distance with respect to $B_1$, $B_2$ and $B_3$ can be obtained in a manner similar to equation (2.46).

The Nutational Parameters.

When considering the nutational parameters $\Delta\epsilon$ and $\Delta\psi$, the situation is more complicated. The series normally used in calculating $\Delta\epsilon$ and $\Delta\psi$ for each epoch contain some 40 terms for $\Delta\epsilon$ of which 24 terms are of short period and 69 terms for $\Delta\psi$ including 46 short periodic terms [65]. To include all the 109 coefficients as parameters in a general adjustment model not confined to solving for only the earth's precessional and nutational terms would necessitate a large number of observations as well as increase greatly the dimensions of the resulting normal matrix. Moreover, the argument in each of the terms of the nutation series is a combination of trigonometric functions of the five so-called "mean longitudes" (of the sun's perigee, the moon's perigee, sun, moon's node and the moon). The "mean longitudes" are also calculated as functions of time (see [65]). The coefficients of the terms in the expressions for the mean angles could therefore be also treated as variables.

There are two possible ways in which the problem of the large number of parameters can be avoided. In the first alternative, the mean longitudes can be regarded as constants, while only a few of the coefficients of the arguments in the nutation series are included as parameters. The other coefficients will have to be held fixed. The choice of the coefficients to be included as parameters is more or less arbitrary, but should include coefficients of both short and long periodic terms. The second way is to replace the orientation of the earth-fixed coordinate system with respect to an inertial system by the three Eulerian angles mentioned earlier, thereby combining the effects of luni-solar precession, nutation and planetary precession. In this case, the angles can be integrated numerically and the number of parameters is reduced

to only the six initial conditions for the three second order equations of motion (see Chapter 4). Expressions for both methods will be given here.

Let the series expressions for $\Delta\epsilon$ and $\Delta\psi$ be given as

$$\Delta\epsilon = \sum_{i=1}^{40} J_i G_i$$

$$\Delta\psi = \sum_{i=1}^{69} K_i Q_i$$

where

$J_i$, $K_i$ are numerical coefficients

$G_i$, $Q_i$ are arguments (functions of the "mean angles").

Also, suppose only n and m coefficients are to be regarded as parameters from $\Delta\epsilon$ and $\Delta\psi$ respectively, such that the reduced expressions are

$$\Delta\epsilon^* = \sum_{i=1}^{n} J_i G_i$$

$$\Delta\psi^* = \sum_{i=1}^{m} K_i Q_i .$$

Then

$$\frac{\partial\Delta\epsilon}{\partial J} = G^T$$

$$\frac{\partial\Delta\psi}{\partial K} = Q^T$$

where

J, K are column vectors of dimension n and m respectively

and G, Q are column vectors of dimension n and m respectively.

Thus

$$\frac{\partial X_T}{\partial J} = \frac{\partial X_T}{\partial \Delta \epsilon} \cdot G^T \tag{2.50}$$

$$\frac{\partial X_T}{\partial K} = \frac{\partial X_T}{\partial \Delta \psi} \cdot Q^T. \tag{2.51}$$

Equations (2.50) and (2.51) can be used together with equations (2.34), (2.35) and equation (2.25) to find the partials of the measured distance $d_1$ with respect to the nutation parameters. The equations for the partials, when Eulerian angles are used will be considered later in this chapter.

<u>The Moon's Eulerian Angles.</u>

The moon's Eulerian angles $\theta$, $\psi$ and $\Phi$ are conventionally computed through the equations given in Section 2.34. Here, the mean angles L, $\Omega$ and I can be regarded as exact while the libration angles $\tau$, $\sigma$ and $\rho$ are variable parameters. Hence, from the expressions for $\theta$, $\psi$ and $\Phi$

$$\begin{aligned} \frac{\partial X_T}{\partial \tau} &= \frac{\partial X_T}{\partial \Phi} \cdot \frac{\partial \Phi}{\partial \tau} \\ \frac{\partial X_T}{\partial \sigma} &= \frac{\partial X_T}{\partial \psi} \cdot \frac{\partial \psi}{\partial \sigma} + \frac{\partial X_T}{\partial \Phi} \cdot \frac{\partial \Phi}{\partial \sigma} \\ \frac{\partial X_T}{\partial \rho} &= \frac{\partial X_T}{\partial \theta} \cdot \frac{\partial \theta}{\partial \rho} . \end{aligned} \tag{2.52}$$

However, since $\tau$, $\sigma$ and $\rho$ are calculated through series expressions, the partials of $X_T$ with respect to the parameters in the series expressions are the required partials. The situation here is similar to that of nutation elements. The expressions for $\tau$, $\sigma$ and $\rho$ contain 18, 11 and 11 terms respectively [65]. Some or all of the 40 fixed coefficients can be regarded as parameters if the arguments are regarded as known, or if numerically integrated Eulerian

angles are used, the six initial values of the integration are the only parameters that need be considered.

The physical libration in node, inclination and longitude have the respective forms:

$$\sigma = \frac{1}{I} \sum_{i=1}^{11} E_i S_i$$

$$\rho = \sum_{i=1}^{11} F_i H_i$$

$$\tau = \sum_{i=1}^{18} G_i U_i$$

where $E_i$, $F_i$ and $G_i$ are constants, $S_i$, $H_i$ and $U_i$ are sine functions of combinations of the Delauny variables and I is the mean inclination. Thus, if E, F, and G represent the column vector of parameters (related to physical libration angles ) to be adjusted, then

$$\frac{\partial \sigma}{\partial E} = \frac{1}{I} \cdot S^T$$

$$\frac{\partial \rho}{\partial F} = H^T \qquad (2.53)$$

$$\frac{\partial \tau}{\partial G} = U^T$$

where

S, H, U are the column vector matrices of arguments.

Furthermore, the mean inclination I can be regarded as a parameter, hence

$$\frac{\partial \sigma}{\partial I} = E^T \cdot S \qquad (2.54)$$

and from Section 2.34

$$\frac{\partial \theta}{\partial I} = 1. \qquad (2.55)$$

Thus,

$$\frac{\partial X_J}{\partial G} = \frac{\partial X_J}{\partial \Phi} \cdot \frac{\partial \Phi}{\partial \tau} \cdot \frac{\partial \tau}{\partial G}$$

$$\frac{\partial X_J}{\partial E} = \frac{\partial X_J}{\partial \psi} \cdot \frac{\partial \psi}{\partial \sigma} \cdot \frac{\partial \sigma}{\partial E} + \frac{\partial X_J}{\partial \Phi} \cdot \frac{\partial \Phi}{\partial \sigma} \cdot \frac{\partial \sigma}{\partial E}$$

$$\frac{\partial X_J}{\partial F} = \frac{\partial X_J}{\partial \theta} \cdot \frac{\partial \theta}{\partial \rho} \cdot \frac{\partial \rho}{\partial F}$$

and

$$\frac{\partial X_J}{\partial I} = \frac{\partial X_J}{\partial \theta} \cdot \frac{\partial \theta}{\partial I} + \frac{\partial X_J}{\partial \Phi} \cdot \frac{\partial \Phi}{\partial} \cdot \frac{\partial \sigma}{\partial I} + \frac{\partial X_J}{\partial \psi} \cdot \frac{\partial \psi}{\partial \sigma} \cdot \frac{\partial \sigma}{\partial I}.$$

Noting from the expressions for the moon's Eulerian angles given in Section 2.34 that

$$\frac{\partial \Phi}{\partial \tau} = \frac{\partial \psi}{\partial \sigma} = \frac{\partial \theta}{\partial \rho} = \frac{\partial \theta}{\partial I} = 1,$$

and

$$\frac{\partial \Phi}{\partial \sigma} = -1,$$

the above equations can be written as:

$$\frac{\partial X_J}{\partial G} = \frac{\partial X_J}{\partial \Phi} \cdot \frac{\partial \tau}{\partial G} \tag{2.56}$$

$$\frac{\partial X_J}{\partial E} = \frac{\partial X_J}{\partial \psi} \cdot \frac{\partial \sigma}{\partial E} - \frac{\partial X_J}{\partial \varphi} \cdot \frac{\partial \sigma}{\partial E} \tag{2.57}$$

$$\frac{\partial X_J}{\partial F} = \frac{\partial X_J}{\partial \theta} \cdot \frac{\partial \rho}{\partial F} \tag{2.58}$$

and

$$\frac{\partial X_J}{\partial I} = \frac{\partial X_J}{\partial \theta} - \frac{\partial X_J}{\partial \Phi} \cdot \frac{\partial \sigma}{\partial I} + \frac{\partial X_J}{\partial \psi} \cdot \frac{\partial \sigma}{\partial I} \tag{2.59}$$

Equations (2.56) to (2.59) can be evaluated because expressions for the partials appearing on the right hand side of the equations have already been given. The size of the matrix obtained from equations (2.56), (2.57) and (2.58) remain $3 \times n$, $3 \times m$ and $3 \times \ell$ where n, m and $\ell$ are the number of parameters represented by the row vectors E, F and G respectively. Similarly, the result of equation (2.59) is a $3 \times 1$ matrix. These equations are to be used together with equation (2.25) to find the partials of the measured distance $d_i$ with respect to these physical libration parameters.

<u>The GAST</u>

The Greenwich Apparent Sidereal Time ($\Theta$) is given by (see [69]):

$$\Theta = UT + 6^h38^m45^s.836 + 8,640,184^s.542\,t_n + 0^s.0929t_n^2 + \Delta\phi \cos\epsilon \quad (2.60)$$

where $t_n$ is the number of Julian centuries of 36525 mean solar days since 1900 Jan. 0.5UT. UT (Universal Time) is the UT1 epoch of observation, the next three terms gives the Mean Sidereal Time (MST) at $0^h$UT, and the last term is generally referred to as the equation of the equinox. $\Delta\phi$ is the nutation in longitude and $\epsilon$ is the true obliquity of the equator of date.

Each UT1 time of observation cannot be taken as a parameter, since this will always introduce one more parameter to the system each time an observation is made. However, general time corrections (clock offset error) can be found for fairly short spans of time. If UT1* is the chronometer time of observation, and $\Delta T$ is the "regional" correction to UT1* in order to obtain the correct UT1, then

$$UT1 = UT1^* + \Delta T.$$

Together with equation (2.60)

$$\frac{\partial \Theta}{\partial \Delta T} = 1.$$

If equation (2.60) is rewritten as

$$\Theta = UT1 + B^{T}T + \Delta\psi \cos \epsilon,$$

then

$$\frac{\partial \Theta}{\partial B} = T^{T}$$

where

$$T = \begin{bmatrix} 1 \\ t_n \\ t_n^2 \end{bmatrix}, \text{ and } B = \begin{bmatrix} B_0 \\ B_1 \\ B_2 \end{bmatrix}.$$

It follows therefore, that

$$\frac{\partial X_T}{\partial \Delta T} = \frac{\partial X_T}{\partial \Theta} \cdot \frac{\partial \Theta}{\partial \Delta T} = \frac{\partial X_T}{\partial \Theta} \tag{2.61}$$

and

$$\frac{\partial X_T}{\partial B} = \frac{\partial X_T}{\partial \Theta} \cdot \frac{\partial \Theta}{\partial B}. \tag{2.62}$$

$\frac{\partial X_T}{\partial \Theta}$ is given by equation (2.41), and $\frac{\partial d_1}{\partial \Delta T, \partial B}$ can be obtained using equation (2.25) as demonstrated earlier.

Since the "variable" parameters $\Delta\psi$ and $\epsilon$ are also used in computing the value of $\Theta$, equations (2.51) and (2.46) can be modified by adding respectively the expressions:

$$\frac{\partial X_T}{\partial K} = \cdots + \frac{\partial X_T}{\partial \Theta} \cdot \frac{\partial \Theta}{\partial \Delta\psi} \cdot \frac{\partial \Delta\psi}{\partial \Theta} \tag{2.63}$$

$$\frac{\partial X_T}{\partial [a_0, \cdots a_3]^T} = \cdots + \frac{\partial X_T}{\partial \Theta} \cdot \frac{\partial \Theta}{\partial \epsilon} \cdot \frac{\partial \epsilon}{\partial [a_0, \cdots a_3]^T} \tag{2.64}$$

The first part of equations (2.63) and (2.64) are given by equations (2.51) and (2.46). From equation (2.60)

$$\frac{\partial \Theta}{\partial \Delta\psi} = \cos \epsilon$$

$$\frac{\partial \Theta}{\partial \epsilon} = -\Delta\psi \sin \epsilon .$$

In practice, since $\Delta\psi \cos \epsilon$ is a small quantity, the equation of the equinox contribution to $\Theta$ can be regarded as errorless and if this is so, it is not necessary to use equations (2.63) and (2.64) in place of equations (2.51) and (2.46) respectively.

Coordinates of the True Pole

The coordinates $x_p$, $y_p$ of the true celestial pole (with reference to the CIO pole) are traditionally determined from the analysis of continuous latitude and/or longitude observations at permanent observatories. Two agencies — the International Polar Motion Service (IPMS) and the Bureau International de l'Heure (BIH) - use the variation of latitude and/or longitude values at these observatories in determining the motion of the pole. The IPMS uses primarily five stations located near a single parallel of latitude, while the other stations participate primarily in the BIH program.

The coordinates of the true pole are published by both the IPMS and the BIH. The final coordinates are given by IPMS at intervals of 0.05 year (18.25 days) but published two years in arreas. The BIH final coordinates are given at intervals of five days and are generally available one month in arrears.

To date, the theory of polar motion is only approximately known. There are no existing mathematical functions which can be used to calculate

the position of the true pole at any epoch such as those that have already been given for other parameters. However, coordinates of the true pole — $x_p$, $y_p$ — cannot be regarded directly as parameters as was noted above. Hence, corrections to known values of $x_p$, $y_p$ will have to be assumed constant for a short length of time (such as five days), or alternatively, the corrections can be obtained in another way.

Recently, polar motion have been obtained from residuals of Doppler satellite observations by J. Anderle and Beuglass of the U.S. Naval Weapons Laboratory [8]. In a similar manner, corrections to the values of $x_p, y_p$ used in predicting laser distances can be obtained by analysing the residuals of the measured distances after adjustments.

The Geocentric Position of the Selenocenter

The position of the moon's center of mass given by $X_{CQ}$, $Y_{CQ}$, $Z_{CQ}$ are, like other variable parameters considered above, computed for each epoch. For this purpose, a lunar ephemeris, analytical or numerical, has to be used. The lunar ephemeris with the smallest estimated uncertainties is the JPL LE16 which is estimated to have uncertainties of 100-150 meters in position and 50 meters in range. The laser ranges are expected to be at least one or two orders of magnitude better in precision than the best ephemeris. It is therefore improper to use any of the existing lunar ephemerides in the prediction equation without allowing for the systematic errors in the ephemeris used.

In order to take care of the systematic errors in the existing lunar ephemeris, such as the numerically integrat : LE16, an empirical model can be used in the observation equations, whose sole purpose would be to absorb the systematic errors in the ephemeris. This will not necessarily lead to an "improved" lunar ephemeris, but will prevent the distortion of

the adjustment due to systematic errors of the ephemeris. Such an empirical model can be a harmonic series, with fixed coefficients and arguments which are linear functions of time, or a general polynominal, the degree of which will depend on some pre-set conditions on the analysis of variance obtained in the adjustment.

Such a harmonic series can be of the form:

$$\sum_i \mu_i \cos(\beta_i t + b_i).$$

Thus, the "true" geocentric coordinates of the selenocenter that will be used in the distance prediction equation as well as in the adjustment model can be of the form:

$$\begin{bmatrix} X_{\mathfrak{C}} \\ Y_{\mathfrak{C}} \\ Z_{\mathfrak{C}} \end{bmatrix} + \begin{bmatrix} \sum_i \mu_i^x \cos(\beta_i^x t + b_i^x) \\ \sum_i \mu_i^y \cos(\beta_i^y t + b_i^y) \\ \sum_i \mu_i^z \cos(\beta_i^z t + b_i^z) \end{bmatrix}.$$

If a polynomial is used to model the systematic errors in the ephemeris, the "true" geocentric coordinates of the moon will become

$$\begin{bmatrix} X_{\mathfrak{C}} \\ Y_{\mathfrak{C}} \\ Z_{\mathfrak{C}} \end{bmatrix} + \begin{bmatrix} C_0^x + C_1^x t + C_2^x t^2 + \cdots \\ C_0^y + C_1^y t + C_2^y t^2 + \cdots \\ C_0^z + C_1^z t + C_2^z t^2 + \cdots \end{bmatrix}.$$

Depending on which model is used, the coefficients $\mu_i$, $\beta_i$, $b_i$ or $C_i$ become part of the parameters to be solved for in the adjustment.

The Geodetic Coordinates

Equation (2.44) gives the partials of the topocentric coordinates of the

moon point with respect to the U, V, W (geodetic) Cartesian coordinates of the laser station. The U, V, W coordinates are functions of the geodetic coordinates ($\varphi$, $\lambda$, h) of the earth point and the parameters of the ellipsoid (a, f) (see equation (2.1)). Optionally, if the position of the earth point is defined in an absolute geodetic system, one can regard $\varphi$, $\lambda$, h, a, f as parameters in place of the Cartesian coordinates. Consequently, equation (2.44) will be replaced by the following equations:

$$\frac{\partial X_T}{\partial \varphi} = -R_1(\epsilon_0)P^T N^T S^T \begin{bmatrix} -(M+h)\sin\varphi\cos\lambda \\ -(M+h)\sin\varphi\sin\lambda \\ (M+h)\cos\varphi \end{bmatrix} \tag{2.65}$$

$$\frac{\partial X_T}{\partial \lambda} = -R_1(\epsilon_0)P^T N^T S^T \begin{bmatrix} -(N+h)\cos\varphi\sin\lambda \\ (N+h)\cos\varphi\cos\lambda \\ 0 \end{bmatrix} \tag{2.66}$$

$$\frac{\partial X_T}{\partial h} = -R_1(\epsilon_0)P^T N^T S^T \begin{bmatrix} \cos\varphi\cos\lambda \\ \cos\varphi\sin\lambda \\ \sin\varphi \end{bmatrix} \tag{2.67}$$

$$\frac{\partial X_T}{\partial a} = -R_1(\epsilon_0)P^T N^T S^T \begin{bmatrix} \frac{\cos\varphi\cos\lambda}{W} \\ \frac{\cos\varphi\sin\lambda}{W} \\ \frac{(1-e^2)\sin\varphi}{W} \end{bmatrix} \tag{2.68}$$

and

$$\frac{\partial X_I}{\partial f} = -R_1(\epsilon_0)P^T N^T S^T \begin{bmatrix} \dfrac{a(1-f)\sin^2\varphi \cos\varphi \cos\lambda}{W^3} \\ \dfrac{a(1-f)\sin^2\varphi \cos\varphi \sin\lambda}{W^3} \\ (M \sin^2\varphi - 2N)(1-f)\sin\varphi \end{bmatrix} \qquad (2.69)$$

where

$$N = \frac{a}{W}$$

$$M = \frac{a(1-e^2)}{W^3}$$

$$W = (1-e^2 \sin^2\varphi)^{-\frac{1}{2}}$$

and a, e, f are respestively the semimajor axis, eccentricity and flattening of the ellipsoid.

The above equations (2.65) to (2.69) are valid only when the U, V, W coordinates are expressed in the "absolute" geodetic ("average" terrestrial) coordinate system. In many instances, coordinates of earth stations are expressed in a "relative" geodetic coordinate system, using any of the conventional reference ellipsoids as the reference figure for the earth. The reference ellipsoid used may not be centered at the geocenter, and the Cartesian axes of such a "relative" system may not be oriented parallel to the axes of the "average" terrestrial coordinate system. If the relative geodetic (curvillinear) coordinates of the earth station is $\bar{\varphi}$, $\bar{\lambda}$, and $\bar{h}$, and the parameters of the reference ellipsoid are $\bar{a}$ and $\bar{f}$, then the "relative" Cartesian coordinates u, v, w are also given by equation (2.1) provided $\bar{\varphi}$, $\bar{\lambda}$, $\bar{h}$, $\bar{N}$ and $\bar{e}$ are substituted for $\varphi$, $\lambda$, h N and e respectively. A general relationship between the "average" terrestrial and the "relative" geodetic coordinates of a point are given by (see [68]):

$$\begin{bmatrix} U \\ V \\ W \end{bmatrix} = \begin{bmatrix} u \\ v \\ w \end{bmatrix} + A \begin{bmatrix} \delta \varphi_o \\ \delta \lambda_o \\ \delta h_o \end{bmatrix} + B \begin{bmatrix} \delta A_o \\ \delta \xi_o \\ \delta \eta_o \end{bmatrix} + s \begin{bmatrix} \Delta u \\ \Delta v \\ \Delta w \end{bmatrix} \qquad (2.70)$$

where:

$$\begin{bmatrix} \Delta u \\ \Delta v \\ \Delta w \end{bmatrix} = \begin{bmatrix} u - u_o \\ v - v_o \\ w - w_o \end{bmatrix},$$

$$A = \begin{bmatrix} \sin \bar{\varphi}_o \cos \bar{\lambda}_o & \sin \bar{\lambda}_o & -\cos \bar{\varphi}_o \cos \bar{\lambda}_o \\ \sin \bar{\varphi}_o \sin \bar{\lambda}_o & -\cos \bar{\lambda}_o & -\cos \bar{\varphi}_o \sin \bar{\lambda}_o \\ -\cos \bar{\varphi}_o & 0 & -\sin \bar{\varphi}_o \end{bmatrix},$$

$$B = \begin{bmatrix} \sin\bar{\varphi}_o \Delta v - \cos\bar{\varphi}_o \sin\bar{\lambda}_o \Delta w & \cos\bar{\varphi}_o \Delta w & -\cos\bar{\varphi}_o \Delta v - \sin\bar{\varphi}_o \sin\bar{\lambda}_o \Delta w \\ -\sin\bar{\varphi}_o \Delta u + \cos\bar{\varphi}_o \cos\bar{\lambda}_o \Delta w & \sin\bar{\lambda}_o \Delta w & \cos\bar{\varphi}_o \Delta u + \sin\bar{\varphi}_o \cos\bar{\lambda}_o \Delta w \\ \cos\bar{\varphi}_o \sin\bar{\lambda}_o \Delta u - \cos\bar{\varphi}_o \cos\bar{\lambda}_o \Delta v & \cos\bar{\lambda}_o \Delta u + \sin\bar{\lambda}_o \Delta v & \sin\bar{\varphi}_o \sin\bar{\lambda}_o \Delta u - \sin\bar{\varphi}_o \cos\bar{\lambda}_o \Delta v \end{bmatrix}$$

$$\begin{bmatrix} \delta \varphi_o \\ \delta \lambda_o \\ \delta h_o \end{bmatrix} = \begin{bmatrix} \bar{\varphi}_o - \varphi_o \\ \bar{\lambda}_o - \lambda_o \\ \bar{h}_o - h_o \end{bmatrix}$$

$\delta A_o$ is the error in azimuth of the relative system

$\delta \xi_o$ is the error in tilt of the system in the meridian plane

$\delta \eta_o$ is the error in tilt in the prime vertical plane

and

$s$ is a scale factor.

It should also be noted that $\delta\varphi_o$ and $\delta\lambda_o$ should be expressed in linear units.

All the variables with zero subscripts denote the values of these variables at the origin of the relative geodetic system.

If equation (2.70) is now substituted in any of the equations (2.10), the topocentric coordinates of the moon point ($\vec{X}_T$) will be obtained. Also, in equation (2.70), seven transformation parameters ($\delta\varphi_o$, $\delta\lambda_o$, $\delta h_o$, $\delta A_o$, $\delta\xi_o$, $\delta\eta_o$ and s) have been introduced in addition to the "relative" geodetic coordinates and the parameters of the reference ellipsoid. The partials of $\vec{X}_T$ with respect to $\bar{\varphi}$, $\bar{\lambda}$, $\bar{h}$, $\bar{a}$ and $\bar{f}$ are given by equations (2.65) to (2.69), provided the relative quantities (with bar) are substituted for their absolute counterparts. Taking the partials of $X_T$ with respect to the seven transformation parameters we obtain:

$$\frac{\partial X_T}{\partial \begin{bmatrix} \delta\varphi_o \\ \delta\lambda_o \\ \delta h_o \end{bmatrix}} = -R_1(\epsilon_o)P^T N^T S^T A \tag{2.71}$$

$$\frac{\partial X_T}{\partial \begin{bmatrix} \delta A_o \\ \delta\xi_o \\ \delta\eta_o \end{bmatrix}} = -R_1(\epsilon_o)P^T N^T S^T B \tag{2.72}$$

and

$$\frac{\partial X_T}{\partial s} = -R_1(\epsilon_o)P^T N^T S^T \begin{bmatrix} \Delta u \\ \Delta v \\ \Delta w \end{bmatrix} . \tag{2.73}$$

The above three equations can be used with equation (2.65) to (2.69) instead of equation (2.44) if it is desired to obtain corrections to the relative geodetic coordinates of the earth station, the parameters of the (relative) reference ellipsoid as well as the seven transformation parameters.

The Selenodetic Coordinates

As in the case of the geodetic coordinates, the Cartesian coordinates of the moon point ($x_M$, $y_M$, $z_M$) are functions of the spherical coordinates ($\ell$, b, r) of the lunar point (see equation (2.2)). Equations for obtaining partials for the $x_M$, $y_M$, $z_M$ coordinates have been given in equation (2.43). If, however, the spherical coordinates b, $\ell$, r replace $x_M$, $y_M$ and $z_M$ as parameters, then the following equations replace equation (2.43):

$$\frac{\partial X_T}{\partial b} = R_1(\epsilon_0)P^T R_1(-\epsilon)T_1^T \begin{bmatrix} -r\sin b\cos\ell \\ -r\sin b\sin\ell \\ r\cos b \end{bmatrix} \tag{2.74}$$

$$\frac{\partial X_T}{\partial \ell} = R_1(\epsilon_0)P^T R_1(-\epsilon)T_1^T \begin{bmatrix} -r\cos b\sin\ell \\ r\cos b\cos\ell \\ 0 \end{bmatrix} \tag{2.75}$$

$$\frac{\partial X_T}{\partial r} = R_1(\epsilon_0)P^T R_1(-\epsilon)T_1^T \begin{bmatrix} \cos b\cos\ell \\ \cos b\sin\ell \\ \sin b \end{bmatrix} \tag{2.76}$$

## 2.5 Observation Equations when Orientation Angles are Obtained through Numerical Integration Process

The idea of obtaining the moon's Eulerian angles through numerical integration of the equations of motion have been discussed in Section 2.34. Also, it has been suggested in Section 2.35 that the conventional precession, nutation and the Greenwich hour angle of the vernal equinox can be replaced by three (Eulerian) angles, which can also be obtained by numerical integration. The numerical integration procedure for obtaining these earth

Eulerian angles is outlined in Chapter 4 of this work.

If

$$E_E = [\theta_E \vdots \psi_E \vdots \Phi_E]$$

and

$$E_M = [\theta_M \vdots \psi_M \vdots \Phi_M]$$

respectively represent the orientation angles of the earth's UVW and the moon's xyz axes (fixed to the bodies) with respect to an inertial system (such as the mean ecliptic coordinate system of 1950.0), then the topocentric coordinates of the moon point is given by equation (2.15):

$$\begin{bmatrix} X_M \\ Y_M \\ Z_M \end{bmatrix}_{topoc.} = R_1(\epsilon_0) \begin{bmatrix} X_{CQ} \\ Y_{CQ} \\ Z_{CQ} \end{bmatrix} + P_M \begin{bmatrix} x_M \\ y_M \\ z_M \end{bmatrix} - P_E \begin{bmatrix} U \\ V \\ W \end{bmatrix} \qquad (2.77)$$

where $P_M$, $P_E$ are 3 x 3 orthogonal matrices given by:

$$P_M = R_3(-\psi_M)R_1(\theta_M)R_3(-\Phi_M)$$

$$P_E = R_3(-\psi_E)R_3(\theta_E)R_3(-\Phi_E).$$

The predicted distance from an earth station to a moon point is computed from equation (2.16):

$$D = (X_{MT}^2 + Y_{MT}^2 + Z_{MT}^2)^{\frac{1}{2}}.$$

The matrix of partials (design matrix A) will be different from those already derived in Section 2.4, since the parameters are different from those listed in equation (2.18). In analogy to equation (2.18)

$$[X_T] = f_3(\epsilon_0, \psi_M, \theta_M, \Phi_M, \psi_E, \theta_E, \Phi_E, U, V, W, x_M, y_M, z_M, X_{CQ}, Y_{CQ}, Z_{CQ}) \qquad (2.78)$$

In addition, since the Eulerian angles are obtained from integration,

$$\begin{bmatrix} \theta_M \\ \psi_M \\ \Phi_M \end{bmatrix} = f_4(\theta_M^o, \psi_M^o, \Phi_M^o, \dot{\theta}_M^o, \dot{\psi}_M^o, \dot{\Phi}_M^o) = f_4[E_M^o \ \vdots \ \dot{E}_M^o] \tag{2.79}$$

and

$$\begin{bmatrix} \theta_E \\ \psi_E \\ \Phi_E \end{bmatrix} = f_5(\theta_E^o, \psi_E^o, \Phi_E^o, \dot{\theta}_E^o, \dot{\psi}_E^o, \dot{\Phi}_E^o) = f_5[E_E^o \ \vdots \ \dot{E}_E^o] \tag{2.80}$$

where superscript o denotes that the quantities are the values of the orientation angles, and their time derivatives at a starting epoch (initial conditions). By differentiating equation (2.77), the following partial differentials are obtained:

$$\frac{\partial X_T}{\partial \epsilon_o} = L_1 R_1(\epsilon_o) \begin{bmatrix} X_{CQ} \\ Y_{CQ} \\ Z_{CQ} \end{bmatrix} \tag{2.81}$$

$$\frac{\partial X_T}{\partial \psi_M} = -L_3 P_M \begin{bmatrix} x_M \\ y_M \\ z_M \end{bmatrix} \tag{2.82}$$

$$\frac{\partial X_T}{\partial \theta_M} = R_3(-\psi_M) L_2 R_1(\theta_M) R_3(-\Phi_M) \begin{bmatrix} x_M \\ y_M \\ z_M \end{bmatrix} \tag{2.83}$$

$$\frac{\partial X_T}{\partial \Phi_M} = -P_M \, L_3 \begin{bmatrix} x_M \\ y_M \\ z_M \end{bmatrix} \tag{2.84}$$

$$\frac{\partial X_T}{\partial \begin{bmatrix} x_M \\ y_M \\ z_M \end{bmatrix}} = \frac{\partial X_T}{\partial X_M} = P_M \tag{2.85}$$

$$\frac{\partial X_T}{\partial \psi_E} = -L_3 \, P_E \begin{bmatrix} U \\ V \\ W \end{bmatrix} \tag{2.86}$$

$$\frac{\partial X_T}{\partial \theta_E} = R_3(-\psi_E) L_1 R_1(\theta_E) R_3(-\Phi_E) \begin{bmatrix} U \\ V \\ W \end{bmatrix} \tag{2.87}$$

$$\frac{\partial X_T}{\partial \Phi_E} = -P_E \, L_3 \begin{bmatrix} U \\ V \\ W \end{bmatrix} \tag{2.88}$$

$$\frac{\partial X_T}{\partial \begin{bmatrix} U \\ V \\ W \end{bmatrix}} = \frac{\partial X_T}{\partial X_P} = -P_E . \tag{2.89}$$

The variable parameters ($\theta_M, \cdots, \Phi_E$) will have to be replaced by the 12 initial conditions in equations (2.79) and (2.80). If

$$[E_M^o \quad \dot{E}_M^o] = [\theta_M^o \ \psi_M^o \ \Phi_M^o \ \dot{\theta}_M^o \ \dot{\psi}_M^o \ \dot{\Phi}_M^o]$$

Then

$$\frac{\partial X_T}{\partial [E_M^o \vdots \dot{E}_M^o]} = \frac{\partial X_T}{\partial E_M} \cdot \frac{\partial E_M}{\partial [E_M^o \vdots \dot{E}_M^o]} \tag{2.90}$$

where $\frac{\partial X_T}{\partial E_M}$ is a 3 x 3 matrix of partials whose columns are given by equations (2.82) to (2.84). Similarly for $[E_E^o \vdots \dot{E}_E^o]$,

$$\frac{\partial X_T}{\partial [E_E^o \vdots \dot{E}_E^o]} = \frac{\partial X_T}{\partial E_E} \cdot \frac{\partial E_E}{\partial [E_E^o \vdots \dot{E}_E^o]} . \tag{2.91}$$

Also, $\frac{\partial X_T}{\partial E_E}$ is a 3 x 3 matrix of partials, whose columns are given by equations (2.86) to (2.88). Each of the expressions $\frac{\partial E_M}{\partial [E_M^o \vdots \dot{E}_M^o]}$ and $\frac{\partial E_E}{\partial [E_E^o \vdots \dot{E}_E^o]}$ is a 3 x 6 matrix which forms part of a matrix, usually referred to as the state transition matrix [ 9 ]. This matrix describes the transition of a differential variation of the initial epoch conditions from the initial epoch $t_o$, to time t. The matrix can be obtained along with the integrated orientation angles by methods which are described in Chapter 4.

The partials of the laser distances with respect to each of the parameters considered in this section can be obtained in the same way as was done in Section 2.4 through the relationship given by equation (2.23)

$$\frac{\partial D}{\partial \varkappa} = \frac{\partial D}{\partial X_T} \frac{\partial X_T}{\partial \varkappa}$$

where D represent the distances, $X_T$ moon point topocentric coordinates and $\varkappa$ the parameters.

## 2.6 Summary

In this chapter, one of the new observational systems which could be used to improve selenodetic control has been considered. A brief description of the laser ranging systems was given and equations relating ranges between an earth point and a moon point to astronomical, geodetic and selenodetic parameters were derived. The range equations are valid for laser ranges as well as any other kind of ranges made between a station on the earth and a moon point.

The range equations were differentiated for the formation of observation equations which can be used with lunar range measurements in an adjustment model to obtain corrections to approximate values of the parameters involved.

In deriving the observation equations, observed ranges are assumed to be corrected for atmospheric, instrumental and other systematic errors. In Appendix B, the effect of the atmosphere on observed laser ranges is briefly discussed.

The range equations can be used in predicting laser lunar ranges for real observations, and can also be used to simulate observational data for experimental adjustments as was done in Chapter 5 of this work.

# 3 APPLICATION OF THE VLBI TO SELENODETIC CONTROL

## 3.1 Introduction.

Radio Interferometry began in 1946, when McCready et al., used an interferometer for solar observation [17]. Later in the same year, the two-element interferometer also came into use at Cambridge. Radio interferometry rapidly developed thereafter with longer baseline observations, but the maximum length of baseline was limited. The conventional interferometry used superheterodyne receivers at each terminal. A common local oscillator signal had to be transported across the baseline by means of a cable connecting the two terminals. Over longer distances, the operations were managed across the baseline by using a radio link containing two repeater stations. The length of baselines for conventional interferometry hardly exceeded 130 km.

The development of atomic frequency and time standards found a useful application in radio interferometry. Using independent atomic standard oscillators, all real-time interconnections between the two interferometer stations could be eliminated. The interferometer signals from each telescope are independently recorded on a magnetic tape along with time, and the tapes are later brought together for processing. This technique of "atomic-clock" interferometry or "independent clock" interferometry (with local freqency standards and tape recorders replacing microwave links or cable interconnections) is now known as Very Long Baseline Interferometry (VLBI).

With the VLBI, resolution of distant radio sources with angular diameter of 0."0006 has been achieved. This compares with a resolution of $\frac{1}{2}$ minute of arc achievable by the largest reflectors, which is roughly the same as the limit for the unaided human eye [16]. The angular resolving power of a radio interferometer system is given by

$$\alpha = \frac{\Lambda}{d} \tag{3.1}$$

where

$\alpha$ is the angular resolution in radians

$\Lambda$ is the wavelength at which the antennas operate

and

d is the length of the baseline.

It is therefore necessary to know the length of the interferometer baseline in order to determine the size or position of the radio sources.

The inverse problem is of more importance to geodesists. If the coordinates of point radio sources are available, then the baseline parameters of the interferometer system can be determined.

Many possible applications of the VLBI in geodesy and geophysics have been suggested by various scientists in recent years. Such areas of application include geodetic ties between continents, continental drift, determination of precession, nutation and the earth's rotation rate, satellite tracking, navigation and time synchronization. In this chapter, the possibility of using the VLBI for determining station positions on the earth and on the moon will be investigated. The relative position of a lunar station to an earth station at any instant is a mathematical function of other parameters apart from the geocentric and selenocentric positions of the earth station and the lunar station respectively. Consequently an updated knowledge of these parameters can be expected when the VLBI is used for earth and moon position determination.

It is envisaged that the establishment of radio antennas on the moon in the future is a possibility, notwithstanding present technological limitations. Consequently, the studies in this chapter include interferometric systems made up of earth-to-earth, moon-to-moon and earth-to-moon baselines.

In the next section, the basic operating principles of an interferometer system will be given. An attempt has been made to make this brief description as non-technical as possible. Its presentation in this chapter should point out the type of observations to be expected from the VLBI, thereby making the rest of this chapter more easily understood.

## 3.2 Basic Operating Principles of the VLBI.

An interferometer is an apparatus for measuring the phase difference between simultaneously received electromagnetic radiation at two stations from a distant source. Alternatively, the elapsed time between the arrival of any particular wave front at each of the two stations (time delay) can be measured. The phase difference $\Delta p$ and the time delay $\tau$ are related by the equation

$$\tau = \frac{\Delta p}{\omega} \qquad (3.2)$$

where

$\omega$ is the nominal frequency of the radiation.

The necessary equipment at each of the interferometer stations include a radio antenna dish, a local oscillator and an atomic clock (both controlled by a highly stable frequency standard such as a hydrogen maser frequency standard generator). Also there should be at each station a mixer, a video

converter, clipper, sampler and a tape recorder. These pieces of equipment are schematically shown in Figure 3.1.

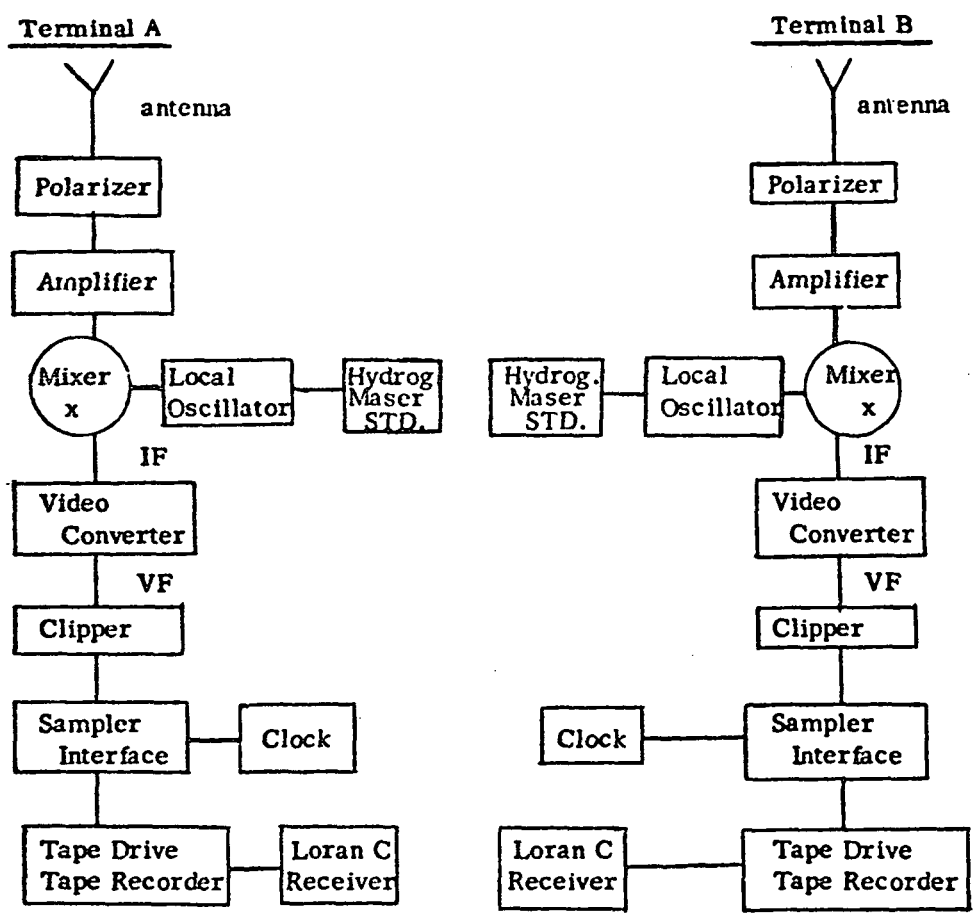


Figure 3.1

Equipment for a VLBI Observing System

The look-angle of the radio source (such as the quasar) at the desired time of observation is pre-computed at each station and each radio antenna is steered to point toward the direction of the radio source. The receiver is also tuned to the desired operating frequency. A synchronizing circuit starts the recording of radio signals received and time, at a pre-set epoch.

The received signal, whose central frequency is $\omega$, is mixed with a local-oscillator produced frequency that is phase-locked. The resulting frequency out of the mixer, known as the intermediate frequency (IF) is passed on to a video converter. The video converter's job is to convert the output signal into a low-frequency signal, suitable for 1-bit digital sampling and recording. The IF signal is amplified, filtered and phase-coherently converted in frequency to obtain a single sideband output signal whose carrier frequency is zero. This output video band signal (limited to 480kHz by available digital recorders) is then passed on to be clipped, sampled and recorded.

Clipping.

The received signal now converted to video band frequency is completely random, a characteristic of the emitting natural radio sources such as the quasars. This signal is clipped "infinitely", thereby retaining the sign of the voltage received and dispensing with the magnitude (see Figure 3.2). A correction can later be applied to the correlator output to compensate for the error introduced by clipping the original wave form. The correction to the correlation output according to the Van Vleck clipping theorem is computed as, [84]:

$$R_x(t) = \sin\left[\frac{\pi}{2} R_y(t)\right] \qquad (3.3)$$

where

$R_x(t)$ is the corrected signal

$R_y(t)$ is the raw output of the correlator

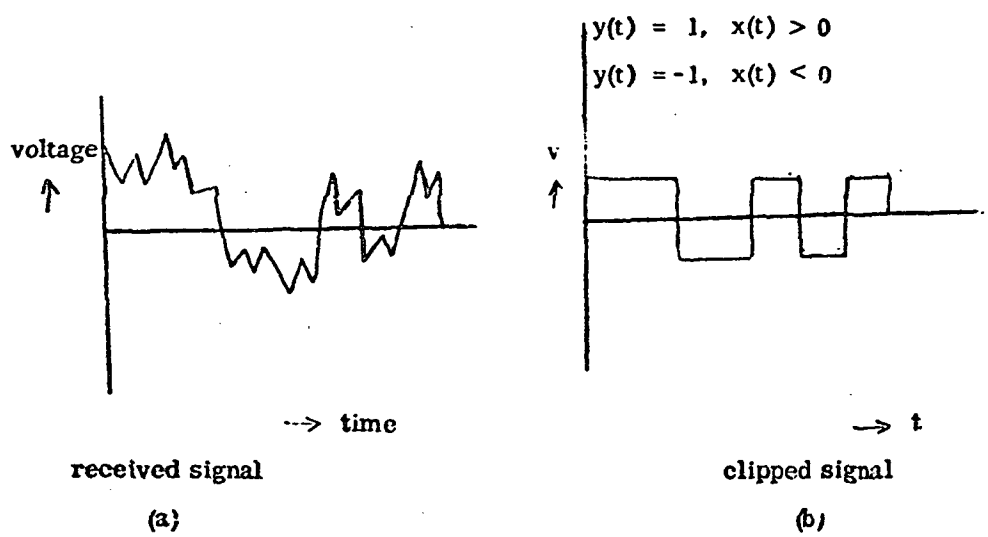


Figure 3.2

Clipped Signal in Relation to the Received Signal

Sampling.

For the purpose of recording the clipped signal on a magnetic tape, the sign of the signal is identified at a regular, spaced interval of time. The sampling rate is, in accordance with the Nyquist theorem, equal to twice the recording bandwith. Thus as an example, the National Radio Astronomy Observatory (NRAO), which uses a bandwidth of 360 kHz, records the data at 720 Kbits/sec. In addition to the clipped and sampled signal,

time is also recorded at intervals of 0.2 sec. The recording of signals and time can be done either on a video tape or on a digital tape. It is more convenient to record on the video tape when sources are being observed since a video tape can last many hours of observations, whereas a digital tape can only record three to four minutes of data. If video tape is used, it is necessary to re-record the data on a digital tape afterwards, for digital computer use.

Data Processing.

The data now on the digital tape consists of the clipped and sampled signal with time, one tape for each of the two interferometer stations. The processing of the tapes is done in two phases, namely:

(a) correlating the tapes

(b) obtaining the true delay.

The correlation of the tapes is done by a digital computer. For each record, the bit streams are shifted relative to one another by an amount that corresponds to the theoretically predicted geometric time delay. The predicted time delay is a function of the baseline length d, and the angle $\beta$ which the baseline makes with the direction of the observed radio source,

$$\tau_g = \frac{d \cos \beta}{c} \qquad (3.4)$$

where c is the velocity of light. The theoretical correlation function is given by

$$R(\tau) = \lim_{T \to \infty} \frac{1}{2T} \int_{-T}^{T} x(t) \cdot x(t + \tau) dt \qquad (3.5)$$

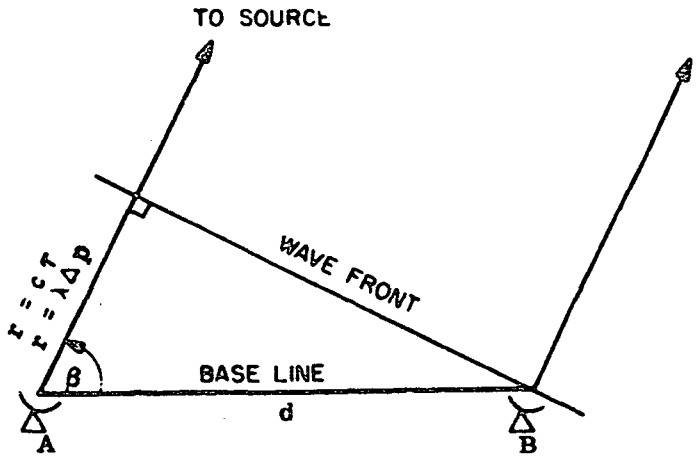


**Figure 3.3 Basic Geometrical Relationships in Interferometry.**

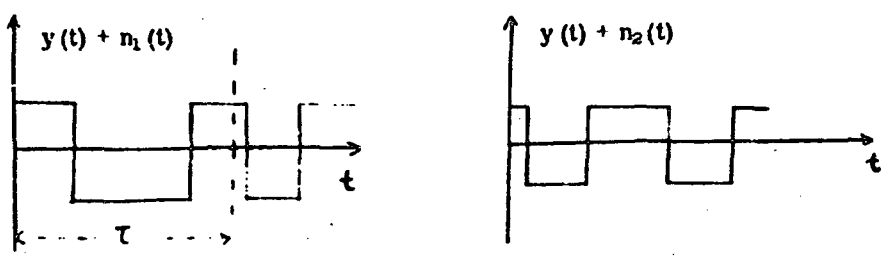


Clipped signal received at A as function of time, starting at $t_o$.

Clipped signal received at B, starting at $t_o$. Note the shift of signal at B w. r. to A

**Figure 3.4 Clipped Signal Received at Two Stations and Time Delay.**

In practice because of finite record length the function is given by numerically integrating over N records, i.e.

$$R'(\tau) = \sum_{n=1}^{N_i} x(t_0 + n\Delta t)\ y(t_0 + n\Delta t + \tau) \qquad (3.6)$$

using a number of values for $\tau$ centered around the predicted geometric delay $\tau_g$, and $N_i$ (number of records over which integration is to be carried out). $N_i$ depends on many factors such as

(1) source strength

(2) antenna size

(3) system noise of receiver

(4) clock stability, i.e. phase stability of the frequency standard.

The first three items put a lower limit on the desirable integration time since weaker sources demand more integration time, and so also do small antennas, and receivers with high system noise. On the other hand, stability of the clock used places a higher limit on the integration time because phase stability must be maintained to high accuracy (1 part in $10^{11}$ or better) within the integration interval.

The correlation function obtained is corrected for finite record length by multiplying $R'(\tau)$ by a weighting function $w(\tau)$ which is chosen to satisfy the following criteria:

$$w(0) = 1 \quad \text{(normality)}$$

$$w(-\tau) = w(\tau) \quad \text{(symmetry)}$$

$$w(\tau)_{\tau \geq \tau_n} = 0$$

where $T_n$ is the total length of the record. The last condition ensures that the corrected function $R''(\tau)$ is defined for all $\tau$. An example of such a weighting function used in practice is given by the "Hanning" function [84]:

$$w(\tau) = \frac{1}{2}\left(1 + \cos\frac{\pi\tau}{T_B}\right), \quad \text{if } |\tau| < T_B$$

$$w(\tau) = 0 \quad , \text{ if } |\tau| > T_B.$$

The weighted correlation function is plotted against time delays and a sharp peak in the graph is an indication of good fringes.

In the plot of the correlation function versus time delays, the central peak of the plot denotes the approximate position of the true delay on the abscissa (see Figure 3.5). The exact peak is determined by fitting a theoretical function to the plot of the correlation function. In a perfect situation, the observed true delay ($\tau_0$) should be the same as the predicted geometric delay ($\tau_g$). Any difference between these two time delays ($\tau_0 - \tau_g$) is due to errors in apriori knowledge of baseline parameters and other effects such as clock offset error, differential refraction and instrumental delays.

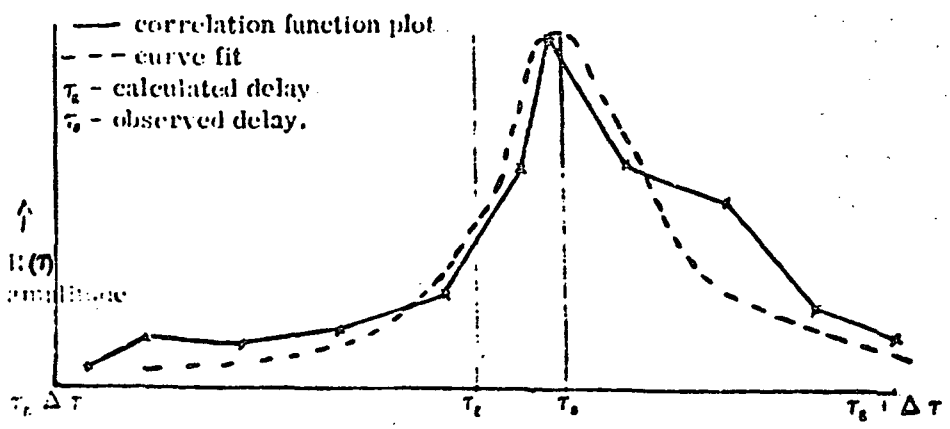


Figure 3.5 Fringe Amplitude Plotted Against Time Delays.

The accuracy with which the time delay is measured depends on the receiver bandwidth, among other factors. When a receiver is tuned to a central frequency $\omega_1$

it receives a broad range of frequencies centered about $\omega$. The width of this range depends on the receiver characteristics and if this bandwidth is $\Delta\omega$, then the accuracy of the delay measurement depends on the correlation interval $\Delta\tau$ given by

$$\Delta\tau = \frac{1}{2 \cdot \Delta\omega} . \qquad (3.7)$$

Thus the accuracy can be increased by narrowing the correlation interval, i.e. increasing the bandwidth. Although there are practical limitations on the bandwidth attainable with a receiver, the effective bandwidth can be made larger by sampling narrow band video signals from many widely separated windows. This method is described in detail by Hinteregger [34].

### 3.3 Equations for the VLBI Measured Time Delays.

It has been shown in the last section how the VLBI operates and that the observed quantities of interest to geodesists is the difference in the time of arrival at two separated antennas of a particular wavefront from a given point source of radio radiation. This relative time delay (or phase delay) is a function of the source direction, the antenna locations, the relative clock error between the two sites and any other influences such as the differential atmospheric refraction. By expressing the measured time delay as a function of the various parameters involved, and with sufficiently large number of observations for each of the observed celestial radio sources, the "best fit" values of the parameters can be estimated by weighted least-squares analysis.

In this section, expressions relating VLBI measured time delays to parameters which influence the measurements will be derived for different

configurations of interferometer stations. The three basic configurations envisaged are those VLBI observations involving:

(1) two stations on the earth (earth-earth VLBI)

(2) two stations on the moon (moon-moon VLBI)

(3) one station each on the earth and on the moon (earth-moon VLBI).

Although the primary interest in this study is the investigation of application of VLBI to selenodetic control, other parameters indirectly connected with the determination of coordinates of points on the moon will also be considered. Thus, the case of the earth-earth VLBI will be treated even though selenodetic control cannot be derived directly from the observations except in the case of the earth stations observing an artificial radio source on the moon.

3.31 Earth-Earth VLBI Equations.

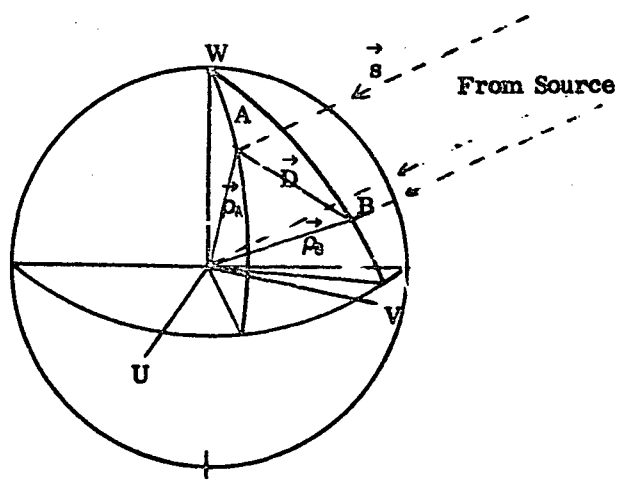


Figure 3.6 Earth-Earth VLBI Observation.

Two radio antennas A and B situated on the earth have position vectors $\vec{\rho}_A$ and $\vec{\rho}_B$ respectively. The inter-site vector $\vec{D}$ is given by

$$\vec{D} = \vec{\rho}_B - \vec{\rho}_A \,. \tag{3.8}$$

The position vectors of $\vec{\rho}_A$ and $\vec{\rho}_B$ can be obtained from the geodetic coordinates of $A(\varphi_A, \lambda_A, h_A)$ and $B(\varphi_B, \lambda_B, h_B)$ as

$$\begin{aligned} \vec{\rho}_A &= U_A \vec{i} + V_A \vec{j} + W_A \vec{k} \\ \vec{\rho}_B &= U_B \vec{i} + V_B \vec{j} + W_B \vec{k} \end{aligned} \tag{3.9}$$

where

$$\begin{bmatrix} U_A \\ V_A \\ W_A \end{bmatrix} = \begin{bmatrix} (N_A + h_A) \cos\varphi_A \cos\lambda_A \\ (N_A + h_A) \cos\varphi_A \sin\lambda_A \\ (N_A (1-e^2) + h_A) \sin\varphi_A \end{bmatrix} \tag{3.10}$$

$$\begin{bmatrix} U_B \\ V_B \\ W_B \end{bmatrix} = \begin{bmatrix} (N_B + h_B) \cos\varphi_B \cos\lambda_B \\ (N_B + h_B) \cos\varphi_B \sin\lambda_B \\ (N_B (1-e^2) + h_B) \sin\varphi_B \end{bmatrix} \tag{3.11}$$

and

$$N = \frac{a}{(1-e^2 \sin^2\varphi)^{\frac{1}{2}}} \,.$$

Also, $\vec{i}, \vec{j}, \vec{k}$ are unit vectors along the U, V, W earth-fixed coordinate system. Thus the vector $\vec{D}$ expressed in the U, V, W coordinate system is given by

$$\vec{D} = d_U \vec{i} + d_V \vec{j} + d_W \vec{k} \tag{3.12}$$

where

$$\begin{bmatrix} d_U \\ d_V \\ d_W \end{bmatrix} = \begin{bmatrix} U_B \\ V_B \\ W_B \end{bmatrix} - \begin{bmatrix} U_A \\ V_A \\ W_A \end{bmatrix} . \qquad (3.13)$$

Let $\vec{s}$ represent the unit vector from the radio source to the geocenter Natural radio sources such as quasars are at extragalactic distances away, so that the geocentric parallax can be neglected. Thus, $\vec{s}$ also represents the vector from the source to any point on the earth. The vector $\vec{s}$ is obtainable from the catalog of radio sources which gives the celestial positions of the sources in a celestial coordinate system (usually the 1950.0 mean equatorial system). If the cataloged source position is $\alpha_o$, $\delta_o$, then the components of the unit vector $\vec{s}_o$ expressed in the 1950.0 mean equatorial Cartesian coordinate system is given by the direction numbers as

$$s_o = \begin{bmatrix} -\cos\delta_o \cos\alpha_o \\ -\cos\delta_o \sin\alpha_o \\ -\sin\delta_o \end{bmatrix} . \qquad (3.14)$$

The true equatorial Cartesian coordinates of the source at the observation epoch is obtained from $\vec{s}_o$ by applying precession and nutation.

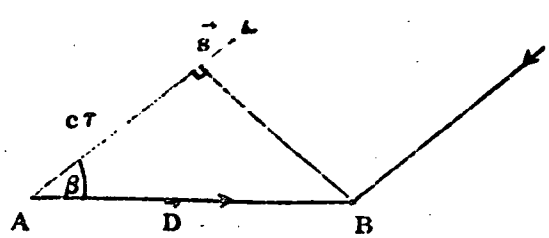

The delay $\tau$ is a function of the baseline length d and the source direction with respect to the baseline as

$$\tau = \frac{d \cos \beta}{c}, \quad c - \text{light velocity.}$$

Thus, if the vectors $\vec{D}$ and $\vec{s}$ are expressed in the same system, then since $\vec{s}$ is a unit vector,

$$\tau = \frac{1}{c} (\vec{D} \cdot \vec{s}). \tag{3.15}$$

The above equation would give the difference between the two times of arrival ($t_2$, $t_1$) of the wavefront at B and A if station B remained stationary during the interval ($t_2$-$t_1$). However, due to the change in the position of B in the interval ($t_2$-$t_1$), the true delay is

$$\tau = \frac{1}{c} [\vec{D} \cdot \vec{s}] \left[ 1 + \frac{\vec{\rho}_B \cdot \vec{s}}{c} \right] \tag{3.16}$$

where $\vec{\rho}_B$ is the velocity of site B in the same coordinate system in which $\vec{s}$ and $\vec{D}$ are expressed.

The vectors $\vec{D}$ and $\vec{s}$ are two vectors in space, and their scalar (dot) product would remain the same irrespective of the coordinate system in which the components of the two vectors are expressed. It is only important that the components of vectors be expressed in the same coordinate system. For convenience, as well as for the desire to work in an inertial coordinate system, the 1950.0 mean equatorial coordinate system can be chosen. Thus, if $\vec{s}_0$ and $\vec{D}_0$ are the vectors $\vec{D}$ and $\vec{s}$ whose components are expressed in the 1950.0 mean equatorial coordinate system, then

$$\vec{D}_0 = [T] \vec{D} \tag{3.17}$$

and $\vec{s}_o$ is given by equation (3.14). [T] is a transformation matrix necessary to transform the $\vec{D}$ vector expressed in the UVW coordinate system to $\vec{D}_o$ vector expressed in the 1950.0 mean equatorial system (XYZ). Thus

$$[T] = P^1 N^1 S^1$$

where P, N, S are 3 x 3 orthogonal transformation matrices, whose full expressions have been given earlier in Chapter 2. Equation (3.17) can now be written as

$$\vec{D}_o = [P^T N^T S^T] \vec{D}. \tag{3.18}$$

In a similar manner, the vector $\vec{\rho}_B$ (in equation (3.9) can be expressed in the 1950.0 mean equatorial coordinate system:

$$\vec{\rho}_{B_o} = [P^T N^T S^T] \vec{\rho}_B. \tag{3.19}$$

In equation (3.16), the rate of change of the vector $\vec{\rho}_{B_o}$ with respect to time is required. Rewriting equation (3.19) by substituting expressions for $S^T$, $N^T$ and $P^T$,

$$\vec{\rho}_{B_o} = [R_3(\zeta_o)R_2(-\theta_1)R_3(z_1)R_1(-\epsilon)R_3(\Delta\psi)R_1(\epsilon + \Delta\epsilon)R_3(-\Theta)R_1(y_P)R_2(x_P)]\vec{\rho}_B. \tag{3.20}$$

Differentiating equation (3.20) with respect to time:

$$\begin{aligned}\frac{d}{dt}\vec{\rho}_{B_o} = \dot{\vec{\rho}}_{B_o} = [&(\dot{\zeta}_o L_3 P^T N^T S^T) - (\dot{\theta}_1 R_3(\zeta_o) L_2 R_2(-\theta_1) R_3(z_1) N^T S^T) + \\ &+ (\dot{z}_1 P^T L_3 N^T S^T) - (\dot{\epsilon} P^T L_1 N^T S^T) + (\dot{\epsilon} P^T N^T L_1 S^T) + \\ &+ (\Delta\dot{\psi} P^T R_1(\epsilon) L_3 R_3(\Delta\psi) R_1(\epsilon + \Delta\epsilon) S^T) + (\Delta\dot{\epsilon} P^T N^T L_1 S^T) + \\ &- (\dot{\Theta} P^T N^T L_3 S^T) + (\dot{y}_P P^T N^T R_3(-\Theta) L_1 R_1(y_P) R_2(x_P) + \\ &+ (\dot{x}_P P^T N^T S^T L_2)]\vec{\rho}_B.\end{aligned} \tag{3.21}$$

In the expression for $\vec{\rho}_{B_o}$, the subscripted L matrices are the Lucas matrices defined in Chapter 2. The dotted quantities are the rate of change of those

quantities which can be obtained by differentiating the expression for each quantity with respect to time. Analytical expressions as functions of time do exist for each of the dotted quantities except for $\dot{x}_p$ and $\dot{y}_p$, whose values, though small, can be calculated from tabulated $x_p$ and $y_p$ values. The $\vec{\rho}_B$ vector, expressed in a geodetic UVW coordinate system, is invariant with time.

If the vectors $\vec{D}_0$, $\vec{s}_0$ and $\vec{\rho}_{B_0}$ have been evaluated from their equations given above, let

$$\begin{aligned} \vec{D}_0 &= D_1\vec{i} + D_2\vec{j} + D_3\vec{k} \\ \vec{s}_0 &= s_1\vec{i} + s_2\vec{j} + s_3\vec{k} \\ \vec{\rho}_{B_0} &= v_1\vec{i} + v_2\vec{j} + v_3\vec{k} \end{aligned} \qquad (3.22)$$

where

$\vec{i}, \vec{j}, \vec{k}$ now represent unit vectors along the X, Y, Z axes that define the 1950.0 mean equatorial Cartesian coordinate system.

Then equation (3.16) can be written as

$$c \cdot \tau = (D_1s_1 + D_2s_2 + D_3s_3)\left[1 + \frac{(v_1s_1 + v_2s_2 + v_3s_3)}{c}\right]. \qquad (3.23)$$

Equation (3.23) represents the prediction equation for the measured time delay for VLBI observations involving two stations which are located on the earth's surface. The predicted values are compared with the observed values and the differences can be used in an adjustment process to correct the parameters which implicitly appear on the right hand side of equation (3.23).

Alternate expressions for the equations for the two vectors $\vec{D}_0$ and $\vec{\rho}_{B_0}$ can be derived by considering that the orientation of the UVW coordinate system with respect to an inertial system is equivalent to three Eulerian

(orientation) angles at observation epoch. This concept, and how to obtain the orientation angles and their time rates is given in Chapter 4 of this work.

Let $\theta$, $\psi$ and $\Phi$ define the orientation of the UVW coordinate system with respect to the mean ecliptic coordinate system of 1950.0. Then, the vector $\vec{D}_o$ is given by

$$\vec{D}_o = [R_1(-\epsilon_o)T^T]\vec{D} = [R_1(-\epsilon_o)R_3(-\psi)R_1(\theta)R_3(-\Phi)]\vec{D} \qquad (3.24)$$

where

$$T = R_3(\Phi)R_1(-\theta)R_3(\psi)$$

$\epsilon_o$ is the mean obliquity of the equator at 1950.0.

Similarly,

$$\vec{\rho}_{B_o} = [R_1(-\epsilon_o)R_3(-\psi)R_1(\theta)R_3(-\Phi)]\vec{\rho}_B = [R_1(\epsilon_o)T^T]\vec{\rho}_B \qquad (3.25)$$

Differentiating equation (3.25) with respect to time

$$\dot{\vec{\rho}}_{B_o} = [-(\dot{\psi}R_1(-\epsilon_o)L_3T^T)+(\dot{\theta}R_1(\epsilon_o)R_3(-\psi)L_1R_1(\theta)R_3(-\Phi))+(-\dot{\Phi}R_1(\epsilon_o)T^TL_3)]\vec{\rho}_B \qquad (3.26)$$

Since $\dot{\psi}$, $\dot{\theta}$ and $\dot{\Phi}$ are obtained from numerical integration as well as $\theta$, $\psi$ and $\Phi$, the equations for $\vec{D}_o$ vector and $\vec{\rho}_{B_o}$ vector can be evaluated. The predicted time delay can then be evaluated from equation (3.23).

Observation Equations for Earth-Earth VLBI.

In order to use the differences between the predicted and the observed time delays in improving the present knowledge of the parameters involved in VLBI observations, it is necessary to derive the partial derivatives of the time delay with respect to the parameters. The paramet[illegible]s involved are the station coordinates, the positions of the sources, t[illegible] precessional elements, nutation and polar motion parameters and the [illegible]wich apparent sidereal time. Alternatively, the Eulerian angles $\theta$, $\psi$ [illegible]an be regar[illegible] as parameters, in addition to the positions of the statio[illegible] and radi[illegible] sources.

The equation for the predicted time delay (equation (3.23)) can be written,

in matrix notation, as

$$\tau = \frac{1}{c}\left[(D^T s) + \frac{1}{c^2}(D^T s\, v^T s)\right] \tag{3.27}$$

where

$$D_0 = D = \begin{bmatrix} D_1 \\ D_2 \\ D_3 \end{bmatrix}$$

$$s_0 = s = \begin{bmatrix} s_1 \\ s_2 \\ s_3 \end{bmatrix}$$

and

$$v = \begin{bmatrix} v_1 \\ v_2 \\ v_3 \end{bmatrix}.$$

The partials of $\tau$ in equation (3.27) are given by

$$\frac{\partial \tau}{\partial D} = \frac{1}{c}\left[s^T\right] + \frac{1}{c^2}\left[s^T v\, s^T\right] \tag{3.28}$$

$$\frac{\partial \tau}{\partial s} = \frac{1}{c}\left[D^T\right] + \frac{1}{c^2}\left[(D^T s v^T) + (v^T s\, D^T)\right] \tag{3.29}$$

$$\frac{\partial \tau}{\partial v} = \frac{1}{c^2}\left[s^T D\, s^T\right] \tag{3.30}$$

Each of the above equations for partials results in a 1 x 3 row matrix. The elements of the matrices D, s, v are functions of parameters, and the matrices will have to be differentiated with respect to these parameters. Hence if the parameter list is represented by vector $\varkappa$, i.e.

$$D = f_1(\varkappa)$$

$$s = f_2(\varkappa)$$

$$v = f_3(\varkappa).$$

Then

$$\frac{\partial \tau}{\partial \varkappa} = \frac{\partial \tau}{\partial D} \cdot \frac{\partial D}{\partial \varkappa} + \frac{\partial \tau}{\partial s} \cdot \frac{\partial s}{\partial \varkappa} + \frac{\partial \tau}{\partial v} \cdot \frac{\partial v}{\partial \varkappa} \tag{3.31}$$

where the partials $\frac{\partial D}{\partial \varkappa}$, $\frac{\partial s}{\partial \varkappa}$ and $\frac{\partial v}{\partial \varkappa}$ are obtained by differentiating expressions for D, s, and v.

From equation (3.14)

$$s = \begin{bmatrix} -\cos\delta_o \cos\alpha_o \\ -\cos\delta_o \sin\alpha_o \\ -\sin\delta_o \end{bmatrix}.$$

Hence

$$\frac{\partial s}{\partial \delta_o} = \begin{bmatrix} \sin\delta_o \cos\alpha_o \\ \sin\delta_o \sin\alpha_o \\ -\cos\delta_o \end{bmatrix}. \tag{3.32}$$

$$\frac{\partial s}{\partial \alpha_o} = \begin{bmatrix} \cos\delta_o \sin\alpha_o \\ -\cos\delta_o \cos\alpha_o \\ 0 \end{bmatrix} \tag{3.33}$$

so that $\frac{\partial \tau}{\partial \delta_o}$, $\frac{\partial \tau}{\partial \alpha_o}$ are obtained using equation (3.31).

From equations (3.18) and (3.13),

$$D = (R_3(\zeta_o)R_2(-\theta_1)R_3(z_1)R_1(-\epsilon)R_3(\Delta\psi)R_1(\epsilon + \Delta\epsilon)R_3(-\Theta)R_1(y_p)R_2(x_p)) \begin{bmatrix} d_u \\ d_v \\ d_w \end{bmatrix}.$$

Hence

$$\frac{\partial D}{\partial \zeta_o} = L_3 P^T N^T S^T \begin{bmatrix} d_u \\ d_v \\ d_w \end{bmatrix} \tag{3.34}$$

$$\frac{\partial D}{\partial \theta_1} = -R_3(\zeta_o)\, L_2\, R_2(-\theta_1) R_3(z_1) N^T S^T \begin{bmatrix} d_u \\ d_v \\ d_w \end{bmatrix} \tag{3.35}$$

$$\frac{\partial D}{\partial z_1} = P^T L_3 N^T S^T \begin{bmatrix} d_u \\ d_v \\ d_w \end{bmatrix} \tag{3.36}$$

$$\frac{\partial D}{\partial \epsilon} = -P^T L_1 N^T S^T \begin{bmatrix} d_u \\ d_v \\ d_w \end{bmatrix} + P^T N^T L_1 S^T \begin{bmatrix} d_u \\ d_v \\ d_w \end{bmatrix} \tag{3.37}$$

$$\frac{dD}{d\Delta\psi} = P^T R_1(-\epsilon) L_3 R_3(\Delta\psi) R_1(\epsilon + \Delta\epsilon) S^T \begin{bmatrix} d_U \\ d_V \\ d_W \end{bmatrix} \tag{3.38}$$

$$\frac{dD}{d\Delta\epsilon} = P^T N^T L_1 S^T \begin{bmatrix} d_U \\ d_V \\ d_W \end{bmatrix} \tag{3.39}$$

$$\frac{dD}{d\Theta} = -P^T N^T L_3 S^T \begin{bmatrix} d_U \\ d_V \\ d_W \end{bmatrix} \tag{3.40}$$

$$\frac{dD}{dy_p} = P^T N^T R_3(-\Theta) L_1 R_1(y_p) R_2(x_p) \begin{bmatrix} d_U \\ d_V \\ d_W \end{bmatrix} \tag{3.41}$$

$$\frac{dD}{dx_p} = P^T N^T S^T L_2 \begin{bmatrix} d_U \\ d_V \\ d_W \end{bmatrix} . \tag{3.42}$$

Since

$$\begin{bmatrix} d_U \\ d_V \\ d_W \end{bmatrix} = \begin{bmatrix} U_B \\ V_B \\ W_B \end{bmatrix} - \begin{bmatrix} U_A \\ V_A \\ W_A \end{bmatrix} ,$$

$$\frac{\partial D}{\partial \begin{bmatrix} U_A \\ V_A \\ W_A \end{bmatrix}} = -P^T N^T S^T \tag{3.43a}$$

$$\frac{\partial D}{\partial \begin{bmatrix} U_B \\ V_B \\ W_B \end{bmatrix}} = P^T N^T S^T \tag{3.43b}$$

As can be expected, both $\vec{\rho}_A$ and $\vec{\rho}_B$ vectors cannot be solved for together and either of the vectors have to be fixed. Also, all the parameters whose partials are given by equations (3.35) to (3.42) are "variable" parameters, and their values vary from instant to instant. However, each of the parameters can be expressed as functions of another set of "non-varying" parameters. It is desirable to replace the "variable" parameters with the "non-varying" set, and this can be done with the same equations given in Section 2.4 of this work.

The alternate expression for D, from equation (3.24) is given by:

$$D = R_1(-\epsilon_0)R_3(-\psi)R_1(\zeta)R_3(-\Phi)\begin{bmatrix} d_u \\ d_v \\ d_w \end{bmatrix} = R_1(-\epsilon_0)T^T\begin{bmatrix} d_u \\ d_v \\ d_w \end{bmatrix}$$

so that

$$\frac{\partial D}{\partial \epsilon_0} = -L_1\ R_1(-\epsilon_0)T^T\begin{bmatrix} d_u \\ d_v \\ d_w \end{bmatrix} \tag{3.44}$$

$$\frac{\partial D}{\partial \psi} = -R_1(-\epsilon_0) L_3 \; T^T \begin{bmatrix} d_u \\ d_v \\ d_w \end{bmatrix} \tag{3.45}$$

$$\frac{\partial D}{\partial \theta} = R_1(-\epsilon_0) R_3(-\psi) L_1 R_1(\theta) R_3(-\Phi) \begin{bmatrix} d_u \\ d_v \\ d_w \end{bmatrix} \tag{3.46}$$

$$\frac{\partial D}{\partial \Phi} = -R_1(-\epsilon_0) T^T L_3 \begin{bmatrix} d_u \\ d_v \\ d_w \end{bmatrix} \tag{3.47}$$

$$\frac{\partial D}{\partial \begin{bmatrix} U_A \\ V_A \\ W_A \end{bmatrix}} = -R_1(-\epsilon_0) T^T \tag{3.48}$$

and

$$\frac{\partial D}{\partial \begin{bmatrix} U_B \\ V_B \\ W_B \end{bmatrix}} = R_1(-\epsilon_0) T^T. \tag{3.49}$$

The "variable" parameters $\theta$, $\psi$ and $\Phi$ can be replaced by the initial conditions ($\theta_0$, $\psi_0$, $\Phi_0$, $\dot{\theta}_0$, $\dot{\psi}_0$ and $\dot{\Phi}_0$) and the partials of $\tau$ with respect to these "non-varying" parameters can be obtained by using the state transition matrix (see Chapter 4), equations (3.45) to (3.47) and equation (3.31).

The expression for $\dot{\vec{\rho}}_{B_O}$ given by equation (3.21) should also be differentiated with respect to the parameters in order to define all the terms appearing in equation (3.31) (the v matrix is represented by the vector $\dot{\vec{\rho}}_{B_O}$). The largest of the terms in equation (3.21) is that dependent on the sidereal rate, i.e.,

$$\dot{\vec{\rho}}_{B_O} = v \approx -\dot{\Theta}(P^T N^T L_3 S^T) \begin{bmatrix} U_B \\ V_B \\ W_B \end{bmatrix} . \tag{3.50}$$

Partials of equation (3.50) are given by:

$$\frac{\partial v}{\partial \dot{\Theta}} \approx -(P^T N^T L_3 S^T) \begin{bmatrix} U_B \\ V_B \\ W_B \end{bmatrix} \tag{3.51}$$

$$\frac{\partial v}{\partial \zeta_0} \approx -\dot{\Theta}(L_3 P^T N^T L_3 S^T) \begin{bmatrix} U_B \\ V_B \\ W_B \end{bmatrix} \tag{3.52}$$

$$\frac{\partial v}{\partial \theta_1} \approx \dot{\Theta}(R_3(\zeta_0)\, L_2\, R_2(-\theta_1) R_3(z_1) N^T\, L_3\, S^T) \begin{bmatrix} U_B \\ V_B \\ W_B \end{bmatrix} \tag{3.53}$$

$$\frac{\partial v}{\partial z_1} \approx -\dot{\Theta}(P^T L_3 N^T L_3 S^T) \begin{bmatrix} U_B \\ V_B \\ W_B \end{bmatrix} \tag{3.54}$$

$$\frac{\partial v}{\partial \epsilon} \approx \dot{\Theta}(P^T L_1 N^T L_3 S^T) - \dot{\Theta}(P^T N^T L_1 L_3 S^T) \begin{bmatrix} U_B \\ V_B \\ W_B \end{bmatrix} \tag{3.55}$$

$$\frac{\partial v}{\partial \Delta\psi} \approx -\dot{\Theta}(P^T R_1(-\epsilon) L_3 R_3(\Delta\psi) R_1(\epsilon + \Delta\epsilon) L_3 S^T) \begin{bmatrix} U_B \\ V_B \\ W_B \end{bmatrix} \tag{3.56}$$

$$\frac{\partial v}{\partial \Delta\epsilon} \approx -\dot{\Theta}(P^T N^T L_1 L_3 S^T) \begin{bmatrix} U_B \\ V_B \\ W_B \end{bmatrix} \tag{3.57}$$

$$\frac{\partial v}{\partial \Theta} \approx \dot{\Theta}(P^T N^T L_3 L_3 S^T) \begin{bmatrix} U_B \\ V_B \\ W_B \end{bmatrix} \tag{3.58}$$

$$\frac{\partial v}{\partial \begin{bmatrix} U_B \\ V_B \\ W_B \end{bmatrix}} = -\dot{\Theta}(P^T N^T L_3 S^T) \quad . \tag{3.59}$$

If the alternate expression for $\vec{\rho}_{B_0}$ is used (equation (3.26)), then the largest

term is the $\dot{\Phi}$ dependent term, so that

$$v \approx -\dot{\Phi}\,(R_1(-\epsilon_0)T^T L_3) \begin{bmatrix} U_B \\ V_B \\ W_B \end{bmatrix}. \tag{3.60}$$

In this case, the partials of v are

$$\frac{\partial v}{\partial \dot{\Phi}} \approx -(R_1(-\epsilon_0)T^T L_3) \begin{bmatrix} U_B \\ V_B \\ W_B \end{bmatrix} \tag{3.61}$$

$$\frac{\partial v}{\partial \epsilon_0} \approx \dot{\Phi}\,(L_1 R_1(-\epsilon_0)T^T L_3) \begin{bmatrix} U_B \\ V_B \\ W_B \end{bmatrix} \tag{3.62}$$

$$\frac{\partial v}{\partial \psi} \approx \dot{\Phi}(R_1(-\epsilon_0)\, L_3\, T^T L_3) \begin{bmatrix} U_B \\ V_B \\ W_B \end{bmatrix} \tag{3.63}$$

$$\frac{\partial v}{\partial \theta} \approx -\dot{\Phi}(R_1(-\epsilon_0)R_3(-\psi)L_1R_1(\theta)R_3(-\dot{\Phi})L_3) \begin{bmatrix} U_B \\ V_B \\ W_B \end{bmatrix} \tag{3.64}$$

$$\frac{\partial v}{\partial \Phi} \approx \dot{\Phi}(R_1(-\epsilon_0)T^T L_3 L_3) \begin{bmatrix} U_B \\ V_B \\ W_B \end{bmatrix} \tag{3.65}$$

$$\frac{\partial v}{\partial \begin{bmatrix} U_B \\ V_B \\ W_B \end{bmatrix}} \approx -\dot{\Phi}\,(R_1(-\epsilon_0)T^T L_3). \tag{3.66}$$

As in the case of the partials of $\lceil D \rceil$, the "variable" parameters in the above expressions for the partials of $\lceil v \rceil$ should be replaced by another set of "non-varying" parameters. Then, equation (3.31) can be evaluated for the partials of the time delay with respect to the parameters (denoted by vector $x$).

The time delay equation, if the small $\dot{\rho}_{B_C}$ — dependent correction term is neglected, and the error in time synchronization is added, is:

$$\tau \approx \frac{1}{c}\,(\vec{D}_0 \cdot \vec{s}_0) + \delta t_c \tag{3.67}$$

where $\delta t_c$ is the clock synchronization error. The $\vec{D}_0$ vector can be expressed as

$$D_0 = \begin{bmatrix} d \cos \delta_L \cos \alpha_L \\ d \cos \delta_L \sin \alpha_L \\ d \sin \delta_L \end{bmatrix} \tag{3.68}$$

where

d is the length of the $\vec{D}_0$ vector

$\alpha_L$, $\delta_L$ are the angular coordinates of the vector $\vec{D}_0$ in the inertial coordinate system.

The changing direction $\vec{D}_0$ in space due to the rotation of the earth changes the angular coordinate $\alpha_L$. The vector $\vec{s}_0$ is given by equation (3.14). Thus equation (3.67) gives

$$\tau = \frac{d}{c}\left[\sin\delta_L \sin\delta_0 + \cos\delta_L \cos\delta_0 \cos(\alpha_L - \alpha_0)\right] + \delta t_c \,. \qquad (3.69)$$

If the transformation parameters involving precession, nutation, polar motion and earth's rotation rate are assumed known, then the number of unknowns are three for the intersite vector, two for the source vector in space of each observed radio source and one for the error in initial clock synchronization. Hence the total number of parameters for n observed sources for a baseline is 2n + 4. However, by assuming the knowledge of the rotation axis direction and rotation rate, the origin of longitude is still not defined. By fixing one more parameter for the definition of longitude origin, the number of independent unknowns reduces to 2n + 3. Any number of observations made to one source from a baseline can only resolve three quantities which are the components of $\vec{D}_0 \cdot \vec{s}_0$ along the earth's axis of rotation plus $\delta t_c$, and the coefficients of the sinusoidally changing components of $\vec{D}_0 \cdot \vec{s}_0$ along two orthogonal directions in the earth's equatorial plane. In order to determine $\vec{D}$, at least three observations must be made of at least n sources where n is the smallest integer that satisfies the equation

$$3n \geq 2n + 3 \qquad (3.70)$$

which gives n to be 3.

The absolute accuracy of the velocity of light in vacuum is about 1 ppm. which is much less accurate than the measurement of time delay. However, whatever value of c is used in the computations merely provides a scale for

the whole system of measurement.

3.32 Moon-Moon VLBI Equations.

The equations in this section are derived for the case in which there are two or more radio antennas located on the moon. These stations, if located at sufficiently large distances, provide a network of selenodetic control, whose positions can be determined by the VLBI method. The observing procedure would remain basically the same as the earth-located VLBI stations although slight modifications may be necessary for practical purposes. It is assumed that the measured quantities would be time delays as in the case of earth-earth VLBI.

Let VLBI observations be made at two stations A, B on the lunar surface, whose position vector from the lunar center in the selenodetic coordinate system (see Section 2.32) are $\vec{r}_A$, $\vec{r}_B$ respectively.

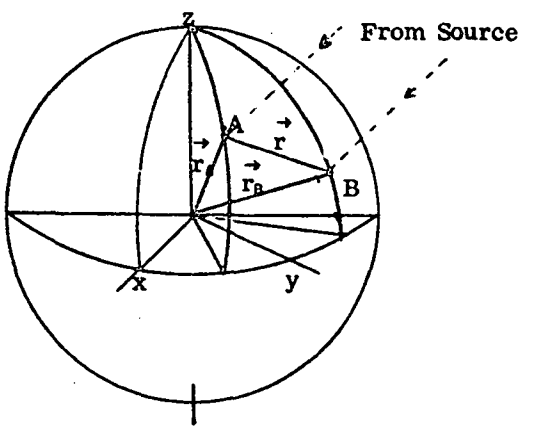


Figure 3.7 Moon-Moon VLBI Observations.

The components of the two vectors, in the xyz selenodetic system are

$$\begin{bmatrix} x_A \\ y_A \\ z_A \end{bmatrix} = \begin{bmatrix} r_A \cos b_A \cos \ell_A \\ r_A \cos b_A \sin \ell_A \\ r_A \sin b_A \end{bmatrix} \tag{3.71a}$$

$$\begin{bmatrix} x_B \\ y_B \\ z_B \end{bmatrix} = \begin{bmatrix} r_B \cos b_B \cos \ell_B \\ r_B \cos b_B \sin \ell_B \\ r_B \sin b_B \end{bmatrix} . \tag{3.71b}$$

If the vector from A to B is $\vec{r}$ then

$$\vec{r} = \vec{r_A} - \vec{r_B} \tag{3.72a}$$

and in matrix notation

$$r = \begin{bmatrix} r_x \\ r_y \\ r_z \end{bmatrix} = \begin{bmatrix} x_B \\ y_B \\ z_B \end{bmatrix} - \begin{bmatrix} x_A \\ y_A \\ z_A \end{bmatrix} . \tag{3.72b}$$

The vector $\vec{s}$ is a unit vector from the lunar center to the radio source. Because of the small diameter of the moon compared to the distances of the radio sources, the vector $\vec{s}$ also represents the unit vector from the radio source in the direction of any point on the lunar surface.

As was pointed out in Section 3.31, the VLBI time delay ($\tau$) can be calculated approximately by

$$\tau \approx \frac{1}{c} (\vec{r_0} \cdot \vec{s_0}) \tag{3.73}$$

where $\vec{r_0}$ and $\vec{s_0}$ are the vectors $\vec{r}$, $\vec{s}$ whose components are expressed in the same coordinate system. The most convenient coordinate system for

space orientation on the moon is the ecliptic coordinate system. Consequently, the $\vec{r}$ and $\vec{s}$ vectors can be expressed in an inertial coordinate system represented by the 1950.0 mean ecliptic system.

If the 1950.0 geocentric mean equatorial coordinates of the source is given as $\alpha_0$, $\delta_0$, the geocentric mean ecliptic coordinates are obtained by a positive $R_1$ rotation through an angle equal to the mean obliquity of the equator of 1950.0 ($\epsilon_0$). Thus the mean ecliptic coordinates $\lambda_0$, $\beta_0$ are obtained from

$$\begin{bmatrix} \cos\beta_0 \cos\lambda_0 \\ \cos\beta_0 \sin\lambda_0 \\ \sin\beta_0 \end{bmatrix} = R_1(\epsilon_0) \begin{bmatrix} -\cos\delta_0 \cos\alpha_0 \\ -\cos\delta_0 \sin\alpha_0 \\ -\sin\delta_0 \end{bmatrix} . \qquad (3.74)$$

The "lunar monthly parallax of the moon" as defined by Kolaczek [50] is very small for the radio sources and the effect of this parallax on translation of the center of the ecliptic coordinate system from the geocenter to the selenocenter can be neglected. Therefore, the selenocentric mean ecliptic coordinates of the source is also given by equation (3.74).

The $\vec{r}$ vector defined in equation (3.72b) has its components $r_x$, $r_y$, $r_z$ along the selenodetic Cartesian coordinate system. This coordinate system is related to the mean ecliptic system of date by the three Eulerian angles $\theta$, $\psi$ and $\varphi$, as defined in Section 2.34. The $\vec{r_0}$ vector, with components along the 1950.0 mean ecliptic Cartesian coordinate axes is given by

$$r_0 = \begin{bmatrix} r_1 \\ r_2 \\ r_3 \end{bmatrix}_{\text{ecl. 1950.0}} = R_1(\epsilon_0) P^T R_1(-\epsilon) T^T \begin{bmatrix} r_x \\ r_y \\ r_z \end{bmatrix} \qquad (3.75)$$

where

P is the precession matrix

and

$$T = R_3(\Psi)R_1(-\theta)R_3(\psi) .$$

In analogy with equation (3.16), the exact equation for the time delay $\tau$, taking into account the motion of one of the two VLBI stations between the interval $\tau$ expressed by equation (3.73) is

$$\tau = \frac{1}{c}(\vec{r}_0 \cdot \vec{s}_0)\left[1 + \frac{\dot{\vec{r}}_{B_0} \cdot \vec{s}_0}{c}\right] \tag{3.76}$$

where

$\dot{\vec{r}}_{B_0}$ is the velocity of site B in the same coordinate system in which $\vec{r}_0$ and $\vec{s}_0$ are defined.

The vector $\dot{\vec{r}}_{B_0}$ is obtained by differentiating with respect to time, the vector $\vec{r}_{B_0}$, which is

$$\vec{r}_{B_0} = R_1(\epsilon_0)P^T R_1(-\epsilon)T^T \vec{r}_B \tag{3.77a}$$

or

$$r_{B_0} = \begin{bmatrix} r_{B_1} \\ r_{B_2} \\ r_{B_3} \end{bmatrix} = R_1(\epsilon_0)P^T R_1(-\epsilon)T^T \begin{bmatrix} x_B \\ y_B \\ z_B \end{bmatrix} . \tag{3.77b}$$

Since $\epsilon_0$ and $\vec{r}_B$ do not vary with time,

$$\frac{\partial \vec{r}_{B0}}{\partial t} = \dot{\vec{r}}_{B0} = R_1(\epsilon_0)\Big[\dot{\zeta}_0 (L_3 P^T R_1(-\epsilon) T^T) - \dot{\theta}_1 (R_3(\zeta_0) L_2 R_2(-\theta_1)$$

$$R_3(z_1) R_1(-\epsilon) T^T) + \dot{z}_1 (P^T L_3 R_1(-\epsilon) T^T) - \dot{\epsilon}(P^T L_1 R_1(-\epsilon) T^T)$$

$$- \dot{\psi}(P^T R_1(-\epsilon) L_3 T^T) - \dot{\theta}(P^T R_1(-\epsilon) R_3(-\psi) L_1 R_1(\theta) R_3(-\Phi))$$

$$- \dot{\Phi}(P^T R_1(-\epsilon) T^T L_3)\Big] \vec{r}_B . \qquad (3.78)$$

Thus if

$$\vec{r}_0 = r_1 \vec{i} + r_2 \vec{j} + r_3 \vec{k}$$

$$\dot{\vec{r}}_{B0} = \dot{r}_{B1} \vec{i} + \dot{r}_{B2} \vec{j} + \dot{r}_{B3} \vec{k} = v_1 \vec{i} + v_2 \vec{j} + v_3 \vec{k}$$

$$\vec{s}_0 = s_1 \vec{i} + s_2 \vec{j} + s_3 \vec{k}$$

where

$\vec{i}, \vec{j}, \vec{k}$ are unit vector along the X, Y, Z axes defind the 1950.0 mean ecliptic system,

then equation for the time delay (from equation 3.76) is

$$\tau = \frac{1}{c} (r_1 s_1 + r_2 s_2 + r_3 s_3) \left[ 1 + \frac{v_1 s_1 + v_2 s_2 + v_3 s_3}{c} \right] . \qquad (3.79)$$

As in the case of the earth-based VLBI, any differences between time delays observed and predicted using equation (3.79) can be used in an adjustment process to correct the assumed values of the parameters which appear in the prediction equation. In order to do this, the partials of $\tau$ with respect to the parameters are needed.

To form the partials, equation (3.79) is rewritten in matrix notation as

$$\tau = \frac{1}{c}\left[(r^T s) + \frac{1}{c^2}(r^T s v^T s)\right] \tag{3.80}$$

where the matrices r, s and v are

$$r = r_0 = \begin{bmatrix} r_1 \\ r_2 \\ r_3 \end{bmatrix}$$

$$s = s_0 = \begin{bmatrix} s_1 \\ s_2 \\ s_3 \end{bmatrix}$$

and

$$v = \begin{bmatrix} v_1 \\ v_2 \\ v_3 \end{bmatrix} = \begin{bmatrix} \dot{r}_{\theta_1} \\ \dot{r}_{\theta_2} \\ \dot{r}_{\theta_3} \end{bmatrix} .$$

The partials of $\tau$ with respect to r, s and v are given by equations (3.28), (3.29) and (3.30) respectively if the matrix r is substituted for the matrix D in those equations. Similarly, since the elements of the matrices r, s and v are functions of parameters (represented by the vector $\varkappa$), the partials of $\tau$ with respect to the parameters $\varkappa$ are given by equation (3.31), replacing D with r. The partials $\frac{\partial r}{\partial \varkappa}$, $\frac{\partial s}{\partial \varkappa}$ and $\frac{\partial v}{\partial \varkappa}$ will be obtained by differentiating expressions for r, s and v.

Since

$$s = \begin{bmatrix} s_1 \\ s_2 \\ s_3 \end{bmatrix} = R_1(\epsilon_0) \begin{bmatrix} -\cos\delta_0 \cos\alpha_0 \\ -\cos\delta_0 \sin\alpha_0 \\ -\sin\alpha_0 \end{bmatrix},$$

$$\frac{\partial s}{\partial \epsilon_0} = L_1 R_1(\epsilon_0) \begin{bmatrix} -\cos\delta_0 \cos\alpha_0 \\ -\cos\delta_0 \sin\alpha_0 \\ -\sin\delta_0 \end{bmatrix} \tag{3.81}$$

$$\frac{\partial s}{\partial \delta_0} = R_1(\epsilon_0) \begin{bmatrix} \sin\delta_0 \cos\alpha_0 \\ \sin\delta_0 \sin\alpha_0 \\ -\cos\delta_0 \end{bmatrix} \tag{3.82}$$

$$\frac{\partial s}{\partial \alpha_0} = R_1(\epsilon_0) \begin{bmatrix} \cos\delta_0 \sin\alpha_0 \\ -\cos\delta_0 \cos\alpha_0 \\ 0 \end{bmatrix} \tag{3.83}$$

and $\frac{\partial \tau}{\partial \delta_0}$, $\frac{\partial \tau}{\partial \alpha_0}$, $\frac{\partial \tau}{\partial \epsilon_0}$ can be obtained by substituting these equations and equation (3.29) into equation (3.31).

Also, from equation (3.75)

$$r = R_1(\epsilon_0)R_3(\zeta_0)R_2(-\theta_1)R_3(z_1)R_1(-\epsilon)R_3(-\psi)R_1(\theta)R_3(-\Phi) \begin{bmatrix} r_x \\ r_y \\ r_z \end{bmatrix}.$$

Hence, taking partials:

$$\frac{\partial r}{\partial \epsilon_0} = L_1 R_1(\epsilon_0) P^T R_1(-\epsilon) T^T \begin{bmatrix} r_x \\ r_y \\ r_z \end{bmatrix} \tag{3.84}$$

$$\frac{\partial \mathbf{r}}{\partial \zeta_0} = R_1(\epsilon_0) L_0 P^T R_1(-\epsilon) T^T \begin{bmatrix} r_x \\ r_y \\ r_z \end{bmatrix} \tag{3.85}$$

$$\frac{\partial \mathbf{r}}{\partial \theta_1} = -R_1(\epsilon_0) R_3(\zeta_0) L_2 R_2(-\theta_1) R_3(z_1) R_1(-\epsilon) T^T \begin{bmatrix} r_x \\ r_y \\ r_z \end{bmatrix} \tag{3.86}$$

$$\frac{\partial \mathbf{r}}{\partial z_1} = R_1(\epsilon_0) P^T L_3 R_1(-\epsilon) T^T \begin{bmatrix} r_x \\ r_y \\ r_z \end{bmatrix} \tag{3.87}$$

$$\frac{\partial \mathbf{r}}{\partial \epsilon} = -R_1(\epsilon_0) P^T L_1 R_1(-\epsilon) T^T \begin{bmatrix} r_x \\ r_y \\ r_z \end{bmatrix} \tag{3.88}$$

$$\frac{\partial \mathbf{r}}{\partial \psi} = -R_1(\epsilon_0) P^T R_1(-\epsilon) L_3 T^T \begin{bmatrix} r_x \\ r_y \\ r_z \end{bmatrix} \tag{3.89}$$

$$\frac{\partial \mathbf{r}}{\partial \theta} = R_1(\epsilon_0) P^T R_1(-\epsilon) R_3(-\psi) L_1 R_1(\theta) R_3(-\psi) \begin{bmatrix} r_x \\ r_y \\ r_z \end{bmatrix} \tag{3.90}$$

$$\frac{\partial \mathbf{r}}{\partial \Phi} = -R_1(\epsilon_0) P^T R_1(-\epsilon) T^T I_3 \begin{bmatrix} r_x \\ r_y \\ r_z \end{bmatrix}. \tag{3.91}$$

Since

$$\begin{bmatrix} r_x \\ r_y \\ r_z \end{bmatrix} = \begin{bmatrix} x_B \\ y_B \\ z_B \end{bmatrix} - \begin{bmatrix} x_A \\ y_A \\ z_A \end{bmatrix} = r_B - r_A ,$$

$$\frac{\partial r}{\partial r_A} = -(R_1(\epsilon_0)P^T R_1(-\epsilon)T^T) \tag{3.92}$$

$$\frac{\partial r}{\partial r_B} = R_1(\epsilon_0)P^T R_1(-\epsilon)T^T . \tag{3.93}$$

As in the case of the earth based VLBI, the coordinates of the two stations cannot be solved for simultaneously. However, the differences in coordinates can be solved for, or alternatively, one station coordinates can be solved if the coordinates of the other station are held fixed.

The partials of time delay $\tau$ with respect to the parameters that appear in the expression for $\vec{r}_{B_0}$ can be obtained in the same way as was in the case of the earth-earth VLBI. In equation (3.78), the most significant term is the $\dot{\Phi}$-dependent term. By neglecting other terms, the equation for v can be approximated by

$$v \approx -\dot{\Phi}[R_1(\epsilon_0)P^T R_1(-\epsilon)T^T L_3] \begin{bmatrix} x_B \\ y_B \\ z_B \end{bmatrix} . \tag{3.94}$$

Partials of equation (3.94) are:

$$\frac{\partial v}{\partial \epsilon_0} \approx -\dot{\Phi}[L_1 R_1(\epsilon_0)P^T R_1(-\epsilon)T^T L_3] \begin{bmatrix} x_B \\ y_B \\ z_B \end{bmatrix} \tag{3.95}$$

$$\frac{\partial v}{\partial \zeta_0} \approx -\dot{\Phi}\,[R_1(\epsilon_0)L_3P^{\prime}R_1(-\epsilon)T^{\prime}L_3]\begin{bmatrix} x_B \\ y_B \\ z_B \end{bmatrix} \tag{3.96}$$

$$\frac{\partial v}{\partial \theta_1} \approx \dot{\Phi}[R_1(\epsilon_0)R_3(\zeta_0)\,L_3\,R_3\,(-\theta_1)R_3(z_1)R_1(-\epsilon)T^{\prime}L_3]\begin{bmatrix} x_B \\ y_B \\ z_B \end{bmatrix} \tag{3.97}$$

$$\frac{\partial v}{\partial z_1} \approx -\dot{\Phi}[R_1(\epsilon_0)P^{\prime}L_3R_1(-\epsilon)T^{\prime}L_3]\begin{bmatrix} x_B \\ y_B \\ z_B \end{bmatrix} \tag{3.98}$$

$$\frac{\partial v}{\partial \epsilon} \approx \dot{\Phi}[R_1(\epsilon_0)P^{\prime}L_1R_1(-\epsilon)\,T^{\prime}L_3]\begin{bmatrix} x_B \\ y_B \\ z_B \end{bmatrix} \tag{3.99}$$

$$\frac{\partial v}{\partial \psi} \approx \dot{\Phi}[R_1(\epsilon_0)P^{\prime}R_1(-\epsilon)L_3\,T^{\prime}L_3]\begin{bmatrix} x_B \\ y_B \\ z_B \end{bmatrix} \tag{3.100}$$

$$\frac{\partial v}{\partial \theta} \approx -\dot{\Phi}\,[R_1(\epsilon_0)P^{\prime}R_1(-\epsilon)R_3(-\psi)L_1R_1(\theta)R_3(-\Phi)L_3]\begin{bmatrix} x_B \\ y_B \\ z_B \end{bmatrix} \tag{3.101}$$

$$\frac{\partial v}{\partial \Phi} \approx \dot{\Phi}\,[R_1(\epsilon_0)P^{\prime}R_1(-\epsilon)T^{\prime}\,L_3\,L_3\,]\begin{bmatrix} x_B \\ y_B \\ z_B \end{bmatrix} \tag{3.102}$$

$$\frac{\partial v}{\partial r_B} \approx -\dot{\Phi}[R_1(\epsilon_0)P^{\prime}R_1(-\epsilon)T^{\prime}L_3]\,. \tag{3.103}$$

The partials of v, with the exception of $\frac{\partial v}{\partial \epsilon_0}$ and $\frac{\partial v}{\partial r_B}$, are partials with respect to parameters varying from instant to instant. Both in this case and in the case of the partials of r, the "variable" parameters can be replaced by "non-varying" ones by expressing each parameter as a function of time or similar "independent" variable. This procedure has been demonstrated in Chapter 2 for the variables involved in this section.

An alternate set of equations for the moon-moon VLBI can be developed if we consider the case in which the orientation of a moon-fixed coordinate system with respect to an inertial system (such as the 1950.0 mean ecliptic system) is obtained directly by numerical integration of the moon's equations of motion. If $\theta, \psi, \Phi$ represent the orientation (Eulerian) angles defining the orientation of the selenodetic coordinate system with respect to the 1950.0 mean ecliptic system, then equations (3.75) and (3.77b) for $r_0$ and $r_{B0}$ become respectively:

$$\begin{bmatrix} r_1 \\ r_2 \\ r_3 \end{bmatrix} = T^T \begin{bmatrix} r_x \\ r_y \\ r_z \end{bmatrix} \tag{3.104}$$

and

$$\begin{bmatrix} r_{B1} \\ r_{B2} \\ r_{B3} \end{bmatrix} = T^T \begin{bmatrix} x_B \\ y_B \\ z_B \end{bmatrix} \tag{3.105}$$

where the transformation matrix $T^T$ is

$$T^T = R_3(-\psi)\, R_1(\theta)\, R_3(-\Phi).$$

Also, $\dot{\vec{r}}_{B0}$ can be obtained by differentiating equation (3.105) for $\vec{r}_{B0}$. Thus

$$\begin{bmatrix} \dot{r}_{B_1} \\ \dot{r}_{B_2} \\ \dot{r}_{B_3} \end{bmatrix} = \begin{bmatrix} v_1 \\ v_2 \\ v_3 \end{bmatrix} = -(\dot{\psi}(L_3 T^T) + \dot{\theta}(R_3(-\psi) L_1 R_1(\theta) R_3(-\Phi)) - \dot{\Phi}(T^T L_3)) \begin{bmatrix} x_B \\ y_B \\ z_B \end{bmatrix}. \tag{3.106}$$

Since the term dependent on $\dot{\Phi}$ is the dominating term in this equation for $\dot{\vec{r}}_{B_0}$,

$$\begin{bmatrix} v_1 \\ v_2 \\ v_3 \end{bmatrix} \approx -(\dot{\Phi} T^T L_3) \begin{bmatrix} x_B \\ y_B \\ z_B \end{bmatrix}. \tag{3.107}$$

With these expressions for $\vec{r}_0$ and $\dot{\vec{r}}_{B_0}$, the time delay can be computed using equation (3.79). The number of parameters involved in computing time delay using this method decreases considerably, with only the six initial conditions for the numerical integration of $\Phi$, $\psi$, $\theta$, $\dot{\Phi}$, $\dot{\psi}$ and $\dot{\theta}$ replacing the precessional elements, mean obliquity of date and the orientation angles of the moon with respect to the mean ecliptic system of date.

The partials of $\vec{r}_0$ and $\dot{\vec{r}}_{B_0}$ are now taken as before:

$$\frac{\partial r_0}{\partial \psi} = -L_3 T^T \begin{bmatrix} r_x \\ r_y \\ r_z \end{bmatrix} \tag{3.108}$$

$$\frac{\partial r_0}{\partial \theta} = R_3(-\psi) L_1 R_1(\theta) R_3(-\Phi) \begin{bmatrix} r_x \\ r_y \\ r_z \end{bmatrix} \tag{3.109}$$

$$\frac{\partial r_O}{\partial \Phi} = -T^T L_3 \begin{bmatrix} r_x \\ r_y \\ r_z \end{bmatrix} \tag{3.110}$$

$$\frac{\partial r_O}{\partial r_A} = -T^T \tag{3.111}$$

$$\frac{\partial r_O}{\partial r_B} = T^T \tag{3.112}$$

$$\frac{\partial v}{\partial \Phi} = -T^T L_3 \begin{bmatrix} x_B \\ y_B \\ z_B \end{bmatrix} \tag{3.113}$$

$$\frac{\partial v}{\partial \psi} = \dot{\Phi}(L_3 T^T L_3) \begin{bmatrix} x_B \\ y_B \\ z_B \end{bmatrix} \tag{3.114}$$

$$\frac{\partial v}{\partial \theta} = -\dot{\Phi}(R_3(-\psi) L_1 R_1(\theta) R_3(-\Phi) L_3) \begin{bmatrix} x_B \\ y_B \\ z_B \end{bmatrix} \tag{3.115}$$

$$\frac{\partial v}{\partial \Phi} = \dot{\Phi}(T^T L_3 L_3) \begin{bmatrix} x_B \\ y_B \\ z_B \end{bmatrix} \tag{3.116}$$

and

$$\frac{\partial v}{\partial r_B} = -\dot{\Phi}(T^T L_3). \tag{3.117}$$

An approximate time delay equation for moon-moon VLBI similar to equation (3.69) for the earth-earth VLBI can be derived from equation (3.73) as:

$$\tau \approx \frac{r}{c}\left[\sin\beta_L \sin\beta_O + \cos\beta_L \cos\beta_O \cos(\lambda_L - \lambda_O)\right] + \delta t_c \qquad (3.118)$$

where

$\beta_L$, $\lambda_L$ are the ecliptic coordinates of the baseline vector $\vec{r_O}$

$r$ is the length of the baseline.

The changing direction of the vector $\vec{r_O}$ in space due to the rotation of the moon, changes the angular coordinate $\lambda_L$, but the rate of change is approximately 27.3 times smaller than the earth-earth VLBI baseline vector.

If the unknowns to be determined in the moon-moon VLBI observations are limited to the radio sources' positions, baseline vectors and time synchronization error, then for each baseline observing n sources, the total number of parameters are 2n + 3 as in the case of the earth-earth VLBI observations. Also, equation (3.70) is valid for the minimum number of sources (three) that should be observed in order to be able to solve for the sources' positions and baseline parameters.

For a good determination of the baseline parameters, the three minimum observations to each observed source should be spaced in time as to allow for large variation in the direction of the source with respect to the baseline. The main factor that accounts for the motion of the source relative to the baseline is the moon's rotation, the sidereal period of which is approximately 27.3 mean solar days. Hence, for a strong solution, observations to sources should be made over this period. This requirement is one of the envisaged

main difficulties of establishing selenodetic control on the moon with moon-moon VLBI observations.

Another technical difficulty in VLBI observations on the moon is the use of accurate time standards and frequency generators, necessary in any VLBI observation. While it is required in VLBI measurements that the generated local oscillator frequency be highly stable, and time accurate to at least one part in $10^{11}$, it is also essential that the VLBI equipment for use on the moon be as compact and light as possible, for easy transportation. Synchronization of the clocks used at moon's VLBI stations also presents another technical difficulty.

One major advantage the moon VLBI stations have over the earth VLBI stations is the fact that the moon has no atmosphere. Hence, if VLBI observations on the moon become a reality, the ever-present problem of refraction, which affects almost all types of observations made on the earth, will be absent.

### 3.33 Earth-Moon VLBI Equations.

In this section, VLBI equations will be derived for the case when the two ends of the baseline are located on the earth and moon. As noted earlier in this chapter, this form of observation is non-existent at present, but it is a future possibility. It is assumed that observations will be made to natural radio sources by the two end stations in a manner similar to the existing earth-earth VLBI observations. The observed quantities are also assumed to be relative time delays. The derivation of the equations in this section essentially follows the methods used in the last two sections.

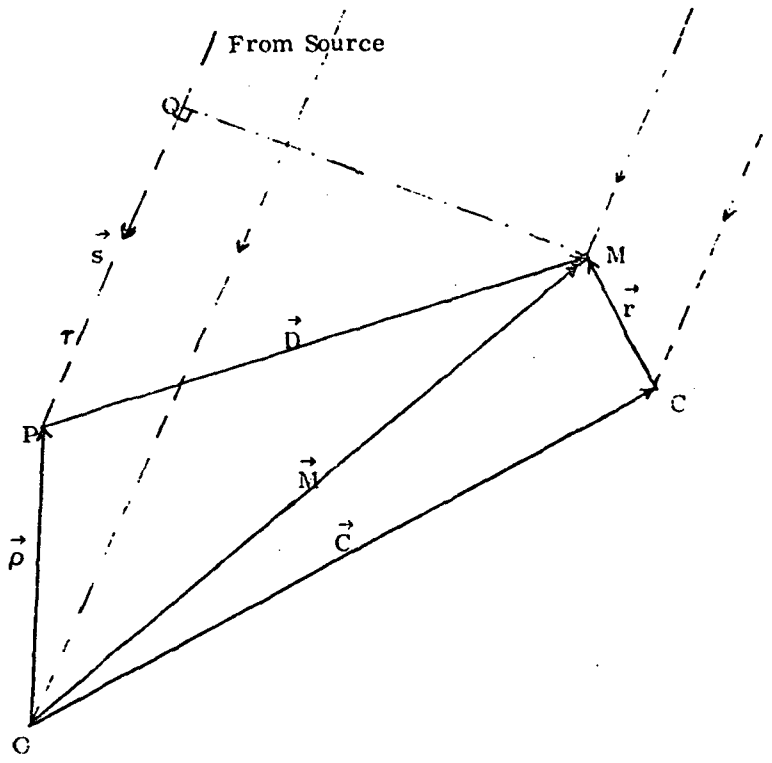


Figure 3.8 Earth-Moon VLBI Observations.

From Figure 3.8,

P is the VLBI station on earth with geodetic coordinate $\varphi$, $\lambda$, h

M is the VLBI station on moon with selenodetic coordinates b, $\ell$, r

O is the geocenter

C is the selenocenter

$\vec{s}$ is the unit vector in the direction from the source to the origin (geocenter)

$\vec{\rho}$ is the vector from O to the earth VLBI station (P)

$\vec{r}$ is the vector from lunar center (C) to the moon VLBI station (M)

$\vec{D}$ is the vector from the earth station to the moon station

$\vec{M}$ is the vector from geocenter to the moon station

and

$\vec{C}$ is the vector from geocenter to the selenocenter.

The following vector relationships hold:

$$\vec{M} = \vec{C} + \vec{r} \tag{3.119}$$

$$\vec{D} = \vec{C} + \vec{r} - \vec{\rho}. \tag{3.120}$$

If the wave front of the observed radio source reaches the station M at time $t_1$ and reaches the station P at $t_2$, $\tau$ seconds later, then the time delay $\tau$ is:

$$\tau = \frac{1}{c}[\vec{D} \cdot \vec{s}]\left[1 + \frac{\vec{M} \cdot \vec{s}}{c}\right]. \tag{3.121}$$

This equation for time delay is valid provided all the vectors are expressed in the same coordinate system. The coordinate system chosen is the mean ecliptic coordinate system of 1950.0.

The vector $\vec{D}$ is given by equation (3.120) as

$$\vec{D} = \vec{C} + \vec{r} - \vec{\rho}.$$

Expressing the vectors $\vec{C}$, $\vec{r}$ and $\vec{\rho}$ in the 1950.0 mean ecliptic coordinate system we have:

$$\vec{C_o} = R_1(\epsilon_o)\vec{C} \tag{3.122a}$$

or

$$\begin{bmatrix} C_1 \\ C_2 \\ C_3 \end{bmatrix} = R_1(\epsilon_o) \begin{bmatrix} X_{cq} \\ Y_{cq} \\ Z_{cq} \end{bmatrix}, \tag{3.122b}$$

$$\vec{r_o} = R_1(\epsilon_o)P^T R_1(-\epsilon)T_M^T \vec{r} \tag{3.123a}$$

or

$$\begin{bmatrix} r_1 \\ r_2 \\ r_3 \end{bmatrix} = R_1(\epsilon_o)P^T R_1(-\epsilon)T_M^T \begin{bmatrix} x \\ y \\ z \end{bmatrix}, \tag{3.123b}$$

and

$$\vec{\rho_o} = R_1(\epsilon_o)P^T N^T S^T \vec{\rho} \tag{3.124a}$$

or

$$\begin{bmatrix} \rho_1 \\ \rho_2 \\ \rho_3 \end{bmatrix} = R_1(\epsilon_o)P^T N^T S^T \begin{bmatrix} U \\ V \\ W \end{bmatrix} \tag{3.124b}$$

where

| | |
|---|---|
| $\epsilon_o$ | is mean obliquity of equator at 1950.0, |
| $X_{cq}$, $Y_{cq}$, $Z_{cq}$ | are the geocentric coordinates of the lunar center in the mean equatorial system of 1950.0 (obtainable from the JPL's DE-69 development ephemeris), |
| x, y, z | are the Cartesian coordinates of the moon's VLBI station in the selenodetic coordinate system. |

| | |
|---|---|
| U, V, W | are the coordinates of the earth VLBI station in the average terrestrial coordinate system, |
| P | is the precession matrix, |
| N | is the nutation matrix, |
| S | is the matrix necessary to transform coordinates in the true celestial system into the average terrestrial coordinate system, |
| $T_M$ | is the matrix which transforms coordinates in the mean ecliptic system of date into the selenodetic coordinate system. |

$$T_M = R_3(\Phi_M) R_1(-\theta_M) R_3(\psi_M).$$

In matrix notation, the vector matrix [D] is

$$[D] = \begin{bmatrix} D_1 \\ D_2 \\ D_3 \end{bmatrix} = \begin{bmatrix} C_1 \\ C_2 \\ C_3 \end{bmatrix} + \begin{bmatrix} r_1 \\ r_2 \\ r_3 \end{bmatrix} - \begin{bmatrix} \rho_1 \\ \rho_2 \\ \rho_3 \end{bmatrix}. \qquad (3.125)$$

The vector $\vec{s}$, from the source to the origin (geocenter) whose components are expressed in the 1950.0 mean ecliptic system ($\vec{s}_0$) can be obtained from the cataloged position of the sources. If $\delta_0$, $\alpha_0$ are the cataloged declination and right ascension of a source (given in 1950.0 mean equatorial system), then

$$\vec{s}_0 = R_1(\epsilon_0)\vec{s} \qquad (3.126a)$$

or

$$\begin{bmatrix} s_1 \\ s_2 \\ s_3 \end{bmatrix} = R_1(\epsilon_0) \begin{bmatrix} -\cos\delta_0 \cos\alpha_0 \\ -\cos\delta_0 \sin\alpha_0 \\ -\sin\delta_0 \end{bmatrix}. \tag{3.126b}$$

For the $\vec{M}_0$ vector, from equation (3.119)

$$\vec{M}_0 = \vec{C}_0 + \vec{r}_0$$

so that

$$\dot{\vec{M}}_0 = \dot{\vec{C}}_0 + \dot{\vec{r}}_0 . \tag{3.127}$$

From equation (3.122a) and (3.122b),

$$\dot{\vec{C}}_0 = R_1(\epsilon_0)\, \dot{\vec{C}}, \tag{3.128a}$$

or

$$\begin{bmatrix} \dot{C}_1 \\ \dot{C}_2 \\ \dot{C}_3 \end{bmatrix} = R_1(\epsilon_0) \begin{bmatrix} \dot{X}_{cq} \\ \dot{Y}_{cq} \\ \dot{Z}_{cq} \end{bmatrix}. \tag{3.128b}$$

The numerically integrated lunar ephemeris (such as the JPL's LE-16) gives both the position vector $\vec{C}$ as well as the velocity vector $\dot{\vec{C}}$ in the mean equatorial coordinate system of 1950.0. Alternatively, $\dot{\vec{C}}$ can be obtained by differentiating the analytical expressions for the position of the moon as given by any analytical lunar ephemeris. The other component of $\dot{\vec{M}}_0$ in equation (3.127), i.e. $\dot{\vec{r}}_0$, can be obtained by differentiating either equation (3.123a) or (3.123b) with respect to time. Thus, similar to equation (3.78),

$$\dot{\vec{r}}_O = \frac{d\vec{r}_O}{dt} = R_1(\epsilon_O)[\dot{\zeta}_O(L_3 P^T R_1(-\epsilon) T_M^T) - \dot{\theta}_1(R_3(\zeta_O) L_2 R_3(-\vartheta_1)$$

$$R_3(z_1) R_1(-\epsilon) T_M^T) + \dot{z}_1(P^T L_3 R_1(-\epsilon) T_M^T) - \dot{\epsilon}(P^T L_1 R_1(-\epsilon) T_M^T)$$

$$- \dot{\psi}_M(P^T R_1(-\epsilon) L_3 T_M^T) + \dot{\theta}_M(P^T R_1(-\epsilon) R_3(-\psi_M) L_1 R_1(\theta_M) R_3(-\Phi_M))$$

$$- \dot{\Phi}_M(P^T R_1(-\epsilon) T_M^T L_3)]\vec{r}. \tag{3.129}$$

In this equation for the $\dot{\vec{r}}_O$, the dominant term is the term dependent on $\dot{\Phi}_M$. Therefore, $\dot{\vec{r}}_O$ is approximately given by

$$\dot{\vec{r}}_O \approx R_1(\epsilon_O)[-\dot{\Phi}_M(P^T R_1(-\epsilon) T_M^T L_3)]\vec{r}. \tag{3.130}$$

Hence, from equations (3.127), (3.128b) and (3.130),

$$[\dot{M}_O] = \begin{bmatrix} \dot{M}_1 \\ \dot{M}_2 \\ \dot{M}_3 \end{bmatrix} \approx R_1(\epsilon_O)\left[\begin{bmatrix} \dot{X}_{CQ} \\ \dot{Y}_{CQ} \\ \dot{Z}_{CQ} \end{bmatrix} - \Phi_M(P^T R_1(-\epsilon) T_M^T L_3) \begin{bmatrix} x \\ y \\ z \end{bmatrix}\right]. \tag{3.131}$$

The time delay can now be calculated from equation (3.121) as

$$\tau = \frac{1}{c}(D_1 s_1 + D_2 s_2 + D_3 s_3)\left[1 + \frac{\dot{M}_1 s_1 + \dot{M}_2 s_2 + \dot{M}_3 s_3}{c}\right] \tag{3.132}$$

i.e., in matrix notation

$$\tau = \frac{1}{c}[(D^T s) + \frac{1}{c}(D^T s\, v^T s)] \tag{3.133}$$

where

$$[v] = \begin{bmatrix} v_1 \\ v_2 \\ v_3 \end{bmatrix} = \begin{bmatrix} \dot{M}_1 \\ \dot{M}_2 \\ \dot{M}_3 \end{bmatrix}.$$

It has been mentioned in Chapter 2 that the orientation of both the earth and the moon with respect to an inertial system (for example, the 1950.0 mean ecliptic coordinate system) can be numerically integrated (see also Chapter 4 and [78]). In this case, if

$\theta_E, \psi_E, \Phi_E$ represent the orientation (Eulerian) angles of the earth-fixed coordinate system (UVW) with respect to the 1950.0 mean ecliptic system

and

$\theta_M, \psi_M, \Phi_M$ are the moon's orientation (Eulerian) angles of the moon-fixed (xyz) coordinate system with respect to the 1950.0 mean ecliptic system,

then the vectors $\vec{\rho}_0$ and $\vec{r}_0$ are respectively:

$$\begin{bmatrix} \rho_1 \\ \rho_2 \\ \rho_3 \end{bmatrix} = T_E^T \begin{bmatrix} U \\ V \\ W \end{bmatrix}, \tag{3.134}$$

$$\begin{bmatrix} r_1 \\ r_2 \\ r_3 \end{bmatrix} = T_M^T \begin{bmatrix} x \\ y \\ z \end{bmatrix} \tag{3.135}$$

where

$$T_E = R_3(\Phi_E)\, R_1(-\theta_E)\, R_3(\psi_E)$$

$$T_M = R_3(\Phi_M)\, R_1(-\theta_M)\, R_3(\psi_M).$$

Consequently,

$$\begin{bmatrix} D_1 \\ D_2 \\ D_3 \end{bmatrix} = R_1(\epsilon_0) \begin{bmatrix} X_{CQ} \\ Y_{CQ} \\ Z_{CQ} \end{bmatrix} + T_M^T \begin{bmatrix} x \\ y \\ z \end{bmatrix} - T_E^T \begin{bmatrix} U \\ V \\ W \end{bmatrix}. \qquad (3.136)$$

Also,

$$\dot{\vec{r}}_O = -[\dot{\psi}_M(L_3 T_M^T) + \dot{\theta}_M(R_3(-\psi_M)L_1R_1(\theta_M)R_3(-\Phi_M)) - \dot{\Phi}_M(T_M^T L_3)]\,\vec{r}. \qquad (3.137)$$

Since the $\dot{\Phi}_M$ term is the dominant term,

$$\dot{\vec{r}}_O \approx -\dot{\Phi}_M(T_M^T L_3)\,\vec{r}. \qquad (3.138)$$

Hence,

$$\begin{bmatrix} \dot{M}_1 \\ \dot{M}_2 \\ \dot{M}_3 \end{bmatrix} \approx R_1(\epsilon_0) \begin{bmatrix} \dot{X}_{CQ} \\ \dot{Y}_{CQ} \\ \dot{Z}_{CQ} \end{bmatrix} - \dot{\Phi}_M(T_M^T L_3) \begin{bmatrix} x \\ y \\ z \end{bmatrix}. \qquad (3.139)$$

The time delay is still computed from equation (3.132) or equation (3.133). The number of parameters that go into the computation of $\tau$ is greatly reduced if the numerical integration method is used to obtain the earth's and moon's orientation angles.

As noted above differences between predicted and observed values of the time delay are used to correct the assumed values of parameters used in predicting the time delay. The partials of time delay $\tau$ are found by taking the partials of equation (3.133) as in the other VLBI cases (Sections 3.31 and 3.32). Thus, the partials of $\tau$ with respect to D, s and v are given by equations (3.28), (3.29) and (3.30) respectively. Also, equation (3.31) gives the expression for the partials of $\tau$ with respect to the parameters. The partials of [D], [s] and [v] with respect to the parameters will now be formed.

From equation (3.129),

$$\begin{bmatrix} D_1 \\ D_2 \\ D_3 \end{bmatrix} = R_1(\epsilon_0) \begin{bmatrix} X_{CQ} \\ Y_{CQ} \\ Z_{CQ} \end{bmatrix} + P^T \; R_1(-\epsilon) T_M^T \begin{bmatrix} x \\ y \\ z \end{bmatrix} - N^T S^T \begin{bmatrix} U \\ V \\ W \end{bmatrix} .$$

This equation for the $\vec{D}$ vector is identical to the equation for $\vec{X}_T$ vector (for laser observations) which is given by equation (2.10) of Chapter 2. Hence the partial derivatives of $\vec{D}$ are equivalent to the partial derivatives of $\vec{X}_T$ in Chapter 2 and are given by equations (2.29) through (2.44). The expression for the $\vec{s}_0$ vector as given by equation (3.126b) is also identical to equation (3.74) in Section 3.32. The partial derivatives of $\vec{s}_0$ with respect to $\epsilon_0$, $\delta_0$ and $\alpha_0$ are therefore given by equations (3.81), (3.82) and (3.83) respectively. Partials for matrix v is obtained from equation (3.131) as follows:

$$\frac{\partial v}{\partial \epsilon_0} = L_1 \begin{bmatrix} v_1 \\ v_2 \\ v_3 \end{bmatrix} \tag{3.140}$$

$$\frac{\partial s}{\partial \begin{bmatrix} \dot{X}_{CQ} \\ \dot{Y}_{CQ} \\ \dot{Z}_{CQ} \end{bmatrix}} = R_1(\epsilon_0) \tag{3.141}$$

$$\frac{\partial v}{\partial \dot{\Phi}_M} = -R_1(\epsilon_0) P^T R_1(-\epsilon) T_M^T L_G) \begin{bmatrix} x \\ y \\ z \end{bmatrix} \tag{3.142}$$

$$\frac{\partial v}{\partial \zeta_0} = -\Phi_M [R_1(\epsilon_0) L_G P^T R_1(-\epsilon) T_M^T L_G)] \begin{bmatrix} x \\ y \\ z \end{bmatrix} \tag{3.143}$$

$$\frac{\partial v}{\partial \theta_1} = \dot{\Phi}_M[R_1(\epsilon_0)R_3(\zeta_0)\ L_2\ R_2\ (-\theta_1)R_3(z_1)R_1(-\epsilon)T_M^T L_3] \begin{bmatrix} x \\ y \\ z \end{bmatrix} \tag{3.144}$$

$$\frac{\partial v}{\partial z_1} = -\dot{\Phi}_M[R_1(\epsilon_0)P^T L_G R_1(-\epsilon)T_M^T L_3] \begin{bmatrix} x \\ y \\ z \end{bmatrix} \tag{3.145}$$

$$\frac{\partial v}{\partial \epsilon} = \dot{\Phi}_M[R_1(\epsilon_0)P^T L_1\ R_1\ (-\epsilon)T_M^T L_3] \begin{bmatrix} x \\ y \\ z \end{bmatrix} \tag{3.146}$$

$$\frac{\partial v}{\partial \psi_M} = \dot{\Phi}_M[R_1(\epsilon_0)P^T R_1(-\epsilon)L_G\ T_M^T\ L_3] \begin{bmatrix} x \\ y \\ z \end{bmatrix} \tag{3.147}$$

$$\frac{\partial v}{\partial \theta_M} = -\dot{\Phi}_M[R_1(\epsilon_0)P^T R_1(-\epsilon)R_3(-\psi_M)L_1R_1(\theta_M)R_3(-\Phi_M)L_3] \begin{bmatrix} x \\ y \\ z \end{bmatrix} \tag{3.148}$$

$$\frac{\partial v}{\partial \Phi_M} = \dot{\Phi}_M[R_1(\epsilon_0)P^T R_1(-\epsilon)T_M^T L_3\ L_3] \begin{bmatrix} x \\ y \\ z \end{bmatrix} \tag{3.149}$$

$$\frac{\partial v}{\partial \begin{bmatrix} x \\ y \\ z \end{bmatrix}} = -\dot{\Phi}_M[R_1(\epsilon_0)P^T R_1(-\epsilon)T_M^T L_3] . \tag{3.150}$$

The partials of $\vec{D}$ and $\vec{v}$ are slightly different if the alternate expressions for them are used (equations (3.136) and (3.139)). Those expressions which differ from the ones given earlier are:

$$\frac{\partial D}{\partial \psi_M} = -L_3 T_M^T \begin{bmatrix} x \\ y \\ z \end{bmatrix} \tag{3.151}$$

$$\frac{\partial D}{\partial \theta_M} = R_3(-\psi_M) L_1 R_1(\theta_M) R_3(-\Phi_M) \begin{bmatrix} x \\ y \\ z \end{bmatrix} \tag{3.152}$$

$$\frac{\partial D}{\partial \Phi_M} = -T_M^T L_3 \begin{bmatrix} x \\ y \\ z \end{bmatrix} \tag{3.153}$$

$$\frac{\partial D}{\partial \begin{bmatrix} x \\ y \\ z \end{bmatrix}} = T_M^T \tag{3.154}$$

with similar expressions for $\frac{\partial D}{\partial \psi_E}$, $\frac{\partial D}{\partial \theta_E}$, $\frac{\partial D}{\partial \Phi_E}$ and $\frac{\partial D}{\partial \begin{bmatrix} U \\ V \\ W \end{bmatrix}}$.

Also,

$$\frac{\partial v}{\partial \Phi_M} = -T_M^T L_3 \begin{bmatrix} x \\ y \\ z \end{bmatrix} \tag{3.155}$$

$$\frac{\partial v}{\partial \psi_M} = \dot{\Phi}_M (L_G \, T_M^T \, L_3) \begin{bmatrix} x \\ y \\ z \end{bmatrix} \tag{3.156}$$

$$\frac{\partial v}{\partial \theta_M} = -\dot{\Phi}_M (R_3(-\psi_M) L_1 R_1(\theta_M) R_3(-\Phi_M) L_G) \begin{bmatrix} x \\ y \\ z \end{bmatrix} \tag{3.157}$$

$$\frac{\partial v}{\partial \Phi_M} = \dot{\Phi}_M (T_M^T \, L_G \, L_3) \begin{bmatrix} x \\ y \\ z \end{bmatrix} \tag{3.158}$$

and

$$\frac{\partial v}{\partial \begin{bmatrix} x \\ y \\ z \end{bmatrix}} = -\dot{\Phi}(T_M^T L_G). \tag{3.159}$$

As it was in the case of laser observation equations, most of the parameters that appear in the derived partials of time delay in their present form are "variable" parameters, varying from epoch to epoch. However, these "variable" parameters can be replaced by another set of parameters which do not vary with time. For example, the integrated Eulerian angles (both for the earth and the moon) are functions of the initial conditions and a few physical parameters. These Eulerian angles, which vary with time, can therefore by replaced by the initial conditions and the physical parameters

in an adjustment program. This principle has been explained in more detail in Chapter 2.

In the earth-moon VLBI observations involving only one station on the earth and another on the moon, if the only unknowns are limited to the inter-site vector between the earth station and the moon station and the vector to the observed sources, then there are $2n+3$ unknowns, where n is the number of observed sources. As in the other two VLBI cases, three simultaneous observations each on three radio sources would uniquely solve the resulting nine unknowns.

### 3.4 Summary.

In the preceeding sections of this chapter, another new observational system - the VLBI - which could be used for selenodetic control determination has been treated. The basic operating principles of the VLBI were given, and equations relating the geometric time delay to geodetic, selenodetic and astronomical parameters were derived. These equations were then differentiated so as to obtain the observation equations for measured time delays. Equations developed in this chapter pertain to earth-earth, moon-moon and earth-moon baselines, and are valid only for observations of natural radio sources.

In deriving the observation equations, the observed time delays are assumed to have been corrected for atmospheric, instrumental and other systematic errors which may affect the measured delays. However, the influence of the earth's atmosphere on VLBI measurements is discussed briefly in Appendix B. Also, modified equations for earth-earth VLBI with artificial radio sources are derived in Appendix A.

# 4. NUMERICAL INTEGRATION OF THE ORIENTATION OF AN EARTH-FIXED COORDINATE SYSTEM WITH RESPECT TO AN INERTIAL SYSTEM

## 4.1 Introduction

The rotation of the earth on its axis and its orbital revolution around the barycenter are of fundamental importance in astronomy. While the circles that these motions describe on the celestial sphere serve as fundamental reference circles, the apparent motion of celestial bodies produced by the earth's motions is the basis of time reckoning.

The two motions of the earth are complex and irregular. The rotation of the earth on its axis is continually disturbed by the gravitational attractions of the sun, moon and the nearer planets. Furthermore, variations in this motion occur due to the fact that the axis of rotation does not coincide with a principal axis of inertia and because of tidal deformations of the earth. Also, mass distribution of the earth is not symmetric, and this distribution changes through transfers of mass upon and within the earth from the operation of geophysical and atmospheric processes.

The variation of the direction of the earth's instantaneous axis of rotation causes a continuous motion of the celestial poles and the equator among the stars, thereby causing variations in the coordinates of celestial objects with respect to time. These variations can be divided into two parts, namely the secular part (precession), and the periodic part (nutation). Also, there is a variation of the position of the instantaneous axis within the earth (polar motion), causing a continual, but small variation of latitudes and longitudes of points on earth. In addition to the variations in the position of the axis of

rotation, there are also variations in the angular rate of rotation, which affect the measurement and determination of time.

In geodetic astronomy, one customarily reduces the cataloged position of an observed star to its position at the epoch of observation using the tabulated values of precessional elements and nutation in longitude and obliquity together with the values of the star's proper motion. The tabulated values of nutation in longitude and obliquity are calculated from the nutation series developed by E.W. Woolard in [94].

The present accuracy to which values of precession and nutation elements are known is consistent with the level of accuracy expected from present instrumentation and observations. Furthermore, if the constant of precession is in error, the error is absorbed into the stars' proper motion values due to the method by which these proper motions are obtained. Thus, as far as present geodetic astronomy is concerned it would not matter one way or the other, whether the value of the precession constant is revised. However, if new observational methods of position determination become feasible (such as the Very Long Baseline Interferometry applied to geodesy) then the need of knowing precession and nutation to better accuracy is of prime importance.

The more precise future observations can be useful in the process of finding more accurate values of precession and nutation. By using a mathematical model in which precession and nutation quantities are parameters in addition to other desired parameters, correction to existing coefficients in the expressions for precession and series for nutation can be obtained. The large number of the parameters involved (109 for nutation and 9 for precession) necessitates a large number of observations over an extended period of time. In order to avoid having to solve for such a large number of parameters, one can do either of two things. The first alternative is to cut down on the number of parameters by fixing some of the coefficients while solving for the remainder.

The second alternative is to devise another way in which the effect of precession and nutation could be computed without resorting to series development, and in such a way as to drastically reduce the number of the parameters involved.

The motion of the earth around its center of mass can be represented mathematically by the equations for the motion of a rigid body. While the earth cannot be regarded as perfectly rigid, the effects of departure from rigidity could be expected to be included in the solution for the equations of motion of a rigid body obtained by fitting real observations to the mathematical model.

The three, second order differential equations of motion of a rigid body have always served as a starting point for finding effects of precession and nutation. Understandably in the past, analytical solutions to these equations have been derived involving large series expressions. The availability of computers in the last decade have now made another approach to the solution of the differential equations of motion possible. The original equations of motion can be integrated numerically without resorting to the various techniques necessary for finding analytic solutions to the equations of motion. The number of parameters involved will reduce to the six initial conditions, which could be solved for in a more convenient way than the present coefficients of nutation series and precession expressions would allow. By using the numerical integration technique, the orientation of any earth-fixed coordinate system (for example the "Average" Terrestrial Coordinate System - UVW) with respect to an inertial system (for example the Mean Ecliptic Coordinate System of 1950.0 - XYZ) could be obtained directly. Thus, the coordinates of an observed celestial object desired in the true equatorial coordinate system could be obtained by first transforming its catalogued position to the UVW coordinate system, and using polar motion values and the GAST to transform to the true equatorial coordinate system.

The equations of motion of the earth derived in the following subsections is generalized, without simplifications other than the assumption of perfect rigidity of the body.

## 4.2 The Equations of Motion of a Rigid Body.

The motion of any rigid body under the influence of external forces can be represented as the resultant of a translation, with the velocity of the center of mass, and a rotation about an axis through the center of mass. The two components of motion are dynamically independent of each other. The center of mass moves as though it were a particle of mass, equal to the total mass of the rigid body, and upon which all external forces were directly exerted. The rotational motion, relative to the moving center of mass, takes place as if the center of mass was at rest. This motion, which will be further investigated here, is determined by the moments of the external forces about the center of mass. Parts of the equations presented below are derived in more detail in text books of celestial and analytical mechanics such as [22], [85] and [79].

Let a rigid body be composed of a system of particles $m_1, m_2, \ldots m_i, \ldots$, whose position vectors from a selected origin of a fixed reference system are respectively $\vec{r}_1, \vec{r}_2, \ldots \vec{r}_i, \ldots$. If external forces $\vec{F}_1, \vec{F}_2, \ldots \vec{F}_i, \ldots$, and internal forces (due to mutual interactions of the particles), $\vec{R}_1, \vec{R}_2, \ldots \vec{R}_i, \ldots$ are the two systems of forces acting upon the system of particles, then the force equation for the i th particle is given by

$$\vec{F}_i + \vec{R}_i = m_i \frac{d^2 \vec{r}_i}{dt^2}. \tag{4.1}$$

For the entire system, the force equation is given by

$$\sum_n \vec{F}_i + \sum_n \vec{R}_i = \sum_n m_i \frac{d^2 \vec{r}_i}{dt^2}. \tag{4.2}$$

The second term on the left hand side of equation (4.2) vanishes since forces due to mutual interactions occur in pairs of equal and oppositely directed forces.

The forces acting on the i th particle is converted to force moments by multiplying each term in equation (4.1) by $\vec{r}_i \times$, which then gives:

$$\vec{r}_i \times \vec{F}_i + \vec{r}_i \times \vec{R}_i = m_i \vec{r}_i \times \frac{d^2\vec{r}_i}{dt^2}. \tag{4.3}$$

Since

$$\vec{r}_i \times \frac{d^2\vec{r}_i}{dt^2} = \frac{d}{dt}\left(\vec{r}_i \times \frac{d\vec{r}_i}{dt}\right)$$

equation (4.3) gives:

$$\vec{r}_i \times \vec{F}_i + \vec{r}_i \times \vec{R}_i = m_i \frac{d}{dt}\left(\vec{r}_i \times \frac{d\vec{r}_i}{dt}\right). \tag{4.4}$$

For the entire system, the force-moment equation becomes

$$\sum_n \vec{r}_i \times \vec{F}_i = \sum_n m_i \frac{d}{dt}\left(\vec{r}_i \times \frac{d\vec{r}_i}{dt}\right) \tag{4.5}$$

by taking $\sum_n \vec{r}_i \times \vec{R}_i$ to be zero.

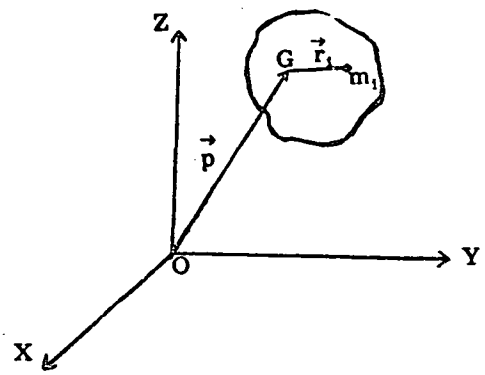


Figure 4.1. Rigid Body and a Fixed System.

Considering Figure 4.1 above, XYZ is a fixed reference system with origin at O, and G is the center of mass of the rigid body. If $\vec{v}_i$ is the velocity of the particle $m_i$ referred to O, then

$$\vec{v}_i = \vec{p} + \vec{r}_i.$$

If the origin O coincides with the center of mass G, then

$$\vec{v}_i = \dot{\vec{r}}_i = \frac{d\vec{r}_i}{dt}$$

and equation (4.5) becomes

$$\sum_n \vec{r}_i \times \vec{F}_i = \frac{d}{dt}[\sum_n m_i \vec{r}_i \times \vec{v}_i] \tag{4.6}$$

or

$$\vec{L} = \frac{d\vec{H}}{dt} \tag{4.7}$$

where

$\vec{L} = \sum_n \vec{r}_i \times \vec{F}_i$ = force moment

$\vec{H} = \sum_n m_i \vec{r}_i \times \vec{v}_i$ = rotational momentum (moment of momentum).

For any particular rigid body the force moment $\vec{L}$ is obtained through the force function while H can be expressed in terms of the inertial constants of the body and its angular velocity. In the section that follows, the principles of rigid body motion will be applied to the case of the earth.

## 4.3 The Rotation of the Earth About its Center of Mass.

### 4.31 The Dynamical Equations of Motion.

In Figure 4.2 let the XYZ axes represent an inertial coordinate system centered at O (for example the mean ecliptic system of 1950.0). Also let the UVW axes represent a coordinate system, fixed to the earth's body and also centered at O (for example, the average terrestrial coordinate system). The instantaneous axis of rotation OP also passes through the earth's center but does not coincide with either the W axis, or the Z axis.

From equations (4.6) and (4.7)

$$\vec{H} = \sum_n m_i \vec{r}_i \times \vec{v}_i. \tag{4.8}$$

Replacing the summation sign by an integration sign and writing dm for the element of mass, $m_i$, equation (4.8) could be written as

$$\vec{H} = \int_M (\vec{r}_i \times \vec{v}_i)\, dm$$

where

$\vec{r}_i$ is the position vector of dm from origin O

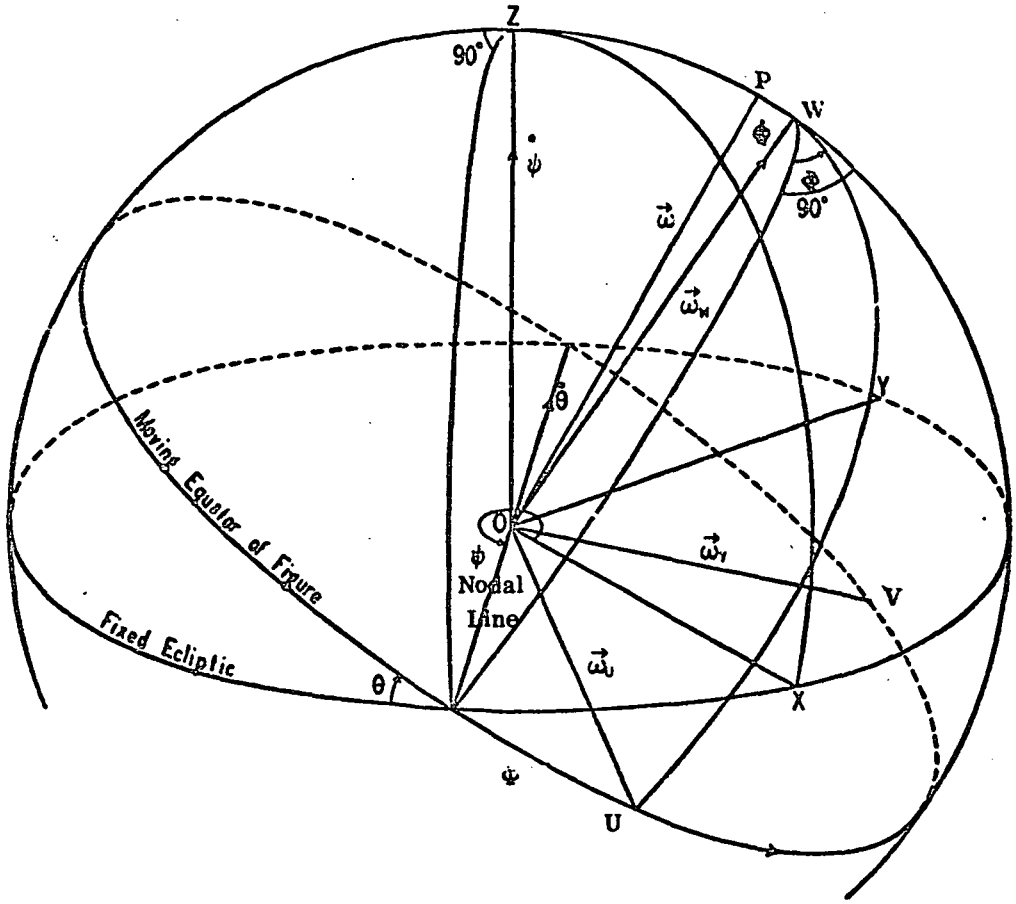


P — Instantaneous Pole

$\omega$ — Earth's Rotational Velocity

XYZ — Mean Ecliptic (1950.0) Coordinate System

UVW — Average Terrestial Coordinate System

$\theta\ \psi\ \Phi$ — Eulerian Angles

Figure 4.2 The Fundamental Coordinate Systems and the Eulerian Angles.

and $\vec{v}_1$ is the velocity of dm referred to the origin.

Also, $\vec{v}_1$ could be expressed as

$$\vec{v}_1 = \vec{\omega} \times \vec{r}_1$$

if $\vec{\omega}$ represents the angular velocity of the earth. Hence

$$\vec{H} = \int_M [\vec{r}_1 \times (\vec{\omega} \times \vec{r}_1)]dm$$

or

$$\vec{H} = \int_M [\vec{\omega}(\vec{r}_1 \cdot \vec{r}_1) - \vec{r}_1(\vec{r}_1 \cdot \vec{\omega})]. \tag{4.9}$$

If the coordinates of the mass element dm is u, v, w in the UVW coordinate system, and $\vec{i}$, $\vec{j}$, $\vec{k}$ are unit vectors along the U, V, W axes respectively, then

$$\vec{r}_1 = u\vec{i} + v\vec{j} + w\vec{z}$$

and

$$\vec{\omega} = \omega_U\vec{i} + \omega_V\vec{j} + \omega_W\vec{z}$$

Subtituting for $\vec{r}_1$ and $\vec{\omega}$ in (4.9) and carrying out the scalar products we obtain:

$$\vec{H} = \int_M [(\omega_U\vec{i} + \omega_V\vec{j} + \omega_W\vec{k})(u^2 + v^2 + w^2) - (u\vec{i} + v\vec{j} + w\vec{k})(u\omega_U + v\omega_V + w\omega_W)]dm.$$

Expanding the above equation further and simplifying we obtain:

$$\vec{H} = (A\omega_U - F\omega_V - E\omega_W)\vec{i} + (B\omega_V - D\omega_W - F\omega_U)\vec{j} + (C\omega_W - D\omega_U - E\omega_V)\vec{k}$$

or (4.10)

$$\vec{H} = H_U\vec{i} + H_V\vec{j} + H_W\vec{k}$$

where A, B, C, D, E, F are the moments of inertial of the earth defined as:

$$A = \int_M (v^2 + w^2)\,dm \qquad D = \int_M vw\,dm$$

$$B = \int_M (u^2 + w^2)\,dm \qquad E = \int_M wu\,dm$$

$$C = \int_M (u^2 + v^2)\,dm \qquad F = \int_M uv\,dm.$$

Equation (4.10) can be rewritten, in matrix notation as

$$[H] = [M_1][\omega] \tag{4.11}$$

where

$$H = \begin{bmatrix} H_U \\ H_V \\ H_W \end{bmatrix}, \quad M_1 = \begin{bmatrix} A & -F & -E \\ -F & B & -D \\ -E & -D & C \end{bmatrix}, \quad \omega = \begin{bmatrix} \omega_U \\ \omega_V \\ \omega_W \end{bmatrix}. \tag{4.12}$$

In order to differentiate $\vec{H}$ with respect to time, one also has to consider the fact that the directions of the unit vectors $\vec{i}, \vec{j}, \vec{k}$ in space do change with respect to time. Thus since

$$\vec{H} = H_U\vec{i} + H_V\vec{j} + H_W\vec{k},$$

$$\frac{d\vec{H}}{dt} = \vec{i}\frac{dH_U}{dt} + H_U\frac{d\vec{i}}{dt} + \vec{j}\frac{dH_V}{dt} + H_V\frac{d\vec{j}}{dt} + \vec{k}\frac{dH_W}{dt} + H_W\frac{d\vec{k}}{dt}.$$

From the above expression we obtain

$$\frac{d\vec{H}}{dt} = (\dot{H}_U - \omega_W H_V + \omega_V H_W)\vec{i} + (\dot{H}_V + \omega_W H_U - \omega_U H_W)\vec{j} + (\dot{H}_W + \omega_U H_V - \omega_V H_U)\vec{k} \tag{4.13}$$

which can also be written as

$$\frac{d\vec{H}}{dt} = \overrightarrow{M_1\dot{\omega}} + \vec{\omega} \times \vec{H}. \tag{4.14}$$

This is the right hand side of equations (4.6) and (4.7). To obtain the left hand side, i.e. $\vec{L}$, we have

$$\vec{L} = \sum_n (\vec{r}_i \times \vec{F}_i)$$

as earlier defined.

The external forces acting on the earth are mainly due to the gravitational attractions of the sun and the moon, and in a much lesser way, to the attractions of the planets. Woolard in [94] considered the moon and the sun as the only external bodies whose gravitational effects cause precession and nutation. Although the effects of the other planets are thought to be negligibly small, the equations to be derived here will include their effects so as to make the equations general. Besides the generality of the equations, however, it is possible that long-term effects of the planets on the rotation of the earth around its center of mass are of such magnitude that can be detected with future observational systems.

If $\vec{U}$ is force function and $\vec{V}$ is potential then

$$\vec{F} = d\vec{U} = -d\vec{V}$$

$$\therefore \quad \vec{L} = d\vec{V} \times \vec{r}.$$

The potential of the earth of mass M at a distant point P is given approximately by the MacCullagh's formula [41] as

$$V = \frac{GM}{R} + \frac{G}{2R^3}(A+B+C-3I) \tag{4.15}$$

where G is the gravitational constant, A, B, C are the principal moments of inertia of the earth with center of mass at O, R is the distance OP and I is the moment inertia of the earth about OP. Equation (4.15) neglects terms depending on $1/R^4$ and on, since these quantities are negligible in astronomical problems because of the great distances involved.

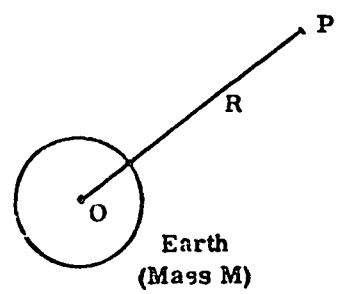


If we now consider, as in the case of the earth, a system of n bodies of finite dimensions, the total potential energy of the system is given by

$$V = G\left[\frac{MM_1}{R_1} + \dots + \frac{MM_n}{R_n} + \frac{M(A_1+B_1+C_1-3I_1)}{2R_1^3} + \dots + \frac{M(A_n+B_n+C_n-3I_n)}{2R_n^3}\right.$$

$$\left. + (A+B+C)\left(\frac{M_1}{2R_1^3} + \dots + \frac{M_n}{2R_n^3}\right) - \frac{3}{2}\left(\frac{M_1I^1}{R_1^3} + \frac{M_2I^2}{R_2^3} + \dots + \frac{M_nI^n}{R_n^3}\right)\right] \tag{4.16}$$

where

| | |
|---|---|
| $R_1 \cdots R_n$ | are distances from earth's mass center to the center of mass of external bodies 1, ...n respectively |
| $M_1 \cdots M_n$ | are masses of external bodies 1, ...n respectively |
| $A_i, B_i, C_i, I_i$ | are the inertia quantities that pertain to the body i, $i = 1 \cdots n$ in the same way as A, B, C, I were defined above, |
| M | is the total mass of the earth |

and $I^i$ is the moment of inertia of the earth about the line joining the earth's center to the center of body i, $i = 1, \ldots n$.

Since V depends on the orientation of the earth only through $I^i$, only the last term of (4.16) need be considered. Thus differentiating (4.16)

$$dV = -\frac{3G}{2}\left[\frac{M_1 dI^1}{R_1^3} + \frac{M_2 dI^2}{R_2^3} + \cdots + \frac{M_n dI^n}{R_n^3}\right]. \tag{4.17}$$

However,

$$I^i = \frac{1}{R_i^2}\,[X][M_i X_i] \tag{4.18}$$

where $X_i$ gives the coordinates of the body i from the earth's center in the UVW coordinate system.

$M_i$ has been defined previously.

Hence

$$dI^i = \frac{2}{R_i^2}\,[M_i\, X_i]$$

and

$$dV = -\left[\frac{3GM_1}{R_1^5}[M_1X_1] + \frac{3GM_2}{R_2^5}[M_1X_2] + \cdots + \frac{3GM_n}{R_n^5}[M_1X_n]\right] \tag{4.19a}$$

or in vector notation

$$d\vec{V} = [d\vec{V}_1 + d\vec{V}_2 + \cdots + d\vec{V}_n]. \tag{4.19b}$$

Since

$$\vec{L} = d\vec{V} \times \vec{r},$$

then

$$\vec{L} = d\vec{V}_1 \times \vec{X}_1 + d\vec{V}_2 \times \vec{X}_2 + \cdots + d\vec{V}_n \times \vec{X}_n$$

or

$$\vec{L} = -\left[\frac{3GM_1}{R_1^5} M_1\vec{X}_1 \times \vec{X}_1 + \frac{3GM_2}{R_2^5} M_1\vec{X}_2 \times \vec{X}_2 + \cdots + \frac{3GM_n}{R_n^5} M_1\vec{X}_n \times \vec{X}_n\right]. \tag{4.20}$$

From equations (4.7) and (4.14),

$$\vec{L} = \frac{d\vec{H}}{dt} = M_1\vec{\dot{\omega}} + \vec{\omega} \times \vec{H}.$$

Therefore, since $\vec{H} = M_1\vec{\omega}$

$$M_1\dot{\vec{\omega}} + \vec{\omega} \times M_1\vec{\omega} = -\left[\frac{3GM_2}{R_1^5} M_1\vec{X}_1 \times \vec{X}_1 + \dots + \frac{3GM_n}{R_n^5} M_1\vec{X}_n \times \vec{X}_n\right]. \qquad (4.21)$$

The above equation (4.21) is the dynamical equation of motion for the earth, assuming rigidity. If it is further assumed that the products of inertia (D, E, F) are zero, the equation reduces to the well-known Euler's equations of motion [79].

4.32 Euler's Geometric Equations.

In the last sub-section, the motion of the earth about its center of mass has been dynamically represented as a rotation about an axis which constantly passes through the center of mass, but whose position within the earth and direction in space varies from instant to instant. The orientation of the earth-fixed UVW coordinate system with respect to the fixed (inertial) coordinate system (XYZ) also varies from instant to instant. This orientation at any instant can be defined by a set of three angles - known as the Euler angles - $\theta$, $\psi$, $\Phi$. These angles are presented in figure 4.2 and are defined as follows:

$\theta$ — the inclination of the average terrestrial equator (moving equator of figure) to the plane of the fixed exliptic (of 1950.0) reckoned positive from the plane of the fixed exliptic to the plane of the moving equator, such that $\theta < 90^\circ$

$\psi$ — the longitude of descending node of the equator of figure reckoned from the fixed equinox

$\Phi$ — the angle in the plane of the equator of figure, between the moving nodal line and the U-axis, reckoned positive eastwards from the descending node to the positive U-axis.

Thus the relationship between the inertial XYZ coordinate system and the moving UVW axes fixed in the earth's body is given by:

$$\begin{bmatrix} U \\ V \\ W \end{bmatrix} = R_3(\Phi)\, R_1(-\theta)\, R_3(\psi) \begin{bmatrix} X \\ Y \\ Z \end{bmatrix} \tag{4.22}$$

where $R_3(\Phi)$, $R_1(-\theta)$ and $R_3(\psi)$ are $3 \times 3$ orthogonal transformation matrices.

The rate of change of the three Eulerian angles $-\dot{\Phi}, \dot{\psi}, \dot{\theta}$ can also be used to represent the motion of the earth about its center of mass. In the figure 4.2, $\dot{\Phi}$ is a rotation about the W-axis, $\dot{\psi}$ a rotation about the Z-axis and $\dot{\theta}$ a rotation about the line of nodes. The relationship between the components of the angular veloctiy $\omega$ along the U, V, W axes — $\omega_U$, $\omega_V$, $\omega_W$ — and $\dot{\Phi}$, $\dot{\psi}$, $\dot{\theta}$ can be obtained, by geometrical considerations, from figure 4.2 to be

$$\begin{aligned} \omega_U &= -\dot{\theta}\cos\Phi - \dot{\psi}\sin\theta\sin\Phi \\ \omega_V &= \dot{\theta}\sin\Phi - \dot{\psi}\sin\theta\cos\Phi \\ \omega_W &= \dot{\psi}\cos\Phi + \dot{\Phi} \end{aligned} \tag{4.23a}$$

which could also be written as:

$$\begin{bmatrix} \omega_U \\ \omega_V \\ \omega_W \end{bmatrix} = S_1 \begin{bmatrix} \dot{\theta} \\ \dot{\psi} \\ \dot{\Phi} \end{bmatrix} \tag{4.23b}$$

or

$$\vec{\omega} = S_1 \dot{\vec{E}} \tag{4.23c}$$

where

$$S_1 = \begin{bmatrix} -\cos\Phi & -\sin\theta\sin\Phi & 0 \\ \sin\Phi & -\sin\theta\cos\Phi & 0 \\ 0 & \cos\theta & 1 \end{bmatrix}, \quad E = \begin{bmatrix} \theta \\ \psi \\ \Phi \end{bmatrix}, \quad \omega = \begin{bmatrix} \omega_U \\ \omega_V \\ \omega_W \end{bmatrix}.$$

Differentiating equation (4.23c) with respect to time,

$$\dot{\vec{\omega}} = S_1 \ddot{\vec{E}} + \dot{S}_1 \dot{\vec{E}} = S_1 \ddot{\vec{E}} + S_2 \dot{\vec{E}}_2 \tag{4.24}$$

where

$$S_2 = \begin{bmatrix} -\cos\theta \sin\Phi & \sin\Phi & -\sin\theta \cos\Phi \\ -\cos\theta \cos\Phi & \cos\Phi & \sin\theta \sin\Phi \\ -\sin\theta & 0 & 0 \end{bmatrix}$$

and

$$E_2 = \begin{bmatrix} \dot{\theta} & \dot{\psi} \\ \dot{\theta} & \dot{\Phi} \\ \dot{\psi} & \dot{\Phi} \end{bmatrix}.$$

From the equations (4.23) and (4.24), the relationship between the $\vec{\omega}$ and $\dot{\vec{\omega}}$ vector and the $\vec{E}$ and $\dot{\vec{E}}$ vector is established. These equations, usually referred to as Euler's geometric (or kinematic) equations, could now be used in conjunction with the dynamical equation (4.21) to obtain three second order differential equations of motion, whose solution would give the orientation of the earth-fixed coordinate system, with respect to the coordinate system fixed in space, at any particular instant.

4.33 Differential Equations of Motion of the Earth.

From the earth's dynamical equations of motion given by (4.21), expressions for $\dot{\vec{\omega}}$ and $\vec{\omega}$ given by (4.23) and (4.24) could be substituted. This gives:

$$M_1\vec{S}_1\ddot{\vec{E}} + M_1\vec{S}_2E_2 + \vec{S}_1\dot{\vec{E}} \times M_1\vec{S}_1\dot{\vec{E}} = -\left[\frac{3GM_1}{R_1^5} M_1\vec{X}_1 \times \vec{X}_1 + \cdots + \frac{3GM_n}{R_n^5} M_1\vec{X}_n \times \vec{X}_n\right]. \tag{4.25}$$

Retaining only $\ddot{\vec{E}}$ on the left hand side,

$$\ddot{\vec{E}} = [M_1S_1]^{-1}\left\{-3G\left[\frac{M_1}{R_1^5} M_1\vec{X}_1 \times \vec{X}_1 + \cdots + \frac{M_n}{R_n^5} M_1\vec{X}_n \times \vec{X}_n\right] - M_1\vec{S}_2E_2 + M_1\vec{S}_1\dot{\vec{E}} \times \vec{S}_1\dot{\vec{E}}\right\}. \tag{4.26}$$

Equation (4.26) is a system of three second-order differential equations of motion, and the solution for $\vec{E}$ gives the motion of the axis of figure - UVW, or equivalently, the orientation of the earth in space. The position of the Earth relative to the instantaneous axis of rotation at any instant can also be obtained

through the angles that this axis makes with the three body-fixed axes - UVW, since the direction cosines of these angles are given by:

$$\cos \alpha_1 = \frac{\omega_U}{\omega}$$

$$\cos \alpha_2 = \frac{\omega_V}{\omega} \qquad (4.27)$$

$$\cos \alpha_3 = \frac{\omega_W}{\omega}$$

$\omega_U, \omega_V, \omega_W$ could be obtained from the Euler's geometric equations given by (4.23).

## 4.4 Numerical Integration of the Earth's Orientation Angles

The simplified form of equation (4.26) has always been the starting equation for the development of the existing solutions of the earth's precession and nutation. The differential equations have been derived with only one assumption — that the earth is a rigid body. In previous solutions, further simplifications are made by assuming that the M (moment of inertia) matrix is a diagonal matrix (putting D = E = F = 0). It is also usually assumed that the earth possesses rotational symmetry about the W axis (i.e., A = B). Furthermore, the external bodies whose attractions influence the earth's motion are limited to the moon and the sun, hence the term "luni-solar" precession and nutation.

The simplified differential equations of motion are, prior to this time, analytically solved by the well-known method of variation of parameters, involving successive approximations. First, the motion that would occur, if all external forces were to vanish is solved for, and this solution is thereafter modified to obtain a solution under actual conditions. The motion of the axis of rotation is generally calculated in two parts. The secular part of the motion is referred to as "luni-solar precession" and the periodic part is called "nutation". A very good example of the classical method of obtaining expressions for precession and nutation can be found in the work

of Woolard [94], which at present serves as the basis for the calculation of nutation tabulated in the various astronomical almanacs.

In this section, an alternate method of using the differential equations of motion (equation (4.26)) to obtain the orientation of the earth with respect to an inertial coordinate system will be given. The method involves the use of digital computers to numerically integrate the earth's equations of motion.

The three second order differential equations (4.26) are transformed into a form suitable for numerical integration by setting

$$Y = \begin{bmatrix} E \\ \dot{E} \end{bmatrix}$$

such that

$$\frac{d}{dt} Y = \begin{bmatrix} \dot{E} \\ \ddot{E} \end{bmatrix}$$

or

$$\dot{Y} = \begin{bmatrix} \dot{E} \\ \ddot{E} \end{bmatrix} = \begin{bmatrix} \dot{E} \\ f(E, \dot{E}) \end{bmatrix} \qquad (4.28)$$

where $f(E, \dot{E})$ is represented by the righthand side of equation (4.26). This is a system of six first order equations, of which the first three are linear and the last three are non-linear.

These six first order equations can be numerically integrated by any standard method. Two methods were used in these studies. The first method is the modified Hamming fourth-order predictor-corrector method. This is an integration procedure that is considered stable and which uses a special Runge-Kutta procedure to obtain starting values. Provisions for controlling local truncation error by changing the step size at each step are included. The detailed algorithm is described by Ralston in [80]. The second method used is the variable order Adams predictor-corrector

method, developed and used by JPL in their Orbital Determination Programs. In addition to being a variable order method, provision is made for making either absolute or relative error tests for the control of local truncation errors for each of the integrated quantities individually. Stepsizes are easily halved or doubled at each step. A description of the integration algorithm is given by Krogh [55].

The variable order Adams method was preferred to the Hamming's method due to its special features. Although the investigations presented in this chapter were started with the Hamming's integration subroutine, it was later replaced by the variable order subroutines. Consequently, results presented later in this chapter were obtained by using the variable order integration subroutines.

4.41 Calculation of Initial Values.

Any numerical integration procedure is formulated for initial-value problems. It is therefore necessary to obtain the starting values:

$$Y_{t_0} = \begin{bmatrix} E \\ \dot{E} \end{bmatrix}_{t_0} = \begin{bmatrix} \theta_0 \\ \psi_0 \\ \Phi_0 \\ \dot{\theta}_0 \\ \dot{\psi}_0 \\ \dot{\Phi}_0 \end{bmatrix} . \qquad (4.29)$$

The starting values were computed in the following way. In Figure 4.3,

XYZ — is the mean ecliptic coordinate system of 1950.0

UVW — is the "average" terrestrial coordinate system

$\theta, \psi, \Phi$ — are the Eulerian angles (orientation angles).

Then let

$\vec{i}, \vec{j}, \vec{k}$ represent unit vectors along XYZ axes respectively

$\vec{i}', \vec{j}', \vec{k}'$ represent unit vectors along the axes UVW respectively,

and

$\vec{n}$ represents the unit vector along the line of nodes, positive toward the descending node of the equator.

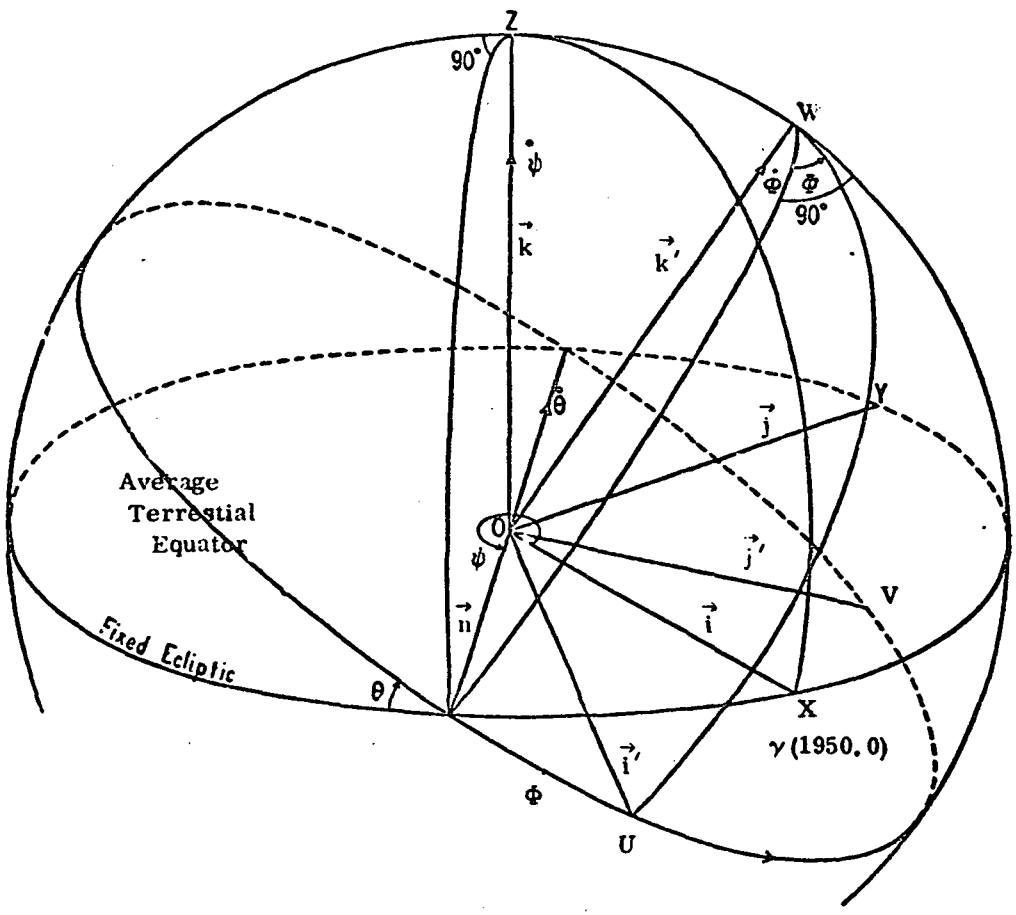


Figure 4.3 Calculation of Eulerian Angles and Their Rates

The transformation from the XYZ coordinate system to the UVW coordinate system is given by

$$\begin{bmatrix} U \\ V \\ W \end{bmatrix}_{epoch} = S\,N\,P\,R_1(-\epsilon_0) \begin{bmatrix} X \\ Y \\ Z \end{bmatrix}_{1950.0} \tag{4.30}$$

or

$$\begin{bmatrix} U \\ V \\ W \end{bmatrix}_{epoch} = T \begin{bmatrix} x \\ y \\ z \end{bmatrix}_{1950.0}$$

where

$$T = S\,N\,P\,R_1(-\epsilon_0)$$

and S, N, P and $\epsilon_0$ have been defined previously. Since the 3 x 3 matrix T transforms a set of coordinates expressed in the 1950.0 mean ecliptic system to the average terrestial system, it follows that

$$\begin{bmatrix} \vec{i}' \\ \vec{j}' \\ \vec{k}' \end{bmatrix} = \begin{bmatrix} T_{11} & T_{12} & T_{13} \\ T_{21} & T_{22} & T_{23} \\ T_{31} & T_{32} & T_{33} \end{bmatrix} \begin{bmatrix} \vec{i} \\ \vec{j} \\ \vec{k} \end{bmatrix}. \tag{4.31}$$

From Figure 4.3 and equation 4.31, $\theta$ is given by

$$\cos\theta = \vec{k}' \cdot \vec{k} = T_{33}$$

Hence

$$\theta = \cos^{-1}(T_{33}) \tag{4.32}$$

Similarly, if

$$\psi' = 360^\circ - \psi$$

$$\cos\psi' = \vec{i} \cdot \vec{n}$$

and

$$\vec{k}' \times \vec{k} = \vec{n} \sin\theta$$

i.e.

$$\vec{n} = \frac{1}{\sin\theta} (T_{32}\vec{i} - T_{31}\vec{j}) .$$

Hence

$$\cos\psi' = \vec{i} \cdot \vec{n} = \frac{T_{32}}{\sin\theta}$$

$$\psi' = \cos^{-1} \left(\frac{T_{32}}{\sin\theta}\right) . \qquad (4.33)$$

For the third angle $\Phi$,

$$\cos\Phi = \vec{i}' \cdot \vec{n}$$

$$\cos\Phi = \frac{1}{\sin\theta} (A_{11} A_{32} - A_{12} A_{31})$$

$$\Phi = \cos^{-1} \left[\frac{A_{11} A_{32} - A_{12} A_{31}}{\sin\theta}\right] . \qquad (4.34)$$

For the initial epoch, the T matrix is calculated. Then the initial values of the three Eulerian angles $\theta$, $\psi$ and $\Phi$ are obtained using equations (4.32), (4.33) and (4.34).

The time derivatives of the angles are obtained by numerical differentiation. The angles are calculated for an epoch $t_o + \Delta t$ and the time rates are obtained from

$$\dot{\theta} = \frac{\theta_{t_o + \Delta t} - \theta_{t_o}}{\Delta t}$$

$$\dot{\psi} = \frac{\psi_{t_o + \Delta t} - \psi_{t_o}}{\Delta t} \qquad (4.35)$$

$$\dot{\Phi} = \frac{\Phi_{t_o + \Delta t} - \Phi_{t_o}}{\Delta t} .$$

$\Delta t$ is a small increment, whose choice is rather arbitrary. However, the increment must be small enough to make the calculated $\dot{\theta}$, $\dot{\psi}$ and $\dot{\Phi}$ close to their true values. From trial runs, it could be concluded that a value of 1/16384 of a day (approximately 5 seconds) is sufficiently small for this purpose.

4.42 Parameters of Integration.

In numerically integrating the system of equation (4.28), the function for calculating $\vec{E}$ has to be evaluated. This function, (equation (4.26)) is given in terms of $\vec{E}$, $\vec{E}$ and some other parameters. These other parameters include the moment of inertia matrix of the earth $M_1$, the masses of the moon, sun and the nearer planets as well as their geocentric positions.

The earth's moment of inertia matrix is given by

$$M_1 = \begin{bmatrix} A & -F & -E \\ -F & B & -D \\ -E & -D & C \end{bmatrix}.$$

The elements of the $M_1$ matrix are related to the second degree spherical harmonic coefficients as follows (see [68])

$$\begin{aligned} C_{20} &= -K[C - \tfrac{1}{2}(A + B)] \\ C_{21} &= K \cdot E \\ C_{22} &= K \cdot \frac{B - A}{4} \\ S_{21} &= K \cdot D \\ S_{22} &= K \cdot \frac{F}{2} \end{aligned} \qquad (4.35)$$

where

$$K = \frac{1}{Ma_e^2}$$

$a_e$, M are the earth's semi-major axis and mass respectively.

From equation (4.36), there are five quantities which explicitly give the six elements of the $M_I$ matrix. Consequently, an additional equation must be defined in order to find the moments of inertia from the spherical harmonic coefficients. From equation (4.36),

$$
\begin{aligned}
A &= C + \frac{1}{K}(C_{20} - 2C_{22}) \\
B &= C + \frac{1}{K}(C_{20} + 2C_{22}) \\
D &= \frac{1}{K} S_{21} \\
E &= \frac{1}{K} C_{21} \\
F &= \frac{2}{K} S_{22} .
\end{aligned}
\tag{4.37}
$$

By putting

$$K' = \frac{C}{Ma_e^2} = C \cdot K$$

$$C = \frac{K'}{K}$$

and equations (4.37) become

$$A = \frac{1}{K}(K' + C_{20} - 2C_{22})$$

$$B = \frac{1}{K}(K' + C_{20} + 2C_{22})$$

and expressions for D, E, F remain the same. If by some other means the value of $K'$ can be found, then the "scaled" moment of inertia matrix can be calculated without using the value of K. It turns out that the scaling of the $M_I$ matrix by $\frac{1}{K}$ does not affect the validity of equation (4.26).

In the integration program, the value used for $K'$ is taken from Kaula [44]

$$K' = \frac{C}{Ma_e^2} = 0.33076.$$

Also, the coefficients of spherical harmonics used were taken from Rapp [81]. Thus,

$$M_1 = \frac{1}{K}\begin{bmatrix} 0.32967 & -0.1692 \times 10^{-5} & 0 \\ -0.1692 \times 10^{-5} & 0.32968 & 0 \\ 0 & 0 & 0.33076 \end{bmatrix}.$$

In addition to the sun and the moon, four other planets were used in equation (4.26). These are Mercury, Venus, Mars and Jupiter. The position of these planets as well as the sun and the moon are obtained in the integration program by reading these values from the JPL Development Ephemeris 69 (DE-69) tape. The DE-69 is the latest of JPL's ephemeris tapes, and contains the position of all the planets, the moon as well as nutation in obliquity and longitude. The positions in the DE-69 were obtained by numerical integration process, and the ephemeris is said to be gravitationally consistent. The planetary masses used are from the JPL system of planetary masses [62]. Table 4.1 gives the gravitational constant for each astronomical body.

| Body | Gravitational Constants ($Km^3/day^{-2}$) |
|---|---|
| Earth | $0.2975542 \times 10^{16}$ |
| Moon | $0.3659906 \times 10^{14}$ |
| Sun | $0.9906936 \times 10^{21}$ |
| Mercury | $0.1655848 \times 10^{15}$ |
| Venus | $0.2425068 \times 10^{16}$ |
| Mars | $0.3197127 \times 10^{16}$ |
| Jupiter | $0.9458682 \times 10^{18}$ |

Table 4.1

Gravitational Constants

## 4.5 Adjustment of Initial Conditions

In order to obtain the earth's orientation angles at epoch t, the six first-order differential equations of motion (equation (4.28)) are numerically integrated from a starting epoch $t_o$. The values obtained for the angles and their rates at the desired epoch t depends to a large extent on the starting values of these quantities at the initial epoch, and on the parameters that are treated in Section 4.42. The method through which the starting values (at $t_o$) can be calculated has been given in Section 4.41 and it necessarily involves the current expressions for precession, nutation and Greenwich Apparent Sidereal Time, as well as a form of numerical differentiation. Small errors in the calculation of the initial values at the starting epoch are propagated through the integration from time $t_o$ to t, and become exaggerated over a long period of time. Consequently, it is important to provide a means

by which initial values and parameters can be corrected in an adjustment process involving some form of observations.

Suppose Z is a set of data which can be computed as a function of the earth's orientation angles together with some other parameters, i.e.

$$Z = Z(Y, \varkappa) \tag{4.37}$$

where

$$Y = \begin{bmatrix} E \\ \dot{E} \end{bmatrix}$$

and $\varkappa$ is a set of parameters also needed in (4.37). Then the variation in Z is obtained through the linearization of equation (4.37) by a Taylor series expansion truncated at the first degree:

$$\delta Z = A_Y \delta Y + A_\varkappa \delta \varkappa \tag{4.38}$$

where

$$A_Y = \frac{\partial Z}{\partial Y}$$

$$A_\varkappa = \frac{\partial Z}{\partial \varkappa} .$$

However, the variation $\delta Y$ in the Eulerian angles and their rates is further related to the variations in the initial conditions $Y_o$ and other parameters $\alpha$ through the solution of the differential equations

$$Y = Y(Y_o, \alpha) \tag{4.39}$$

where

$$Y_o = \begin{bmatrix} E_o \\ \dot{E}_o \end{bmatrix} .$$

The variation in Y obtained in a manner similar to equation (4.38), is given

by:

$$\delta Y = U\delta Y_o + V d\alpha. \tag{4.40}$$

The matrix of partial derivatives

$$U = \begin{bmatrix} U_1 & U_2 \\ U_3 & U_4 \end{bmatrix} = \begin{bmatrix} \frac{\partial E}{\partial E_o} & \frac{\partial E}{\partial \dot{E}_o} \\ \frac{\partial \dot{E}}{\partial E_o} & \frac{\partial \dot{E}}{\partial \dot{E}_o} \end{bmatrix} \tag{4.41}$$

is known as the state transition matrix, which describes the transition of a differential variation of the initial epoch conditions from time $t_o$ to time t. Also, the matrix of partials:

$$V = \begin{bmatrix} V_1 \\ V_2 \end{bmatrix} = \begin{bmatrix} \frac{\partial E}{\partial \alpha} \\ \frac{\partial \dot{E}}{\partial \alpha} \end{bmatrix} \tag{4.42}$$

is called the parameter sensitivity matrix. It describes the effect of a differential variation in the parameters $\alpha$ on the integrated quantities E, $\dot{E}$.

When equation (4.40) is substituted in equation (4.38), the variation in Z is obtained as:

$$\delta Z = A_Y \cdot U \cdot \delta Y_o + A_Y \cdot V \cdot \delta\alpha + A_\chi \delta\chi. \tag{4.43}$$

The matrices of partials $A_Y$ and $A_\chi$ can be evaluated from the formulas obtained by forming the partials of the various parameters which are functions of the observables. Such expressions for the laser distances were given in Section 2.4 and for VLBI, in Sections 3.31, 3.32 and 3.33. However, the solution of the differential equations (equation (4.39)) cannot be written in a closed form.

Consequently, approximate expressions for the U and V matrices have to be found which can be evaluated by numerical differentiation or integration.

4.51 Evaluation of the State Transition and the Parameter Sensitivity Matrices.

One way by which the U and V matrices can be evaluated is by numerical differentiation (also called numerical variant) method. In this method, the desired partial derivatives are obtained by incrementing each of the initial conditions, and integrating the differential equations of motion to the required time t. Then the nominal values of the angles (obtained using the original initial conditions) are subtracted from the values obtained when each initial condition is incremented and the result is divided by the increment.

Thus a set of forty-two differential equations of motion can be integrated together, six for the nominal initial conditions ($Y_{O_N}$) and six for each of the six initial values varied. If, for example the first initial condition $Y_O^1$ is varied from $Y_{O_N}^1$ to $Y_{O_V}^1$, then

$$U_{n,1} = \frac{Y_{(Y_{O_V}^1)} - Y_{(Y_{O_N})}}{Y_{O_V}^1 - Y_{O_N}^1} \qquad (4.42)$$

and similarly for other values varied.

In these studies, the numerical differentiation method was used to obtain the U matrix. The choice of increment is rather arbitrary, although it must be such as to give as close approximations to the partials as is possible. A number of increments is tried, until by trial and error, the U matrix can be considered stable. The stability of the U matrix is ensured when a small change in the increment does not affect the U matrix appreciably.

The V matrix can be obtained in the same way as described for the U matrix. The parameters of interest are varied one by one and the equations of motion integrated to the desired time t. Then the nominal values of the angles are subtracted from the values obtained by varying any of the parameters and the result divided by the increment.

An alternative way of evaluating U and V is by numerical integration [9]. The equations of motion (4.28) can be written in the form

$$\dot{Y} = \dot{Y}(Y, \alpha)$$

and the variation in $\dot{Y}$ is given by

$$\delta\dot{Y} = B\delta Y + H\delta\alpha. \tag{4.43}$$

Substitute equation (4.40) into equation (4.43) to obtain the equation:

$$\delta\dot{Y} = B\cdot U\cdot\delta Y_0 + (B\cdot V + H)\delta\alpha. \tag{4.44a}$$

However, equation (4.44a) can also be obtained by differentiating equation (4.40) with respect to time:

$$\delta\dot{Y} = \dot{U}\delta Y_0 + \dot{V}\delta\alpha. \tag{4.44b}$$

It follows from equations (4.44a) and (4.44b) that

$$\dot{U} = B\cdot U \tag{4.45}$$

and

$$\dot{V} = B\cdot V + H. \tag{4.46}$$

Equations (4.45) and (4.46) are differential equations whose integration will result in the state transition matrix U and the parameter sensitivity matrix V. The solution to equation (4.45) depends on the solution to the equations of motion because the matrix B is a function of the integrated values of Y. Once expressions for B and H have been derived, the differ-

ential equations (4.45) and (4.46) can be integrated along with the six equations of motion (4.28). The matrices B and H are given by

$$B = \frac{\partial \dot{Y}}{\partial Y} = \begin{bmatrix} \frac{\partial \dot{E}}{\partial E} & \frac{\partial \dot{E}}{\partial \dot{E}} \\ \frac{\partial \ddot{E}}{\partial E} & \frac{\partial \ddot{E}}{\partial \dot{E}} \end{bmatrix} = \left[\begin{array}{c|c} O & I \\ \hline B_{21} & B_{22} \end{array}\right] \tag{4.47}$$

$$H = \frac{\partial \dot{Y}}{\partial \alpha} = \begin{bmatrix} \frac{\partial \dot{E}}{\partial \alpha} \\ \frac{\partial \ddot{E}}{\partial \alpha} \end{bmatrix} = \begin{bmatrix} O \\ H_2 \end{bmatrix}. \tag{4.48}$$

Expressions for $B_{21}$, $B_{22}$, and $H_2$ can be obtained by differentiating the second order differential equations represented by equation (4.26). This differentiation was not carried out in this work since another method was chosen for the evaluation of the state transition matrix.

4.52 Numerical Fit of the Numerically Integrated Angles to the Calculated Angles.

In order to investigate the feasibility of numerically integrating the earth's orientation angles, the differential equations of motion (4.26) were integrated for a limited period of time. The results are presented in Section 4.6 of this work. As would be expected however, the numerically integrated angles differed from the calculated angles. Also, the differences grew larger as the epoch of integration moved away from the initial epoch. The differences in values of the integrated angles and the calculated angles are due, at least in part, to the inaccurate values of the initial conditions. Better initial conditions can be obtained through adjustment processes involving real observations together with the use of the state transition matrix and the parameter sensitivity matrix already treated in Sections 4.5 and 4.51.

Without available real observations, it is still possible to obtain corrections to the initial values. In this case, the calculated angles could serve as pseudo-observations, while the integrated angles are "approximate" values. This idea originated from the work of JPL in the development of their numerical ephemeris. The lunar ephemeris obtained by numerical integration was fitted to the Brown-Eckert ephemeris in order to adjust the initial conditions for their integration [29]. It is important to note that such a numerical fit of integrated quantities to their corresponding values obtained through other means does not distort the numerical integration process. It merely seeks to relate the integrated values to the values obtained through other proven means. This is clearly permissible in this case because classical methods of calculating the earth's orientation are known to yield results very close to the actual orientation of the earth.

Let

$$E_b = \begin{bmatrix} \theta \\ \psi \\ \Phi \end{bmatrix}_b$$

be the earth's Eulerian angles obtained through precession, nutation and GAST. Also, let

$$E_c = \begin{bmatrix} \theta \\ \psi \\ \Phi \end{bmatrix}_c$$

be the corresponding values from numerical integration with initial conditions:

$$Y_o = \begin{bmatrix} E_o \\ \dot{E}_o \end{bmatrix} = \begin{bmatrix} \theta_o \\ \psi_o \\ \Phi_o \\ \dot{\theta}_o \\ \dot{\psi}_o \\ \dot{\Phi}_o \end{bmatrix} .$$

In a perfect situation, it is expected that

$$E_c - E_b = \begin{bmatrix} \theta \\ \psi \\ \Phi \end{bmatrix}_c - \begin{bmatrix} \theta \\ \psi \\ \Phi \end{bmatrix}_b = \begin{bmatrix} 0 \\ 0 \\ 0 \end{bmatrix} .$$

In general, however, there are differences between $E_c$ and $E_b$, i.e.

$$\Delta E = E_c - E_b = \begin{bmatrix} \Delta\theta \\ \Delta\psi \\ \Delta\Phi \end{bmatrix} . \tag{4.49}$$

Since $E_c$ is a function of $Y_o$, it follows that

$$\Delta E = \begin{bmatrix} \Delta\theta \\ \Delta\psi \\ \Delta\Phi \end{bmatrix} = f(Y_o) = f \begin{bmatrix} \theta_o \\ \psi_o \\ \Phi_o \\ \dot{\theta}_o \\ \dot{\psi}_o \\ \dot{\Phi}_o \end{bmatrix} . \tag{4.50}$$

Using the principles of least squares, the weighted sum of squares of $\Delta E$ is minimized. Thus, using the notations of Uotila [93], the corrections, X, to the approximate values of the initial conditions $Y_0^0$ is given by

$$X = -(A^T PA)^{-1} (A^T PL) \tag{4.51}$$

where

$$A = \frac{\partial(\Delta E)}{\partial(Y_0)} \tag{4.52}$$

$$L = \begin{bmatrix} \theta_c - \theta_b \\ \psi_c - \psi_b \\ \Phi_c - \Phi_b \end{bmatrix} \tag{4.53}$$

and P is a weight matrix. In obtaining the design matrix A, the state transition matrix is also needed.

$$A = \frac{\partial(\Delta E)}{\partial(Y_0)} = \frac{\partial(\Delta E)}{\partial E} \cdot \frac{\partial E}{\partial(Y_0)} . \tag{4.54}$$

However,

$$\frac{\partial \Delta E}{\partial E} = I \text{ (identity matrix)}$$

and

$$\frac{\partial E}{\partial(Y_0)} = \begin{bmatrix} \frac{\partial E}{\partial E_0} & \frac{\partial E}{\partial \dot{E}_0} \end{bmatrix} = [U_1 \quad U_2].$$

Hence the A matrix can be evaluated along with the integration of Y, if the $U_1$, $U_2$ submatrices are obtained through one of the methods in Section 4.51.

The L matrix is easily obtained by calculating the Eulerian angles at each epoch of comparison (using precession, etc.) and subtracting these values from the integrated angles. In general, the size of the A matrix is 3n x 6 and that of L is 3n x 1 where n is the number of discrete epochs over which the adjustment is to be made.

The choice of the function to be minimized in a case like this must be made carefully. If the $\Delta E$ quantities are large, it may be necessary to find other functions to minimize. The sum of squares of the $\Delta E$ quantities have been minimized in these studies because they are quite small. Numerical results from the adjustment and the improvement it made to the integration made with the unadjusted initial conditions are presented in Section 4.6.

## 4.6 Numerical Experiments and Results.

In the previous sections of this chapter, a method by which the orientation of the average terrestrial coordinate system with respect to a fixed celestial coordinate system (such as the mean ecliptic system of 1950.0) can be obtained by direct numerical integration of the earth's equations of motion has been outlined. The earth's dynamical (rotational) equations of motion were derived in a more complete form, without assumptions as to the mass distribution and dynamic shape of the earth. Since the integrated angles and their time rates at any epoch depend on the initial conditions and physical parameters used in integrating the equations of motion, an outline of a method through which corrections to the initial conditions and the physical parameters can be obtained was also given. Such a new theoretical approach to an old problem as this needs some confirmation as to the validity of the method numerically. It is therefore the purpose of this section to provide such needed numerical support for the theoretical parts of the chapter.

An extensive numerical experiment on this subject is well beyond the scope of the present study. Consequently, the experiments reported in this section are limited to those necessary to verify the correctness of the equations derived and the computer programs developed for the numerical integration of the Eulerian angles and their time rates. Also, the ability to adjust the initial conditions with the adjustment computer programs based on the method presented in Section 4.5 was verified.

An important aid in verifying the computer programs developed in connection with this study was the Simulated Earth-Moon Environment data (hereafter referred to in this section as the simulated data) which was developed by Papo [78]. The generated simulated data are based on a moderately complex model of the earth-moon dynamic system consisting of a rotationally symetric rigid earth and a perfectly rigid moon whose dynamical shape is that of a triaxial ellipsoid. Details of the model and the mathematical formulation of the equations of motion of this simplified earth-moon system are contained in [78].

A simulated ephemeris of the earth and the moon was created for a period of one year beginning at 2440222.5 JD (1969.0). The ephemeris consists of numerically integrated geocentric position and velocity of the moon, the Eulerian angles and their time rates for the earth and the moon recorded at half daily intervals. In addition, a fifth-order modified Everett interpolation formula [77] was available for use in interpolating the 18 quantities at epochs which fall between tabulated values.

The following two numerical experiments are reported in this section.

(1) Fitting the numerically integrated earth's Eulerian angles to those obtained from the simulated data.

(2) Comparing the numerically integrated Eulerian angles to their counterparts obtained through classical method (using

precession, nutation and polar motion as outlined in Section 4.41).

4.61 Fitting the Numerically Integrated Eulerian Angles to the Simulated Angles.

As previously mentioned, the availability of the simulated data enables one to independently check the equations of motion of the earth as developed in this chapter and the computer programs written on the basis of the equations. Therefore, the first task that was performed was to compare the numerically integrated angles to the simulated angles. In order to make the two sets of angles compatible, the numerical integration program written for the real case had to be slightly modified to accomodate the following restrictions imposed by the simulated environment model:

(1) For the elements of the moment of inertial matrix, $A = B$ and $D = E = F = 0$.

(2) Only the moon is the external celestial body whose potential affects the rotation of the earth.

(3) The geocentric position of the moon at any epoch is that given by the simulated data rather than the one obtainable from a real lunar ephemeris.

It turned out that these modifications to the real integration program were easily achieveable through the alteration of a few statements in the program and data cards.

The integrating subroutine used to integrate the equations of motion is the DVDQ subroutine, a variable step, variable order Adams integrator [55]. A comparison of angles integrated and their counterparts from the simulated data shows residuals which were less than $0.''0001$ for $\theta$ and $0.''001$ for $\psi$ and $\Phi$ over the one year interval. These results indicate perfect agreement between the two numerical integration programs which are results of equations derived independently, using different methods and expressed in different forms.

The next step was to test the adjustment program and the ability of the adjustment method to recover the initial conditions. For this purpose, the theoretical initial conditions (values of the integrated quantities at the initial epoch of 2440222.5 JD), read from the simulated data were varied. Three test runs were made in which

(1) only the initial angles were varied

(2) both the initial angles and their time rates were varied

(3) only the time rates of the angles were varied.

The adjustment was performed over an interval of forty days beginning at 2440222.5 JD and ending at 2440262.5 JD. Values of the angles integrated with wrong initial conditions were compared with the "true" values at half daily intervals. Table 4.2 shows the "correct" initial conditions, and the initial conditions used in each of the three cases mentioned above.

| Symbol | Correct Initial Values | Initial Values for Case 1 | Initial Values for Case 2 | Initial Values for Case 3 |
|---|---|---|---|---|
| $\theta$ | 0.4091596226 | 0.4091693189 | 0.4091644707 | 0.4091596226 |
| $\psi$ | $-0.131898 \times 10^{-5}$ | $-0.110152 \times 10^{-4}$ | $-0.616711 \times 10^{-5}$ | $-0.131898 \times 10^{-5}$ |
| $\Phi$ | 4.8950936587 | 4.8951033498 | 4.8950985068 | 4.8950936587 |
| $\dot{\theta}$ | $0.659363 \times 10^{-7}$ | $0.659363 \times 10^{-7}$ | $0.725299 \times 10^{-7}$ | $0.725299 \times 10^{-7}$ |
| $\dot{\psi}$ | $-0.300932 \times 10^{-8}$ | $-0.30093 \times 10^{-8}$ | $-0.303942 \times 10^{-8}$ | $-0.303942 \times 10^{-8}$ |
| $\dot{\Phi}$ | 6.3003883741 | 6.3003883741 | 6.3003943826 | 6.3003943826 |

Table 4.2 Starting Initial Conditions for Three Test Cases.

($\theta$, $\psi$, $\Phi$ in radians, $\dot{\theta}$, $\dot{\psi}$, $\dot{\Phi}$ in rad/day)

| Symbol | Correct Initial Values | Recovered Initial Values for Case 1 | Recovered Initial Values for Case 2 | Recovered Initial Values for Case 3 |
|---|---|---|---|---|
| $\theta$ | 0.4091596226 | 0.4091596227 | 0.4091596227 | 0.4091596226 |
| $\psi$ | $-0.131898 \times 10^{-5}$ | $-0.131869 \times 10^{-5}$ | $-0.131880 \times 10^{-5}$ | $-0.131860 \times 10^{-5}$ |
| $\Phi$ | 4.8950936587 | 4.8950936584 | 4.8950936585 | 4.8950936584 |
| $\dot{\theta}$ | $0.659363 \times 10^{-7}$ | $0.652045 \times 10^{-7}$ | $0.654780 \times 10^{-7}$ | $0.649609 \times 10^{-7}$ |
| $\dot{\psi}$ | $-0.300932 \times 10^{-8}$ | $-0.298465 \times 10^{-8}$ | $-0.299432 \times 10^{-8}$ | $-0.300307 \times 10^{-8}$ |
| $\dot{\Phi}$ | 6.3003883741 | 6.3003883718 | 6.3003883727 | 6.3003883735 |

Table 4.3 Recovered Initial Conditions for Three Test Cases after Two Iterations.
($\theta$, $\psi$, $\Phi$ in radians, $\dot{\theta}$, $\dot{\psi}$, $\dot{\Phi}$ in rad/day)

Table 4.3 presents the adjusted values of the initial conditions for the three cases after two iterations. Comparison of the recovered parameters with their correct values shows agreement up to the ninth decimal figure (equivalent to 0.″0002 for the angles, and 0.″0002/day for their time rates). The residuals obtained from the comparison of the integrated angles and those from the simulated data were, for all three angles and in all three cases, less than 0.″0001 throughout the adjustment interval. Since Case 2 is the most general case, the residuals before and after adjustments are presented in Figure 4.4 for $\theta$ and $\psi$ and in Figure 4.5 for $\Phi$.

From the adjustment results, it appears as if some of the parameters in the solution have poor separation from other parameters. This can be seen in Table 4.4 which presents the correlation matrix obtained from the adjustment. The correlation matrix for all three test cases is identical up to the first two significant digits. Also, the inverted normal matrix (weight coefficient matrix) for all three cases is very similar, and Table 4.5 shows the weight coefficient matrix for Case 2. In spite of the high correlation between certain parameters (especially between $\dot{\psi}$ and $\dot{\Phi}$) the results of these experiments show that the

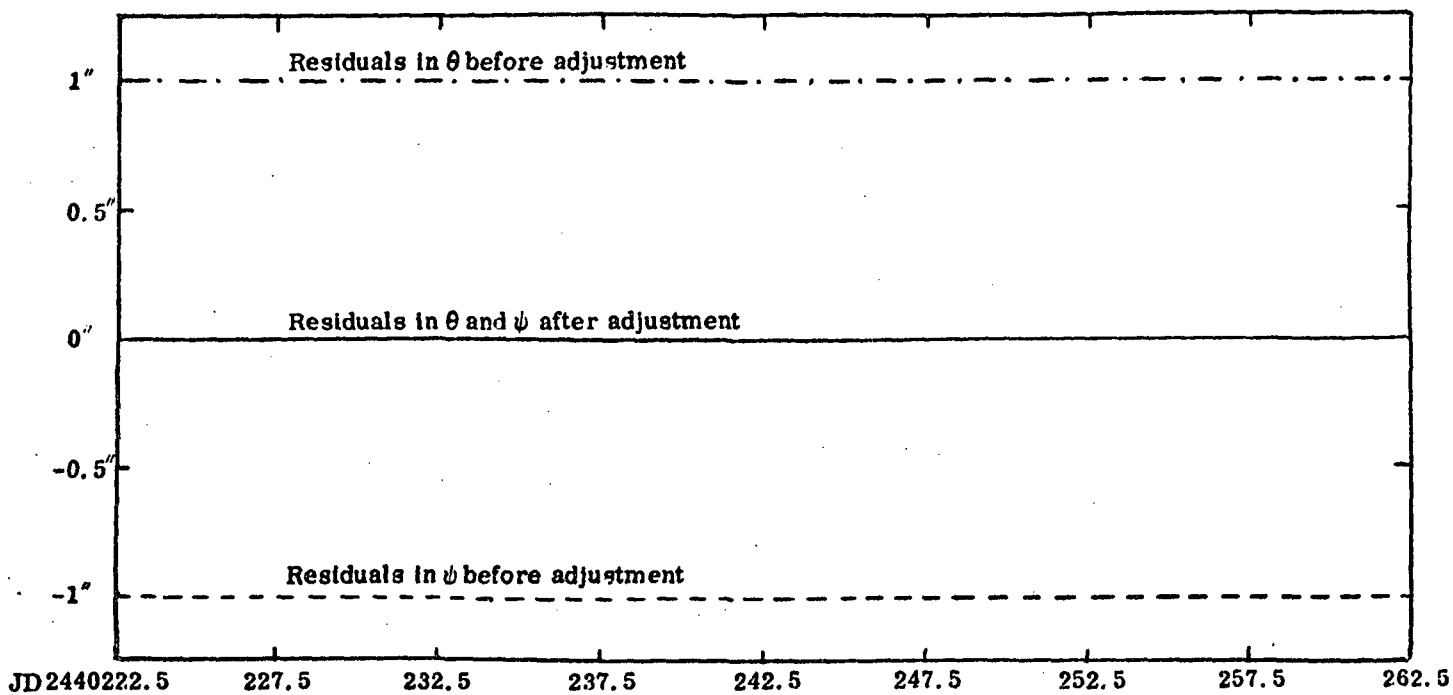


Figure 4.4 Residuals in θ and ψ Before and After Adjustment.

(Simulated Case)

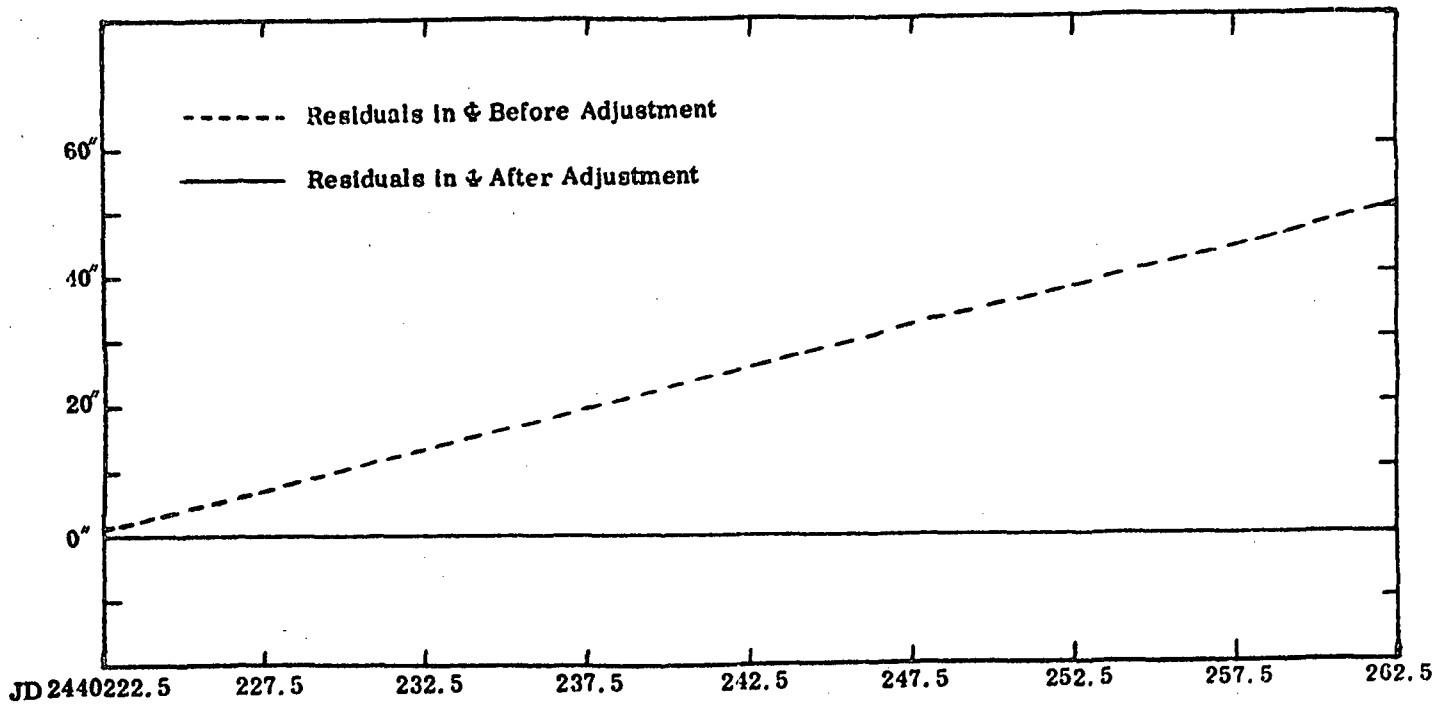


Figure 4.5 Residuals in Φ Before and After Adjustment.

(Simulated Case)

solutions for all the parameters do actually converge to their true values. The adjustment performed over a 40-day interval with two iterations takes approximately five minutes to run on an IBM 360/75 computer.

| | $\theta$ | $\psi$ | $\Phi$ | $\dot{\theta}$ | $\dot{\psi}$ | $\dot{\Phi}$ |
|---|---|---|---|---|---|---|
| $\theta$ | 1.00 | | | | | |
| $\psi$ | -0.17 | 1.00 | | | | |
| $\Phi$ | 0.10 | -0.35 | 1.00 | | | |
| $\dot{\theta}$ | 0.22 | -0.76 | 0.46 | 1.00 | | |
| $\dot{\psi}$ | 0.41 | -0.41 | 0.25 | 0.54 | 1.00 | |
| $\dot{\Phi}$ | -0.41 | 0.41 | -0.26 | -0.54 | -0.99 | 1.00 |

Table 4.4

Correlation Matrix for Adjusted Initial Values in the Simulated Case.

| | $\theta$ | $\psi$ | $\Phi$ | $\dot{\theta}$ | $\dot{\psi}$ | $\dot{\Phi}$ |
|---|---|---|---|---|---|---|
| $\theta$ | $1.5\times10^{-2}$ | | | | | |
| $\psi$ | $-3.5\times10^{-3}$ | $2.9\times10^{-2}$ | | | | |
| $\Phi$ | $3.0\times10^{-3}$ | $-1.5\times10^{-2}$ | $6.2\times10^{-2}$ | | | |
| $\dot{\theta}$ | $8.6\times10^{-3}$ | $-4.2\times10^{-2}$ | $3.8\times10^{-2}$ | $1.1\times10^{-1}$ | | |
| $\dot{\psi}$ | $3.9\times10^{-2}$ | $-5.6\times10^{-2}$ | $4.9\times10^{-2}$ | $1.4\times10^{-1}$ | $6.3\times10^{-1}$ | |
| $\dot{\Phi}$ | $5.3\times10^{-1}$ | $5.1\times10^{-2}$ | $-4.6\times10^{-2}$ | $-1.3\times10^{-1}$ | $-5.7\times10^{-1}$ | $5.3\times10^{-1}$ |

Table 4.5

Weight Coefficient Matrix for Adjusted Initial Values in the Simulated Case.

4.62 Comparison of Numerically Integrated Eulerian Angles to those Obtained through Classical Method.

The experiments performed in Section 4.61 have demonstrated that the method and equations developed in the previous sections of this chapter can be used to accurately integrate earth's Eulerian angles and, if necessary, to adjust initial conditions in a simulated model. Nevertheless, the ultimate test of this method as to its applicability to the real world rests on how such numerically integrated angles compare with their counterparts using existing methods. The purpose of this section is to evaluate, through numerical experiments, whether or not the equations and methods presented earlier can be used in a real situation. In this case, there is no known "true" solution, and only good estimates of the solution can be obtained, usually through an adjustment process. Consequently, the experiments reported in this section show:

(1) How close the values of the angles integrated are, compared to corresponding angles obtained through classical methods

(2) Results obtained, if the initial conditions are adjusted.

In Section 4.41, a method has been outlined through which the three Eulerian angles $\theta$, $\psi$, $\Phi$ can be obtained at any epoch (using values of precessional and nutational elements, and the GAST). The initial values of the angles for the numerical integration as well as the angles compared with the integrated angles at selected epochs were computed using this method. The time rates of the initial angles were obtained by dividing the difference between computed angles at the initial epoch and at 1/65536 day later by the time interval.

The integration was performed over an interval of approximately one year between 2437610.5 JD and 2437970.5 JD. The earth's equations of motion were integrated by the DVDQ subroutine. The geocentric position of the sun, the moon and the planets (see Section 4.42) at the epoch of

integration were read off the JPL's latest numerical development ephemeris — DE69. The constants of integration were those given in Section 4.42. The integration over the one-year period took approximately five minutes on the IBM 360/75 computer.

Instead of the Cowell type of integration performed in the simulated case, the Encke type of integration was used in this case. This can be done by modifying the original equations of motion from Cowell's to Encke's type, i.e. defining a reference case of motion for which analytical expressions can be given, and obtaining the difference between Cowell's equations of motion and the equations of motion of the reference case. Thus, the equations integrated are "perturbations" of the reference case. In addition to this modification, it was decided to integrate perturbations of the quantities $\theta$, $\psi$, $\psi + \Phi$ and their time rates instead of $\theta$, $\psi$, $\Phi$ and their time rates. The main reason for doing this was to find out whether or not the strong correlation between $\dot{\psi}$ and $\dot{\Phi}$ can be removed. As it turns out, this affected, very little, the high correlation between the two parameters.

The quantities integrated (in the Encke mode) were:

$$\begin{bmatrix} \delta_1 \\ \delta_2 \\ \delta_3 \\ \delta_4 \\ \delta_5 \\ \delta_6 \end{bmatrix} = \begin{bmatrix} \theta - \theta_c \\ \psi - \psi_c \\ \Phi + \psi - K_0 - K_1 t \\ \dot{\theta} \\ \dot{\psi} \\ \dot{\Phi} + \dot{\psi} - K_1 \end{bmatrix}$$

where

$\theta_c$ = 0.409170 rad.

$\psi_c$ = 6.280350 rad.

$K_0 = \Phi_c + \psi_c$ = 7.082407

$K_1$ = 6.30038810 rad/day (sidereal rate)

and

$$t = \text{time in JD from the initial epoch.}$$

Also, the quantities compared at each epoch with the computed values were $\theta$, $\psi$ and $\Phi + \psi$. The initial values of the integrated quantities were

$$\delta_1 = 7.00084121 \times 10^{-7}\text{rad.} \quad \delta_4 = -1.85309594 \times 10^{-7}\text{rad/day}$$
$$\delta_2 = 4.42734527 \times 10^{-7}\text{rad.} \quad \delta_5 = -3.32660736 \times 10^{-7}\text{rad/day}$$
$$\delta_3 = 1.30133957 \times 10^{-6}\text{rad.} \quad \delta_6 = -6.40369792 \times 10^{-7}\text{rad/day.}$$

All quantities integrated refer to the mean ecliptic system of 1950.0.

The residuals in $\theta$, $\psi$ and $\Phi + \psi$ are presented in Figures 4.6 and 4.7. It can be seen from these figures that residuals in $\theta$ and $\psi$ exhibit a semi-monthly period while residuals in $\Phi + \psi$ have a dominant secular trend. However, the residuals were very small, not exceeding $0\overset{''}{.}02$ in $\theta$, $0\overset{''}{.}05$ in $\psi$ and $0\overset{''}{.}3$ in $\theta + \psi$ over the period of one year.

An attempt was also made at adjusting the initial conditions by fitting the numerically integrated angles over the computed ones. For this purpose, a relatively short interval of forty days beginning at 2437610.5 JD was chosen. The initial values of the integrated quantities ($\delta_1$ to $\delta_6$) were those given above. After a single iteration, the corrections to the starting values of the initial conditions were less than $0\overset{''}{.}01$ and the adjusted values of these quantities were:

$$\delta_1 = 7.23518822 \times 10^{-7} \qquad \delta_4 = -1.96953572 \times 10^{-7}$$
$$\delta_2 = 4.99809019 \times 10^{-7} \qquad \delta_5 = -3.21460406 \times 10^{-7}$$
$$\delta_3 = 1.30475169 \times 10^{-6} \qquad \delta_6 = -6.36575208 \times 10^{-7}$$

This single solution took approximately three minutes on the IBM 360/75 computer.

The correlation matrix as shown by Table 4.6 shows in general less correlation between parameters compared to the simulated case (Table 4.4).

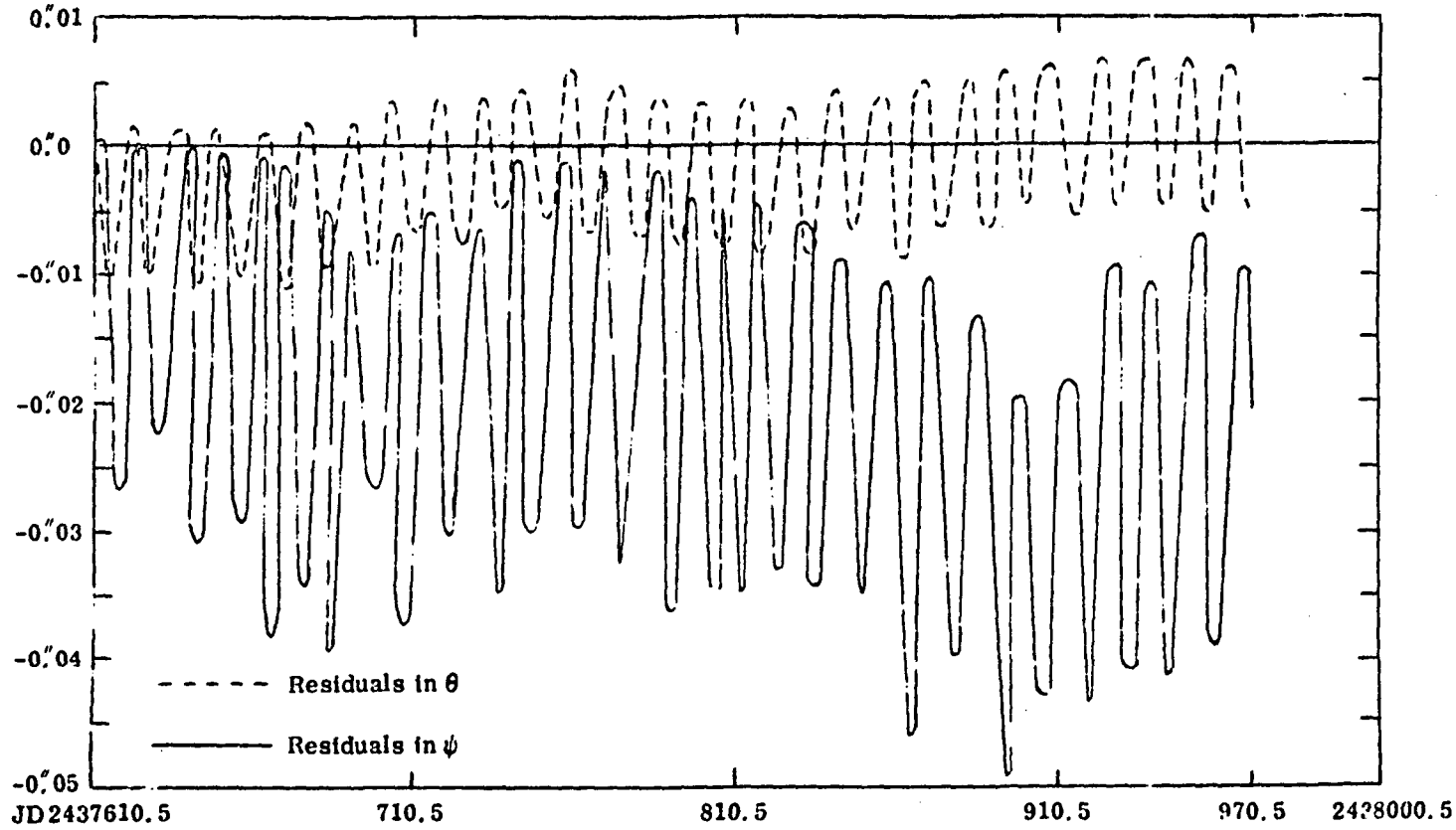


Figure 4.6 Residuals in θ and ψ Over One Year Period.

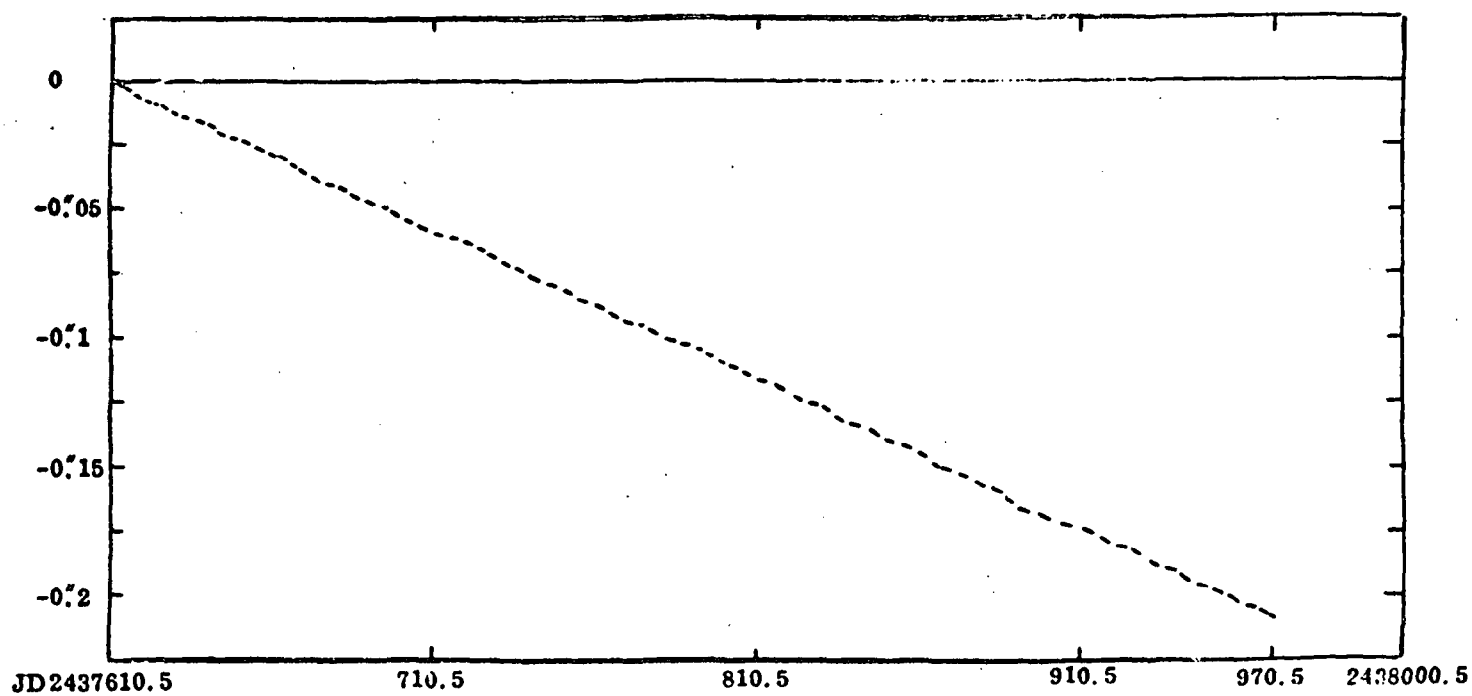


Figure 4.7 Residuals in $\Phi + \psi$ Over One Year Period.

However, the high correlation between $\delta_5$ and $\delta_6$ is almost the same as that between $\dot{\psi}$ and $\dot{\Phi}$ in the simulated case. Table 4.7 also presents the weight coefficient matrix for the adjusted initial conditions.

| | $\delta_1$ | $\delta_2$ | $\delta_3$ | $\delta_4$ | $\delta_5$ | $\delta_6$ |
|---|---|---|---|---|---|---|
| $\delta_1$ | 1.00 | | | | | |
| $\delta_2$ | -0.13 | 1.00 | | | | |
| $\delta_3$ | 0.04 | -0.08 | 1.00 | | | |
| $\delta_4$ | 0.15 | -0.80 | 0.01 | 1.00 | | |
| $\delta_5$ | 0.33 | -0.44 | 0.14 | 0.48 | 1.00 | |
| $\delta_6$ | 0.33 | -0.40 | 0.00 | 0.44 | 0.98 | 1.00 |

Table 4.6

Correlation Matrix for Adjusted Initial Conditions in the Real Case.

| | $\delta_1$ | $\delta_2$ | $\delta_3$ | $\delta_4$ | $\delta_5$ | $\delta_6$ |
|---|---|---|---|---|---|---|
| $\delta_1$ | $6.2\times10^{-3}$ | | | | | |
| $\delta_2$ | $-1.6\times10^{-3}$ | $2.2\times10^{-2}$ | | | | |
| $\delta_3$ | $5.1\times10^{-4}$ | $-1.7\times10^{-3}$ | $2.2\times10^{-2}$ | | | |
| $\delta_4$ | $3.7\times10^{-3}$ | $-4.1\times10^{-2}$ | $4.1\times10^{-3}$ | $1.0\times10^{-2}$ | | |
| $\delta_5$ | $1.2\times10^{-2}$ | $-2.9\times10^{-2}$ | $3.0\times10^{-3}$ | $6.9\times10^{-2}$ | $1.9\times10^{-1}$ | |
| $\delta_6$ | $8.8\times10^{-4}$ | $-2.0\times10^{-3}$ | $-4.4\times10^{-5}$ | $4.8\times10^{-3}$ | $1.5\times10^{-2}$ | $1.2\times10^{-3}$ |

Table 4.7

Weight Coefficient Matrix for Adjusted Initial Conditions in the Real Case.

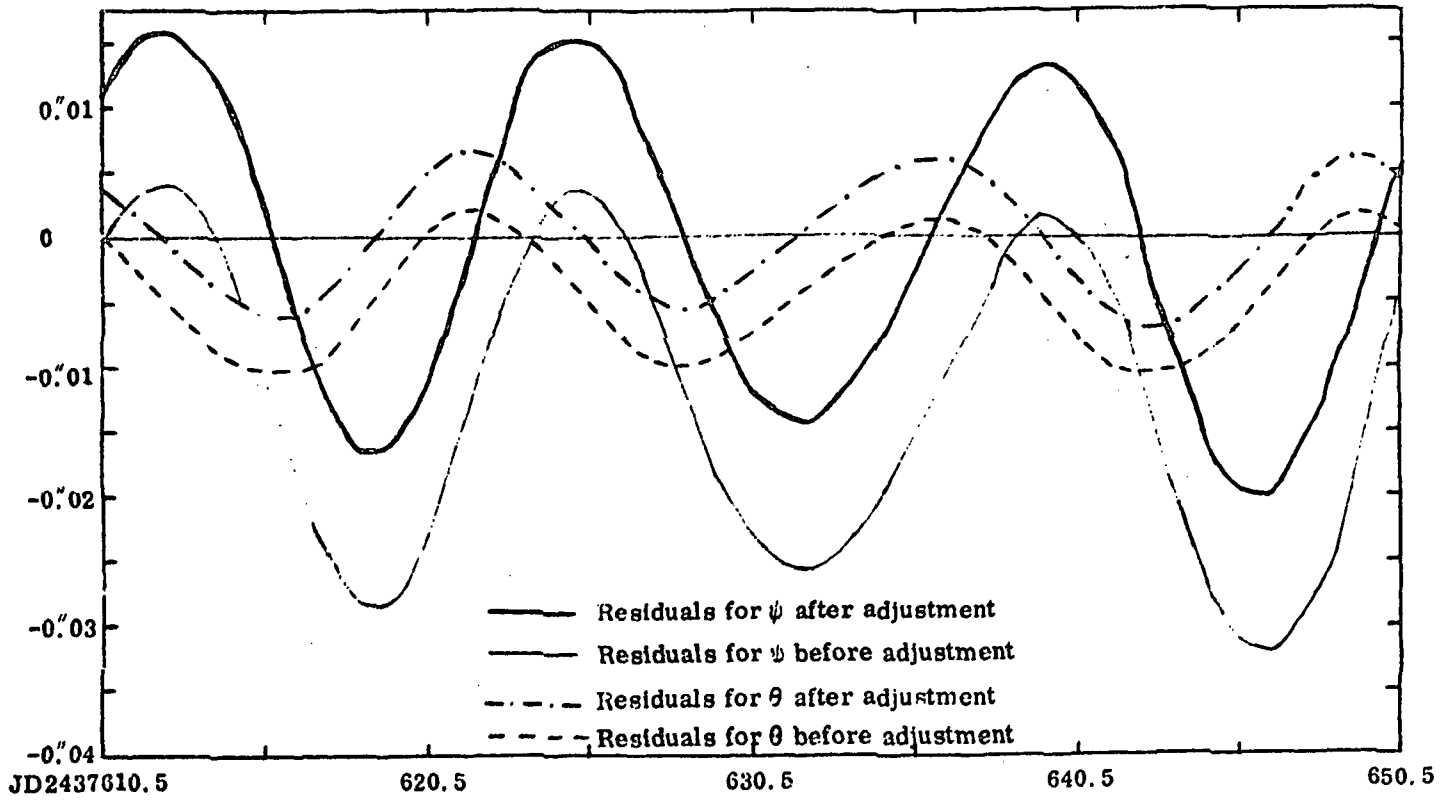


**Figure 4.8** Residuals for θ and ψ Before and After Adjustment.

(Real Case)

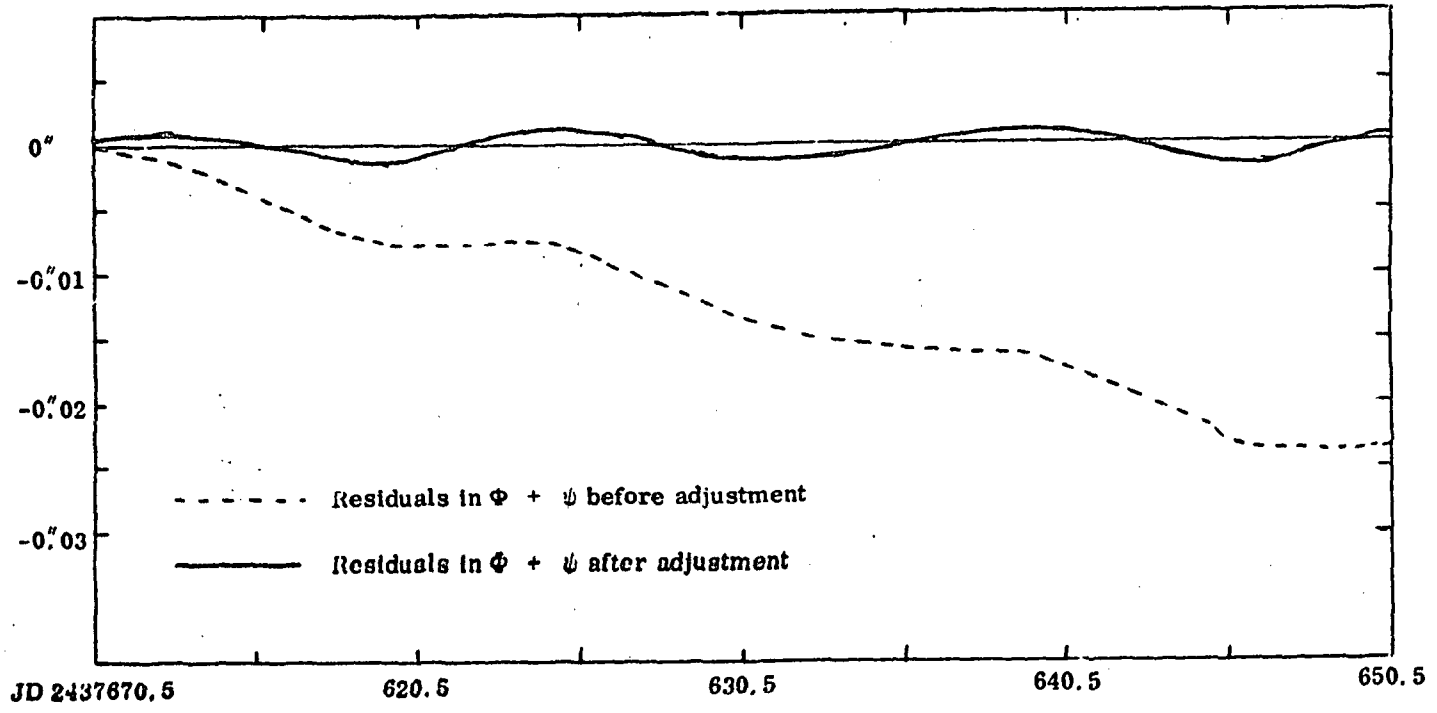


Figure 4.9 Residuals in $\Phi + \psi$ Before and After Adjustment.

(Real Case)

The residuals in $\theta$, $\psi$ and $\theta + \psi$ before and after the adjustment are shown in Figures 4.8 and 4.9. It can be seen from these two figures that the basic form of the residuals remained after adjustment, but the residuals were more or less centered around the zero line. The semi-monthly period present before the adjustment remained after the adjustment.

One basic conclusion that could be made on the basis of tests performed in this section is that it is possible to obtain, by the numerical integration method, the orientation of the average terrestrial coordinate system with respect to a coordinate system fixed in space (such as the mean ecliptic system of 1950.0). It has been demonstrated that over a period of one year, the integrated angles compare well with the angles computed by classical means to within $0\overset{''}{.}2$. Also, it is possible to adjust the initial conditions through the method given in this chapter in order to obtain a better fit of the integrated angles with computed ones using the classical method. Nevertheless, it is important to note that the most desireable goal is to adjust the initial conditions, using real observations.

# 5 ADJUSTMENT MODEL FOR LASER AND VLBI OBSERVATIONS.

## 5.1 Introduction.

In the previous chapters, we have treated two basic types of new observations which can be used to obtain more accurate position determination on the moon. In both Chapters 2 and 3, the prediction equations for the observables have been developed as functions of certain physical and astronomical parameters. Also partial derivatives essential to the formation of observation equations have been derived. In general, the observed values of the observables and their computed values will be different, the differences resulting from errors in the observations as well as errors in the assumed values of parameters used in the prediction equations. These assumed values of parameters can then be "corrected" using the deviations of the observed values from their predicted counterparts through an adjustment procedure. Much more often than not, there are more equations available than unknowns (due to large number of observations), and a unique solution is usually obtained through the use of the principles of least squares. This technique involves the minimization of a quadratic form, which is the total weighted sum of squares of the residuals.

In this study, the two observation types we are concerned with are the laser distances and the VLBI time delays. Furthermore, VLBI observations have been classified under three types namely

earth- earth VLBI observations
earth-moon VLBI observations
moon-moon VLBI observations.

Although the earth- earth VLBI observations cannot be used directly to obtain coordinates of points on the moon (except in the case of observations made to artificial radio sources located on the lunar surface), they can be used to determine more accurately the orientation of the earth-fixed axes in space. In turn, the knowledge of the earth's orientation in space is essential to the determination of selenodetic control through earth-based observations. Therefore, the adjustment equations developed in this chapter will be applicable to the four types of observation as follows:

(i) lasers
(ii) earth-earth VLBI
(iii) earth-moon VLBI
(iv) moon-moon VLBI.

In developing the adjustment model, consideration is given to the fact that values for most of the parameters to be solved for are available through some sort of previous determinations. Therefore, since these "approximate" values of parameters have some variances associated with them, they could also be considered as "observations" with corresponding residuals and weights. It is also recognized that laser observations are currently under way, while the other observation types are only a future possibility. Therefore, a sequential solution of the normal equations is desirable, whereby the laser observations could be adjusted first, and the result later combined directly with other observation types whenever they are available. Lastly, it is recognized that there are many parameters involved in the adjustment of this kind, some of which are either undesirable (nuisance parameters) or known more accurately through other means than can be obtained using the observation

types considered in this study. For example, parameters related to refraction models and clock synchronization errors are nuisance parameters while geocentric Cartesian coordinates of earth stations may be obtained more accurately through other means, such as artificial satellite data analysis.

In summary, the adjustment model to be developed will be a generalized model in which parameters will be regarded as "observations" associated with their corresponding weights. The solution of the normal equations will be of a sequential nature, and parameters whose solutions are not required will be eliminated from the normal equations while their contribution to the solution of the other desired parameters will be accounted for. The derivation of the normal equations and their solution follow, in most part, the method used by Uotila in [93].

## 5.2 Classification of Parameters in the Solution.

It has been noted in Section 5.1 that all parameters in the general adjustment model will be regarded as observations with corresponding weights. In addition to these quasi-observations, we also have observations made with either laser or VLBI instrumentation. These observations are divided into four groups as follows:

(a) laser — (F - group)
(b) earth-earth VLBI — (G - group)
(c) earth-moon VLBI — (H - group)
(d) moon-moon VLBI — (J - group).

The parameters (or quasi-observations) are also in two categories. The first class of parameters are of direct interest, and their solution is the main goal of these studies. Parameters in the second class can be described as transient. They are needed for the mathematical modeling of the observation groups, but they are either of no direct interest (nuisance parameters) or they are not as sensitive to the observation types being con-

sidered here as other known types of observations.

In this work, parameters are classified into four groups - $X_1$, $X_2$, $X_3$, $X_4$ - through the consideration of the above defined classes of desired and non-desired parameters as well as other factors.

Parameters $X_1$

This group includes the Cartesian (x, y, z) coordinates of the lunar stations in the selenodetic coordinate system. These are the main set of parameters in which we are interested. Transformation into polar coordinates can be done easily (since the lunar figure approximates a sphere).

Also in the $X_1$ parameter group are the lunar orientation parameters. In this chapter, the orientation of the moon with respect to an inertial system will be assumed to be defined by the three Eulerian angles obtained through the numerical integration of the moon's equations of motion. Consequently, the orientation parameters consist of the initial values of the Eulerian angles and their time rates at a standard epoch. This set of parameters which is non-variant, is related to the moon's orientation angle at each epoch through a 6 x 6 partial derivatives matrix known as the state transition matrix. The partials of the mathematical functions with respect to this set of parameters are obtained by using the state transition matrix together with the partials of the functions with respect to the orientation angles at each epoch of observation. Thus, the moon's orientation parameters to be solved remain six, irrespective of the number of epochs at which observations are made.

The last set of parameters in this group relate to the dynamic figure of the moon. These are the moon's principal moments of inertia, or the lower degree and order harmonic coefficients of the moon. These constants appear explicitly in the moon's equations of motion which are integrated in

order to obtain the moon's orientation angles (see [78]).

All the three sets of parameters in this group are desirable parameters. In addition to this, they also appear in the mathematical functions for the three observation types F, H and J.

Parameters $X_2$

The parameters in this group are the geocentric Cartesian coordinates of the observing stations on the earth and the earth's orientation with respect to an inertial system. They feature in the mathematical functions for F, G and H-type observations, since these observations require at least one station on the earth.

The orientation parameters are defined in the same way as the moon's orientation parameters above. In Chapter 4, the numerical integration of the earth's orientation (Eulerian) angles and their time rates have been suggested. In this way, the number of parameters reduce to the six initial conditions which are related to the Eulerian angles and their time rates at any observing epoch by the 6 x 6 state transition matrix.

Also included in this group are the parameters of polar motion (coordinates of the true (instantaneous) pole from the average pole). For easy parametisation, it is reasonable to regard these coordinates as constant over short intervals of time.

The $X_2$ group of parameters may or may not be regarded as desirable depending on the purpose of adjustment. In this work we shall treat them as desirable parameters. However, it is clear that the coordinates of stations determined from the types of observations considered in these studies will be less accurate than those obtainable with current methods of station position determination on the earth.

Parameters $X_3$

This group of parameters consists of the undesirable (nuisance) parameters which are necessary for modeling observation types F, G and H only. The group includes parameters necessary for modeling the systematic errors in the existing lunar ephemeris. Also, included in this group of parameters are the corrections to the error models used in computing corrections to the observed quantities, for systematic observational errors such as atmospheric refraction and earth tides (see Appendix B). The parameters will not be solved explicitly, but their contributions will be included in the solution for the desired parameters.

Parameters $X_4$

This group of parameters is also undesirable, but does appear in the mathematical functions for the G, H and J observation types (VLBI). The parameters include the radio source positions and clock synchronization errors. Also, residual instrumental errors (which are systematic in nature) can be included in this group. The $X_4$ group of parameters can be treated in the same way as the $X_3$ parameters.

Summary

In summary, the following tables present the classification of observations in the general adjustment model.

| Type (Symbol) | Description |
|---|---|
| F | Earth to Moon laser observations |
| G | Earth to Earth VLBI observations |
| H | Earth to Moon VLBI observations |
| J | Moon to Moon VLBI observations. |

Table 5.1

Types of Observations

| Symbol | Parameter Types | Comments |
|---|---|---|
| $X_1$ | (i) Cartesian coordinates of moon stations | |
| | (ii) Orientation parameters of the moon at initial epoch | Desired parameters |
| | (iii) Principal moments of inertia of the moon | |
| $X_2$ | (i) Cartesian coordinates of the earth station | |
| | (ii) Earth's orientation parameters at an initial epoch | Desired parameters |
| | (iii) Polar motion parameters | |
| $X_3$ | (i) Lunar ephemeris systematic error model | |
| | (ii) Residual refraction errors | Undesired parameters |
| | (iii) Residual earth-tidal errors | |
| $X_4$ | (i) Radio source positions | |
| | (ii) Clock offset errors | Undesired parameters |
| | (iii) Residual instrumental error | |

Table 5.2

Types of Parameters (Pseudo Observations)

## 5.3 Generalized Adjustment Model.

### 5.31 Formation of Normal Equations.

The mathematical structure for the adjustment can be written, using Uotila's notations [93] as:

$$F(L_F^a,\ L_{x_1}^a,\ L_{x_2}^a,\ L_{x_3}^a) = 0 \qquad (5.1)$$

$$G(L_G^a,\ L_{x_2}^a,\ L_{x_3}^a,\ L_{x_4}^a) = 0 \qquad (5.2)$$

$$H(L_M^a,\ L_{x_1}^a,\ L_{x_2}^a,\ L_{x_3}^a,\ L_{x_4}^a) = 0 \qquad (5.3)$$

$$J(L_J^a,\ L_{x_1}^a,\ L_{x_4}^a) = 0 \qquad (5.4)$$

where

F, G, H, and J are mathematical functions of observations

$L_F$ is a set of laser observations

$L_G$ is a set of Earth-Earth VLBI observations

$L_M$ is a set of Earth-Moon VLBI observations.

$L_J$ is a set of Moon-Moon VLBI observations

$L_{x_1}, L_{x_2}, L_{x_3}, L_{x_4}$ are "observation" groups defined in Section 5.2.

The superscripts denote the following:

a = adjusted value

b = observed value

o = estimated value.

Linearization of equations (5.1) to (5.4) through Taylor series yields the following corresponding equations:

$$B_F V_F + B_{F\,x_1} V_{x_1} + B_{F\,x_2} V_{x_2} + B_{F\,x_3} V_{x_3} + W_F = 0 \qquad (5.5)$$

$$B_G V_G + B_{G\,x_2} V_{x_2} + B_{G\,x_3} V_{x_3} + B_{G\,x_4} V_{x_4} + W_G = 0 \qquad (5.6)$$

$$B_M V_M + B_{M\,x_1} V_{x_1} + B_{M\,x_2} V_{x_2} + B_{M\,x_3} V_{x_3} + B_{M\,x_4} V_{x_4} + W_M = 0 \qquad (5.7)$$

$$B_J V_J + B_{J\,x_1} V_{x_1} + B_{J\,x_4} V_{x_4} + W_J = 0 \qquad (5.8)$$

where

$V_{x_1}, V_{x_2}, V_{x_3}, V_{x_4}$ are corrections to the estimated values of parameters

$V_F$, $V_G$, $V_M$ and $V_J$ are observation residuals

$$B_F = \frac{\partial F}{\partial L_F}, \quad B_{Fx_1} = \frac{\partial F}{\partial L_{x_1}}, \quad W_F = F(L_F^b, L_x^o)$$

and similar expressions for $B_G$, $B_H$, $B_{Gx_1}$, $B_{Hx_1}$, $W_G$ and $W_H$. In addition, let $P_F$, $P_G$, $P_H$, $P_J$ and $P_{x_1}$ represent weight matrices corresponding to $L_F$, $L_G$, $L_J$ and $L_{x_1}$, assuming that these groups of observations are not correlated to one another.

The determination of the corrections (V's) through least squares require the minimization of the quadratic form $V^T PV$. Introducing a function $\Gamma$ and Lagrange multipliers $K_F$, $K_G$ and $K_H$, it is desired to minimize:

$$\begin{aligned}\Gamma = {} & (V_F^T P_F V_F + V_G^T P_G V_G + V_H^T P_H V_H + \sum_{i=1}^{4} (V_{x_i}^T P_{x_i} V_{x_i})) \\ & -2K_F^T(B_F V_F + B_{Fx_1} V_{x_1} + B_{Fx_2} V_{x_2} + B_{Fx_3} V_{x_3} + W_F) \\ & -2K_G^T(B_G V_G + B_{Gx_2} V_{x_2} + B_{Gx_3} V_{x_3} + B_{Gx_4} V_{x_4} + W_G) \\ & -2K_H^T(B_H V_H + B_{Hx_1} V_{x_1} + B_{Hx_2} V_{x_2} + B_{Hx_3} V_{x_3} + B_{Hx_4} V_{x_4} + W_H) \\ & -2K_J^T(B_J V_J + B_{Jx_1} V_{x_1} + B_{Jx_4} V_{x_4}). \qquad (5.9)\end{aligned}$$

Differentiating equation (5.9) with respect to $V_F$, $V_G$, $V_H$, $V_J$ and $V_{x_i}$, setting the result to zero and taking equations (5.5) to (5.8) into account, the system of equation (5.10) is obtained in matrix form. This is a system of normal equations of the form

$$NX + U = 0$$

and the solution

$$X = -N^{-1} U$$

usually requires the inversion of the N (normal) matrix

$$
\begin{bmatrix}
-P_F & & & & & & & & B_F^T & 0 & 0 & 0 \\
 & -P_G & & & & & & & 0 & B_G^T & 0 & 0 \\
 & & -P_H & & & & & & 0 & 0 & B_H^T & 0 \\
 & & & -P_J & & & & & 0 & 0 & 0 & B_J^T \\
 & & & & -P_{x_1} & & & & B_{Fx_1}^T & 0 & B_{Gx_1}^T & B_{Jx_1}^T \\
 & & & & & -P_{x_2} & & & B_{Fx_2}^T & B_{Gx_2}^T & B_{Hx_2}^T & 0 \\
 & & & & & & -P_{x_3} & & B_{Fx_2}^T & B_{Gx_3}^T & B_{Hx_3}^T & 0 \\
 & & & & & & & -P_{x_4} & 0 & B_{Gx_4}^T & B_{Hx_4}^T & B_{Jx_4}^T \\
B_F & 0 & 0 & 0 & B_{Fx_1} & B_{Fx_2} & B_{Fx_3} & 0 & 0 & 0 & 0 & 0 \\
0 & B_G & 0 & 0 & 0 & B_{Gx_2} & B_{Gx_3} & B_{Gx_4} & 0 & 0 & 0 & 0 \\
0 & 0 & B_H & 0 & B_{Hx_1} & B_{Hx_2} & B_{Hx_3} & B_{Hx_4} & 0 & 0 & 0 & 0 \\
0 & 0 & 0 & B_J & B_{Jx_1} & 0 & 0 & B_{Jx_4} & 0 & 0 & 0 & 0
\end{bmatrix}
\begin{bmatrix} V_F \\ V_G \\ V_H \\ V_J \\ V_{x_1} \\ V_{x_2} \\ V_{x_3} \\ V_{x_4} \\ K_F \\ K_G \\ K_H \\ K_J \end{bmatrix}
=
\begin{bmatrix} 0 \\ 0 \\ 0 \\ 0 \\ 0 \\ 0 \\ 0 \\ 0 \\ -W_F \\ -W_G \\ -W_H \\ -W_J \end{bmatrix}
\qquad (5.10)
$$

5.32 Solution of Normal Equations.

The solution of equation (5.10) using matrix algebra can be obtained; however the dimensions of the normal matrix are large and it is desirable to eliminate some of the parameters from the system. From the first three sets of equations, expressions can be obtained for the observation residuals $V_F$, $V_G$ and $V_H$ as:

$$
\begin{aligned}
V_F &= P_F^{-1} B_F^T K_F \\
V_G &= P_G^{-1} B_G^T K_G \qquad (5.11) \\
V_H &= P_H^{-1} B_H^T K_H \\
V_J &= P_J^{-1} B_J^T K_J .
\end{aligned}
$$

By inserting the expressions for V's above into the last three sets of equations of equation (5.10) and re-arranging, the system of equations reduces to:

$$
\begin{bmatrix}
M_F & 0 & 0 & 0 & B_{Fx_1} & B_{Fx_2} & B_{Fx_3} & 0 \\
0 & M_G & 0 & 0 & 0 & B_{Gx_2} & B_{Gx_3} & B_{Gx_4} \\
0 & 0 & M_H & 0 & B_{Hx_1} & B_{Hx_2} & B_{Hx_3} & B_{Hx_4} \\
0 & 0 & 0 & M_J & B_{Jx_1} & 0 & 0 & B_{Jx_4} \\
B^T_{Fx_1} & 0 & B^T_{Gx_1} & B^T_{Jx_1} & -P_{x_1} & 0 & 0 & 0 \\
B^T_{Fx_2} & B^T_{Gx_2} & B^T_{Hx_2} & 0 & 0 & -P_{x_2} & 0 & 0 \\
B^T_{Fx_3} & B^T_{Gx_3} & B^T_{Hx_3} & 0 & 0 & 0 & -P_{x_3} & 0 \\
0 & B^T_{Gx_4} & B^T_{Hx_4} & B^T_{Jx_2} & 0 & 0 & 0 & -P_{x_4}
\end{bmatrix}
\begin{bmatrix} K_F \\ K_G \\ K_H \\ K_J \\ V_{x_1} \\ V_{x_2} \\ V_{x_3} \\ V_{x_4} \end{bmatrix}
=
\begin{bmatrix} -W_F \\ -W_G \\ -W_H \\ -W_J \\ 0 \\ 0 \\ 0 \\ 0 \end{bmatrix}
\qquad (5.12)
$$

where

$$
\begin{aligned}
M_F &= B_F P_F^{-1} B_F^T \\
M_G &= B_G P_G^{-1} B_G^T \\
M_H &= B_H P_H^{-1} B_H^T \\
M_J &= B_J P_J^{-1} B_J^T .
\end{aligned}
$$

The equation set (5.12) can be re-written as:

$$
\begin{bmatrix} M & B_x \\ B_x^T & -P_x \end{bmatrix}
\begin{bmatrix} K \\ V_x \end{bmatrix}
=
\begin{bmatrix} -W \\ 0 \end{bmatrix}
\qquad (5.13)
$$

where

$$
M = \begin{bmatrix} M_F & 0 & 0 & 0 \\ 0 & M_G & 0 & 0 \\ 0 & 0 & M_H & 0 \\ 0 & 0 & 0 & M_J \end{bmatrix}, \quad
B_x = \begin{bmatrix} B_{Fx_1} & B_{Fx_2} & B_{Fx_3} & 0 \\ 0 & B_{Gx_2} & B_{Gx_3} & B_{Gx_4} \\ B_{Hx_1} & B_{Hx_2} & B_{Hx_3} & B_{Hx_4} \\ B_{Jx_1} & 0 & 0 & B_{Jx_4} \end{bmatrix}
$$

$$P_x = \begin{bmatrix} P_{x_1} & 0 & 0 & 0 \\ 0 & P_{x_2} & 0 & 0 \\ 0 & 0 & P_{x_3} & 0 \\ 0 & 0 & 0 & P_{x_4} \end{bmatrix}, \quad V_x = \begin{bmatrix} V_{x_1} \\ V_{x_2} \\ V_{x_3} \\ V_{x_4} \end{bmatrix}$$

$$K = \begin{bmatrix} K_F \\ K_G \\ K_H \\ K_J \end{bmatrix}, \quad W = \begin{bmatrix} W_F \\ W_G \\ W_H \\ W_J \end{bmatrix}.$$

From the first equation of (5.13),

$$K = -M^{-1}(B_x V_x + W)$$

and from the second equation,

$$V_x = -(B_x^T M^{-1} B_x + P_x)^{-1} B_x^T M^{-1} W. \tag{5.14}$$

Then,

$$L_x^a = L_x^b + V_x.$$

Equation (5.14) above gives the combined solution for the residuals of all parameters ("observations") using all the four types of observations. The weight coefficient matrix of $L_x^a$(adjusted values of parameters ("observations")) is given by:

$$Q_{L_x^a} = [P_x + B_x^T M^{-1} B_x]^{-1}. \tag{5.15}$$

It was already noted above that there are two classes of parameters, the first class containing parameters we wish to solve explicitly, while the solution to the other class of parameters is not needed. Therefore let the $V_x$ matrix be divided into two groups namely:

$V_{x_D}$ - desired parameters

$V_{x_U}$ - undesired parameters

where, according to the parameter classification of Section 5.2,

$$V_{x_D} = \begin{bmatrix} V_{x_1} \\ V_{x_2} \end{bmatrix}; \quad P_{x_D} = \begin{bmatrix} P_{x_1} & 0 \\ 0 & P_{x_2} \end{bmatrix}$$

$$V_{x_U} = \begin{bmatrix} V_{x_3} \\ V_{x_4} \end{bmatrix}; \quad P_{x_U} = \begin{bmatrix} P_{x_3} & 0 \\ 0 & P_{x_4} \end{bmatrix}.$$

Furthermore, since laser observations will most probably be available before the VLBI observations, the solution of $V_{x_D}$ using only F-type (laser) observations can first be found followed by the sequential solution of $V_{x_D}$ with the addition of the other observation types.

For the first case (using only F-type observations) the normal equations can be written as

$$\begin{bmatrix} M_f & B_{fx_D} & B_{fx_U} \\ B_{fx_D}^T & -P_{x_D} & 0 \\ B_{fx_U}^T & 0 & -P_{x_U} \end{bmatrix} \begin{bmatrix} K_f \\ V_{x_D} \\ V_{x_U} \end{bmatrix} = \begin{bmatrix} -W_f \\ 0 \\ 0 \end{bmatrix}. \tag{5.16}$$

Eliminating both $K_f$ and $V_{x_U}$ from the system, the expression for $V_{x_D}$ is

$$V_{x_D} = -[P_{x_D} + B_{fx_D}^T(M_f + M_{fx_U})^{-1}B_{fx_D}]^{-1}B_{fx_D}^T(M_f + M_{fx_U})^{-1}W_f \tag{5.17}$$

where

$$M_{fx_U} = (B_{fx_U}P_{x_U}^{-1}B_{fx_U}^T).$$

Also,

$$V_{x_U} = P_{x_U}^{-1}B_{fx_U}^T K_f \tag{5.18}$$

and

$$K_r = -[M_r + M_{r_U}]^{-1}[B_{r_D}V_{x_D} + W_r]. \qquad (5.19)$$

The weight coefficient matrix for the adjusted parameters - $L^a_{x_D}$ is

$$Q_{L^a_{x_D}} = P^{-1}_{x_D} - P^{-1}_{x_D}B^T_{r_D}(M_r + M_{r_D})^{-1}B_{r_D}P^{-1}_{x_D} + P^{-1}_{x_D}B^T_{r_D}(M_r + M_{r_D})M_{r_U}(M_r + M_{r_D})^{-1}B_{r_D}P^{-1}_{x_D} \qquad (5.20)$$

where

$$M_{r_{x_D}} = B_{r_{x_D}}P^{-1}_{x_D}B^T_{r_{x_D}}.$$

The last part of the above equation is the contribution to the weight coefficient matrix, of the "folded-in" (unsolved) parameter set $L_{x_U}$

Introducing the G, H and J-types of observations (VLBI), the normal equations can be written as:

$$\begin{bmatrix} M_r & 0 & B_{r_D} & B_{r_U} \\ 0 & M_c & B_{c_D} & B_{c_U} \\ B_{r_D} & B_{c_D} & -P_{x_D} & 0 \\ B_{c_D} & B_{c_U} & 0 & -P_{x_U} \end{bmatrix} \begin{bmatrix} K_r \\ K_c \\ V_{x_D} \\ V_{x_U} \end{bmatrix} = \begin{bmatrix} -W_r \\ -W_c \\ 0 \\ 0 \end{bmatrix} \qquad (5.21)$$

$$M_c = \begin{bmatrix} M_G & 0 & 0 \\ 0 & M_H & 0 \\ 0 & 0 & M_J \end{bmatrix}; \quad B_{c_{x_D}} = \begin{bmatrix} B_{G_{x_D}} \\ B_{H_{x_D}} \\ B_{J_{x_D}} \end{bmatrix};$$

$$W_c = \begin{bmatrix} W_G \\ W_H \\ W_J \end{bmatrix}, \quad K_c = \begin{bmatrix} K_G \\ K_H \\ K_J \end{bmatrix}.$$

The solution of $V_{x_D}$ from equation (5.21) is

$$V_{x_D} = -[P_{x_D} + B^T_{r_D}(M_r + M_{r_U})^{-1}B_{r_D}]^{-1}[B^T_{r_D}(M_r + M_{r_U})^{-1}W_r + (B^T_{r_D}(M_r + M_{r_U})S_{rc} - B^T_{c_D})K_c]. \qquad (5.22)$$

where

$$S_{Fc_j} = B_{Fk_j} P^{-1}_{k_j} B^T_{Ck_j}.$$

Comparison of equations (5.17) and (5.22) shows that the latter equation could be written as

$$V_{k_b} = V^{*}_{k_b} + \delta V_{k_b}$$

where

$V^{*}_{k_b}$ is given by equation (5.17)

and

$$\delta V_{k_b} = [P_{k_b} + B^T_{Fk_b}(M_b + M_{Fk_j})^{-1} B_{Fk_b}]^{-1}[(B^T_{Ck_b} - B^T_{Fk_b}(M_b + M_{Fk_j}) S_{Fc_j}) K_c].$$

The term $\delta V_{k_b}$ gives the contribution of the G-, H- and J-sets of observations if these sets are sequentially used to find $V_{k_b}$ after an initial adjustment with the F-set of observations.

An alternative way of carrying out this sequential adjustment is to use the system of equations (5.16) where the F-set matrices are replaced by the C-set. However, the "observed" $L^b_{k_b}$ should in this case be the adjusted $L^a_{k_b}$, obtained from the adjustment of the F-set of observations. Also, the weight matrix $P_{k_b}$ should be changed accordingly to the inverse of the variance-covariance matrix resulting from the adjustment of the F-set of observations.

## 5.4 Numerical Experiments.

In this study, a few numerical experiments were performed for the purpose of investigating the expected accuracies of position determinations, using lunar laser distances as observations. The adjustment system is based on the laser observation equations derived in Chapter 2, and the adjustment equations presented in the previous sections of this chapter. Since no real data were available, laser distances were simulated for the purpose of these experiments. No strong conclusions can be drawn

from the results of adjustments performed with simulated data concerning the results one would obtain using real data. Nevertheless, in the absence of real observations, simulated data are often used in evaluating a proposed model, as well as investigating the relative accuracies of the various parameters in the model.

In an earlier report [25], eight lunar control points, arbitrarily, but uniformly located over the lunar near-side were used to represent positions of lunar retroreflectors, to which eight laser stations, located on earth, observe lunar ranges. The design of the numerical experiments to be reported in this section reflects the existing configuration of lunar ranging stations and retroreflectors. The three retroreflectors deposited on the moon by U. S. astronauts serve as the moon stations to distances which are measured from laser stations on the earth. A set of numerical experiments were performed for the case when the only actively observing laser station - the McDonald Observatory at Ft. Davis, Texas - ranges to the three lunar reflectors. Similar experiments were also performed for the case when three laser stations observe laser ranges to the lunar reflectors in order to determine any improvement in expected accuracies of parameters in the adjustment model as a result of observations from multiple laser stations on earth. For this purpose, two laser stations were chosen, in addition to the McDonald Observatory, such that the stations are located as distant as possible from the McDonald Observatory. The two stations are located at the Crimean Observatory, USSR and the Mt. Stromlo Observatory in Canberra, Australia. The establishment of permanent laser observing station at these two observatories has also been proposed. Tables 5.3 and 5.4 present the coordinates of the three laser stations and the three lunar retroreflectors. The location of the lunar retroflectors is also shown in Figure 5.1.

For the limited objectives of the experiments performed, only the following parameters were included in the adjustment model as unknowns.

| Point No. | U(km) | V(km) | W(km) | Location |
|---|---|---|---|---|
| 1 | -1330.81462 | -5328.78935 | 3235.69752 | Ft. Davis, Texas |
| 2 | -4466.54586 | 2683.24104 | -3667.44266 | Mt. Stromlo, Australia |
| 3 | 3784.28692 | 2552.21344 | 4440.46175 | Crimean, USSR |

Table 5.3

The Geocentric Cartesian Coordinates of Three Laser Stations

| Point No. | x(km) | y(km) | z(km) | Remarks |
|---|---|---|---|---|
| 1 | 1591.42945 | 691.97322 | 19.26380 | Apollo 11 Mission |
| 2 | 1652.86823 | -520.44969 | -110.54128 | Apollo 14 Mission |
| 3 | 1554.85951 | 99.26753 | 762.35841 | Apollo 15 Mission |

Table 5.4

Selenodetic Cartesian Coordinates of Three Lunar Retroreflectors

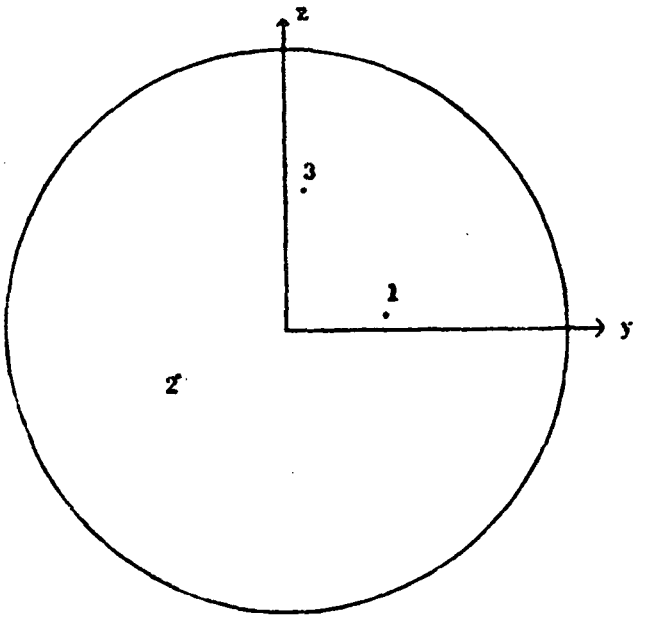


Figure 5.1

Location of the Three Lunar Retroreflectors

(1) The geocentric Cartesian (U, V, W) coordinates of the laser stations on the earth.

(2) The parameters of the orientation of the U, V, W coordinate system with respect to the mean ecliptic coordinate system of a standard epoch, which was chosen to be 1969.0 (2440222.5 JD). These parameters are represented by the three Eulerian angles and their time rates for the epoch of 1969.0.

(3) The selenodetic Cartesian (x,y,z) coordinates of the lunar retroreflectors, to which laser distances were simulated.

(4) The parameters of the orientation of the x,y,z coordinate system with respect to the mean ecliptic system of 1969.0,

represented by the physical libration parameters - $\tau, \sigma, \rho$ - *and their time derivatives at the epoch of 1969.0.*

(5) Three physical parameters of the moon, represented by the spherical harmonic coefficients $C_{30}$, $C_{22}$ and the moment of inertia ratio $\beta = \frac{C-A}{B}$.

The simulated data were assumed to be completely free from systematic errors, and the geocentric coordinates of the moon's center of mass were assumed to be known.

The mathematical model used to simulate the laser distances was that presented in Section 2.5, whereby the topocentric coordinates of the lunar *retroreflector is expressed as (see equation 2.77):*

$$\begin{bmatrix} X_{MT} \\ Y_{MT} \\ Z_{MT} \end{bmatrix} = \begin{bmatrix} X_C \\ Y_C \\ Z_C \end{bmatrix} + P_M \begin{bmatrix} x_M \\ y_M \\ z_M \end{bmatrix} - P_E \begin{bmatrix} U \\ V \\ W \end{bmatrix}, \qquad (5.23)$$

where

$X_C, Y_C, Z_C$ are the geocentric coordinates of the center of mass of the moon in the 1969.0 mean ecliptic coordinate system.

The orientation matrices $P_E$, $P_M$ are obtained from integrated Eulerian angles of the earth and the moon respectively.

The two cases of experiments reported in this section are as follows:

(1) Obtaining the weight coefficient matrix of the adjusted values of parameters, using simulated laser distances obtained from the Simulated Earth-Moon Environment Data.

(2) Investigating how well the parameters in the adjustment model can be recovered if their "true" values are altered. This investigation was also performed with the simulated environment data

Simulation of laser distances.

The flow of computation for the simulation of laser distances are as follows:

(a) The rotational equations of motion of the earth are numerically integrated so as to find the earth's Eulerian angles and their time rates at regular half day intervals, over a one-year period. All the integrated quantities refer to the initial epoch of 1969.0. An additional output of this step is the $6 \times 6$ state transition matrix. The state transition matrix, the Eulerian angles and their time rates, and the epoch of computation are then stored on a temporary storage device for later use.

(b) Step (a) is repeated for the moon.

(c) The U, V, W coordinates of the laser stations, and the x, y, z coordinates of the moon points are read as input into a program which generates laser distances.

(d) At each half-day interval, all the "observable" laser distances are computed, using information from steps (a), (b), (c) and a lunar ephemeris. These distances are then punched out on cards for later screening.

A laser distance is deemed "observable" if the observing conditions are such that

(i) The altitude of the moon point is between $30^\circ$ and $70^\circ$

(ii) The observed moon point is on the front side of the moon's disc (with respect to the laser station) and is at least $10^\circ$ off the lunar limb.

Integration of the Eulerian angles.

The numerical integration of the earth's Eulerian angles follow the method outlined in Chapter 4. The Encke-type integration was used, in which the quantities integrated are given as

$$\begin{bmatrix} \delta_1 \\ \delta_2 \\ \delta_3 \\ \delta_4 \\ \delta_5 \\ \delta_6 \end{bmatrix} = \begin{bmatrix} \theta - \theta_c \\ \psi - \psi_c \\ \Psi + \psi - K_0 - K_1 t \\ \dot{\theta} \\ \dot{\psi} \\ \dot{\Psi} + \dot{\psi} - K_1 \end{bmatrix} \tag{5.24}$$

where $\theta_c$, $\psi_c$, $K_0$ and $K_1$ are constants. The expression for the state transition matrix U, which was obtained by numerical differentiation is given as

$$U = \frac{\partial \delta}{\partial \delta_0} \tag{5.25}$$

where

$$\delta = [\delta_1 \ \delta_2 \ \delta_3 \ \delta_4 \ \delta_5 \ \delta_3]^T$$

and

$\delta_0$ is the value of $\delta$ at the initial epoch of 1969.0.

For the moon's Eulerian angles, the equations developed by Papo [78], for the integration of the physical libration quantities ($\tau$, $\sigma$, $\rho$, $\dot{\tau}$, $\dot{\sigma}$ and $\dot{\rho}$) and the state transition matrix ($U^*$), were used. The Eulerian angles are then obtained from the physical libration quantities and the expressions for the Cassini laws:

$$\begin{bmatrix} \Psi \\ \psi \\ \theta \\ \dot{\Psi} \\ \dot{\psi} \\ \dot{\theta} \end{bmatrix} = \begin{bmatrix} L + \pi - \Omega \\ \Omega \\ I \\ \dot{L} - \dot{\Omega} \\ \dot{\Omega} \\ 0 \end{bmatrix} + \begin{bmatrix} \tau - \sigma \\ \sigma \\ \rho \\ \dot{\tau} - \dot{\sigma} \\ \dot{\sigma} \\ \dot{\rho} \end{bmatrix} \tag{5.26}$$

Apart from the physical libration quantities and the state transition matrix, the integration program also computes the 3 x 6 parameter sensitivity matrix, S, which is given by:

$$S = \frac{\partial [\tau \ \sigma \ \rho \ \dot{\tau} \ \dot{\sigma} \ \dot{\rho}]^T}{\partial [C_{22} \beta C_{20}]^T} .$$

A similar expression for the U* matrix is

$$U^* = \frac{\partial [\tau \ \sigma \ \rho \ \dot{\tau} \ \dot{\sigma} \ \dot{\rho}]^T}{\partial [\tau_0 \ \sigma_0 \ \rho_0 \ \dot{\tau}_0 \ \dot{\sigma}_0 \ \dot{\rho}_0]^T} .$$

Weighting.

The adjustment method used regards all the parameters, in addition to the simulated distances, as observations with associated weights. The relative weight of each of the parameters was computed as the inverse of its estimated variance, thereby choosing the variance of unit weight to be 1.

The values of the variances of parameters were selected to conform with the level of uncertainties in the present knowledge of these quantities. The standard deviation of the parameters are as follows:

| | | | |
|---|---|---|---|
| U, V, W coordinates, | m | = | 25 meters |
| x, y, z coordinates, | m | = | 1 kilometer |
| $\delta_1, \delta_2, \delta_3$ | m | = | 1.0 sec |
| $\delta_3, \delta_4, \delta_5$ | m | = | 0.5 sec /day |
| $\tau, \rho, \sigma$ | m | = | 20.0 sec |
| $\dot{\tau}, \dot{\rho}, \dot{\sigma}$ | m | = | 10.0 sec/day |
| $C_{22}$ | m | = | 0.5 sec |
| $\beta$ | m | = | 2.0 sec |
| $C_{20}$ | m | = | 0.01 sec . |

The standard deviation of each "observed" distance was assumed to be 15 cm, which is the precision currently expected from lunar laser ranges.

Experiment (1).

The purpose of this experiment is to investigate the internal precision of the adjustment system. An idea about the internal precision of the adjustment system can be obtained through the inspection of the variance-covariance matrix, particularly the diagonal elements (variance.), and the associated matrix of correlation coefficients.

The simulated distances used in this experiment were computed using the Simulated Environment Data [78]. From laser distances simulated according to the procedure already outlined above, a number of them are chosen over a certain period of time, for adjustment. There were three cases of experimental computer runs:

(1) In the first case, laser distances were simulated between one laser station (at the McDonald Observatory), and the three lunar retroreflectors. Different numbers of observations over differing periods of time were chosen for the formation of the normal matrix. These were as follows: 50 observations over a three-month period, 100 observations over a six-month period, 150 observations over a nine-month period, and 200 observations over one year.

(2) In order to have an idea about how the parameter variances improve with increase in the period of time over which observations are made, the second case consists of computer runs where the number of observations was held fixed, while the period of observations was varied.

(3) In the third case, the simulated distances used, comprised of distances between all the three laser stations already mentioned above and the three lunar retroreflectors. The total numbers of observations and the observation periods chosen were the same as in case (1).

The partials of distances with respect to the parameters were evaluated using the equations developed in Section 2.5. Since the orientation parameters (of both the earth and the moon) defined in Section 2.5 are slightly different for those in this adjustment model, a simple transformation had to be made as follows:

$$\frac{\partial D}{\partial \delta_0} = \frac{\partial D}{\partial E^{\varepsilon}} \cdot \frac{\partial E^{\varepsilon}}{\partial \delta} \cdot \frac{\partial \delta}{\partial \delta_0} \quad \text{for the earth's orientation angles}$$

and

$$\frac{\partial D}{\partial \xi_0} = \frac{\partial D}{\partial E^{M}} \cdot \frac{\partial E^{M}}{\partial \xi} \cdot \frac{\partial \xi}{\partial \xi_0} \quad \text{for the moon's orientation angles}$$

where

$$\delta = [\delta_1 \ \delta_2 \ \delta_3 \ \delta_4 \ \delta_5 \ \delta_6]^T$$

$$E^{\varepsilon} = [\theta_{\varepsilon} \ \psi_{\varepsilon} \ \varphi_{\varepsilon} \ \dot{\theta}_{\varepsilon} \ \dot{\psi}_{\varepsilon} \ \dot{\varphi}_{\varepsilon}]^T$$

$$\xi = [\tau \ \sigma \ \rho \ \dot{\tau} \ \dot{\sigma} \ \dot{\rho}]^T$$

$$E^{M} = [\theta_{M} \ \psi_{M} \ \varphi_{M} \ \theta_{M} \ \psi_{M} \ \varphi_{M}]^T$$

and

D is the distance.

It follows form equations (5.24) and (5.26) that

$$\frac{\partial E^{\varepsilon}}{\partial \delta} = \left[\begin{array}{ccc|ccc} 1 & 0 & 0 & 0 & 0 & 0 \\ 0 & 1 & 0 & 0 & 0 & 0 \\ 0 & -1 & 1 & 0 & 0 & 0 \\ \hline 0 & 0 & 0 & 1 & 0 & 0 \\ 0 & 0 & 0 & 0 & 1 & 0 \\ 0 & 0 & 0 & 0 & -1 & 1 \end{array}\right]$$

and

$$\frac{\partial E''}{\partial \xi} = \left[\begin{array}{ccc|ccc} 0 & 0 & 1 & 0 & 0 & 0 \\ 0 & 1 & 0 & 0 & 0 & 0 \\ 1 & -1 & 0 & 0 & 0 & 0 \\ \hline 0 & 0 & 0 & 0 & 0 & 1 \\ 0 & 0 & 0 & 0 & 1 & 0 \\ 0 & 0 & 0 & 1 & -1 & 0 \end{array}\right] .$$

The expressions for the partials of distances with respect to the orientation parameters can thus be evaluated.

Table 5.5 gives the diagonal elements of the variance-covariance matrix of case (1), where the only laser station observing is located at the McDonald Observatory. The general pattern shows, as can be expected, that the parameter variances decrease as more observations are made over longer periods of time. It can also be seen from the table that, in addition to a general improvement in lunar position determination through the use of laser ranges, we can also expect an improvement in the determination of geocentric positions of stations on the earth's surface. A general improvement in the accuracy of determining the orientation parameters of both the earth and the moon, and the moon's lower order spherical harmonic coefficients can also be expected by using lunar laser ranges. The exception to this is the variances obtained for the moon's physical libration in the node and its time derivative ($\sigma$ and $\dot{\sigma}$). Even with 200 observations over a one year period, the variance obtained for $\sigma$ and $\dot{\sigma}$ are 250".7 and 29.5 $sec^2/day^2$ respectively, compared to the a priori values of 400" and 100 $sec^2/day^2$. A good explanation for this poor determination of $\sigma$ and $\dot{\sigma}$ cannot be found, especially since the dominant term of libration in node has a period of about one month. On the other hand, it should be realized that the node itself is defined by the intersection of two planes at an angle of only 1°.5.

| Parameters | 50 Observations 3 Months | 100 Observations 6 Months | 150 Observations 9 Months | 200 Observations 12 Months | A Priori Variance |
|---|---|---|---|---|---|
| | meter$^2$ | meter$^2$ | meter$^2$ | meter$^2$ | meter$^2$ |
| U | 312.7 | 1.0 | 0.3 | 0.08 | 625 |
| V | 19.6 | 0.07 | 0.02 | 0.01 | 625 |
| W | 36.0 | 8.9 | 1.8 | 1.4 | 625 |
| $x_1$ | 16.3 | 2.9 | 1.2 | 0.5 | $1 \times 10^6$ |
| $y_1$ | 57.1 | 10.1 | 4.2 | 1.9 | $1 \times 10^6$ |
| $z_1$ | 646.3 | 220.9 | 85.8 | 57.7 | $1 \times 10^6$ |
| $x_2$ | 10.5 | 2.3 | 1.1 | 0.4 | $1 \times 10^6$ |
| $y_2$ | 138.7 | 27.6 | 10.6 | 4.4 | $1 \times 10^6$ |
| $z_2$ | 627.4 | 191.9 | 66.6 | 50.1 | $1 \times 10^6$ |
| $x_3$ | 17.5 | 14.4 | 10.1 | 6.0 | $1 \times 10^6$ |
| $y_3$ | 113.2 | 26.7 | 9.8 | 6.3 | $1 \times 10^6$ |
| $z_3$ | 539.6 | 171.5 | 63.2 | 44.6 | $1 \times 10^6$ |
| | second$^2$ | second$^2$ | second$^2$ | second$^2$ | second$^2$ |
| $\delta_1$ | $0.6 \times 10^{-3}$ | $0.1 \times 10^{-3}$ | $0.2 \times 10^{-4}$ | $0.1 \times 10^{-4}$ | 1.0 |
| $\delta_2$ | $0.3 \times 10^{-2}$ | $0.2 \times 10^{-3}$ | $0.8 \times 10^{-4}$ | $0.6 \times 10^{-4}$ | 1.0 |
| $\delta_3$ | 0.5 | $0.1 \times 10^{-2}$ | $0.3 \times 10^{-3}$ | $0.1 \times 10^{-3}$ | 1.0 |
| $\tau$ | 1.5 | 0.3 | 0.1 | 0.04 | 400 |
| $\sigma$ | 397.8 | 382.0 | 318.7 | 250.7 | 400 |
| $\rho$ | 1.4 | 1.2 | 0.8 | 0.4 | 400 |
| $C_{22}$ | $0.3 \times 10^{-2}$ | $0.2 \times 10^{-3}$ | $0.5 \times 10^{-4}$ | $0.2 \times 10^{-4}$ | 0.25 |
| $\beta$ | $0.4 \times 10^{-3}$ | $0.3 \times 10^{-4}$ | $0.8 \times 10^{-5}$ | $0.3 \times 10^{-5}$ | 4.0 |
| $C_{20}$ | $0.1 \times 10^{-3}$ | $0.1 \times 10^{-3}$ | $0.1 \times 10^{-3}$ | $0.1 \times 10^{-3}$ | $0.1 \times 10^{-3}$ |
| | sec$^2$/day$^2$ | sec$^2$/day$^2$ | sec$^2$/day$^2$ | sec$^2$/day$^2$ | sec$^2$/day$^2$ |
| $\delta_4$ | $0.2 \times 10^{-2}$ | $0.2 \times 10^{-3}$ | $0.1 \times 10^{-3}$ | $0.8 \times 10^{-4}$ | 0.25 |
| $\delta_5$ | $0.6 \times 10^{-1}$ | $0.7 \times 10^{-2}$ | $0.6 \times 10^{-3}$ | $0.3 \times 10^{-3}$ | 0.25 |
| $\delta_6$ | $0.4 \times 10^{-3}$ | $0.5 \times 10^{-4}$ | $0.4 \times 10^{-5}$ | $0.2 \times 10^{-5}$ | 0.25 |
| $\dot{\tau}$ | $0.8 \times 10^{-3}$ | $0.6 \times 10^{-4}$ | $0.1 \times 10^{-4}$ | $0.6 \times 10^{-5}$ | 100 |
| $\dot{\sigma}$ | 98.2 | 81.3 | 55.1 | 29.5 | 100 |
| $\dot{\rho}$ | 0.02 | 0.015 | 0.011 | 0.009 | 100 |

Table 5.5

Variances of Parameters for Case (1), With One Laser Station Observing

Another trend that could be noticed in Table 5.5 is that, in general, the x coordinates of the lunar reflectors are better determined than the y and z coordinates. The z-coordinates are the ones with the poorest determination. This phenomena can be explained through the fact that the ranges are likely to be more sensitive to changes in the X coordinates of lunar stations since the X-axis is always oriented approximately toward the earth. This same conclusion cannot be made for the geocentric coordinates of points on the earth which are likely to depend more on the geometry of the simulated distances chosen for adjustment.

Table 5.6 displays the variances of parameters for case (2), where the number of observations are held fixed and the periods of observation are varied. All the parameters show sensitivity to the length of the period of observations as can be seen from decreases in the variances of parameters when the period of observation is increased. The sharpest change in the variances occurs when the period of observation is increased from three months to six months. A further increase in the period to nine months shows further decrease in the variances, but to a lesser degree.

In Table 5.7, the diagonal elements of the variance-covariance matrix (variances of parameters) for case (3) are tabulated. In this case, there are three observing laser stations on the earth. The characteristics of this table are similar to those of Table 5.5 for case (1), where only one laser station is ranging to the lunar retroreflectors. From both tables, it can be seen that the accuracy of determining the parameters increase with increase in the number of observations and the period of observations. The largest degree of improvement is obtained when the number and period of observations are increased from 50 and three months to 100 and six months respectively. Also, the least sensitive parameter in the adjustment model remains the moon's physical libration in node and its time derivative ($\sigma$ and $\dot{\sigma}$).

| Parameters | 50 Observations 3 Months | 50 Observations 6 Months | 50 Observations 9 Months | 100 Observations 6 Months | 100 Observations 9 Months |
|---|---|---|---|---|---|
| | meter$^2$ | meter$^2$ | meter$^2$ | meter$^2$ | meter$^2$ |
| U | 312 | 3.03 | 1.2 | 1.0 | 0.43 |
| V | 19.6 | 0.2 | 0.1 | 0.07 | 0.03 |
| W | 36.0 | 30.0 | 10.7 | 8.9 | 2.88 |
| $x_1$ | 16.3 | 5.4 | 4.9 | 2.9 | 2.0 |
| $y_1$ | 57.1 | 16.9 | 13.4 | 10.1 | 7.1 |
| $z_1$ | 646.3 | 563.1 | 241.7 | 220.9 | 117.4 |
| $x_2$ | 10.5 | 3.7 | 3.1 | 2.3 | 1.6 |
| $y_2$ | 138.7 | 48.0 | 35.4 | 27.6 | 16.8 |
| $z_2$ | 627.4 | 531.2 | 211.5 | 191.9 | 92.2 |
| $x_3$ | 17.5 | 16.3 | 14.4 | 14.4 | 12.3 |
| $y_3$ | 113.2 | 45.1 | 28.0 | 26.7 | 19.8 |
| $z_3$ | 539.6 | 437.2 | 168.0 | 171.5 | 85.5 |
| | second$^2$ | second$^2$ | second$^2$ | second$^2$ | second$^2$ |
| $\delta_1$ | $0.6 \times 10^{-3}$ | $0.3 \times 10^{-3}$ | $0.7 \times 10^{-4}$ | $0.1 \times 10^{-3}$ | $0.2 \times 10^{-4}$ |
| $\delta_2$ | $0.3 \times 10^{-2}$ | $0.5 \times 10^{-3}$ | $0.7 \times 10^{-3}$ | $0.2 \times 10^{-3}$ | $0.1 \times 10^{-3}$ |
| $\delta_3$ | 0.5 | $0.4 \times 10^{-2}$ | $0.2 \times 10^{-2}$ | $0.1 \times 10^{-2}$ | $0.6 \times 10^{-3}$ |
| $\tau$ | 1.5 | 0.48 | 0.4 | 0.3 | 0.2 |
| $\sigma$ | 397.8 | 392.4 | 372.2 | 382.0 | 348.5 |
| $\rho$ | 1.4 | 1.38 | 1.2 | 1.2 | 1.0 |
| $C_{22}$ | $0.3 \times 10^{-2}$ | $0.4 \times 10^{-3}$ | $0.2 \times 10^{-3}$ | $0.2 \times 10^{-3}$ | $0.9 \times 10^{-4}$ |
| $\beta$ | $0.4 \times 10^{-3}$ | $0.4 \times 10^{-4}$ | $0.3 \times 10^{-4}$ | $0.3 \times 10^{-4}$ | $0.2 \times 10^{-4}$ |
| $C_{20}$ | $0.1 \times 10^{-3}$ | $0.1 \times 10^{-3}$ | $0.1 \times 10^{-3}$ | $0.1 \times 10^{-3}$ | $0.1 \times 10^{-3}$ |
| | sec$^2$/day$^2$ | sec$^2$/day$^2$ | sec$^2$/day$^2$ | sec$^2$/day$^2$ | sec$^2$/day$^2$ |
| $\delta_4$ | $0.2 \times 10^{-2}$ | $0.5 \times 10^{-3}$ | $0.1 \times 10^{-2}$ | $0.2 \times 10^{-3}$ | $0.2 \times 10^{-3}$ |
| $\delta_5$ | $0.6 \times 10^{-1}$ | $0.2 \times 10^{-1}$ | $0.6 \times 10^{-2}$ | $0.7 \times 10^{-2}$ | $0.8 \times 10^{-3}$ |
| $\delta_6$ | $0.4 \times 10^{-3}$ | $0.1 \times 10^{-3}$ | $0.4 \times 10^{-4}$ | $0.5 \times 10^{-4}$ | $0.6 \times 10^{-6}$ |
| $\dot{\tau}$ | $0.8 \times 10^{-3}$ | $0.1 \times 10^{-3}$ | $0.5 \times 10^{-4}$ | $0.6 \times 10^{-4}$ | $0.2 \times 10^{-4}$ |
| $\dot{\sigma}$ | 98.2 | 94.5 | 80.9 | 81.3 | 68.9 |
| $\dot{\rho}$ | 0.02 | 0.015 | 0.014 | 0.015 | 0.013 |

Table 5.6

Variances of Parameters for Case (2), Period of Observation Varied

| Parameters | 50 Observations 3 Months | 100 Observations 6 Months | 150 Observations 9 Months | 200 Observations 12 Months | A Priori Variances |
|---|---|---|---|---|---|
| | meter$^2$ | meter$^2$ | meter$^2$ | meter$^2$ | meter$^2$ |
| $U_1$ | 169.43 | 1.17 | 0.1 | 0.04 | 625 |
| $V_1$ | 10.61 | 0.08 | 0.02 | 0.01 | 625 |
| $W_1$ | 9.69 | 2.49 | 1.26 | 0.75 | 625 |
| $U_2$ | 43.04 | 0.34 | 0.04 | 0.02 | 625 |
| $V_2$ | 119.04 | 0.81 | 0.08 | 0.03 | 625 |
| $W_2$ | 8.08 | 2.14 | 1.05 | 0.62 | 625 |
| $U_3$ | 38.88 | 0.25 | 0.03 | 0.01 | 625 |
| $V_3$ | 85.47 | 0.59 | 0.06 | 0.03 | 625 |
| $W_3$ | 9.83 | 2.51 | 1.26 | 0.76 | 625 |
| $x_1$ | 10.50 | 2.51 | 0.97 | 0.47 | $1 \times 10^6$ |
| $y_1$ | 43.26 | 6.92 | 3.09 | 1.61 | $1 \times 10^6$ |
| $z_1$ | 243.70 | 131.25 | 82.21 | 49.60 | $1 \times 10^6$ |
| $x_2$ | 6.71 | 2.08 | 0.87 | 0.46 | $1 \times 10^6$ |
| $y_2$ | 81.66 | 22.11 | 8.23 | 3.96 | $1 \times 10^6$ |
| $z_2$ | 207.30 | 96.73 | 62.80 | 42.57 | $1 \times 10^6$ |
| $x_3$ | 17.05 | 13.90 | 9.62 | 6.25 | $1 \times 10^6$ |
| $y_3$ | 67.06 | 17.71 | 8.21 | 3.83 | $1 \times 10^6$ |
| $z_3$ | 197.62 | 98.69 | 64.18 | 40.77 | $1 \times 10^6$ |
| | second$^2$ | second$^2$ | second$^2$ | second$^2$ | second$^2$ |
| $\delta_1$ | $0.14 \times 10^{-3}$ | $0.38 \times 10^{-4}$ | $0.21 \times 10^{-4}$ | $0.15 \times 10^{-5}$ | 1.0 |
| $\delta_2$ | $0.11 \times 10^{-3}$ | $0.39 \times 10^{-4}$ | $0.23 \times 10^{-4}$ | $0.14 \times 10^{-4}$ | 1.0 |
| $\delta_3$ | 0.25 | $0.17 \times 10^{-2}$ | $0.15 \times 10^{-3}$ | $0.63 \times 10^{-4}$ | 1.0 |
| $\tau$ | 0.94 | 0.23 | $0.83 \times 10^{-1}$ | $0.39 \times 10^{-1}$ | 400 |
| $\sigma$ | 397.58 | 378.84 | 335.64 | 247.27 | 400 |
| $\rho$ | 1.44 | 1.14 | 0.76 | 0.44 | 400 |
| $C_{22}$ | $0.17 \times 10^{-2}$ | $0.20 \times 10^{-3}$ | $0.38 \times 10^{-4}$ | $0.14 \times 10^{-4}$ | 0.25 |
| $\beta$ | $0.48 \times 10^{-3}$ | $0.25 \times 10^{-4}$ | $0.80 \times 10^{-5}$ | $0.33 \times 10^{-5}$ | 4.0 |
| $C_{20}$ | $0.1 \times 10^{-3}$ | $0.1 \times 10^{-3}$ | $0.1 \times 10^{-3}$ | $0.1 \times 10^{-3}$ | $0.1 \times 10^{-3}$ |
| | sec$^2$/day$^2$ | sec$^2$/day$^2$ | sec$^2$/day$^2$ | sec$^2$/day$^2$ | sec$^2$/day$^2$ |
| $\delta_4$ | $0.50 \times 10^{-3}$ | $0.18 \times 10^{-3}$ | $0.12 \times 10^{-3}$ | $0.63 \times 10^{-4}$ | 0.25 |
| $\delta_5$ | $0.99 \times 10^{-2}$ | $0.18 \times 10^{-2}$ | $0.68 \times 10^{-3}$ | $0.23 \times 10^{-3}$ | 0.25 |
| $\delta_6$ | $0.67 \times 10^{-4}$ | $0.12 \times 10^{-4}$ | $0.46 \times 10^{-5}$ | $0.16 \times 10^{-5}$ | 0.25 |
| $\dot{\tau}$ | $0.55 \times 10^{-3}$ | $0.55 \times 10^{-4}$ | $0.13 \times 10^{-4}$ | $0.53 \times 10^{-5}$ | 100 |
| $\dot{\sigma}$ | 97.37 | 78.40 | 51.74 | 30.10 | 100 |
| $\dot{\rho}$ | $0.16 \times 10^{-1}$ | $0.15 \times 10^{-1}$ | $0.13 \times 10^{-1}$ | $0.93 \times 10^{-2}$ | 100 |

Table 5.7

Variances of Parameters for Case (3),

With Three Laser Stations Observing

The correlation coefficient matrix presented in Table 5.8 is that of Case (3) with 200 observations over a one year period. The correlation matrix obtained for the other cases are similar to the one presented here, but, in general, correlation between parameters are higher for cases involving less observations performed over less periods of time.

The first striking feature of the correlation matrix (Table 5.8) is the high correlation that exists between the U and V coordinates of the same laser station on the one hand, as well as the high correlation between the x and y coordinates of the retroreflectors on the other. Also, the U coordinates are correlated among one another, and the same applies to the U, W, x, y, z coordinates. These phenomena may be due to the fact that the orientation of both the earth and the moon, as well as the geocenter are part of the parameters in the solution. It can also be noticed in Table 5.8 that there is a high correlation between $\delta_5$ and $\delta_6$, as well as between $\delta_2$ and $\delta_4$. This was also the case in Chapter 4 (see Tables 4.4 and 4.6). For the moon's orientation parameters, high correlation exists between $\sigma$ and $\dot{\rho}$, and $\rho$ and $\dot{\sigma}$. The coordinates of laser stations were neither correlated with the selenodetic coordinates of the reflectors, nor with the orientation parameters of the moon.

Experiment (2).

This experiment was performed in order to investigate how well the parameters in the adjustment model can be recovered, if known shifts are introduced into the starting parameters (as approximate values of the parameters). The computational methods in this experiment are similar to that of Experiment (1), except that arbitrary shifts were introduced into the "known" values of parameters. The experiment was performed for the case when three stations are observing to the three retroreflectors, with only 50 observations over a three month period.

REPRODUCIBILITY OF THE ORIGINAL PAGE IS POOR

| $U_1$ | $V_1$ | $W_1$ | $U_2$ | $V_2$ | $W_2$ | $U_3$ | $V_3$ | $W_3$ |
|---|---|---|---|---|---|---|---|---|
| 1.000 | -0.536 | 0.009 | -0.770 | -0.957 | 0.018 | -0.879 | 0.925 | 0.011 |
| -0.536 | 1.000 | 0.107 | 0.793 | 0.430 | 0.131 | 0.175 | -0.737 | 0.104 |
| 0.009 | 0.107 | 1.000 | -0.276 | 0.134 | 0.957 | -0.099 | -0.037 | 0.995 |
| -0.770 | 0.793 | -0.276 | 1.000 | 0.646 | -0.265 | 0.524 | -0.866 | -0.277 |
| -0.957 | 0.430 | 0.134 | 0.646 | 1.000 | 0.121 | 0.892 | -0.869 | 0.132 |
| 0.018 | 0.131 | 0.957 | -0.265 | 0.121 | 1.000 | -0.135 | -0.043 | 0.951 |
| -0.879 | 0.175 | -0.099 | 0.524 | 0.892 | -0.135 | 1.000 | -0.718 | -0.108 |
| 0.925 | -0.737 | -0.037 | -0.866 | -0.869 | -0.043 | -0.718 | 1.000 | -0.035 |
| 0.011 | 0.104 | 0.995 | -0.277 | 0.132 | 0.951 | -0.108 | -0.035 | 1.000 |

| $\delta_1$ | $\delta_2$ | $\delta_3$ | $\delta_4$ | $\delta_5$ | $\delta_6$ |
|---|---|---|---|---|---|
| 1.000 | 0.190 | 0.085 | -0.263 | 0.394 | 0.393 |
| 0.190 | 1.000 | 0.231 | -0.826 | 0.395 | 0.395 |
| 0.085 | 0.231 | 1.000 | -0.199 | 0.337 | 0.337 |
| -0.263 | -0.826 | -0.199 | 1.000 | -0.502 | -0.503 |
| 0.394 | 0.395 | 0.337 | -0.502 | 1.000 | 1.000 |
| 0.393 | 0.395 | 0.337 | -0.503 | 1.000 | 1.000 |

| $x_1$ | $y_1$ | $z_1$ | $x_2$ | $y_2$ | $z_2$ | $x_3$ | $y_3$ | $z_3$ |
|---|---|---|---|---|---|---|---|---|
| 1.000 | -0.969 | -0.299 | -0.880 | -0.977 | -0.162 | 0.247 | -0.396 | -0.234 |
| -0.969 | 1.000 | 0.162 | 0.815 | 0.961 | 0.034 | -0.136 | 0.444 | 0.093 |
| -0.299 | 0.162 | 1.000 | 0.624 | 0.224 | 0.937 | -0.869 | -0.166 | 0.968 |
| -0.880 | 0.815 | 0.624 | 1.000 | 0.842 | 0.504 | -0.653 | 0.266 | 0.560 |
| -0.977 | 0.961 | 0.224 | 0.842 | 1.000 | 0.051 | -0.173 | 0.303 | 0.139 |
| -0.162 | 0.034 | 0.937 | 0.504 | 0.051 | 1.000 | -0.844 | -0.005 | 0.958 |
| 0.247 | -0.136 | -0.869 | -0.653 | -0.173 | -0.844 | 1.000 | 0.102 | -0.863 |
| -0.396 | 0.444 | -0.166 | 0.266 | 0.303 | -0.005 | 0.102 | 1.000 | -0.111 |
| -0.234 | 0.093 | 0.968 | 0.560 | 0.139 | 0.958 | -0.863 | -0.111 | 1.000 |

| $\tau$ | $\sigma$ | $\rho$ | $\tau$ | $\sigma$ | $\rho$ | $C_{22}$ | $\beta$ | $C_{20}$ |
|---|---|---|---|---|---|---|---|---|
| 1.000 | 0.296 | 0.215 | -0.510 | 0.216 | -0.300 | -0.960 | -0.068 | -0.000 |
| 0.296 | 1.000 | -0.294 | -0.457 | -0.302 | -0.997 | -0.282 | 0.215 | -0.000 |
| 0.216 | -0.294 | 1.000 | 0.722 | 0.958 | 0.287 | -0.205 | -0.436 | -0.000 |
| -0.510 | -0.457 | 0.722 | 1.000 | 0.723 | 0.453 | 0.499 | -0.329 | 0.000 |
| 0.216 | -0.302 | 0.998 | 0.723 | 1.000 | 0.295 | -0.205 | -0.431 | -0.000 |
| -0.300 | -0.997 | 0.287 | 0.453 | 0.295 | 1.000 | 0.285 | -0.186 | 0.000 |
| -0.960 | -0.282 | -0.205 | 0.499 | -0.205 | 0.285 | 1.000 | 0.046 | -0.269 |
| -0.068 | 0.215 | -0.436 | -0.329 | -0.431 | -0.186 | 0.046 | 1.000 | 0.000 |
| -0.000 | -0.000 | -0.000 | 0.000 | -0.000 | 0.000 | -0.268 | 0.000 | 1.000 |

Table 5.8

Correlation Matrix for Case (3),

200 Observations Over A One Year Period

| | $U_1$ | $V_1$ | $W_1$ | $U_2$ | $V_2$ | $W_2$ | $U_3$ | $V_3$ | $W_3$ |
|---|---|---|---|---|---|---|---|---|---|
| $\delta_1$ | 0.071 | 0.083 | 0.386 | -0.042 | -0.048 | 0.137 | -0.084 | 0.030 | 0.399 |
| $\delta_2$ | 0.224 | -0.181 | -0.042 | -0.211 | -0.231 | -0.078 | -0.131 | 0.239 | -0.045 |
| $\delta_3$ | 0.975 | -0.584 | 0.008 | -0.801 | -0.937 | 0.008 | -0.846 | 0.939 | 0.012 |
| $\delta_4$ | -0.190 | 0.152 | -0.018 | 0.189 | 0.178 | 0.024 | 0.107 | -0.191 | -0.016 |
| $\delta_5$ | 0.317 | -0.173 | 0.037 | -0.232 | -0.313 | -0.002 | -0.292 | 0.292 | 0.040 |
| $\delta_6$ | 0.318 | -0.174 | 0.037 | -0.233 | -0.314 | -0.002 | -0.293 | 0.293 | 0.039 |
| $x_1$ | -0.137 | 0.069 | -0.089 | 0.138 | 0.117 | -0.135 | 0.141 | -0.127 | -0.089 |
| $y_1$ | 0.172 | -0.062 | -0.002 | -0.116 | -0.169 | 0.043 | -0.184 | 0.153 | -0.001 |
| $z_1$ | 0.028 | 0.072 | 0.567 | -0.154 | 0.044 | 0.564 | -0.087 | -0.026 | 0.566 |
| $x_2$ | 0.123 | 0.055 | 0.104 | -0.051 | -0.129 | 0.143 | -0.181 | 0.061 | 0.104 |
| $y_2$ | 0.145 | -0.025 | 0.009 | -0.083 | -0.146 | 0.066 | -0.172 | 0.120 | 0.008 |
| $z_2$ | 0.018 | 0.074 | 0.620 | -0.170 | 0.056 | 0.620 | -0.080 | -0.030 | 0.619 |
| $x_3$ | -0.024 | 0.002 | -0.139 | 0.050 | 0.016 | -0.129 | 0.028 | 0.001 | -0.140 |
| $y_3$ | -0.053 | 0.093 | 0.021 | 0.071 | 0.048 | 0.035 | -0.005 | -0.081 | 0.025 |
| $z_3$ | 0.040 | 0.030 | 0.566 | -0.196 | 0.041 | 0.584 | -0.083 | 0.000 | 0.562 |
| $\tau$ | -0.141 | 0.016 | -0.067 | 0.099 | 0.133 | -0.120 | 0.171 | -0.112 | -0.067 |
| $\sigma$ | 0.002 | -0.013 | 0.088 | -0.046 | -0.007 | 0.055 | 0.001 | 0.007 | 0.086 |
| $\rho$ | -0.029 | -0.006 | -0.106 | 0.035 | 0.022 | -0.113 | 0.035 | 0.002 | -0.106 |
| $\dot{\tau}$ | 0.073 | -0.025 | -0.059 | -0.039 | -0.072 | -0.021 | -0.083 | 0.080 | -0.060 |
| $\dot{\sigma}$ | -0.026 | -0.018 | -0.124 | 0.030 | 0.020 | -0.122 | 0.038 | 0.008 | -0.125 |
| $\dot{\rho}$ | 0.015 | 0.003 | -0.096 | 0.033 | -0.011 | -0.061 | -0.015 | 0.013 | -0.095 |
| $C_{z0}$ | 0.132 | -0.014 | 0.063 | -0.090 | -0.124 | 0.114 | -0.161 | 0.102 | 0.063 |
| $\beta$ | -0.005 | 0.107 | -0.133 | 0.105 | -0.028 | -0.118 | -0.013 | -0.051 | -0.139 |
| $C_{z0}$ | 0.000 | -0.000 | 0.000 | -0.000 | -0.000 | 0.000 | -0.000 | 0.000 | 0.000 |

**Table 5.8 (Continued).**

| | $\delta_1$ | $\delta_2$ | $\delta_3$ | $\delta_4$ | $\delta_5$ | $\delta_6$ |
|---|---|---|---|---|---|---|
| $x_1$ | 0.082 | -0.026 | -0.113 | 0.074 | -0.077 | -0.076 |
| $y_1$ | -0.092 | -0.009 | 0.154 | -0.073 | 0.086 | 0.087 |
| $z_1$ | 0.207 | 0.004 | -0.013 | -0.047 | 0.096 | 0.097 |
| $x_2$ | -0.013 | 0.017 | 0.079 | -0.073 | 0.098 | 0.099 |
| $y_2$ | -0.117 | -0.004 | 0.116 | -0.068 | 0.094 | 0.095 |
| $z_2$ | 0.247 | 0.003 | -0.004 | -0.025 | 0.048 | 0.048 |
| $x_3$ | -0.104 | -0.042 | 0.038 | 0.055 | -0.076 | -0.077 |
| $y_3$ | -0.064 | -0.094 | -0.024 | 0.018 | -0.113 | -0.113 |
| $z_3$ | 0.117 | -0.012 | 0.010 | -0.015 | 0.062 | 0.063 |

| | $\delta_1$ | $\delta_2$ | $\delta_3$ | $\delta_4$ | $\delta_5$ | $\delta_6$ |
|---|---|---|---|---|---|---|
| $\tau$ | 0.090 | 0.006 | -0.115 | 0.065 | -0.076 | -0.077 |
| $\sigma$ | 0.085 | 0.024 | 0.016 | 0.019 | -0.071 | -0.072 |
| $\rho$ | -0.063 | -0.035 | 0.014 | 0.051 | -0.104 | -0.105 |
| $\dot{\tau}$ | -0.149 | -0.044 | 0.093 | 0.012 | -0.047 | -0.048 |
| $\dot{\sigma}$ | -0.097 | -0.040 | 0.017 | 0.055 | -0.107 | -0.109 |
| $\dot{\rho}$ | -0.089 | -0.018 | -0.001 | -0.019 | 0.079 | 0.079 |
| $C_{22}$ | -0.090 | -0.007 | 0.107 | -0.059 | 0.067 | 0.068 |
| $\beta$ | -0.041 | -0.055 | -0.039 | 0.054 | 0.031 | 0.031 |
| $C_{20}$ | -0.000 | -0.000 | 0.000 | -0.000 | 0.000 | 0.000 |

| | $x_1$ | $y_1$ | $z_1$ | $x_2$ | $y_2$ | $z_2$ | $x_3$ | $y_3$ | $z_3$ |
|---|---|---|---|---|---|---|---|---|---|
| $\tau$ | 0.940 | -0.075 | -0.217 | -0.139 | -0.984 | -0.073 | 0.149 | -0.406 | -0.142 |
| $\sigma$ | 0.223 | -0.262 | 0.377 | 0.068 | -0.339 | 0.596 | -0.525 | 0.265 | 0.446 |
| $\rho$ | 0.305 | -0.191 | -0.876 | -0.083 | -0.261 | -0.700 | 0.964 | 0.238 | -0.837 |
| $\dot{\tau}$ | -0.424 | 0.511 | -0.620 | -0.014 | 0.456 | -0.618 | 0.739 | 0.503 | -0.629 |
| $\dot{\sigma}$ | 0.304 | -0.191 | -0.884 | -0.086 | -0.267 | -0.773 | 0.967 | 0.233 | -0.835 |
| $\dot{\rho}$ | -0.228 | 0.264 | -0.305 | -0.062 | 0.348 | -0.599 | 0.523 | -0.310 | -0.443 |
| $C_{22}$ | -0.953 | 0.935 | 0.206 | 0.024 | 0.943 | 0.069 | -0.142 | 0.401 | 0.134 |
| $\beta$ | -0.094 | 0.063 | 0.298 | 0.253 | 0.099 | 0.265 | -0.429 | -0.082 | 0.247 |
| $C_{20}$ | -0.000 | 0.000 | 0.000 | 0.000 | 0.000 | 0.000 | -0.000 | 0.000 | 0.000 |

**Table 5.8 (Continued).**

Table 5.9 presents the shifts introduced into the various parameters, and the corrections obtained from the solution. The coordinates of the laser stations were recovered to within 10 meters in almost all the cases while the coordinates of retroreflectors were recovered to within 70 meters for most of them. The earth's Eulerian angles are well recovered although their time rates (except $\dot{\theta}_8$) are not. Except for $\dot{\tau}$ and $\dot{\rho}$, the physical libration parameters are poorly recovered, especially $\sigma$ and $\dot{\sigma}$. The moon's physical parameters $C_{22}$, $\beta$ and $C_{20}$ were all well recovered.

The degree of recovery of parameters for this experiment, especially for the coordinates of the laser stations and retroreflectors are somewhat lower than might be expected. Nevertheless, it is not utterly surprising because of the high correlation that exists between some of the parameters. Moreover, only one adjustment cycle was performed for the case presented here, and two or more iterations on this solution might have brought the magnitudes of the corrections closer to the respective shifts introduced.

| Parameters | Shifts | Solution | Parameters | Shifts | Solution |
|---|---|---|---|---|---|
| | Meters | Meters | | Seconds | Seconds |
| $U_1$ | 14.6 | - 26.2 | $\delta_1$ | - 2.1 | 2.1 |
| $V_1$ | 89.4 | - 89.6 | $\delta_2$ | 2.1 | - 2.0 |
| $W_1$ | - 97.5 | 90.4 | $\delta_3$ | - 2.1 | 1.6 |
| $U_2$ | 45.9 | - 39.8 | $\tau$ | 4.3 | -14.2 |
| $V_2$ | - 41.0 | 51.0 | $\sigma$ | 45.1 | - 4.6 |
| $W_2$ | 42.7 | - 48.1 | $\rho$ | - 5.4 | - 2.6 |
| $U_3$ | - 86.9 | 92.5 | $C_{\alpha\alpha}$ | 0.7 | - 0.8 |
| $V_3$ | - 13.4 | 5.0 | $\beta$ | 0.8 | - 0.8 |
| $W_3$ | - 61.8 | 54.7 | $C_{\alpha\rho}$ | 0.0 | 0.0 |
| | | | | Sec/Day | Sec/Day |
| $x_1$ | -429.4 | 394.7 | $\delta_4$ | 0.001 | - 0.1 |
| $y_1$ | -973.2 | 1059.0 | $\delta_5$ | 0.006 | 0.3 |
| $z_1$ | -263.8 | 304.1 | $\delta_6$ | 0.0 | 0.0 |
| $x_2$ | -868.2 | 897.1 | $\dot{\tau}$ | - 1.5 | 1.5 |
| $y_2$ | 449.7 | - 371.9 | $\dot{\sigma}$ | -62.7 | - 1.2 |
| $z_2$ | 541.3 | - 517.6 | $\dot{\rho}$ | - 2.6 | 2.4 |
| $x_3$ | -859.5 | 827.8 | | | |
| $y_3$ | -267.5 | 336.1 | | | |
| $z_3$ | -358.4 | 394.7 | | | |

Table 5.9

Shifts Introduced to Parameters, and Corrections from Solution

## 6. SUMMARY AND CONCLUSIONS.

The main purpose of this study has been that of deriving the observation equations necessary to utilize the lunar laser ranging and the VLBI measurements for the establishment of a primary control network on the moon. The control network consists of coordinates of moon points in the selenodetic Cartesian coordinate system, which is fixed to the lunar body, centered at the moon's center of mass and has its axes coincident with the three principal axes of the moon. The control points are those moon points to which range measurements have been made from terrestrial stations, or those points which have been used in conjunction with terrestrial or other lunar stations for VLBI observations of natural radio sources.

The problem of determining coordinates of points on the moon in the above-defined selenodetic Cartesian coordinate system using earth-based observations is rigorously tied to the knowledge of the following dynamic behavior of the earth and the moon: the orbital motion of the moon about the barycenter, the rotational motion of the moon on its axis and the motion of the earth about its center of mass. In addition, the knowledge of the geocentric positions of the terrestrial stations is essential. Therefore, it can be expected that our knowledge of the parameters related to the above phenomena of the earth-moon dynamic system as well as the geocentric positions of earth stations can be improved simultaneously with the determination of coordinates of lunar points. For this reason, the derived observation equations for the laser ranges and the VLBI time delays were based on a general model, in which the following groups of unknown parameters were included:

1. The selenodetic Cartesian coordinates of lunar points.

2. The geocentric Cartesian coordinates of earth stations.

3. The parameters of the orientation of the selenodetic coordinate system with respect to a celestial coordinate system fixed in space. These may be given by three Eulerian angles, obtainable either through the numerical integration of the moon's equations of motion, or through the Cassini laws and the physical libration angles determined through the classical method.

4. The parameters of the orientation of the average terrestrial coordinate system (U, V, W) with respect to a fixed celestial coordinate system. Traditionally, these have usually been given in terms of the precessional elements, the nutations in obliquity and in longitude, the Greenwich Apparent Sidereal Time and the motion of the true pole with respect to the CIO pole. It has been shown in this study that the orientation of an earth-fixed coordinate system with respect to a fixed celestial system can be represented by three Eulerian angles, which can be obtained through numerical integration of three second-order differential equations.

5. The geocentric coordinates of the center of mass of the moon as given by a lunar ephemeris.

The laser and the VLBI equations were developed in Chapters 2 and 3. In Chapter 4, some effort was devoted to the derivation of the earth's equations of motion (rotational) and an outline of how these differential equations can be numerically integrated was presented. The justification for the extensive treatment of this subject in this study lies in the fact that the knowledge of the earth's orientation in space is an important factor for accurate determination of selenodetic coordinates of points on the moon. Moreover, the number of parameters defining the earth's orientation is greatly reduced when the angles are obtained through numerical integration process. This eases up the important practical problem of computer storage in handling the solution of a huge

system of normal equations, which would have resulted from the inclusion of precessional and nutational parameters in the adjustment model. A general adjustment model, based on the theory of adjustment computations using matrix algebra, was developed for the analysis of laser and VLBI observations in Chapter 5.

A few numerical experiments were performed in this study, basically for the purpose of checking the models and equations developed in parts of this work. The first group of experiments are limited to the numerical verification of the equations and methods developed for the numerical integration of the earth's orientation angles, and the computer programs based on these equations. From the results obtained, it was demonstrated that, over a period of one year, the numerically integrated angles compare very well to the classically computed ones, to within 0".2 in the worst case. It was also shown that the solutions for the initial conditions of the integration do converge inspite of high correlations between some of the parameters.

Another group of experiments was performed for the purpose of investigating the accuracies of determining geodetic and selenodetic coordinates as well as the orientation parameters of the earth and the moon, when laser ranges are used. For this purpose, the three retro-reflectors on the moon deposited by U. S. astronauts served as the lunar bench marks and simulated ranges were obtained to their reflec...s from three laser stations located on the earth's surface. Results of the experiments indicate significant improvement in the accuracy of determining station positions (both on the earth and on the moon). Also, the results indicate that the orientation of the earth and the moon, represented by 6 parameters each, can be more accurately solved for with the use of laser ranges. However, it was clear from the results that a good number of the parameters in the solution were highly correlated. This fact seems to have affected the degree to which parameters could be recovered, if their known values are arbitrarily altered.

One logical extension of the study performed here is the numerical verification of the observation equations for the VLBI, and the improvement that might be expected in the adjustment system if VLBI observations are combined with laser ranges. Another problem area is the investigation of the possibility of conbining the types of observations treated in this work with other types such as earth-based optical observations, satellite-borne photography, lunar laser altimetry and range/range-rate observations to lunar satellites. In deriving the observation equations for the laser and the VLBI, as well as the equations of motion of the earth, both the earth and the moon were assumed to be rigid bodies. The effects of non-rigidity of the earth and the moon on these equations still remain to be investigated.

Finally, the ultimate goal in the application of the findings contained in this study to Geodetic Science and other related academic disciplines would be reached when the equations presented here are successfully applied to actual laser and/or VLBI observations.

## APPENDIX A

### Equations for Earth-Based VLBI Observations of an Artificial Source

The use of a radio beacon, deposited on the moon, as an artificial source for an independent clock interferometric system was one of the recommendations of the Lunar Science and Exploration Conference of 1967 [75]. The radio source could be a transponder, whose transmitted signals are observed by two or more radio telescopes widely separated on the earth. The main advantage of using an artificial radio source is the stronger signal reception expected because of the proximity of the artificial source. The differences in the arrival times of the radio signal at the two interferometer stations (time delay) are obtained through the usual VLBI technique of delay mapping (described in Section 3.2). The difference between the observed and the predicted time delays can be used to obtain corrections to approximate or assumed values of parameters used in the prediction equation.

Since the source is at a finite distance from the earth, the equations for the earth-based VLBI observations of natural sources derived in Section 3.31 is no longer valid, and a corrected equation will be derived in this appendix.

In Figure A.1,

O is the geocenter

C is the selenocenter

A, B are the VLBI stations on earth

M is the position of the radio source on the moon

$\vec{C}$ is the vector from geocenter to selenocenter

$\vec{M}$ is the vector from geocenter to the radio source

$\vec{R}_A$, $\vec{R}_B$ are vectors from geocenter to A and B respectively

$\vec{S}_A$, $\vec{S}_B$ are vectors from A, B to the radio source

$\vec{D}$ is the vector from A to B.

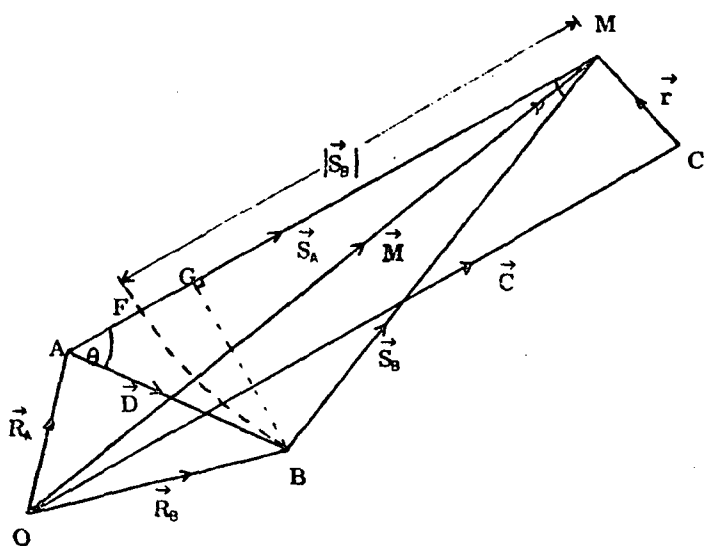


Figure A.1 Earth-Based VLBI with Artificial Source.

From the figure,

$$MF = MB = |\vec{S}_B|.$$

Hence, the delay distance (d) is given by AF. If c is the velocity of light, the time delay $\tau$, is given by

$$\tau = \frac{d}{c}. \qquad (A.1)$$

However,

$$d = AG + GM - MB$$

or

$$d = |\vec{D}| \cos\theta + |\vec{S}_B| \cos\gamma - |\vec{S}_B| \tag{A.2}$$

and since

$$|\vec{S}_B| \sin\gamma = |\vec{D}| \sin\theta,$$

it follows that

$$d = |\vec{D}| \cos\theta - |\vec{D}| \sin\theta \left(\frac{1-\cos\gamma}{\sin\gamma}\right). \tag{A.3}$$

Therefore,

$$\tau = \frac{|\vec{D}|}{c}\left[\cos\theta - \sin\theta\left(\frac{1-\cos\gamma}{\sin\gamma}\right)\right] \tag{A.4}$$

represents the corrected equation for the time delay, which is the difference in the arrival times ($t_2$, $t_1$) of the radio signal at stations B and A respectively.

If the various vectors in Figure A.1 are expressed in the same coordinate system (for example, the mean ecliptic system of a standard epoch), then the following vector relationships hold:

$$\begin{aligned} \vec{D} &= \vec{R}_B - \vec{R}_A \\ \vec{S}_A &= \vec{C} + \vec{r} - \vec{R}_A \\ \vec{S}_B &= \vec{C} + \vec{r} - \vec{R}_B. \end{aligned}$$

Also,

$$\cos\theta = \frac{\vec{S}_A \cdot \vec{D}}{|\vec{S}_A||\vec{D}|} \tag{A.5}$$

and

$$\cos\gamma = \frac{\vec{S}_A \cdot \vec{S}_B}{|\vec{S}_A||\vec{S}_B|}. \qquad \text{(A.6)}$$

In matrix form equations (A.5) and (A.6) can be written as

$$\cos\theta = \frac{D^T S_A}{(D^T D S_A^T S_A)^{\frac{1}{2}}}$$

and

$$\cos\gamma = \frac{S_B^T S_A}{(S_B^T S_B S_A^T S_A)^{\frac{1}{2}}}$$

where D, $S_A$, $S_B$ are column matrices of vectors $\vec{D}$, $\vec{S}_A$ and $\vec{S}_B$ respectively.

The equation for the time delay (equation (A.4)) can be evaluated for any epoch through vectors $\vec{D}$, $\vec{S}_A$ and $\vec{S}_B$. As noted earlier, the components of these vectors must be expressed in the same coordinate system, such as the mean ecliptic system of any standard epoch.

The vector $\vec{D}$ which is the inter-site vector, is a function of the geocentric position vectors of the two observing stations and a transformation matrix which varies with time. Both $S_A$ and $S_B$ depend on the geocentric position of the lunar center of mass, the selenocentric position of the radio source and transformation matrices that vary with time.

## APPENDIX B

### Systematic Errors Affecting Earth-Based Lunar Observations

Most of the systematic errors which have effects upon all observations made to points or objects on or near the moon can be classified under the following two main groups:

A. Instrumental errors

B. Errors due to physical effects.

In the development of observation equations for the two types of observations considered in the main chapters of this work (i.e. the laser and the VLBI), it was assumed that these observations have been corrected for all systematic errors. This assumption is a reasonable one, in view of the fact that most observers go to a great deal of effort to correct their observations for known instrumental and other systematic errors. Nevertheless, it often happens that inadequacy in the theoretical knowledge of the physical phenomena involved and incomplete identification of all sources of instrumental errors may result in incomplete systematic error modelling and the treatment of observations, thereby leaving residual errors in the corrected observations presumed to be free from all systematic errors. Consequently, the correct procedure in adjusting any set of observations should include provisions for the inclusion of mathematical models capable of absorbing all or most of the residual systematic errors. While the development of such models for laser and VLBI observations is beyond the scope of this present study, the purpose of this appendix is to identify and discuss possible sources of systematic errors in the types of observations already mentioned above.

A. Instrumental Errors.

Instrumental errors are those errors which are inherent in the measuring systems. Their sources are not easily identifiable in new and complex observational systems. Full identification of all the sources of errors comes with experience in the usage of such new measuring systems, and through the analyses of measured quantities. However, once the sources have been identified, instrumental errors can be controlled or corrected very accurately.

Since both the laser and the VLBI are new observational systems, all their sources of errors have not yet been identified. Nevertheless, a few sources of errors can be mentioned for each system.

For the laser, these sources include errors in the time interval measuring circuitry, and in the determination of the physical point in the transmitting/receiving telescope, to which the measured distances are referred. Another source of instrumental error in the laser is in the determination of total instrumental delay of the signal, due to the optical path length of the telescope and the delay through the photomultiplier.

The main source of instrumental error for the VLBI is in the possible drift of the generated local frequency standard, and the limited phase stability of the locally generated signal. This results in a clock offset error which can be easily incorporated into the mathematical adjustment model as one of the parameters to be solved. Also, inaccurate determination of the "system zero bias" is one of the sources of VLBI instrumental errors. The "system zero bias" is dependent on the determination of the focal point of the telescope, and on the instrumental delays of the observed radio signal.

Most of the instrumental errors are expected to be eliminated from the observations, leaving only residual errors which, if large enough, can be determined by the incorporation of suitable mathematical models into the adjustment model.

B. Errors Due to Physical Effects.

Systematic errors in this group are caused by the fact that earth-bound observations to moon points are made through the earth's atmosphere, and that certain geophysical phenomena (such as earth-tides) do change the positions of earth stations relative to the geocenter. Therefore, errors in this group can be treated under the following headings:

(1) Atmospheric refraction errors

(2) Earth tidal effects

(3) Continental drift

1. Atmospheric refraction errors.

Atmospheric effects on radio or optical signals can be classified under the two following headings:

(a) Tropospheric effects

(b) Ionospheric effects.

The lower part of the atmosphere ( the troposphere) contains both dry air and water vapor, while the ionosphere (the upper part of the atmosphere) is made up of layers of free, electrically charged particles (ions). The electron densities of the ionospheric layers vary considerably with solar activity, geography and the time of the day.

The refractive index in both the troposphere and the ionosphere departs from unity, thereby causing both a deviation of the ray from the straight line path, and a change in the phase velocity of the signal from its velocity in vacuum. Thus:

$$v_p = \frac{c}{n} \qquad \text{(B. 1)}$$

where

$v_p$ is the phase velocity in the atmosphere

c is the velocity of electromagnetic radiation in vacuum

and

n is the refractive index of the medium.

The departure of the ray path from a straight line is usually very small for normal observing conditions, and it is non-existent in the zenith direction. Neglecting this deviation, the difference between the path in free space and the actual path is given by:

$$\delta d = \int dh - \int n dh,$$

or

$$\delta d = \int (1-n) dh \qquad \text{(B. 2)}$$

where the integration is to be performed over the entire path.

The above equation (B. 2) is exact for an electromagnetic signal observation in the direction of the zenith, and corrections for observations made at other elevations are functions of the correction in the zenith direction, provided no horizontal gradient is present at the time of observation.

Tropospheric effects.

In the troposphere, the refractive index (n) is greater than unity. The correct evaluation of equation (B. 2) requires the knowledge of the refractive indices along the entire ray path at the time of observation. Since this is practically impossible, numerous methods have been proposed for the prediction of the value of the integral equation. These methods include radio-optical dispersion techniques, range measurements at two optical wavelengths, and prediction from surface weather data. Hopfield in [35] shows how, with the use of surface weather data, the dry air component of the range correction for laser and radio observations, in the zenith direction can be predicted with a root mean square error of few millimeters (out of a total correction of about 2. 3 meters). However, the range error prediction for the more variable but smaller wet part of the troposphere is not as accurate as that for the dry part. The residual tropospheric refraction error is larger for the VLBI observations, than for laser ranges because of the increased influence of water vapor in the radio spectral region. At optical frequencies, the effect of

water vapor is so much decreased as to be almost negligible.

Ionospheric effects.

Unlike the troposphere, the ionospheric medium is such that its refractive index is less than unity. Consequently, the two effects (tropospheric and ionospheric) tend to cancel each other. For a microwave radio path which traverses both the troposphere and the ionosphere, the overall effect is a negative differential phase path length.

The calculation of the ionospheric refraction error, which depends on the frequency of the wave, the electron density, the earth's magnetic field and the collision frequency can be done using ionospheric models and the ray-tracing technique [61]. In general, the ionospheric correction is inversely proportional to the square of the signal. From [45], an approximate equation for the average day-time ionospheric correction for the observed range is given by:

$$|\delta d| \approx \frac{3 \times 10^{21}}{2 f^2} \text{ cm} \qquad \text{(B. 3)}$$

where

$\delta d$ is range error

and

$f$ is propagation frequency.

The observations made at radio frequencies are much more affected by the ionosphere than those at optical frequency. Consequently, it is desirable that VLBI observations be made at high frequencies, subject to other limiting conditions.

From the above discussion, it is evident that corrections due to atmospheric effects are usually calculated from theoretical models. Residual refraction errors are almost certainly bound to remain in the corrected observations, the magnitudes of which depend on the departure of the actual atmospheric conditions from the model used in calculating the corrections.

VLBI observations involve two stations, and the residual refraction error in the corrected time delay depends on the residual refraction errors at both stations. The determination of the residual errors, if large enough can be done by introducing suitable mathematical models into the adjustment model, and regarding these residual errors as unknowns in the adjustment.

2. Earth tidal effects.

The tidal phenomenon, which is a result of the varying attractive forces of the moon and the sun, produces periodic deformations of the geoid known as earth tides. These deformations cause small variations in the intensity of gravity, in the direction of the vertical, and in geoidal heights. On an absolutely rigid crust, the periodic variations in the magnitude and direction of the gravity vector can be calculated from the potential of the bodies which causes these variations. Theoretically, the magnitudes of the variations are 0.″04 and 0.″2 milligals for the deflection of the vertical and the intensity of gravity respectively. However, the globe as a whole cannot be truly regarded as rigid, since the earth is somewhat elastic and viscous. Consequently, the theoretical deformations of the earth due to luni-solar attractions and their phases are altered by the earth's elasticity and viscosity. Furthermore, the non-rigidity of the earth gives rise to tensions and cubic expansions which would not be present with a rigid globe.

In lunar laser ranging and earth-based VLBI, the observations are made with instruments rigidly attached to the earth's crust. The periodic variations of the radial distances of observing stations introduce systematic errors into both the laser and the VLBI observations, which should be eiliminated before adjusting the observations.

From the static theory of tides, the theoretical height of the observed tide ($\xi$) at a point is given by [63]:

$$\xi = \frac{W_2}{g} \qquad \text{(B. 4)}$$

where

$W_2$ is the potential (to the second degree) of the force-producing bodies (sun and moon) at the point

g is the value of gravity.

For the moon, if z is the geocentric altitude, the height of the theoretical tide is

$$\xi_{☾} = 26.7\ (\cos 2z_{☾} + 1/3)\ \text{cm}. \qquad \text{(B.5)}$$

The geoidal height therefore increases by a maximum of 35.6 cm and decreases by a maximum of 17.8 cm, giving a total range of 53.4 cm. For the sun,

$$\xi_{\odot} = 12.3\ (\cos 2z_{\odot} + 1/3)\ \text{cm} \qquad \text{(B.6)}$$

which is equivalent to an oscillation from 16.4 cm to -8.2 cm or a total range of 24.6 cm. Thus the combined luni-solar effect would give an oscillation of of 78 cm for the geoid, if the earth were a perfect liquid.

From observations of tides, the actual response of the earth to the tidal generating forces results in a rise and fall of the elevation of the earth's surface on the order of 25 to 30 cm in the midlatitudes and of 50 cm near the equator. The projected precision of both the laser and the VLBI measurements shows that for both instruments, the systematic errors due to earth tides cannot be ignored, and observations made by both instruments must be corrected for tidal effects.

In the classical method of determining tides, earth tides are broadly classified under three types namely:

(i) long periodic

(ii) diurnal

(iii) semi-diurnal.

Within each type, there are several tidal waves of differing amplitudes and frequencies. The instruments used in earth tide observations include horizontal pendulums, tidal gravimeters and extensometers. From a continuous

record of observations made with these instruments, the amplitude and phase of each wave is determined, using methods of harmonic analysis which are based on the theory of the combination of ordinates [63]. The laser and the VLBI can play important roles in the determination of earth-tides in future provided measurements made by them are of a continuous nature.

It is relevant to mention here that solid tides on the surface of the moon do exist, and that tidal effects on the moon are relatively larger, at least theoretically [63]. So far, very little is known about the moon's internal constitution, and no observations have been made on the surface of the moon for the purpose of determining lunar tides. Consequently, lunar tides for the present, can only be considered theoretically.

3. Continental drift.

During the past few years, some geodetic evidence has been accumulated, which shows that the earth's surface is mobile. Large blocks of the earth's outer layer appear to be moving with respect to one another at varying rates from 1 cm/year to as high as 15 cm/year [45]. This "drifting of the continents" causes changes in the geocentric positions of earth stations, to which laser and VLBI instruments are rigidly fixed. However, the average rate of motion is small enough to have no appreciable effects on lunar laser ranging and VLBI measurements, if the observations cover a relatively short span of time. For observations taken over a long period, the effect of crustal motion may become appreciable, and the observations should therefore be corrected before they are used for adjustment purposes.

## BIBLIOGRAPHY


[1] Alley, C.O. et al. (1965). "Optical Radar Using a Corner Reflector on the Moon." Journal of Geophysical Research, Vol. 70, p. 2267.

[2] Alley, C.O. and P.L. Bender. (1968). "Information Obtainable from Laser Range Measurements to a Lunar Corner Reflector." Symposium No. 32 of the IAU/IUGG on Continental Drift, Secular Motion of the Pole and Rotation of the Earth, edited by W. Markowitz and B.Guinot. D.Reidel Publishing Co. Dordrecht, Holland.

[3] Alley, C.O. et al. (1969). "Some Implications for Physics and Geophysics of Laser Range Measurements from Earth to a Lunar Retro-Reflector." Proceedings of NATO Advanced Study Institute on the Application of Modern Physics to the Earth and Planetary Interiors, edited by S.K. Runcorn. John Wiley and Sons, London.

[4] Alley, C.O. et al. (1970). "Apollo 11 Laser Ranging Retro-Reflector: Initial Measurements from the McDonald Observatory." Science, Vol. 167, pp. 368-370, January 23.

[5] Alley, C.O. et al. (1970). "Laser Ranging Retroreflector: Continuing Measurements and Expected Results." Science, Vol. 167, pp. 458-460. January 30.

[6] AMS. (1960). "Horizontal and Vertical Control for Lunar Mapping (Part One: Methods)." Army Map Service Technical Report No. 29. August.

[7] AMS and ACIC. (1967). "Department of Defence Selenodetic Control System 1966." Defence Intelligence Agency Technical Report. January.

[8] Anderle, R.J. (1970). "Polar Motion Determinations by U.S. Navy Doppler Satellite Observations." NWL Technical Report, TR-2432. July.

[9] Anderson, J.D. (1964). "Theoretical Basis of the JPL Oribt Determination Program." Technical Memorandum 312-409. Jet Propulsion Laboratory, Pasadena, California.

[10] Bare, C., et al. (1967). "Interferometer Experiment with Independent Local Oscillators." Science, Vol. 157, No. 3785, pp. 189-191. July 14.

[11] Brown, E.W. (1896). An Introductory Treatise on the Lunar Theory. Cambridge University Press (Dover Edition published in 1960).

[12] Brown, E.W. (1908). "Theory of the Motion of the Moon." Memoirs of the Royal Astronomical Society, Vol. 59, pp. 1-103.

[13] Brouwer, D. and G.M. Clemence. (1961). Methods of Celestial Mechanics. Academic Press, New York.

[14] Burke, Bernard F. (1969). "Long-Baseline Interferometry." Physics Today, Vol. 22, No. 7, pp. 54-63. July.

[15] Cohen, M.H. et al. (1968). "Radio Interferometry at One-Thousandth Second of Arc." Science, Vol. 162, No. 3849, p. 88. October 4.

[16] Cohen, M.H. et al. (1968). "Radio Interferometry at One-Thousandth Second of Arc." Science, Vol. 162, pp. 88-94. October 4.

[17] Cohen, M.H. (1969). "High-Resolution Observations of Radio Sources." Annual Review of Astronomy and Astrophysics, Vol. 7, p. 619.

[18] Department of Geodetic Science. (1969). "Investigation Related to Geodetic Control on the Moon: First Quarterly Status Report." Prepared for NASA-MSC. The Ohio State University, Columbus. December.

[19] Doyle, Frederick J. (1968). "Photogrammetric Geodesy on the Moon." Paper presented at the Annual Meeting of the American Society of Photogrammetry. March.

[20] Eckert, W.J., R. Jones and H.K. Clark. (1954). "Construction of the Lunar Ephemeris." Improved Lunar Ephemeris 1952-1959, Supplement to the American Ephemeris and Nautical Almanac. U.S. Government Printing Office, Washington, D.C.

[21] Eckhardt, D.H. (1970). "Lunar Libration Tables." The Moon, Vol. 1, No. 2. February.

[22] Edwards, Hiram W. (1964). Analytic and Vector Mechanics. Dover Publications, Inc., New York.

[23] Escobal, P.R. (1965). Methods of Orbit Determination. John Wiley and Sons, Inc., New York.

[24] Escobal, P.R. (1968). Methods of Astrodynamics. John Wiley and Sons, Inc., New York.

[25] Fajemirokun, F.A. (1971). "Application of New Observational Systems for Selenodetic Control." Dissertation, The Ohio State University, Columbus, September.

[26] Faller, James E. et al. (1969). "Laser Beam Directed at the Lunar Retro-Reflector Array: Observations of the First Returns." Science, Vol. 166, p. 99. October 3.

[27] Franz, J. (1898). "Die Figure des Mondes." Astro. Beob. Königsberg, 38.

[28] Franz, J. (1901). "Ortsbestimmung von 150 Mondkratern." Mitteilungen der Koniglichen Universitats-Sternwarte zu Breslau, Vol. 1, pp. 1-51.

[29] Garthwaite, K. et al. (1970). "A Preliminary Special Perturbation Theory for the Lunar Motion." Astronomical Journal, Vol. 75, No. 10, pp. 1133-1139. December.

[30] Gold, T. (1967). "Radio Method for the Precise Measurement of the Rotation Period of the Earth." Science, Vol. 157, pp. 302-304. July 21.

[31] Goldstein, Herbert. (1950). Classical Mechanics. Addison-Wesley Publishing Company, Inc., Reading, Massachusetts.

[32] Gurevich, V.B. (1967). "Astronomical Determination of Position on the Moon. Soviet Astronomy - AJ, Vol. 11, No. 1, pp. 137-147. Translated from Astronomicheskii Zhernal, Vol. 44, No. 1, pp. 178-192. January - February.

[33] Hayn, F. (1904). "Selenographische Koordinaten." Leipzig Sächs. Gesell. der Wiss. II Abh.

[34] Hinteregger, H.F. (1968). "A Long Base Line Interferometer System with Extended Band Width." Nerem Record Vol. 10, IEEE Catalogue No. 68 C22 - NEREM. November.

[35] Hopfield, H.S. (1971). "Tropospheric Effect on Electromagnetically Measured Range: Prediction from Surface Weather Data." Radio Science, Vol. 6, No. 3, pp. 357-367. March.

[36] Hopfield, H.S. (1971). "Tropospheric Range Error at the Zenith." Paper presented at the 14th Plenary Meeting of COSPAR, Working Group 1, Seattle, Washington. June - July.

[37] Hopmann, J. (1967). "The Accuracy of the Information on Absolute Heights on the Moon, and the Problem of its Figure." Mantles of the Earth and Terrestrial Planets, S.K. Runcorn, (ed.), pp. 175-182. John Wiley and Sons, Inc., New York.

[38] Howard, W.E. and S.P. Maran. (1965). "General Catalogue of Discrete Radio Sources." The Astrophysical Journal, Supplement Series, Vol. X. The University of Chicago Press, Chicago.

[39] Hunt, Mahlon S. (1966). "Progress in Selenodesy." AFCRL Special Report No. 39. Project 8654. January.

[40] Hunt, Mahlon S. (1967). "Selenodesy and Lunar Laser Experiments." Presented at the 14th General Assembly of the IUGG/IAG, Lucerne, Switzerland. September - October.

[41] Jeffreys, Sir Harold. (1970). The Earth: Its Origin, History and Physical Constitution, 5th Edition. Cambridge University Press, New York.

[42] Jennison, R.C. (1966). Radio Astronomy. George Newnes, Ltd., Tower House, London.

[43] Jones, Harold E. (1969). "Geodetic Ties Between Continents by Means of Radio Telescopes." The Canadian Surveyor, Vol. XXIII, No. 4, pp. 379-388. September.

[44] Kaula, W.M. (1968). An Introduction to Planetary Physics: The Terrestrial Planets. John Wiley and Sons, Inc., New York.

[45] Kaula, W.M. (ed.). (1969). "The Terrestrial Environment, Solid- Earth and Ocean Physics: Application of Space and Astronomic Techniques." Report of a study at Williamstown, Massachusetts to the National Aeronautics and Space Administration. August.

[46] Kaula, W.M. (1971). "Geophysical Implications of Laser Ranging to the Moon." Paper presented at the IUGG/IAG Lunar Ranging Symposium, Moscow. August 6.

[47] Ko, H.C. (1964). "Radio Telescope Antennas." Microwave Scanning Antennas, Vol. 1, Edited by R.C. Hansen. Academic Press, New York.

[48] Kokurin, Yu. L. et al. (1965). "Optical Radar Method for Measuring the Parameters of the Moon's Figure and Orbit." Translated from Kosmicheskie Issledovaniya, Vol. 4, No. 3, pp. 414-426. May - June, 1966.

[49] Kokurin, Yu. L. et al. (1966). "Possibilities for Improving Certain Astronomical Parameters of the Earth-Moon System by the Optical Radar Method." Translated from Kosmicheskie Issledovaniya, Vol. 5, No. 2, pp. 219-224. March - April, 1967.

[50] Kolaczek, B. (1968). "Selenocentric and Lunar Topocentric Spherical Coordinates." Smithsonian Astrophysical Observatory Special Report 286. September 20.

[51] Kopal, Zdenek. (1969). The Moon. D. Reidel Publishing Company, Dordrecht, Holland.

[52] Kopal, Z. and C. L. Goudas. (eds). (1967). Measure of the Moon. D. Reidel Publishing Company, Dordrecht, Holland.

[53] Koziel, K. (1948). Acta Astronomica, 4, p. 61, June 27.

[54] Kraus, John D. (1966). Radio Astronomy. McGraw-Hill Book Company, New York.

[55] Krogh, Fred T. (1969). "VODQ/SVDQ/DVDQ - Variable Order Integrators for the Numerical Solution of Ordinary Differential Equations." Section 314, Subroutine Write-up, Jet Propulsion Laboratory, Pasadena, California. May.

[56] Lengyel, B. A. (1962). Lasers, Generation of Light by Stimulated Emission. John Wiley and Sons, Inc., New York.

[57] Lehr, Carlton G. (1969). "Geodetic and Geophysical Application of Laser Satellite Ranging." IEEE Transactions on Geoscience Electronics, Vol. GE-7, No. 4, pp. 261-267. October.

[58] Lucas, James. (1963). "Differentiation of Orientation Matrix." Photogrammetric Engineering. Vol. 29, No. 7, July.

[59] MacDonald, Gordon J. F. (1967). "Implications for Geophysics of the Precise Measurement of the Earth's Rotation." Science, Vol. 157, pp. 304-305. July 21.

[60] Marshall, S. L. (ed). (1968). Laser Technology and Applications. McGraw-Hill, Inc., New York.

[61] Mathur, N.C. (1969). "Ray-Tracing Analysis of Ionospheric and Tropospheric Effects on Interferometric Distance Determination." Presented at the Fall National Meeting of the American Geophysical Union, San Francisco, California. December 15-18.

[62] Melbourne, W.G. et al. (1968). "Constants and Related Information for Astrodynamic Calculations, 1968." Technical Report 32-1306, Jet Propulsion Laboratory, Pasadena, California.

[63] Melchior, Paul. (1966). The Earth Tides. Pergamon Press, Ltd., New York.

[64] Melchior, Paul and B. Georis. (1968). "Earth Tides, Precession-Nutation and the Secular Retardation of the Earth's Rotation." Physics of the Earth and Planetary Interiors, Vol. 1, pp. 267-287.

[65] Mendez, J.C. and R.J. Stern. (1969). "Geographic and Selenographic Coordinate Transformation Program." TRW1176-H203-R0-00, TRW Note No. 69-FMT-749, Project Apollo, Task MSC/TRW A-193. April 18.

[66] Meyer, Donald L. and Byron W. Ruffin. (1965). "Coordinates of Lunar Features, Group I and II Solutions." ACIC Technical Paper No. 15. March.

[67] Moran, James M. (1968). "Interferometric Observations of Galactic OH Emission." Ph. D. Dissertation, Massachusetts Institute of Technology, Cambridge. September.

[68] Mueller, Ivan I. (1964). Introduction to Satellite Geodesy. Frederick Ungar Publishing Co., New York.

[69] Mueller, Ivan I. (1969). Spherical and Practical Astronomy as Applied to Geodesy. Frederick Ungar Publishing Co., New York.

[70] Mueller, Ivan I. (ed). (1969). "A General Review and Discussion on Geodetic Control on the Moon." Reports of the Department of Geodetic Science, No. 127. The Ohio State University, Columbus. December.

[71] Mulholland, J.D. (1968). "Proceedings of the JPL Seminar on Uncertainties in the Lunar Ephemeris." Technical Report 32-1247, Jet Propulsion Laboratory, Pasadena, California. May.

[72] Mulholland, J.D. et al. (1968). "Gravitational Inconsistency in the Lunar Theory. Part I: Numerical Determination. Part II: Confirmation by Radio Tracking." Technical Report 32-1290, Jet Propulsion Laboratory, Pasadena, California. Reprinted from Science. May 24.

[73] Munk, W.H. and G.J.F. MacDonald. (1960). The Rotation of the Earth: A Geophysical Discussion. Cambridge University Press, New York.

[74] NASA. (1965). Summer Conference on Lunar Science and Exploration. NASA SP-88. U.S. Government Printing Office. July.

[75] NASA. (1967). Summer Study of Lunar Science and Exploration. NASA SP-157. U.S. Government Printing Office. October.

[76] Nautical Almanac Offices of the United Kingdom and the United States of America. (1961). Explanatory Supplement to the Astronomical Ephemeris and the American Ephemeris and Nautical Almanac. H.M. Stationery Office, London.

[77] O'Handley, D.A. et al. (1969). "JPL Development Ephemeris No. 69." Technical Report 32-1465, Jet Propulsion Laboratory, Pasadena, California. December 15.

[78] Papo, H.B. (1971). "Optimal Selenodetic Control." Department of Geodetic Science Report No. 156, The Ohio State University.

[79] Plummer, H.C. (1960). An Introductory Treatise on Dynamical Astronomy. Dover Publications, Inc., New York.

[80] Ralston and H. Wolf (eds). (1960). Mathematical Methods for Digital Computers. John Wiley and Sons, Inc., New York.

[81] Rapp, R.H. (1969). "The Geopotential to (14,14) from a Combination of Satellite and Gravimetric Data." Bulletin Geodesique, No. 91, March.

[82] Robinson, W.G. (1970). "Q-Switched Ruby Laser for Lunar Ranging Experiments." Laser Journal, pp. 29-30. January/February.

[83] Rogers, Alan E.E. (1970). "Very Long Baseline Interferometry with Large Effective Bandwidth for Phase-Delay Measurements." Radio Science, Vol. 5, No. 10, pp. 1239-1247. October.

[84] Ross, S. (1968). "Interferometer Systems." Investigation of Continental Drift, Phase-I Effort. SAO Report for NASA. November.

[85] Routh, E.J. (1960). Dynamics of a System of Rigid Bodies: Elementary Part, 7th Edition. Dover Publications, Inc., New York.

[86] Routh, E.J. (1955). Advanced Dynamics of a System of Rigid Bodies, 6th Edition. Dover Publications, Inc., New York.

[87] Saastamoinen, J. (1970). "The Atmospheric Correction for Laser Ranging of Satellites." Paper presented at the Annual AGU Meeting, Washington D.C. April.

[88] Scharn, Hermann O.F. (1970). "Geodetic Application of Long Base-Line Interferometry." Final Report ORA-70-0005, Office of Research Analyses, Holloman Air Force Base, New Mexico. May.

[89] Schrutka-Rechtenstamm, G. (1958). "Neureduktion der 150 Mondpunkte der Breslauer Messungen von J. Franz." Sitz. Osterr. Akad. Wiss. Math. - Naturw. Klasse, Abt. II, Vol. 167. January.

[90] Shapiro, I.I. (1968). "Possible Experiments with Long-Baseline Interferometers." Nerem Record Vol. 10, IEEE Catalogue No. 68C22-NEREM. November.

[91] Smart, W.M. (1953). Celestial Mechanics. Longmans, Green and Company, New York.

[92] Swenson, G.W. and N.C. Mathur. (1968). "The Interferometer in Radio Astronomy." Proceedings of the IEEE, Vol. 56, No. 12, pp. 2114-2130. December.

[93] Uotila, U.A. (1967). "Introduction to Adjustment Computations with Matrices." Unpublished class notes. The Ohio State University.

[94] Woolard, E.W. (1953). "Theory of the Rotation of the Earth Around its Center of Mass." Astronomical Papers prepared for the use of the American Ephemeris and Nautical Almanac, Vol. XV, Part 1. U.S. Government Printing Office, Washington, D.C.